
Process stabilization of cartridge case ironing

AN INVESTIGATION OF THE STABILIZING EFFECTS INTRODUCED BY USING A CIRCULAR
DIE LAND IN CARTRIDGE CASE IRONING

By

JAKOB B. PEDERSEN



AALBORG UNIVERSITY
STUDENT REPORT

MAIN REPORT



AALBORG UNIVERSITY
STUDENT REPORT

**Study Board of Industry and Global
Business Development**

Fibigerstræde 16

DK - 9220 Aalborg Øst

Tlf. 99 40 93 09

ift@m-tech.aau.dk

www.en.ses.aau.dk

Title:

Process stabilization of cartridge case
ironing

Semester:

VT-4

Theme:

Master thesis

Project period:

February 2017 - June 2017

ECTS:

30

Synopsis

This project is conducted in collaboration with the Danish munition manufacturer DENEX, and concerns the investigation and implementation of a die design with a circular die land, CDL, to the ironing process of 5.56mm NATO cartridge cases.

The first part of the project concerns an investigation of the effects an implementation of the CDL design have on the ironing process.

In the second part of the project is a CDL design determined in regards to implementing it to the production at DENEX. It was determined that the design should use a CDL radius of 11mm.

In the third and final part of the project is the chosen CDL design implemented and tested in the production at DENEX, and it was here discovered that the design was not able to produce conforming cartridge cases due to fracture during the third draw.

Jakob B. Pedersen

Supervisor:

Benny Ørtoft Endelt

Contact at DENEX:

John Bach

Censor:

Lars-Erik Braüner

Pages: 69

Appendix: 5

Preface

This report documents the master thesis composed by Jakob Bengtson Pedersen at the 4th and final semester of the master program in Manufacturing Technology at Aalborg University during the period from the 1st of February to the 2nd of June 2017. The theme for the project is *Master Thesis*.

The project is completed under supervision of Associate Professor Benny Ørtoft Endelt, and in collaboration with DENEX through John Bach

In regards to confidentiality, it is desired to keep the report public available, hence confidential material will not be present in the report. In order to gain access to this material, the reader would have to make personal contact to DENEX at:

DENEX
Tuenvej 120
9900 Frederikshavn
Denmark
www.denex.dk
expal@expal.biz

Reading guide

Through the report source references in the form of the Harvard method will appear and these are all listed at the back of the report. References from books, homepages or the like will appear with the last name of the author and the year of publication in the form of [Author, Year]. They can furthermore appear with specific reference to a chapter, page, figure or table.

Figures and tables in the report are numbered according to the respective chapter. In this way the first figure in chapter 3 has number 3.1, the second number 3.2 and so on. Explanatory text is found under the given figures and tables. Figures without references are composed by the author.

As for figures and tables, equations are also numbered according to their respective chapter. Furthermore the used notation style for math is that matrices and vectors are typeset in boldface, whereas scalars are typeset italic. In order to distinguish between matrices and vectors, matrices are always represented by capital letters e.g **M**, and vectors by lower case letters e.g **v**. Please note that variables may have multiple meanings, depending on the chapter.

Danish abstract

Dette projekt er lavet i samarbejde med ammunitions fabrikken DENEX, og omhandler en undersøgelse og implementering af et matrice design, der anvender en cirkulær anlægsflade, til strækningsreduktionsprocessen for 5.56mm NATO patronhylstre. Konceptet bag anvendelsen af en cirkulær anlægsflade stammer fra [Danckert, 2005], hvor det er vidst, at dette design har en stabiliserende effekt på strækningsreduktionsprocessen, hvis matricen er udsat for et lille tilt, hvilket både kan skyldes en upræcis fremstilling, eller manglende præcision under montagen.

Med udgangspunkt i at undersøge hvilken effekt dette design har på den omtalte strækningsreduktionsproces, omhandler projektet derved først en undersøgelse, af hvilke effekter en implementering af designet har på processen, hvorefter der foretages en designundersøgelse, med henblik på at finde et design der vil kunne implementeres i praksis. Efter at der er blevet udvalgt et design, bliver dette fremstillet, hvorefter det testes i DENEX's produktionen.

Ved test af værktøjet blev det konstateret, at det fundne design ikke var i stand til at fremstille brugbare patronhylstre, idet de blev revet over under strækningsreduktionsprocessen

Table of contents

| | |
|--|------------|
| Danish abstract | vii |
| Nomenclature | 1 |
| Chapter 1 Introduction | 3 |
| 1.1 Company profile and case | 3 |
| 1.2 Production of cartridge cases | 4 |
| 1.3 Summery of preliminary work | 9 |
| 1.4 Problem statement | 16 |
| Chapter 2 Problem approach | 17 |
| 2.1 Investigation of CDL effects | 17 |
| 2.2 Determination of CDL design | 18 |
| 2.3 Process implementation of CDL dies..... | 18 |
| Chapter 3 The CDL design | 19 |
| 3.1 The CDL design concept | 19 |
| 3.2 Design of CDL dies | 22 |
| Chapter 4 Model modifications | 25 |
| 4.1 Geometric modifications | 25 |
| 4.2 Implementaion of punch deflection | 27 |
| Chapter 5 Investigation of CDL effects | 29 |
| 5.1 Investigation approach | 29 |
| 5.2 The CDL designs influence on the ironing process | 30 |
| 5.3 CDL performance when introducing a small die tilt | 39 |
| Chapter 6 Determination of CDL design | 43 |
| 6.1 Determination approach | 43 |
| 6.2 Evaluation of strains | 45 |
| 6.3 Inspection of process stability | 49 |
| 6.4 Design performance when introducing a small die tilt | 52 |
| Chapter 7 Evaluation of die implementation | 57 |
| 7.1 Process implementation of the CDL design | 57 |
| 7.2 Discussion of the CDL dies performance..... | 58 |
| Chapter 8 Conclusion | 61 |
| Chapter 9 Perspectives | 63 |
| List of Figures | 65 |

| | |
|---|----|
| List of Tables | 68 |
| Bibliography | 69 |
| Appendix A Drawings | |
| Appendix B Reading guide for chapter C and D | |
| Appendix C Initial investigation of CDL effects | |
| Appendix D Determination of final CDL radius | |
| Appendix E LS-Dyna model | |

Nomenclature

| Symbol | Explanation | Unit |
|-----------|---|--------------------------|
| α | Semi die angle | [°] |
| ρ | Density | [Tonne/mm ³] |
| ν | Poisson's ratio | [-] |
| a | Die tilt angle | [°] |
| $D_{i,n}$ | Inner diameter after the n th draw, n=0..3 | [mm] |
| $D_{o,n}$ | Outer diameter after the n th draw, n=0..3 | [mm] |
| E | Young's modulus | [MPa] |
| FD | Dynamic coefficient of friction | [-] |
| FS | Static coefficient of friction | [-] |
| h_i | Initial cup height | [mm] |
| h_f | Final cup height | [mm] |
| h_n | Cartridge case height after the n th draw, n=1..3 | [mm] |
| K | Strength coefficient | [MPa] |
| L | Die land length | [mm] |
| n | Strain hardening exponent | [-] |
| P | Punch force | [N] |
| r_i | Inner cup radius | [mm] |
| $r_{o,f}$ | Final outer cup radius | [mm] |
| $r_{o,i}$ | Initial outer cup radius | [mm] |
| t_f | Final wall thickness | [mm] |
| t_i | Initial wall thickness | [mm] |
| t_n | Cartridge case thickness after the n th draw, n=1..3 | [mm] |
| VC | Viscous coefficient of friction | [-] |

Chapter 3

| | | |
|---------------|---|------|
| a | Die tilt angle | [°] |
| $D_{car,o}$ | Outer cartridge diameter | [mm] |
| $D_{die,i}$ | Inner die diameter | [mm] |
| F_{total} | Total radial force | [N] |
| $F_{DieLand}$ | Radial force at the die land | [N] |
| $F_{conical}$ | Radial force at the conical part of the die | [N] |
| g_{tilt} | Contact gap introduced by die tilt | [mm] |
| h_{die} | Die height | [mm] |
| h_{tilt} | Die tilt height | [mm] |
| L | Die land length | [mm] |
| L_{top} | Minimum length of die core top surface | [mm] |
| r_{cdl} | Circular die land radius | [mm] |

Continued on next page...

...Continued from previous page

| Symbol | Explanation | Unit |
|------------------|---|------|
| $r_{cdl,max}$ | Maximum CDL radius | [mm] |
| $r_{cdl,min}$ | Minimum CDL radius | [mm] |
| SC_{inlet} | Safety clearance | [mm] |
| Chapter 5 | | |
| α | Inlet angle | [°] |
| Δh | Cartridge case height difference | [mm] |
| $F_{friction}$ | Friction force between the cartridge case and the punch | [N] |
| F_n | Normal force | [N] |
| F_{nose} | Force transmitted through the cartridge case nose | [N] |
| F_{punch} | Punch force | [N] |
| F_x | x-force | [N] |
| F_y | y-force | [N] |
| F_z | z-force | [N] |
| r_{cdl} | Circular die land radius | [mm] |
| t | Time | [s] |
| Chapter 6 | | |
| Δh | Cartridge case height difference | [mm] |
| ε | Strain | [-] |
| F_z | z-force | [N] |
| r_{cdl} | Circular die land radius | [mm] |

Introduction

1

This project is made as a continuation of the work and conclusions made by the author in [Pedersen, 2016] at the 9th semester of the master program in manufacturing engineering at Aalborg university. As well as for the previous work, this project is made in collaboration with DENEX, who have provided a case for a product and a process which is in their interest to get analysed with regards to optimization of process stability. This chapter will thereby first contain an introduction to the company, the case and the process, whereafter important aspects and conclusions from the previous project will be presented. Note that it will only be a brief introduction to the company, the case and process, since these are already described in [Pedersen, 2016].

1.1 Company profile and case

DENEX is an Elling based company that produces and develops ammunition, pyrotechnics and explosives. The company tracks back to the year 1676, where they were founded as ammunition supplier for the Danish armed forces. Today they are a part of the MAXAM corporations defence business unit EXPAL.

The product which DENEX have provided as case is the 5.56mm NATO cartridge, see figure 1.1, with focus on the ironing process of the cartridge case. The 5.56mm NATO cartridge is one of DENEX's high volume activities, with a production capability of 200000 cartridges a day, hence even small improvements of the product or the processes have the potential of providing notable impact. When having focus on the ironing process, the desired improvements is to maximise material utilization i.e reduced the amount of material scrapped due to cut off, and to extend the tool life expectancy by reducing wear.



Figure 1.1. 5.56mm NATO cartridge

1.2 Production of cartridge cases

The 5.56mm NATO cartridge case is a small arms calibre cartridge that is used in weapons as the M/10 rifle, which is the standard weapon for the Danish armed forces. The terminology for the components composing a cartridge can be seen at figure 1.2, along with the terminologies for the cartridge case.

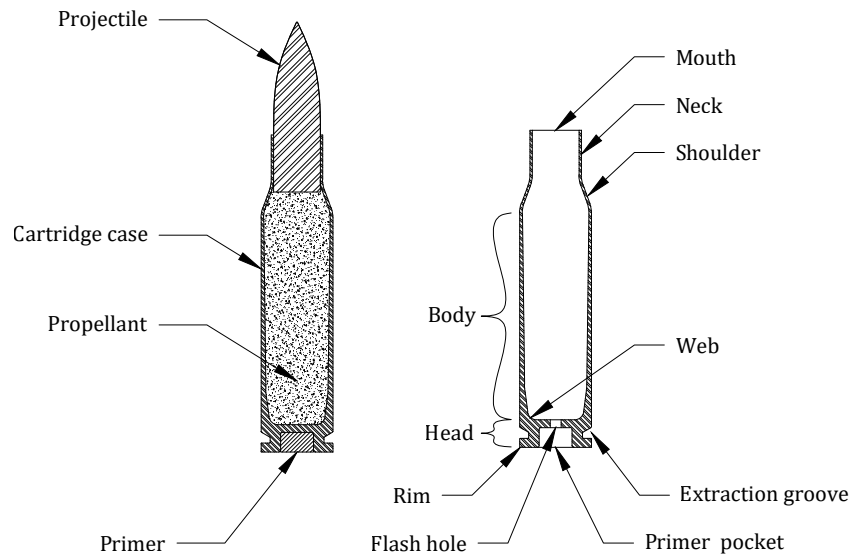


Figure 1.2. Cartridge terminology

When producing the cartridge case, the production can be divided into 6 stages:

1. Blanking, deep drawing and annealing
2. Ironing and clipping
3. Annealing and washing
4. Forming of the primer pocket, punching of the flash hole, and tapering
5. Cutting of extraction groove
6. Mouth and neck annealing, pickling and washing

When produced at DENEX, the first stage with blanking, deep drawing and annealing is performed by an external supplier i.e the in-house manufacturing process of the cartridge cases starts at the ironing stage.

In the following a description of the ironing process will be presented, followed by a description of the setup used for the cartridge cases. The remaining operations on the cartridge will not be described further due to that ironing process being the process of interest.

1.2.1 Ironing

Ironing is a cold forming process used for thickness reduction and elongation of the cup wall on pre-produced cups. At figure 1.3, an example of a basic ironing setup is illustrated before, during, and after performing the ironing operation.

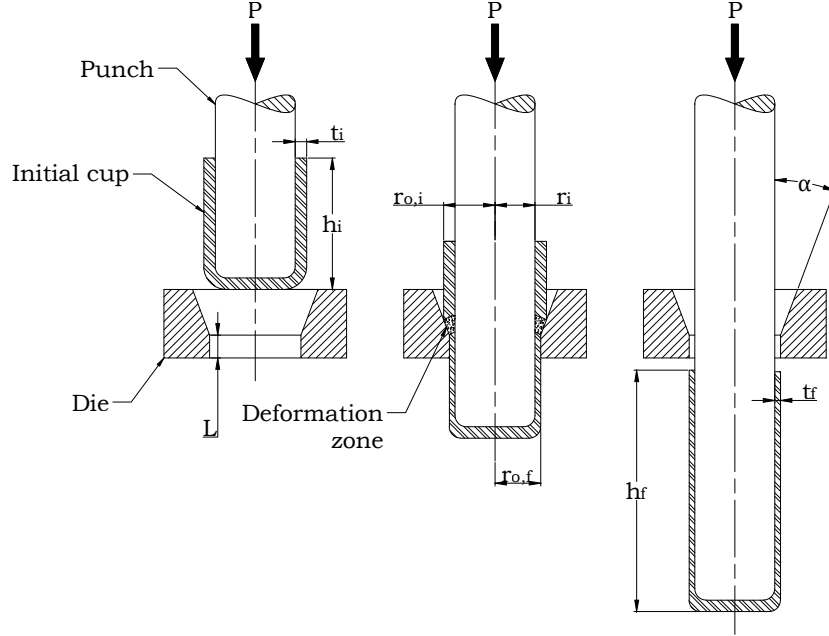


Figure 1.3. Basic ironing setup, based on figure 11.5 and 11.6 in [Avitzur, 1983]

Where:

| | | | |
|----------|--------------------|-----------|--------------------------|
| α | Semi die angle | r_i | Inner cup radius |
| h_f | Final cup height | $r_{o,f}$ | Final outer cup radius |
| h_i | initial cup height | $r_{o,i}$ | Initial outer cup radius |
| L | Die land length | t_f | Final wall thickness |
| P | Punch force | t_i | Initial wall thickness |

As seen at figure 1.3 does the setup consist of a pre-drawn cup, a punch, and a die, where the punch forces the pre-produced cup through the die. By having a die radius, R_f smaller than the outer cup radius, R_o , the wall thickness of the cup is reduced from the initial thickness, t_i , to the final thickness, t_f , and the cup is elongated from having the initial height, h_i , to the final height, h_f .

When reducing the wall thickness the reduction ratio is defined as [Danckert, 2005]:

$$\text{Reduction ratio [\%]} = \frac{t_i - t_f}{t_i} \cdot 100 \quad (1.1)$$

The amount of reduction that a cup can be subjected to without introducing instability to the process, is defined by a the maximum reduction ratio, which is a result of both depended and independent process variables:

- Independent variables:
 - Die land length, L
 - Semi-cone angle, α
 - Material properties
- Dependent variables:
 - Friction
 - * Lubrication
 - * Temperature
 - * Surface roughness
 - * Material properties
 - * Drawing speed

By choosing a proper set of process variables is it theoretically possible to obtain an unlimited reduction ratio, though in praxis the maximum reduction ratio is limited to 50% when using a single die [Avitzur, 1983].

1.2.2 Ironing of cartridge cases

The ironing process of cartridge cases at DENEX is performed on a New Lachaussee 702 horizontal transfer cartridge case press, see figure 1.4, with two parallel tool groups and a total capacity of 90 cartridge cases pr. minute.



Figure 1.4. New Lachaussee 702 cartridge case press [New Lachaussee, 2017]

The tool setup used at each of the tool groups consist of five stations that are connect by a transfer system which transports the cartridge cases sequentially. The stations composing each tool group are:

1. Feeding station
2. Ironing station 1
3. Ironing station 2
4. Ironing station 3
5. Clipping station

At ironing station 1 and 2 a stacked tool design is used when performing the ironing operation i.e the cartridge cases are drawn trough two dies by the same punch stroke, whereas only a single die is used at ironing station 3. At figure 1.5 a simplified sketch of the stations composing each tool group are illustrated.

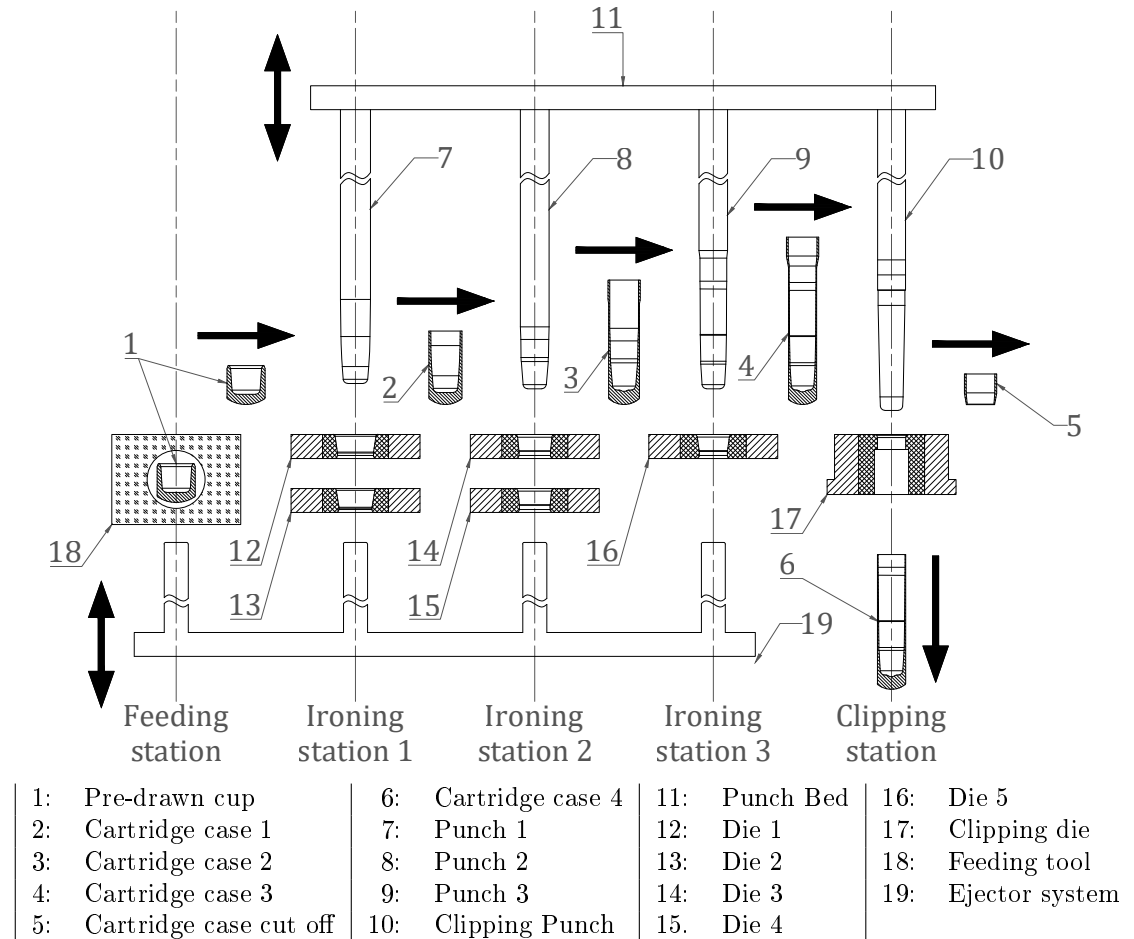


Figure 1.5. Simplified illustration of the ironing setup for 5.56mm cartridge cases

From figure 1.5 can it be seen that the pre-drawn cup (1) enters the tool group at the feeding station, from where the ejector system pushes it into the transfer system which transfers it to ironing station 1. Note that the transfer system is not included at the sketch. When the pre-drawn cup is placed at ironing station 1, punch 1 (7) draws it through the two first dies (12) and (13). After being drawn through the dies, the ejector system pushes the drawn cartridge case (2) back through the dies to the transfer system, where it is transported to ironing station 2. Ironing station 2 and 3 follows the same procedure as for ironing station 1. At the clipping station the collar of the cartridge case is cut off, leaving the cartridge case at the desired length. This process is done by having a sharp rim at the punch with the same diameter as the clipping die. When the cartridge case (6) have passed through the clipping die, it is not pushed back trough the die by the ejector system, but pushed forward to a accumulation container by the subsequent cartridge cases. After ended clipping operation the cut off drops down onto a conveyor, transporting it to a scrap deposit. It have to be noted that the punches (7), (8) and (9) are attached to the same

punch bed (11), driven by a crankshaft, and thereby performs their drawing operations simultaneously. The movement of the punches and both the transfer and ejector system are linked and thereby concludes a continuous processing of the cartridge cases. In regards to lubrication, each station is supplied with a continues flow of lubricant, in order to ensure consistent lubrication and cooling of the cartridge cases.

1.2.3 Cartridge case specifications

From the technical documentation provided for the cartridge cases, the following informations are derived, see figure 1.6 and table 1.1.

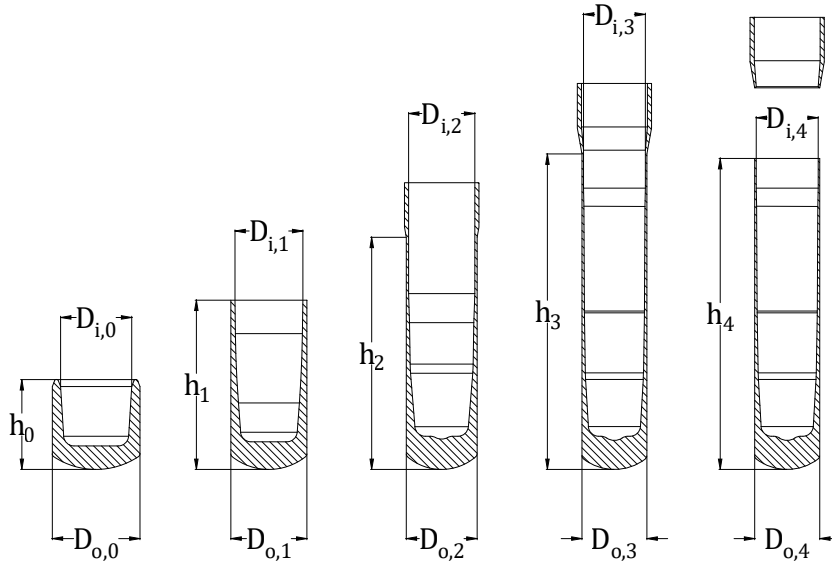


Figure 1.6. 5.56mm cartridge case specifications

The dimensions displayed at figure 1.6 and specified at table 1.1 are derived from the technical documentation provided by DENEX. The dimensions for the drawing height, h_n , and the outer diameter, $D_{o,n}$, can be directly read in the technical documentation, whereas the inner diameter, $D_{i,n}$ is not specified. The inner diameter, $D_{i,n}$, of the cartridge case top is derived using information of the cartridge case height and bottom thickness along with the respective punch dimensions. It have to be noted that the reduction ratios displayed in table 1.1 are for the thinnest point at the cartridge cases i.e. at the drawing height, h_n .

| | | Initial cup | 1 st draw | 2 nd draw | 3 rd draw | Clipping | Total |
|--------------------------------|------|-------------|----------------------|----------------------|----------------------|----------|--------|
| Cartridge number, n | | 0 | 1 | 2 | 3 | 4 | - |
| Outer diameter, $D_{o,n}$ | [mm] | 12.60 | 11.00 | 10.25 | 9.40 | 9.40 | - |
| Outer diameter reduction | [%] | - | 12.7 | 6.82 | 8.29 | 0 | 25.40 |
| Inner diameter, $D_{i,n}$ | [mm] | 10.30 | 9.81 | 9.58 | 8.96 | 8.96 | - |
| Inner diameter reduction ratio | [%] | 0 | 4.72 | 2.38 | 6.47 | 0 | 13.01 |
| Thickness, t_n | [mm] | 1.15 | 0.59 | 0.34 | 0.22 | 0.22 | - |
| Thickness reduction ratio | [%] | - | 48.44 | 43.51 | 34.33 | 0 | 80.87 |
| Drawing height, h_n | [mm] | 13.00 | 24.50 | 33.60 | 45.65 | 45.00 | - |
| Height elongation | [%] | - | 88.46 | 37.14 | 5.86 | - | 246.15 |

Table 1.1. 5.56mm cartridge case specifications

In regards to material, the cartridge cases are made of CuZn30 cartridge brass, where the initial cup have a weight of 7.2g. After the clipping process the cartridge case have a weight of 6.2g, i.e. 1g of material is processed as scrap due to the cut off. Considering that 45 million 5.56mm cartridges are produced annually, this results in 4.5 tonnes of brass returned as scrap.

1.3 Summery of preliminary work

As mentioned above is this project a continuation of the work conducted in [Pedersen, 2016], which main focus was to construct a LS-Dyna FEA model for simulating the ironing process of cartridge cases. It have to be noted that the regarded cartridge in [Pedersen, 2016] was the 7.62mm NATO cartridge, whereas this project deals with the 5.56mm NATO cartridge. Though the model dealt with a different cartridge case the production setup and procedures remains, hence only the cartridge case dimensions are different.

The problems statements that was regarded were:

1. How can a LS-Dyna model, representing the ironing process for 7.62mm NATO cartridge cases at DENEX, be constructed, so it provides a sufficient accuracy compared to the components produced at DENEX?
2. Are there any issues in regards to the ironing process, that influences the quality off the components, and can the LS-Dyna model be used for determining a possible cause for these issues?

For answering the problems listed above, three main topics were regarded:

1. Construction of the FEA ironing model
2. Validation of the FEA ironing model
3. Investigation of process issues

In the following, a summery of these three topic will be given, elaborating on major aspects and conclusions.

1.3.1 Construction of the FEA ironing model

For simulating the ironing process of 7.62mm NATO cartridge cases, a 3D model was developed for the FEA software LS-Dyna. In order to make a model where a simulation could be terminated within a reasonable time frame the following simplifications were introduced:

- Only components essential to the ironing process were included:
 - Cartridge case
 - Punch
 - Die cores
- Symmetry conditions were applied, reducing the model to a quarter of the process's physical extent
- The ejector system was neglected, thereby excluding the cartridge cases back travel through the dies after ended draw

At figure 1.7 the geometric representation of station 1 is illustrated when using these simplification for the representation of the ironing process. Besides the dimensions of the tools, the representation is identical for station 2 and 3.

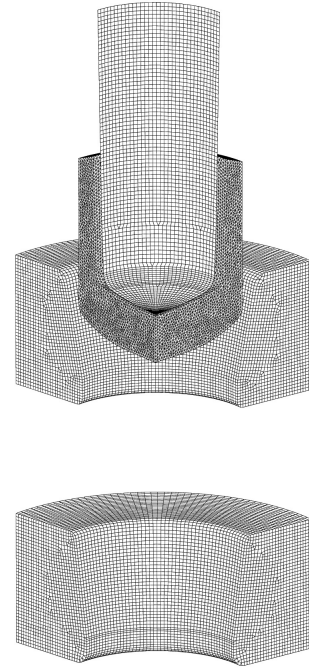


Figure 1.7. Simplified ironing model

The general settings and parameters used for the model is displayed in table 1.2 along with the settings and parameters for the cartridge case and the tools.

| General parameters and settings | | | |
|---|-------------------------------|-----------------------|------------------|
| Time integration type | Explicit | | |
| Termination time [s] | 0.0288 | | |
| Time step size | $5E - 7$ | | |
| Mass scaling ratio | 249 | | |
| Contact formulation | CONSTRAINT_SURFACE_TO_SURFACE | | |
| Remeshing frequency [s] | 0.00576 | | |
| FS | 0.10 | | |
| FD | 0.08 | | |
| VS | $\frac{50MPa}{\sqrt{3}}$ | | |
| Cartridge case and tool parameters and settings | | | |
| | Cartridge case | Dies | Punch |
| Element format | Solid tetrahedron | Solid hexagon | shell |
| Element formulation | 13 | 1 | 1 |
| No. elements | $\approx 1.9E05$ | $\approx 5E04$ (each) | $\approx 2.3E04$ |
| Material | Brass, CuZn30 | Tungsten Carbide | Steel |
| Material model | POWER_LAW_PLASTICITY | ELASTIC | RIGID |
| Density, ρ , [$\frac{tonne}{mm^3}$] | 8.53E-9 | 15.5E-9 | 7.85E-9 |
| Young's modulus, E, [GPa] | 110 | 650 | 206 |
| Poissons ratio, ν | 0.35 | 0.2 | 0.3 |
| Strain hardening exponent, n | 0.49 | - | - |
| Strength coefficient, K , [MPa] | 860 | - | - |

Table 1.2. Model parameters and settings

It have to be noted that the parameters and settings listed above are for station 1. The settings for station 2 and 3 are similar to those for station 1, only with small changes in the termination time, mass scaling ratio, and number of elements in the tools.

At figure 1.8 the cartridge case output for each of the ironing stations is displayed with their respective effective plastic strain.

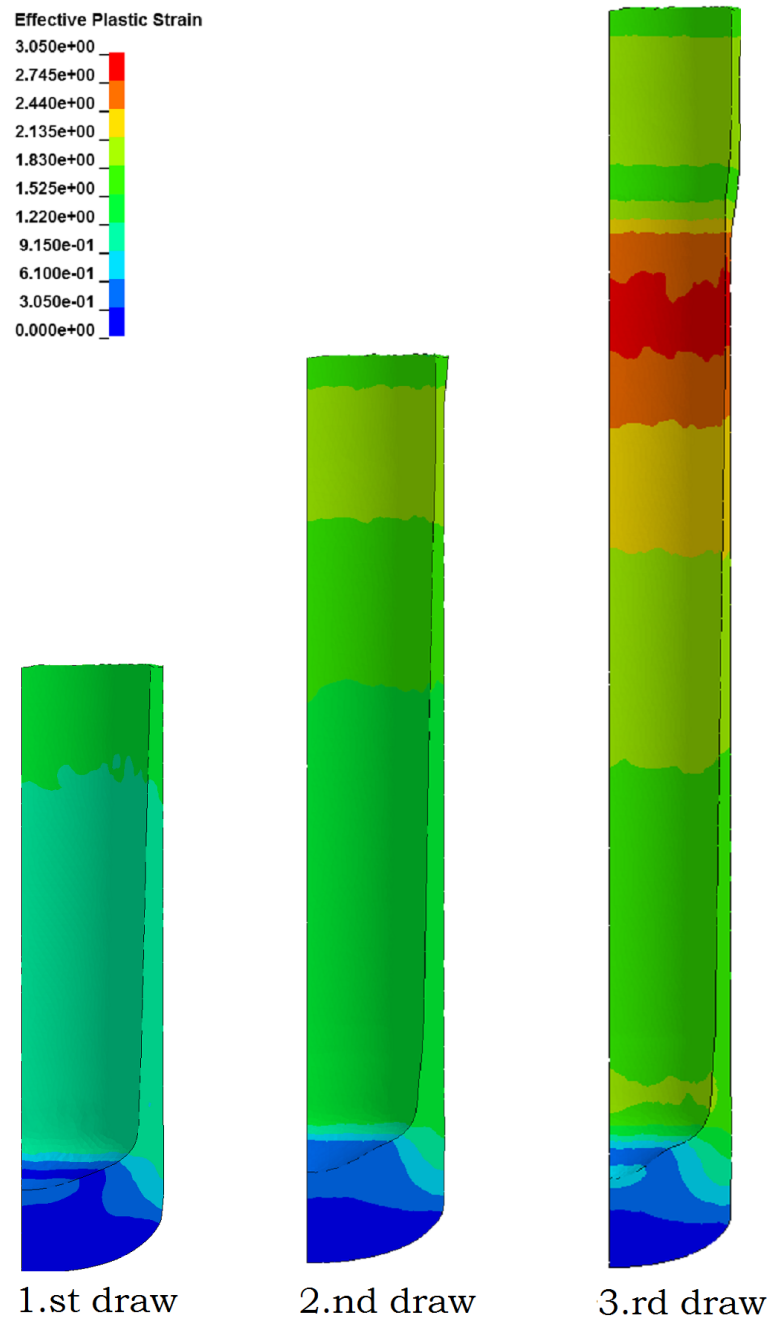


Figure 1.8. Output cartridges for ironing station 1, 2 and 3

In regards to the method used for handling the simulation of a process that consists of multiple operations, the used approach for the model is displayed at figure 1.9. From the figure can it be seen that a model of the pre-draw cup is loaded into LS-Dyna along with models for the tools, station specific parameters and setting and the global settings for the simulations. After ended simulation the results are processed by LS-PrePost, that outputs a model of the drawn cartridge case's geometry, element stresses and strains. The new model for the cartridge case is then processed to the input for station 2 which follows the same procedure as for station 1. The same operations are conducted for station 3 which likewise after ended simulations outputs the final model and result of the simulated ironing sequence.

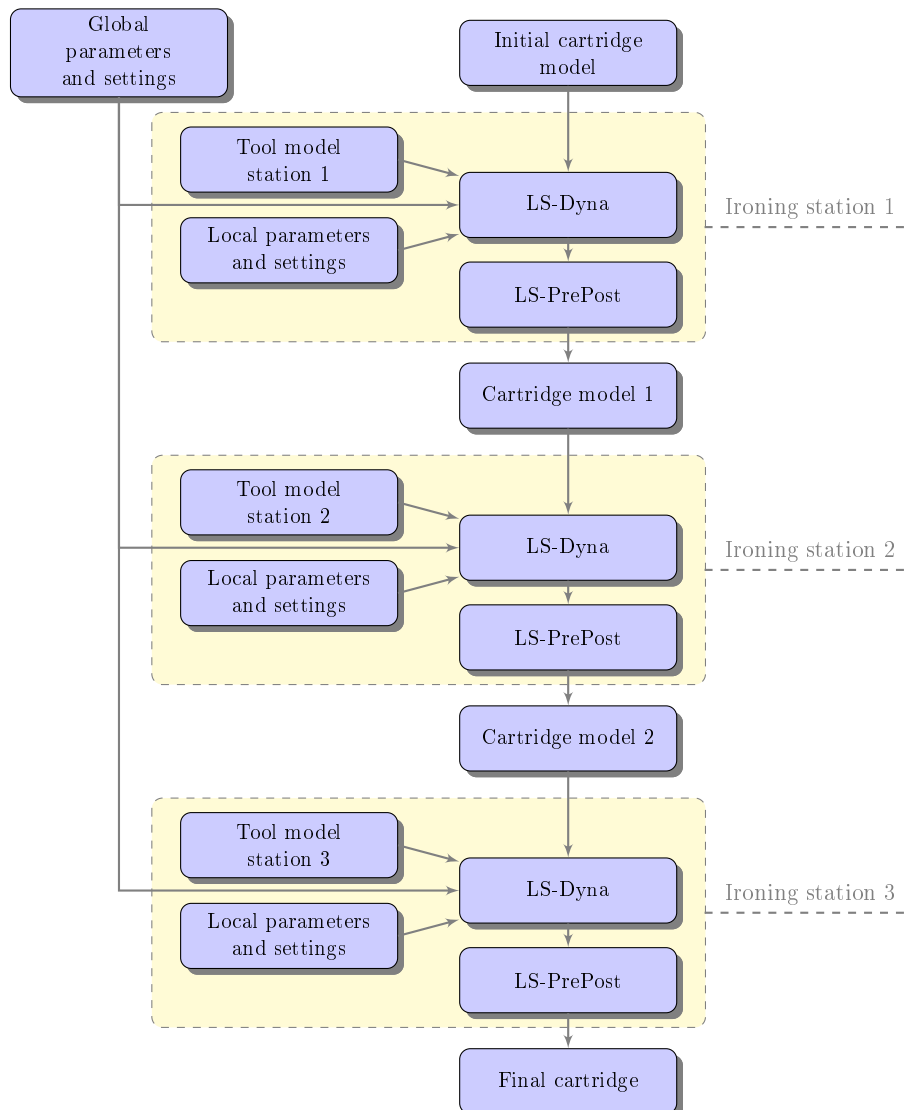


Figure 1.9. Approach for multi-station ironing simulation

1.3.2 Validation of the FEA ironing model

In order to determine if the model provided a sufficient accuracy compared to the cartridge cases produced at DENEX, the wall thickness from the simulated cartridge cases was evaluated in regards to the wall thickness of the manufactured cartridge cases. Figure 1.10 shows the thickness's of the cartridge case after ended draw at each of the three ironing stations, for both the simulated ironing sequence and the manufactured cartridge cases at each of the two tool groups on the press.

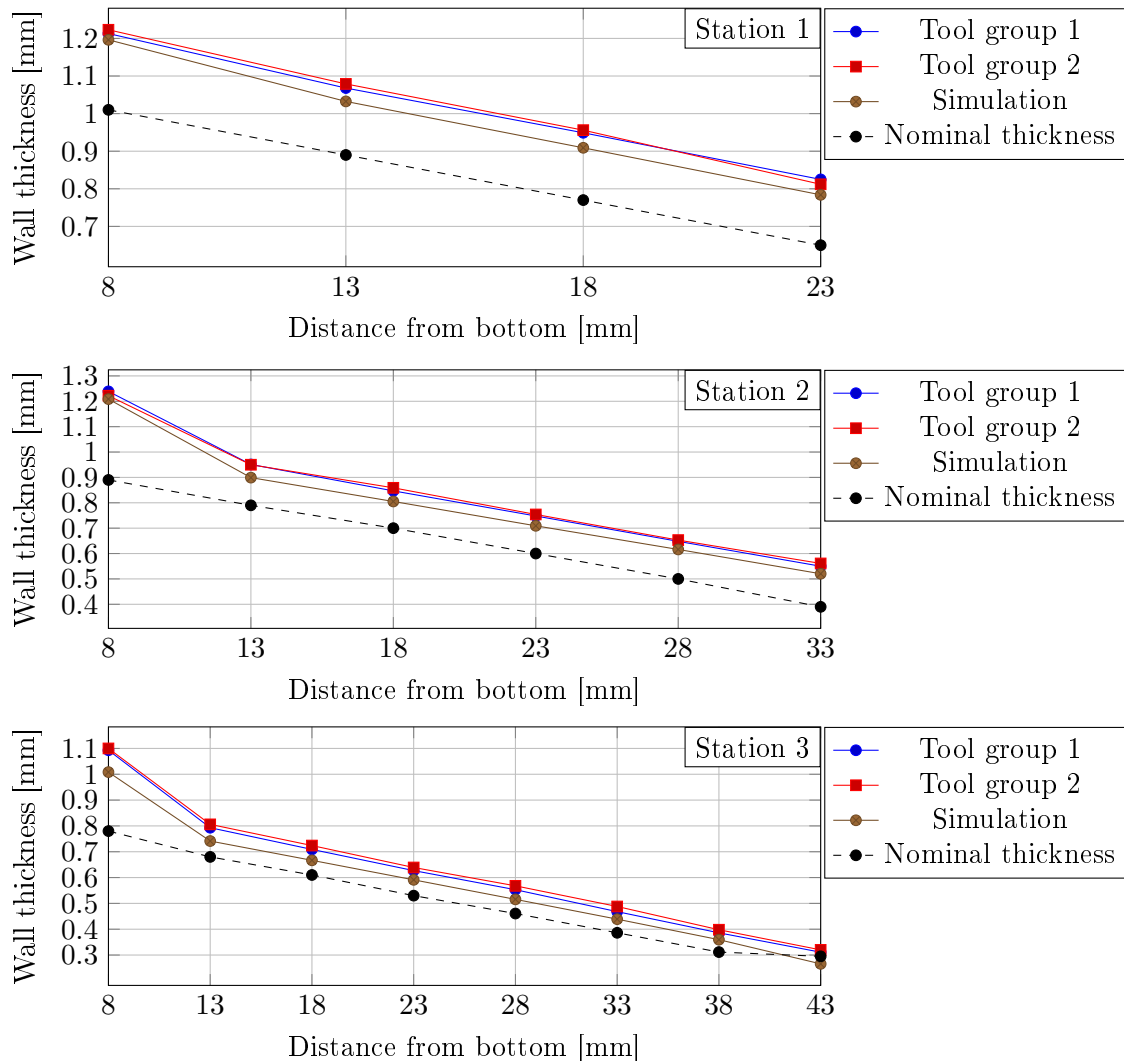


Figure 1.10. Evaluation of model accuracy

In order to determine if the model provided a sufficient accuracy compared to the manufactured cartridge cases, a success criterion was established, specifying that the wall thickness gained from the simulations should be within the boundaries formed by manufactured cartridge cases, and the nominal thickness obtain from the technical documentation for the cartridge cases, see figure 1.10. Furthermore was it specified that the development of wall thickness profile should be similar to the one for the manufactured cartridge cases. Based on these requirement was is concluded that the model provided a sufficient accuracy.

1.3.3 Investigation of process issues

For the investigation of process issues, a visual inspection was conducted on the manufactured cartridge cases, see figure 1.11.

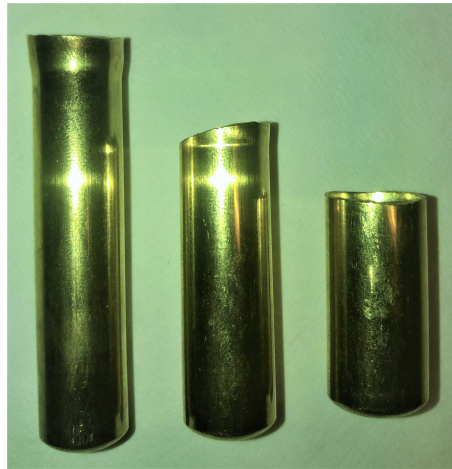


Figure 1.11. Visual inspection of the manufactured cartridge cases

From the inspection was it concluded that the cartridge cases was subjected to an issue regarding a skewness in the cup height. This effect represents an issue since it is an indication of having a non uniform wall thickness distribution. Furthermore does a reduction of the skewness introduce a possible cost reduction, since a more uniform height will reduce the amount of material needed for the cut-off, thereby allowing less material in the initial cup.

For the investigation of this issue was two scenarios investigated:

1. An initial eccentric alignment of the cartridge case, compared to the alignment of the dies, see figure 1.12
2. Presence of a small tilt of the dies, due to inaccurate manufacturing or mounting in the press, see figure 1.13

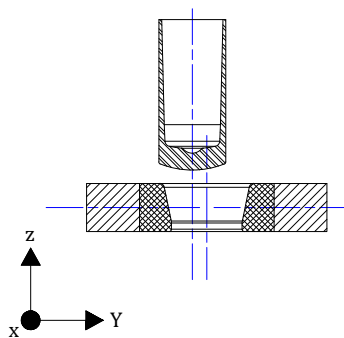


Figure 1.12. Eccentric alignment of the cartridge case

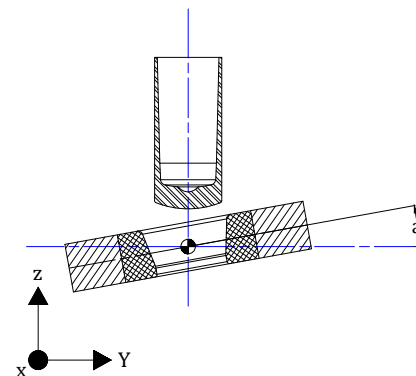


Figure 1.13. Die tilt

For the investigation, the two scenarios were implemented individually to the model and tested. In the first scenario a 0.1mm offset in the y-direction was considered, and it was concluded that the eccentric alignment did not present a notable issue, since the dies

conical inlet provides a centring effect of the cartridge case. For the second scenario, three sub-scenarios was constructed, where the all the dies was subjected to a die tilt of with a consistent die tilt of 0.05° , 0.15° and 0.25° , respectively. From these investigations was it concluded, that even small tilts of the dies had a notable effect in regards to introducing skewness to the cartridge case height, see figure 1.14.

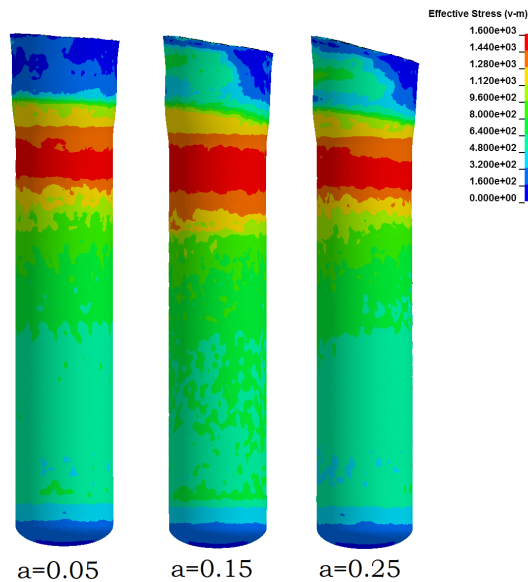


Figure 1.14. Results of tilt scenarios

1.3.4 Conclusion and continuation of the preliminary work

By regarding the topics presented in section 1.3.1, 1.3.2 and 1.3.3, in respect to the problems presented in section 1.3, was it concluded that a FEA model of the ironing process had been constructed in way that provided sufficient accuracy in regards to the manufactured cartridge cases, and that an issue regarding skewness of the cartridge case height was present, where a possible cause could be linked to a small tilt of the dies.

After concluding the project, possibilities for future work on the process was discussed. One of the possible directions that were discussed was to make further investigation of the stability issue introduced by a die tilt. Here it was introduced that the work conducted in [Danckert, 2005] shows that implementing a die design with a circular die land to the ironing process has a stabilizing effect on the issues caused by a tilted die.

1.4 Problem statement

As mentioned in section 1.3.4 does the work conducted in [Danckert, 2005] state that introducing a die design with a circular die land (CDL) have stabilizing effect on the ironing process in regards to the effects introduces by having dies subjected to a small tilt. In collaboration with DENEX is it decided to investigate if implementing the CDL design to the ironing process of 5.56mm NATO cartridge cases have a stabilizing effect in regards to minimizing the skewness of the cartridge case height, and how the CDL design otherwise affects the process. In order to test the effects of the CDL design outside a numerical environment, has DENEX agreed to aid in manufacturing and implementing of a set of CDL dies.

Thereby, the following problem statements are constructed:

Which effects does the implementation of a circular die land design have on the ironing process of 5.56mm NATO cartridge cases?

What would be a suitable die design for the test and implementation of the circular die land design to the process?

How does the circular die land design perform when implemented to the production setup at DENEX?

Problem approach 2

As described in 1.4, three problems are formulated as objective for the project. The topics of these three problems can be describes as: investigation of CDL effects, determination of CDL design, and die implementation. This chapter will regard how each of these problems are approached, thereby providing an introduction to the following chapters.

2.1 Investigation of CDL effects

The first problem statement formulated in section 1.4, regards which effects an implementation of the CDL design have on the ironing process of 5.56mm NATO cartridge case. In order to make this investigation, it is first necessary to elaborate on why the implementation of the CDL design have an stabilizing on the ironing process. Secondly, in order to investigate the CDL designs effects on the 5.56mm cartridge cases, is it necessary to establish a design space for the CDL design when implemented to this specific ironing process. The elaboration on the CDL designs stabilizing effects and the die designs design space is be presented in chapter 3, section 3.1 and 3.2, respectively.

For the means of investigating the CDL designs effect on the ironing process, is the LS-Dyna model developed in [Pedersen, 2016] modified to represent the ironing process of 5.56mm NATO cartridge cases instead of the 7.62mm NATO cartridge cases. Along with the changes in the part and tool geometries, is a series of additional features required for the investigation implemented to the model. The modifications introduced to the model is described in chapter 4. It have to be noted that when introducing the modification to the model, is it assumed that the model still provides representative results for the cartridge case ironing process, and thereby is no further work be conducted in order to test the model accuracy.

After modifying the LS-Dyna model is the investigation of the CDL designs effect on the ironing process conducted by implementing the design to a single die in the setup, wherafter the results are evaluated. After evaluating the designs influence on the process is the designs assumed stabilizing effects on a die tilt investigated. Besides using the observations to determine the effects of using the CDL design, the results will be used as an indication for where in CDL designs design space the further determination of a CDL design should be conducted. The investigation of the CDL designs effects is presented in chapter 5.

2.2 Determination of CDL design

For the determination of a suitable CDL design for the implementation in the process setup at DENEX, the results from the investigation of the CDL designs effects in chapter 5, will be used as indication for where within the CDL dies design space to conduct the investigation. From this, a series of different designs are constructed in the selected area of the design space, and subjected to different tilt scenarios using the LS-Dyna model. By evaluating the results, the design assessed to provide the best trade-off between the CDL effects and process stability is chosen. The determination of the CDL die design will be presented in chapter 6, whereas the technical documentation for the chosen dies can be seen in appendix A

2.3 Process implementation of CDL dies

In order to test how the CDL design performs when implemented to the ironing setup at DENEX, is the die design determined in 6 manufactured. When implementing the design to the ironing setup, the approach depends of the outcome obtained by using the CDL dies. If the CDL dies conclude produces conforming part, the obtained cartridge case will be measured in order to evaluate the quality of the produced cartridges and the CDL design assumed stabilizing effect on the process. If the implementation of the CDL dies does not conclude a successful ironing sequence, will the observations and obtained cartridge cases be evaluated in regards to determining a cause for the CDL designs failure. The evaluation of implementing the CDL design to the ironing process is presented in chapter 7.

The CDL design 3

In this chapter, the concept behind introducing a die design with a circular die land is presented, along with an explanation of why this design approach has a stabilizing effect on the ironing process. After the CDL concept has been explained, the design space for the dies used in the ironing process of 5.56mm NATO cartridge cases is determined.

3.1 The CDL design concept

The CDL design is a design concept for ironing dies, that in [Danckert, 2005] is shown to decrease the process sensitivity to stability issues caused by having dies subjected to a small tilt, which is a result of inaccurate machining or mounting. At figure 3.1 an example of a CDL die design is shown next to a conventional die design.

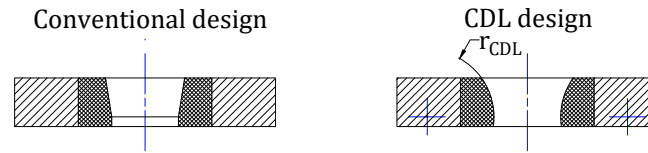


Figure 3.1. Conventional and CDL die design

In order to elaborate on the CDL designs stabilizing effect on a small die tilt, it is first necessary to give an introduction to a die tilts effects on the process when using a conventional die design.

By considering a 2D example of the ironing process, the radial forces on each side of the die can be described as the sum of the forces acting on the die land and the conical inlet, where the magnitude of these forces are a function of the reduction radius, see figure 3.2 and 3.3.

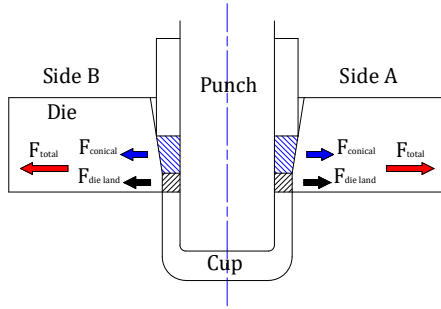


Figure 3.2. Radial forces on the die

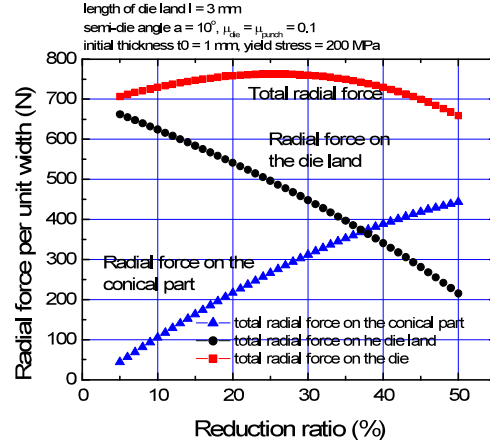


Figure 3.3. Radial force as function of reduction ratio [Danckert, 2005, figure 56]

When observing the ironing process at figure 3.2 and 3.3 in steady state, there have to be equilibrium between the radial forces at side A and B of the die, hence a process with equal conditions at each side of the die, die land length, semi-die angle, friction etc., yields the same reduction ratio for the cup wall at each side.

When introducing a small tilt to the die, the process conditions on the die changes due to contact loss between the cup and the die land at one side of the die, see figure 3.4 side A.

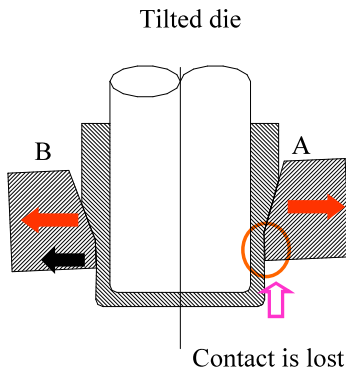
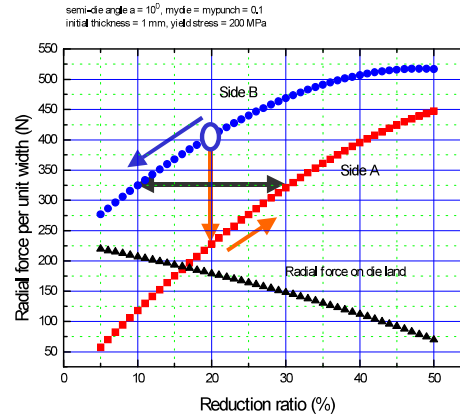


Figure 3.4. The effect on the radial forces introduced by a small die tilt [Danckert, 2005, figure 56]



By having a contact loss between the die land and the cup, the radial forces at side A are only composed by the radial forces on the conical part of the die, $F_{conical}$, hence a new equilibrium between the radial forces at side A and B have to be established. As seen on figure 3.4 this equilibrium is obtained by increasing the reduction ratio at side A while lowering it at side B, thereby resulting in a non-uniform wall thickness to the cup and a skewness to the cup height. The die tilt required to introduce the contact loss is theoretically infinitely small if elastic deformation of the die is neglected, hence only a small tilt of the die are required in order to result in the contact loss [Danckert, 2005].

For the investigation of the CDL designs effects and the determination of a CDL design in chapter 5 and 6, tilt scenarios are used, where the dies are subjected to a die tilt, a , at $a = 0.20^\circ$ and $a = 0.40^\circ$. At figure 3.5 and in table 3.1, the geometric effects of introducing the die tilt to the conventional die design are illustrated.

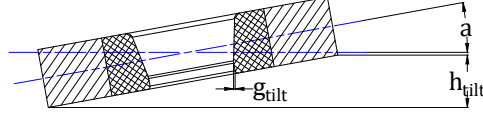


Figure 3.5. Geometric effects of introducing a die tilt

| a | h_{tilt} [mm] | g_{tilt} [mm] | | | | |
|--------------|-----------------|-----------------|--------|--------|--------|--------|
| | | Die 1 | Die 2 | Die 3 | Die 4 | Die 5 |
| 0.20° | 0.15 | 0.0030 | 0.0016 | 0.0049 | 0.0049 | 0.0048 |
| 0.40° | 0.30 | 0.0060 | 0.0031 | 0.0098 | 0.0098 | 0.0095 |

Table 3.1. Geometric effects of introducing a small die tilt

From the technical documentation for the dies is it given that the die land have a concentric tolerance zone at 0.005mm i.e it is possible to obtain the geometric effect equal to those for a 0.20° die tilt solely due to the tolerances in the manufacturing of the dies.

By introducing the CDL die design, the contact surface between the die and the cup have a circular profile, hence a small die tilt does not result in contact loss and thereby changes in the radial forces as seen for the conventional design at figure 3.4. At figure 3.6 the contact differences between the conventional and CDL design is illustrated when introducing a small die tilt. It have to be noted that the illustration displays the contact before equilibrium in the radial forces are established i.e. the cup have the same reduction ratio at both side A and B.

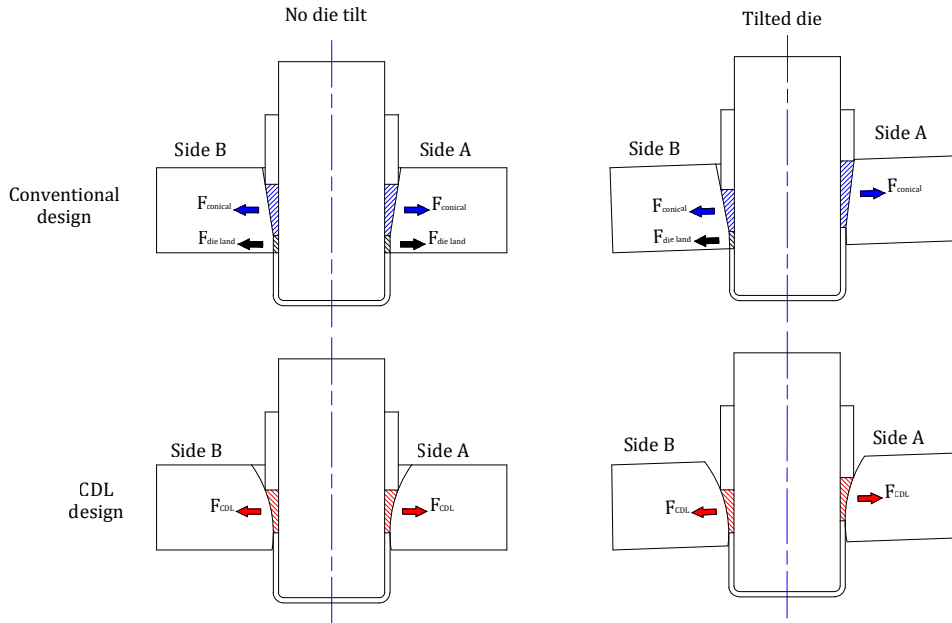


Figure 3.6. Comparison of conventional and CDL design when introducing a small die tilt

3.2 Design of CDL dies

In order to establish a design space for the CDL dies it is first necessary to determine the general outline for the new design. Since the scope of the project is to investigate and compare the effects of implementing the CDL design to an existing process, the governing geometric properties from the current die design will be transferred to the CDL design of the dies. The transferred geometries can be seen on figure 3.7 and are:

- Die height, h_{die}
- Outer diameter of the die cores, $D_{die,o}$
- Inner die diameter, $D_{die,i}$, i.e. no changes are made to the reduction ratios.
- The die land length, L , is used as an offset from the die bottom surface for the origin of the CDL radii

When having the general outline for the new die design it is possible to establish a set of boundaries for the dies die land radius, r_{cdl} i.e. the design space can be determined. The boundaries exist in the form of a minimum and a maximum die land radius for each die.

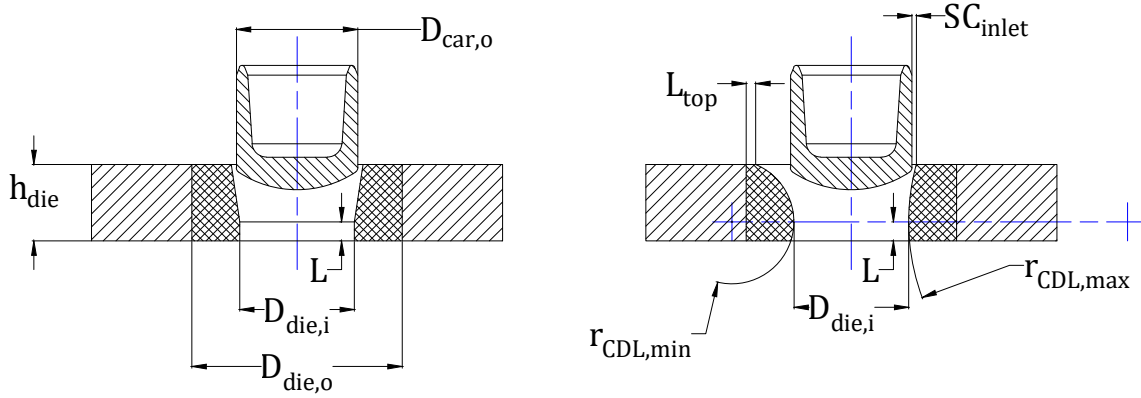


Figure 3.7. Design of CDL dies

Where:

| | | | |
|-------------|----------------------------|---------------|--|
| $D_{car,o}$ | Outer cartridge diameter | L_{top} | Minimum length of die core top surface |
| $D_{die,i}$ | Inner die diameter | $r_{cdl,max}$ | Maximum CDL radius |
| $D_{die,o}$ | Outer diameter of die core | $r_{cdl,min}$ | Minimum CDL radius |
| h_{die} | Die height | sc_{inlet} | Safety clearance |
| L | Die land length | | |

3.2.1 Minimum die land radius:

When determining the minimum radii for the CDL design, two conditions have to be satisfied. The first condition is that the die land radius have to be larger than the distance from the die lands horizontal centreline, see figure 3.7, to the top surface of the die:

$$r_{cdl,min} \geq h_{die} - L \quad (3.1)$$

This requirement is made in order to make sure that the circular die land intersects with the top surface at the die.

The second requirement for minimum CDL radius is that there, as a minimum, has to be a given distance, L_{top} , between the inlet and the outer wall of the die core, see figure 3.7. The second condition can be described using the following formula:

$$r_{cdl,min} \geq \frac{(h_{die} - L)^2 + (\frac{1}{2} \cdot (D_{die,o} - D_{die,i}) - L_{top})^2}{D_{die,o} - D_{die,i} - 2 \cdot L_{top}} \quad (3.2)$$

This requirement is due to that the die cores are mounted in the outer die part using shrink fitting. It is assessed that having a minimum length of 1mm from the die cores outer wall to the inlet is sufficient in order to avoid interfering with the performance of the shrink fitting.

By calculating the minimum CDL radius for the two conditions, the results in table 3.2 are obtained. The minimum radius for each die is then the radius that satisfy both condition i.e. the largest value for condition 1 or 2.

| | Condition 1 [mm] | Condition 2 [mm] | $r_{cdl,min}$ [mm] |
|-------|------------------|------------------|--------------------|
| Die 1 | 6.00 | 6.50 | 6.50 |
| Die 2 | 6.40 | 6.80 | 6.80 |
| Die 3 | 5.50 | 5.56 | 5.56 |
| Die 4 | 5.50 | 5.54 | 5.54 |
| Die 5 | 5.50 | 5.50 | 5.50 |

Table 3.2. Minimum die land radii

3.2.2 Maximum die land radius:

The maximum radius for the CDL design is determined by the diameter of the cartridge case at arrival to the die. This is due to that the die's inlet diameter decreases with an increasing die land radius i.e if the die land radius exceeds a certain limit, the dies inlet diameter becomes smaller than the cartridges case's outer diameter. If introducing a safety clearance, SC_{inlet} , between the cartridge case and the inlet, the condition for the maximum die land radius, $r_{cdl,max}$, can be describes as:

$$r_{cdl,max} \leq \frac{(h_{die} - L)^2 + (\frac{1}{2} \cdot (D_{car,o} - D_{die,i}) + SC_{inlet})^2}{D_{car,o} - D_{die,i} + 2 \cdot SC_{inlet}} \quad (3.3)$$

By using a safety clearance between the cartridge case and the inlet of $SC_{inlet} = 0.5\text{mm}$, the following maximum radii's are obtained for the different dies:

| | $r_{cdl,max}$ [mm] |
|-------|--------------------|
| Die 1 | 22.90 |
| Die 2 | 20.98 |
| Die 3 | 20.54 |
| Die 4 | 24.51 |
| Die 5 | 16.81 |

Table 3.3. Maximum die land radii

3.2.3 Determination of design space

By having calculated the boundaries for the individual CDL dies die land radius, the design space for the individual dies can thereby be determined as:

| | Design space [mm] |
|-------|--------------------------------|
| Die 1 | $6.50 \leq r_{cdl} \leq 22.90$ |
| Die 2 | $6.80 \leq r_{cdl} \leq 20.98$ |
| Die 3 | $5.56 \leq r_{cdl} \leq 20.54$ |
| Die 4 | $5.54 \leq r_{cdl} \leq 24.51$ |
| Die 5 | $5.50 \leq r_{cdl} \leq 16.81$ |

Table 3.4. Design space for the CDL dies die land radius

Model modifications 4

In order to investigate the effects of implementing the CDL design to the ironing process of 5.56mm NATO cartridge cases, is it necessary to make modifications to the model developed in [Pedersen, 2016]. These modification is due to that the previous model was developed for the ironing of 7.62mm NATO cartridge cases in a setup where punch deflection was not considered, which is a necessary feature when investigation the consequences of a small die tilt. Thereby will this chapter concern both the geometric changes introduced to the model and the implementation of punch deflection. The LS-Dyna code for the modified ironing model can be seen in appendix E

4.1 Geometric modifications

For the conversion of the model representing the ironing of 7.62mm NATO cartridge cases, to a representation for the ironing process of 5.56mm NATO cartridge cases, for scenarios with a small die tilt, the following modification are introduced to the model:

- The dimensions for both the tools and the pre-drawn cup are changed to represent the geometries for the 5.56mm NATO cartridge case ironing process. The process setup and geometries are the same, hence only the dimensions are modified.
- The model is expanded to a 180° symmetrical representation, see figure 4.1, instead of a 90° representation. This is necessary in order obtained the effect on the radial forces and reduction ratio introduced by a die tilt as described in section 3.1.
- The element and material representation of the tools have been changed from using solid elements with an elastic material model, to being represented by shell elements and a material model for rigid materials, thereby removing elastic deformation of the tools from the model. At figure 4.1 the result of this simplification can can be seen when applied to station 1. This simplification is introduced both in order to reduces the number of factors influencing the simulation results when introducing a small die tilt, and to reduce the needed computational time needed for solving the simulations. By using this simplification is it assumed that changes in the radial forces, caused by a die tilt, only have a minor effect on the elastic deformation of the dies during the draw, thereby not interfering with the results in the investigation of the effects introduced by implementing the CDL design.

- The dies are divided into two parts, see figure 4.2, each representing a 90° cut of the 180° die representation. By implementing this feature it is possible to obtain a measurement for the radial forces acting on the die, by monitoring the x-forces acting on each die part. In regards to notation, the top die at each ironing station will forwardly be referred to as die 1 and the bottom die as die 2 in combination with the number of the ironing station e.g. die 4 will be referred to as die 1 at station 2. When referring to one of the two die parts composing each die, the parts are named in accordance to their x-position in regards to the models centreline e.g. die parts on the right side (in relation to the orientation on figure 4.2) are noted x^+ and the dies on the left part are noted x^- . Thereby the right part of die 1 will be noted die 1 x^+ and vice versa.

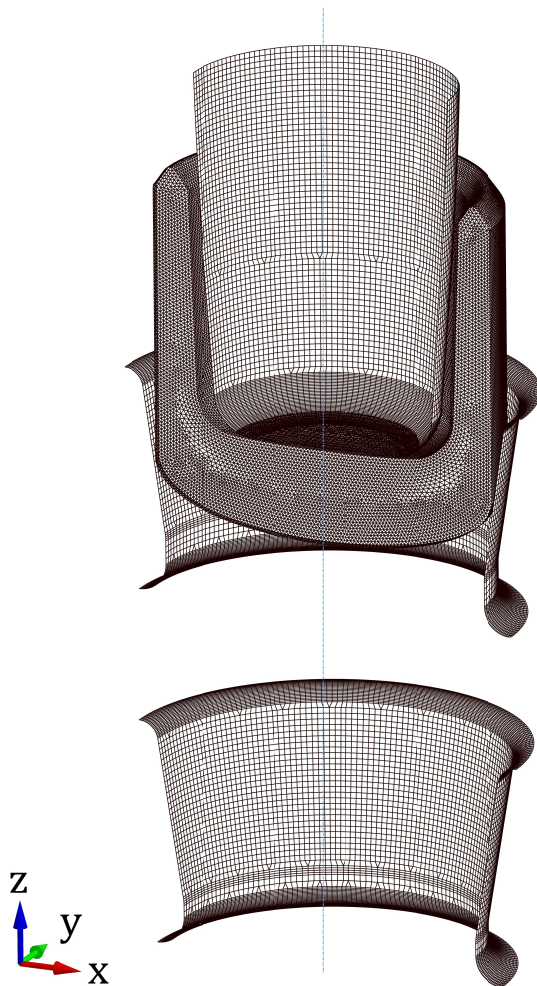


Figure 4.1. Geometric representation of ironing station 1

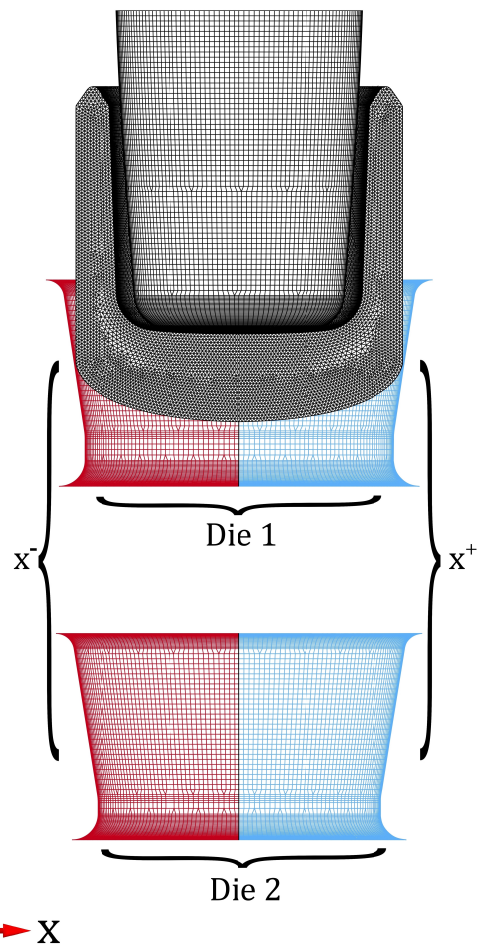


Figure 4.2. Die notation

4.2 Implementaion of punch deflection

As described in section 3.1 introduces a small die tilt changes to the radial force between the dies and the cartridge case, which results in a differentiated reduction ratio of the cartridge cases cup wall, hence either the punch is subjected to deflected or the dies are displaced, if mounted in a floating setup, in order to re-establish equilibrium between the radial forces.

A way to implement this behaviour to the model is to simulate the punch travel by moving the dies instead of the punch, and having a fully constrained punch, except for translation in the x-direction. Thereby are the tools in the model subjected to the constraints listed in table 4.1.

| Part | Constraints | |
|-------|---------------|------------|
| | Translational | Rotational |
| Punch | y z | x y z |
| Dies | x y | x y z |

Table 4.1. Applied constraints

When using this approach for implementing punch deflection is it important to note that the implementation is a simplified representation of punch deflection. This is due to that the punch have translational freedom in the x-direction and thereby is it not a contributing part in the force balance for the radial forces between the cartridge case and the dies.

A consequence of implementing punch deflection to the model, is that the contact formulation for contact between the cartridge case and the punch have to be switched to a penalty based formulation from the previously used constrained based formulations. This is due to that the constrained based contact formulation does not transmit forces to rigid bodies, hence no displacement of the punch will be obtained. When using a penalty based contact formulation, the contact forces are obtained by introducing a force penalty to nodes at the cartridge case that penetrates elements in the punch, hence small penetrations are present during the simulation. When using a penalty based contact formulation for a part that uses remeshing during the simulation i.e. the cartridge case, is it necessary enable the `soft` option for the contact formulation, since the simulation otherwise will crash due to registering initial penetration when restarting the simulation after the remeshing. When using the `soft` option, the initial penetration depth is used as offset for the following calculation of the contact forces. The consequence of using the `soft` option is that it has a cumulative effect on the penetration depth each time a remeshing is performed, thereby influencing the wall thickness and the reduction ratio. In order to minimize the effect of the `soft` option on the wall thickness, the amount of performed remeshings are reduced from five at each simulated ironing station to one at ironing station 1 and two, just before ended simulation. To compensate for the reduced amount of remeshings, the amount of elements composing the cartridge case have been increased from the $\approx 1.9E05$ elements used in the previous model to $\approx 6.2E05$ elements.

Investigation of the CDL designs effects on the ironing process

5

This chapter concerns the investigation of the effects an implementation of the CDL design to the LS-Dyna model have on the ironing process of 5.56mm NATO cartridge cases. For this purpose will this chapter first concern the approach used for the investigation, and secondly and evaluation of the observed effects the CDL design have on the ironing process when implemented to a single die. The evaluation of the CDL designs effects will firstly be conducted with focus on the designs general impact on the ironing process and secondly with focus on the stability issues caused by a small die tilt.

5.1 Investigation approach

For investigating which effects an implementation of the CDL design have on the ironing process of 5.56mm NATO cartridge cases, the used approach is firstly to test how the design affects the general performance of the process i.e how does the die design affect the process when no die tilt are present. After investigating the designs general effects on the ironing process, scenarios with the presence of a small die tilt is introduced, and the designs assumed stabilizing effect on the process is evaluated in comparison to the conventional die design.

In order to limit the expanse of the investigation, the following limitations are applied to the investigation:

- The effects are investigated by implementing the CDL design to a single die, and observing the effects when only drawing the cartridge case through that specific die. For the investigation the CDL design is implemented to die 2 at station 1. This is due to that when drawing the cartridge case through the dies at station 1 is it only in contact with one die at a time i.e the observed effects will only be a result of the regarded die. The reason for using die 2 is that die 1 is used for reducing the outer diameter of the cartridge case i.e. only a minor thickness reduction is obtained due to the initial gap between the cartridge and the punch, see figure 4.2 or 4.1.

- In order to determine the influence from the CDL radius, r_{cdl} , different radii within the design space for die 2 are implement. The considered radii are the upper and lower boundary of the design space for die 2 along with three radii equally positioned between the boundaries, see table 5.1.

$$r_{cdl} = [6.80\text{mm} \quad 10.34\text{mm} \quad 13.89\text{mm} \quad 17.44\text{mm} \quad 20.98\text{mm}]$$

Table 5.1. Implemented CDL radii

- For evaluating the stabilizing effects of the CDL design, two tilt scenarios are considered, where the die are subjected to a 0.20° and a 0.40° die tilt.

5.2 The CDL designs influence on the ironing process

In the following section, the effects of implementing the CDL design to die 2 at station 1 in the ironing process of 5.56mm NATO cartridge cases are evaluated. This will be done by observing and evaluating the effects the CDL design have on the process, and how the use of different CDL radii affects the process. For evaluating the effects, the following topics will be regarded:

- Cartridge cases effective plastic strain
- Force observations
- Contact pressure
- Geometric effects

After discussing the the effects the CDL design have on the ironing process, the results from using the different CDL radii will be compared to the results from using the conventional design. This is done in order to determine in which general area of the design space the further determination of a CDL design, for implementing at the production at DENEX, should be conducted.

It have to be noted that only selected data from the simulation will be presented during evaluations. For a full overview of the collected data see appendix C. Furthermore can a description of how the data is collected and processed be found in appendix B.

5.2.1 Evaluation of the CDL designs influence on the ironing process

By starting the evaluation of the CDL designs effects on the ironing process with observing how the cartridge cases plastic strain are affected, the following results are obtained:

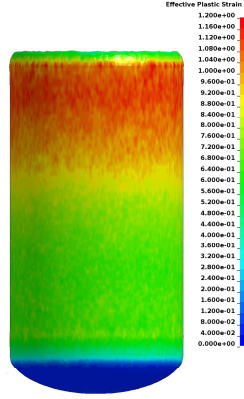


Figure 5.1. Effective plastic strain - Station 1
- 0.00° die tilt - Conventional die design

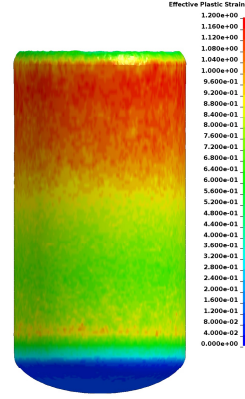


Figure 5.2. Effective plastic strain - Station 1
- 0.00° die tilt - $r_{cdl} = 6.80mm$

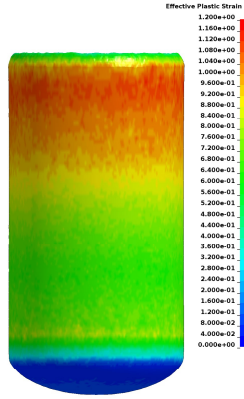


Figure 5.3. Effective plastic strain - Station 1
- 0.00° die tilt - $r_{cdl} = 10.34mm$

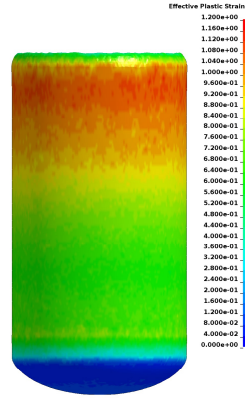


Figure 5.4. Effective plastic strain - Station 1
- 0.00° die tilt - $r_{cdl} = 13.89mm$

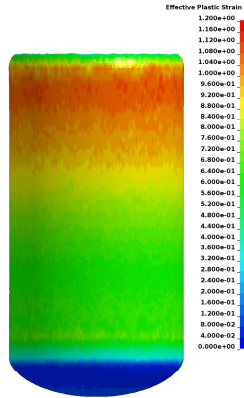


Figure 5.5. Effective plastic strain - Station 1
- 0.00° die tilt - $r_{cdl} = 17.44mm$

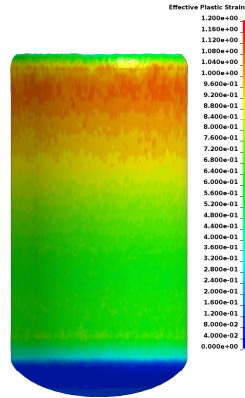


Figure 5.6. Effective plastic strain - Station 1
- 0.00° die tilt - $r_{cdl} = 20.98mm$

As seen on figure 5.2 to 5.6, are the strains in the cartridge cases affected by the CDL design, in a way where an increasing die land radius, r_{cdl} , results in lower strains in the cartridge cases. This effect on the strain can be linked to how the die land radius affects the radial forces on the punch, and thereby the friction force between the punch and the cartridge case. At figure 5.7 the y-forces acting on the punch are displayed, which can be interpreted as measurement for the radial force on the punch.

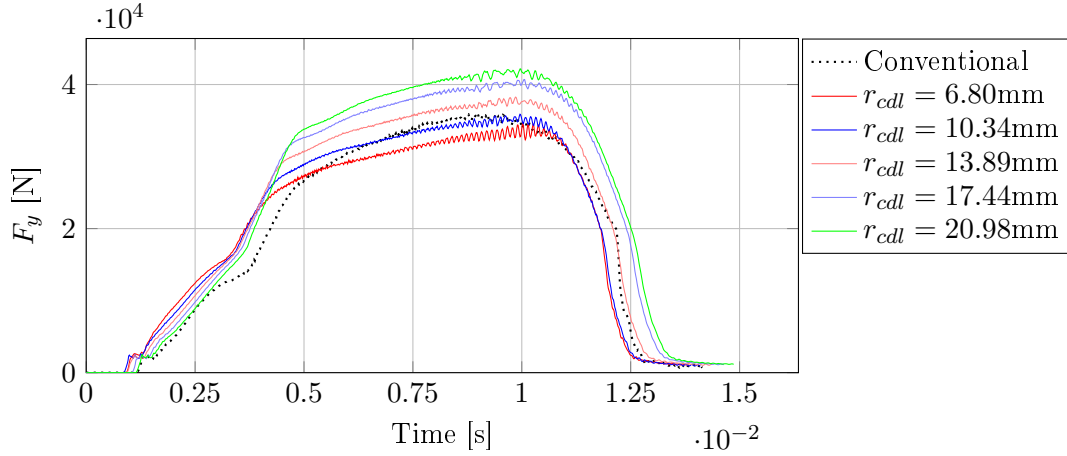


Figure 5.7. F_y - Station 1 - Punch - 0.00° die tilt

From figure 5.7 can it be seen that the radial forces on the punch increases with an increasing die land radius, r_{cdl} , hence an increasing die land radius, r_{cdl} , yields a higher friction force between the cartridge case and the punch. As described in [Adamic et al., 2008] can the punch force, F_{punch} , be described as the sum of the force transmitted to the cartridge case through the punch nose, F_{nose} and the friction force between the cartridge case and the punch at the deformation zone, $F_{friction}$, see equation 5.1 and figure 5.8.

$$F_{punch} = F_{nose} + F_{friction} \quad (5.1)$$

If considering an ironing process with a constant punch force, F_{punch} , then a decreasing friction force, $F_{friction}$, results in higher forces transmitted through the punch nose, hence the cup wall have to carry a higher load, which causes additional elongation and thereby thickness reduction of the cup wall, that are not controlled by the die.

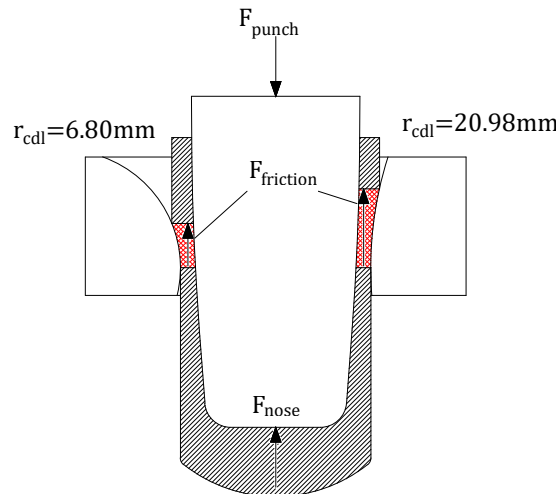


Figure 5.8. Punch force components

If considering this effect, where a decreasing radial force on the punch results in increasing forces transmitted through the punch nose, F_{nose} , for the ironing process of cartridge cases, then the observation for the different CDL radii, where a decreasing CDL radius, r_{cdl} , yields a decrease in the radial force on the punch and thereby the friction force, $F_{friction}$, the observations seems to be in agreement, since larger strains are observed in the cartridge cases for a decreasing CDL radius, r_{cdl} .

If observing the punch force, F_{punch} , see figure 5.9, can it be seen that the changes in the friction force, not only affects the process by altering how much force is transmitted through the punch nose, but also affects the total amount of needed punch force. The observation is, that an increasing CDL radius, r_{cdl} , results in a higher punch force i.e. an increasing CDL radius and thereby increasing friction force, $F_{friction}$, results a higher punch force, F_{punch} . It has to be noted that this effect only are present during the draw, and not during the cartridge cases entry to the die, which is from $t = 0s$ to $t \approx 0.0035s$.

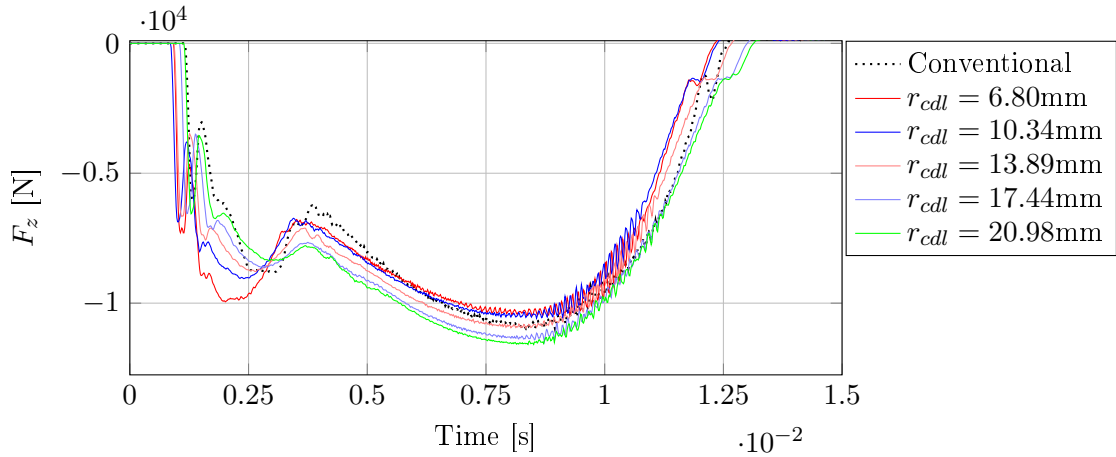


Figure 5.9. F_z - Station 1 - Punch - 0.00° die tilt

When observing the punch force during the cartridge cases entry to the die, see figure 5.9, can it be seen that two force peaks are present at $t \approx 0.001s$ and $t \approx 0.0025s$. If observing the z-forces at one of the die parts instead of the punch, see figure 5.10, can it be seen that only the force peak at $t \approx 0.0025s$ are present i.e. the peak at $t \approx 0.001s$ is the impact between the cartridge case and the punch at the start of the simulation, and can be neglected in the further discussion.

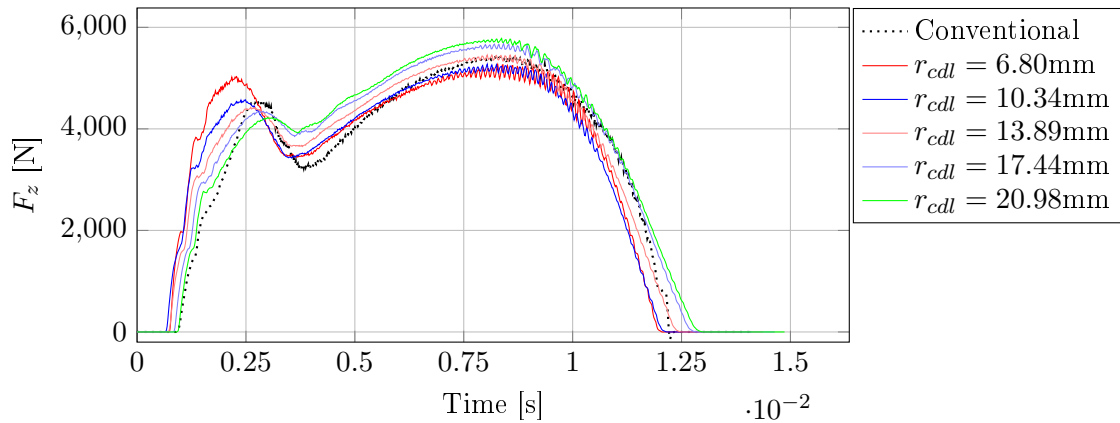


Figure 5.10. F_z - Station 1 - Die 2 x^- - 0.00° die tilt

From figure 5.10 can it be seen that there are a decrease in the z-force, for the cartridge cases impact with the die, when increasing the CDL radius. This change in the impact force is due to that when having a circular die land, the inlet angle, α , is increasing with a decreasing CDL radius, see figure 5.11, hence the force component in the z-direction is increasing.

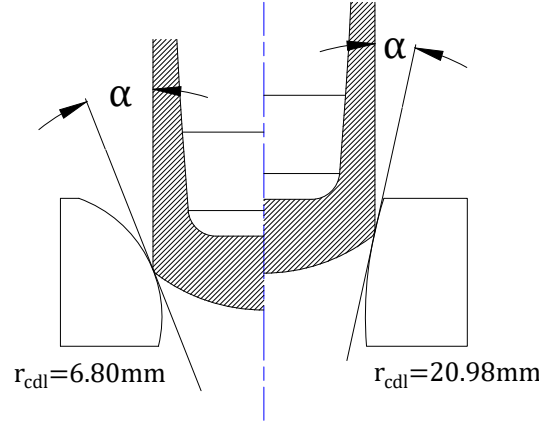


Figure 5.11. The CDL radius, r_{cdl} , influence on the inlet angle, α

If observing the radial force on the die in regards to the cartridge cases entry, see figure 5.12, can it be seen, in opposition to the z-forces, that using a smaller CDL radius, r_{cdl} , results in higher radial forces on the die. If observing both the x and z-forces on the die, see figure 5.12 and 5.10, can it be seen that increasing the CDL radius, r_{cdl} , gives a more smooth transition in the forces from the cartridge case entry at the die, to the drawing of the cartridge case through the die.

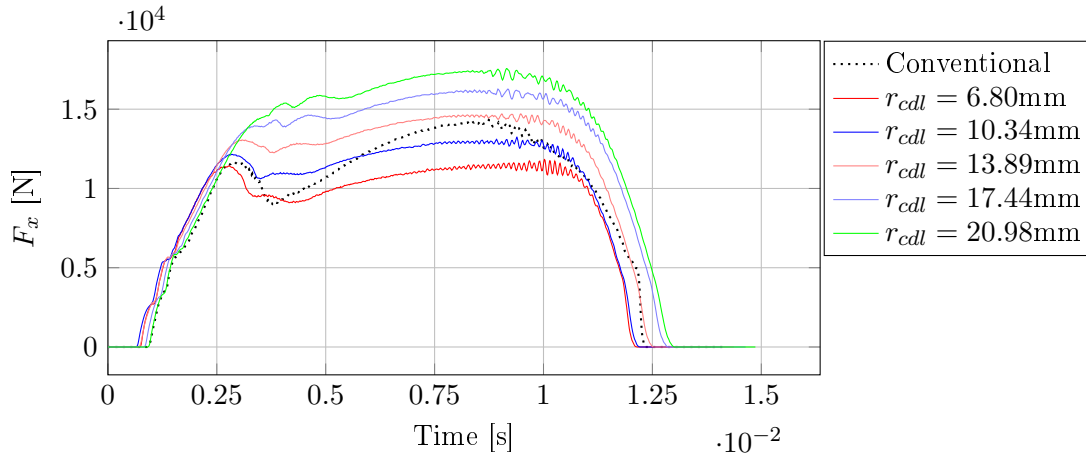


Figure 5.12. F_x - Station 1 - Die 2 x^- - 0.00° die tilt

Another observation that is made in connection to the inlet angle, α , is that the geometric profile of the cartridge cases bottom changes when using different CDL radii. On figure 5.13 a section cut of the cartridge case along the y-normal plane is displayed, where it can be seen that the distance from the bottom surface of the punch to the cartridge case is increasing with an increasing CDL radius, r_{cdl} .

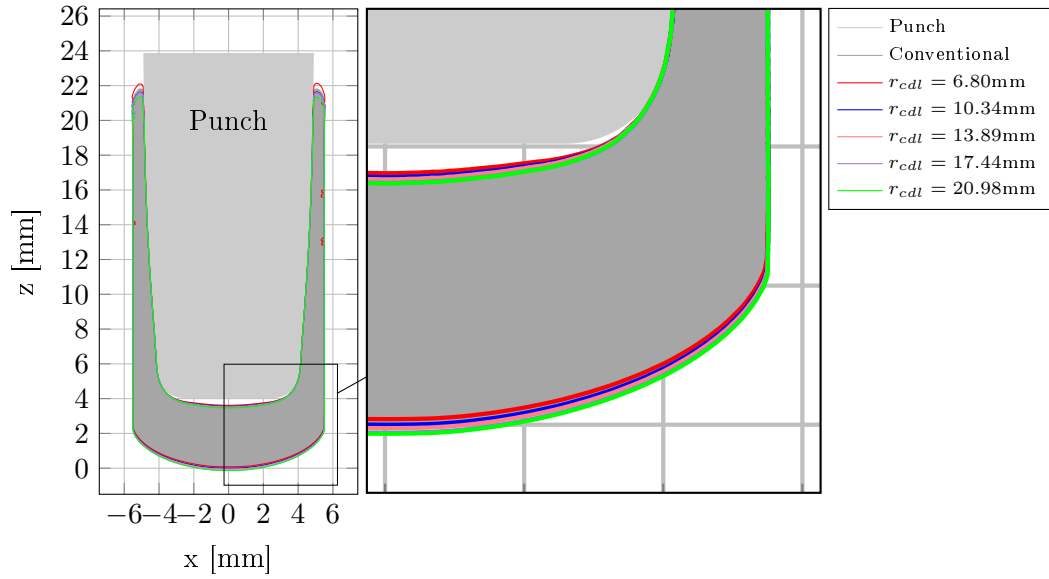


Figure 5.13. Cartridge bottom profile - Station 1 - 0.00° die tilt

The observed effect on figure 5.13 is assumed to be a consequence of the inlet angle, α , since it is determining for the distribution of the force components during the cartridge cases entry to the die, see figure 5.14. On the figure can it be seen that a larger CDL radius results in a lower z -force, F_z , than for the lower CDL radius, hence the material in bottom of the cartridge case is compressed, rather than being pushed upwards in the z -direction, causing it to bulge away from the punch nose.

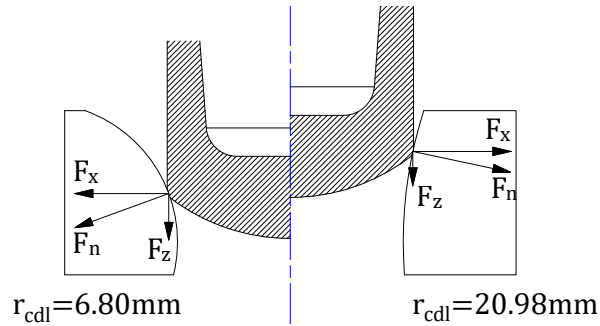


Figure 5.14. Force distribution at the cartridge case entry to the die

Besides displaying the geometric changes of the cartridge case bottom, when using different CDL radii, can it from figure 5.13 be seen that the CDL design also influences the height of the cartridge cases. On figure 5.15 are the cartridge case height along the top edge displayed for the investigated CDL radii.

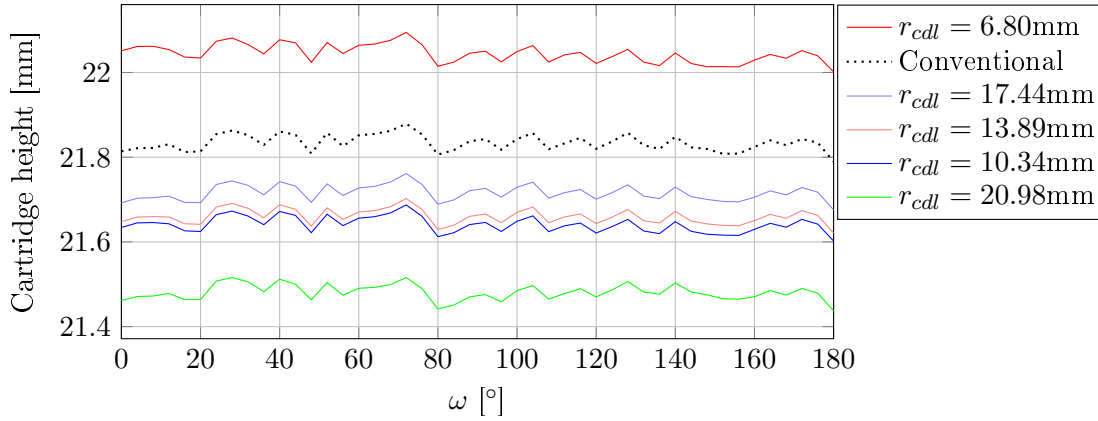


Figure 5.15. Cartridge height - Station 1 - 0.00° die tilt

When considering the development of the strains in the cartridge cases for the different CDL radii, see figure 5.1 to 5.6, the assumption would be that the cartridge case height follows the same tendency i.e. an increasing CDL radii would result in a decreasing cup height. On figure 5.15 can it be seen that the measured cartridge case height does not following the assumed tendency, note that the entries in the legend are sorted in regards to cartridge height in descending order. If considering the section cut of the cartridge case, as seen on figure 5.13, but with focus on the cartridge case top, see figure 5.16, can it be seen that the cartridge case height, in relation to the punch nose, follows the assumed tendency, where the cartridge case height increases with increasing strains caused by a decreasing CDL radius. Furthermore is it observed that the increment in the cartridge case height between each investigated CDL radius, r_{cdl} , is not equally distributed i.e. the height increment at to the boundary radii are significantly larger than for the radii in between.

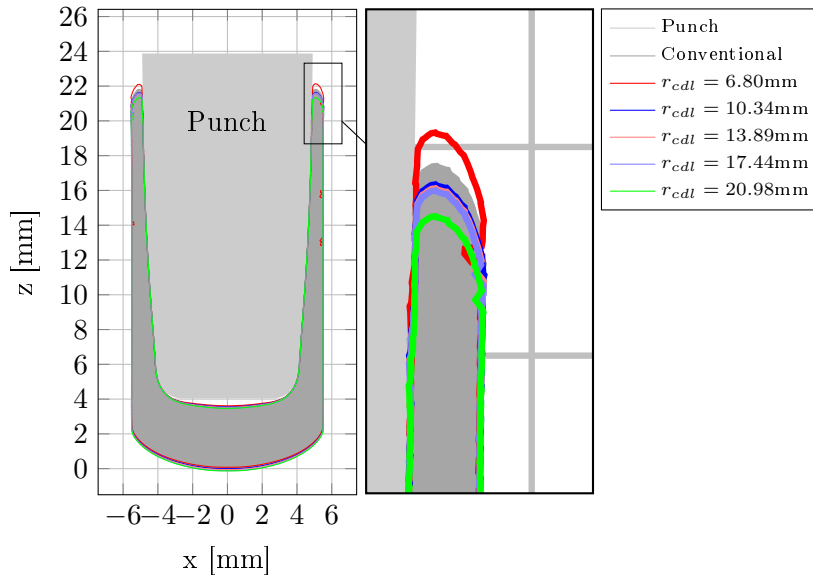


Figure 5.16. Cartridge bottom profile - Station 1 - 0.00° die tilt

By considering the CDL designs influence on the cartridge case height, it is evident that, the height is a result of an interrelationship between the CDL designs influence on the strain and the direction in which the material in cartridge case bottom is led during the

entry to the die.

Another effect that have been investigated for the implementation of the CDL design to the ironing process of 5.56mm NATO cartridge cases, is how the different radii influences the contact pressure between the cartridge case and the die. By comparing the contact pressure obtained for the different CDL radii, an indication can be obtained for how the CDL designs performs in regards to tool wear. It has to be noted that this report will only regard this topic by using the assuming that contact pressure can be used as a measurement for tool wear i.e. a higher contact pressure results in a higher tool wear. Furthermore will the contact pressure be presented in the form of the maximum pressure, observed for the contact between the cartridge case the regarded die part. Note that the pressures appears as being negative, which is a result of the master and slave definition in the contact formulation.

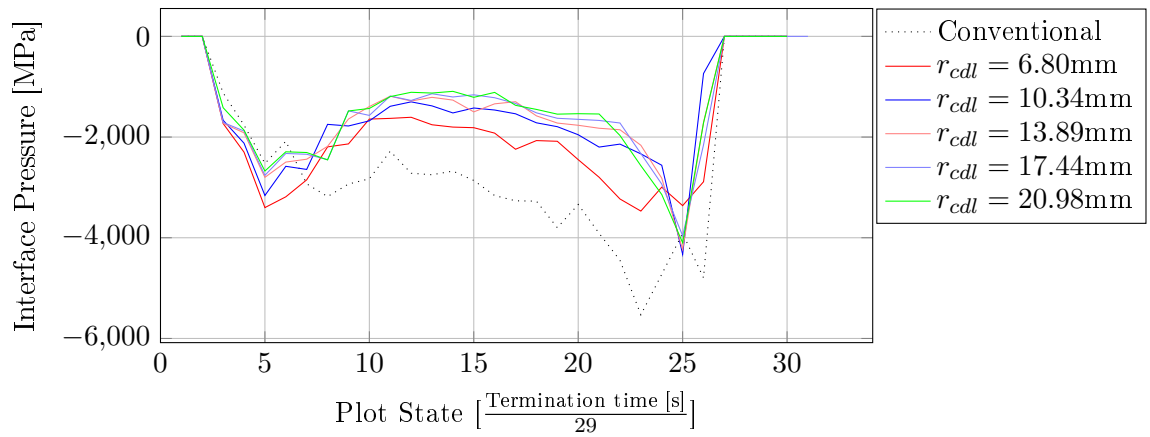


Figure 5.17. Maximum interface pressure - Station 1 - Die 2 x^- - 0.00° die tilt

From figure 5.17 can it be seen that observed pressures for the CDL design in general have a lower magnitude than the pressure observed for the conventional die design and that the contact pressure are decreasing with an increasing CDL radius. If firstly considering the decrease in contact pressure when increasing the CDL radius, this effect can be connected to that increasing the die land radius results in a larger contact area during the draw, see figure 5.18. It have to be considered that this tendency might be problem depended, since the radial forces, displayed for the die on figure 5.12, shows that these are increasing with the CDL radius, hence for another problem the radial forces might be the dominant factor for the contact pressures tendency.

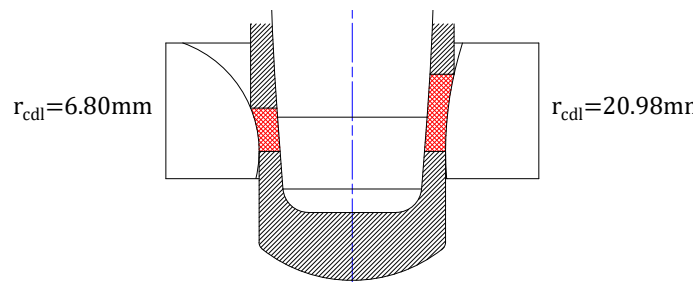


Figure 5.18. Contact zone for the CDL design

If considering the observed higher contact pressure for the conventional design, compared to the CDL design, this can be connected to that the circular design has a more equal distribution of the contact forces than the conventional, where the contact forces are concentrated at the transition between the inlet and the die land, which can be seen on figure 5.19 and 5.20, where the contact pressure between the cartridge case and die 2 x^- are displayed for state 15 ($t \approx 0.007s$).

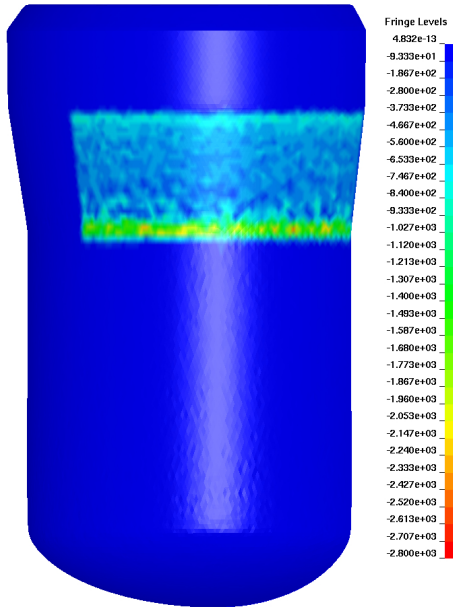


Figure 5.19. Contact pressure - Station 1
- Die 2 x^- - 0.00° die tilt -
Conventional die design

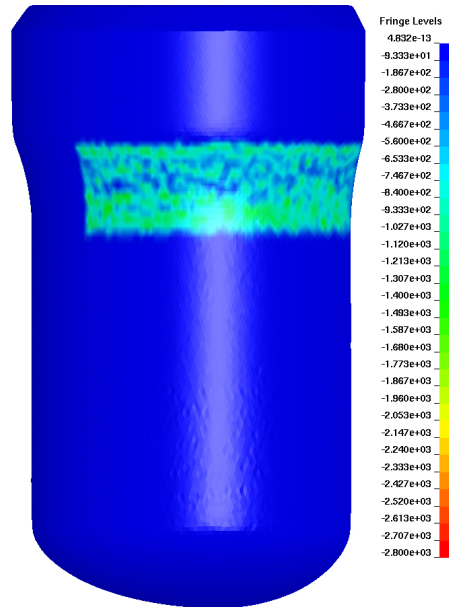


Figure 5.20. Contact pressure - Station 1
- Die 2 x^- - 0.00° die tilt -
 $r_{cdl} = 6.80\text{mm}$

From the discussions above, the CDL design effects on the ironing process of 5.56mm NATO cartridge cases can be summarized to have the effects on the on the ironing process that are shown on table 5.2, when considering an increasing die land radius, r_{cdl} .

| Evaluated effect | Observed tendency |
|-----------------------------------|-------------------|
| Strain | ↘ |
| Cartridge height, absolute | Mixed |
| Cartridge height, From punch nose | ↘ |
| Radial punch force | ↗ |
| Radial die force | ↗ |
| Punch force | ↘ |
| Impact force | ↘ |
| Contact pressure | ↘ |

Table 5.2. The CDL designs effect on the ironing process when increasing the CDL radius, r_{cdl}

5.2.2 Comparison to the conventional die design

In order to determine where in the CDL dies design space, the further investigation of the CDL design should be conducted, in regards to selecting a die land radius, r_{cdl} , for implementing in the ironing process at DENEX, the evaluated data in section 5.2.1 will be compared to the data obtained for the conventional die design. This is due to that using the conventional die design represents a functional ironing process, hence a CDL design with similar conditions and parameters are assumed to conclude a functional design.

The comparison of the different die designs are conducted by evaluating the data presented in section 5.2.1 in regards to identifying which CDL design that provides the closest resemblance to the conventional die design. The comparison can be seen on table 5.3 where the discussed effects in section 5.2.1 are presented along with the CDL design(s) that are assessed to be the closest fit to the conventional design.

| Evaluated effect | Closest fit, r_{cdl} , | Observation reference |
|-----------------------------------|--------------------------|-----------------------|
| Strain | 10.34mm - 13.89mm | Figure 5.1 to 5.6 |
| Cartridge height, absolute | 17.44mm | Figure 5.15 |
| Cartridge height, From punch nose | 10.34mm | Figure 5.16 |
| Radial punch force | 10.34mm | Figure 5.7 |
| Radial die force | 10.34mm | Figure 5.12 |
| Punch force | 10.34mm | Figure 5.9 an 5.10 |
| Impact force | 10.34mm | Figure 5.10 |
| Contact pressure | None | Figure 5.17 |

Table 5.3. CDL designs resemblance to the conventional design

From the information in table 5.3 can it be seen that the design that provide the most similar results, compared to the conventional die design, is when using $r_{cdl} = 10.34\text{mm}$

5.3 CDL performance when introducing a small die tilt

After investigating which effects the CDL design has on the ironing process, the next step is to investigate how the design performs when introducing a small die tilt to the die, and if the design have a stabilizing effect on the process when compared to the conventional design. For this investigation, each of the regarded designs are subjected to two tilt scenarios where the die is tilted 0.20° and 0.40° around the y-axis, respectively.

As stated in section 3.1, the effect of introducing a small die tilt to the the conventional design is that contact is lost between the cartridge case and the die land at one side of the die, which results in non-equal thickness reduction of the die i.e punch displacement are introduced, whereas the CDL design should be unaffected. By taking this effect into consideration can the performance of the CDL design be measured by monitoring the punch displacement during the draw, along with measuring the height of the cartridge cases after completed draw.

On figure 5.21 and 5.22 are the punch displacement displayed for the different die design when subjected to the considered tilt scenarios.

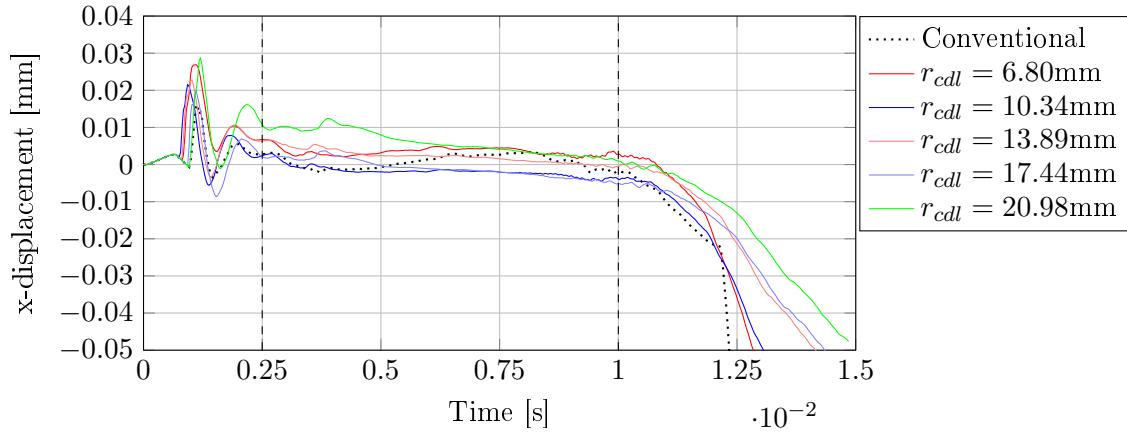


Figure 5.21. x-displacement - Station 1 - Punch - 0.20° die tilt

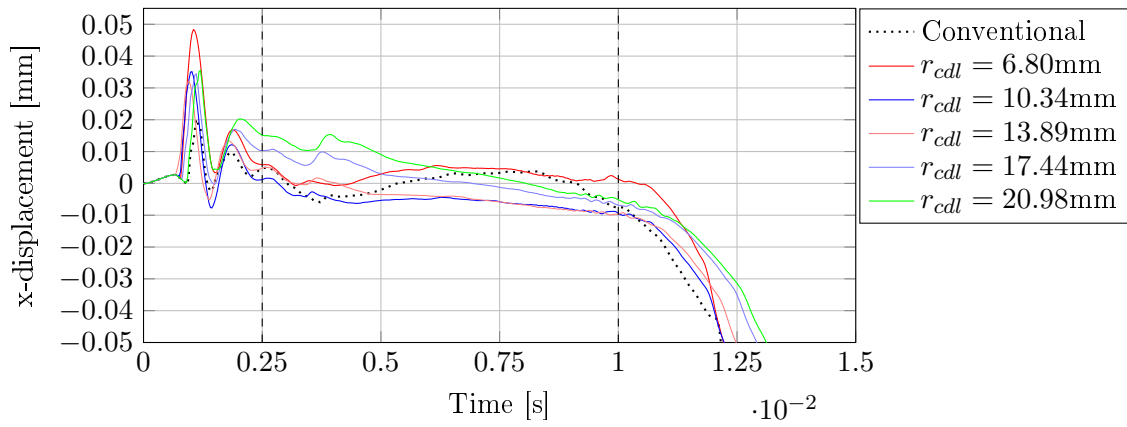


Figure 5.22. x-displacement - Station 1 - Punch - 0.40° die tilt

If firstly considering the punch displacement at figure 5.21 and 5.22 from $t = 0$ s to $t \approx 0.0025$ s can it be seen that the x-position of the punch is subjected to a single oscillation. This effect is a results of both the die tilt and the method used for representing the punch deflection. This is due to that using a tilted die affects the impact between the cartridge case and the die i.e contact is established earlier at the raised side of the die. When using a model for the punch deflection where the punch can float freely in the x-direction, the earlier impact in one side of the die causes both the punch and the die to be shot away from the impacted side i.e. oscillations in the displacement occurs until full contact between the punch and the die is established.

By considering the earlier impact on one die side, and that the ironing process of 5.56mm NATO cartridge case also are performing a reduction of the inner cartridge case diameter, see figure 5.23, is it observed from the simulation that a tilted die not only results in a contact loss, but also is causing an initial misalignment of the cartridge case compared to the punch, in the form of a small counter-clockwise rotation of the cartridge, see figure 5.24, thereby introducing an initial skewness of the cartridge case.

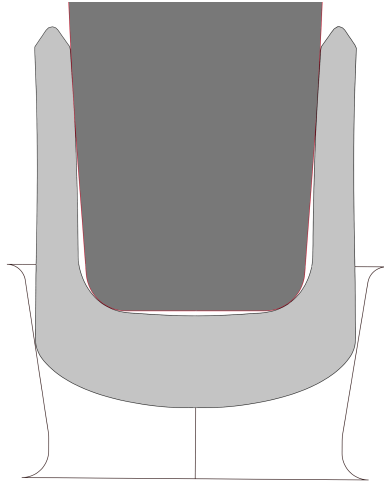


Figure 5.23. Initial position of the cartridge case for the conventional design
- $t = 0\text{s}$ - 0.40° die tilt

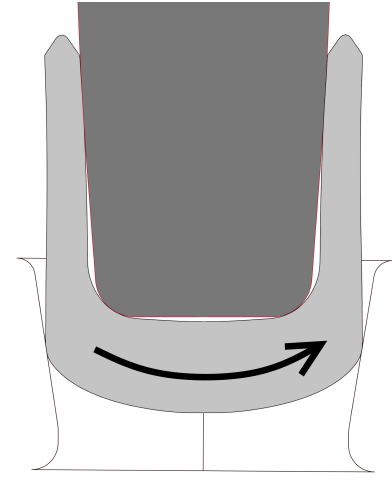


Figure 5.24. Initial cartridge rotation due to impact for the conventional design - $t = 0.001\text{s}$ - 0.40° die tilt

When considering the last part of the draw, from $t \approx 0.01$ to $t \approx 0.015$, can it be seen that the punch starts to drift rapidly in the x^- -direction. Note that the range for the negative x -displacement on figure 5.21 and 5.22, have been limited to -0.05mm in order to make the displacements for the different designs distinguishable. The observed behaviour can be linked to the effect a skewness in the cartridge case height have on the reduction ratio in the last part of the draw i.e when non of the initial geometry is left in the inlet. As seen on figure 5.25 does a skewness of the cup height result in having more material left in the inlet for the higher part of the cartridge case, hence a larger thickness reduction is needed than for the lower part. This causes an imbalance to the radial forces on the die, hence the punch is displaced in the x^- -direction in order establish equilibrium between the radial forces.

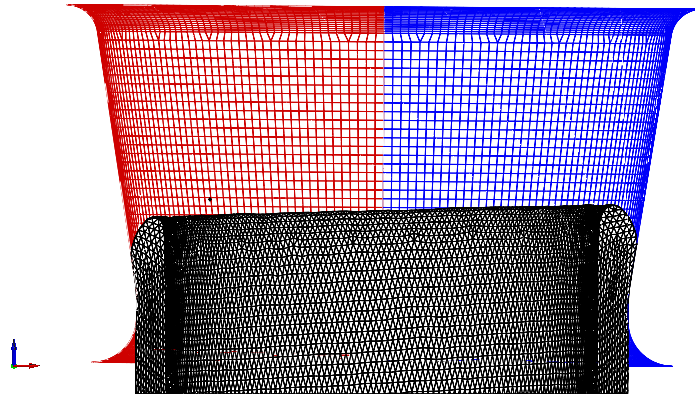


Figure 5.25. Material distribution in the cartridge case top - $t = 0.011\text{s}$ - 0.40° die tilt - Conventional design

For the actual draw of the cartridge case, from $t \approx 0.0025\text{s}$ to $t \approx 0.01\text{s}$ at figure 5.21 and 5.22, can it be seen that non of the tested design manages to establish a continuous 0mm displacement of the punch during the draw, and that there is a general tendency of

a drift in the x^- direction. Furthermore can it be seen that the punch displacement for the different CDL radii does not follow a ordered tendency in regards to offset from the centreline. If observing the punch displacement for the conventional die design, can it be seen that the displacement does not have the same tendency for drifting towards the x^- direction, but instead is oscillating around the centreline. From these observations is it deemed that there is no direct indication for the CDL design to perform better than the conventional design in regards to neutralizing punch displacement.

Besides observing the punch displacement, another way of evaluating the CDL designs performance, when introducing a small die tilt, is to measure the skewness of the cartridge case height, Δh , after completed draw, see figure 5.26.

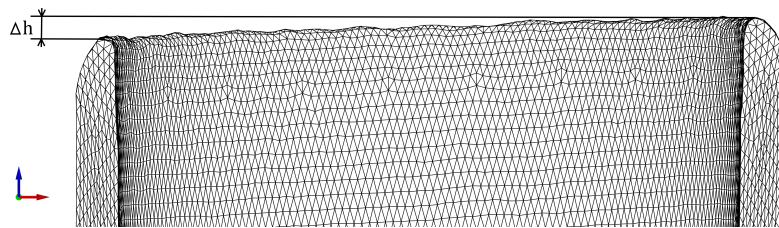


Figure 5.26. Cartridge case height difference, Δh

In table 5.4 are the cartridge case height displayed for the different die designs and scenarios.

| Die design | Δh [mm] | |
|--------------|-----------------|----------------|
| | 0.20° die tilt | 0.40° die tilt |
| Conventional | 0.1884 | 0.3370 |
| r=6.80mm | 0.1305 | 0.1980 |
| r=10.34mm | 0.1155 | 0.1856 |
| r=13.89mm | 0.1167 | 0.1945 |
| r=17.44mm | 0.1168 | 0.1980 |
| r=20.98mm | 0.1120 | 0.1843 |

Table 5.4. Cartridge case height difference

As seen in table 5.4 is there a notable difference in the skewness between the cartridge cases simulated using a CDL design and those for the conventional design, with the cartridge case for the conventional design having the largest height difference. When comparing the results for the different CDL radii, then does the different radii provide similar results, where the only deviation is the cartridge case height for $r_{cdl} = 6.80\text{mm}$.

Based on the results presented in table 5.4 can it be concluded that introducing the CDL design to the ironing process have an stabilizing effect the cartridge case height when a small die tilt are introduced, though the excepted stabilizing effect on the punch displacement was not observed.

Determination of CDL design 6

This chapter concerns the second part of the problem statement presented in section 1.4, which states that a suitable design have to be determined for the CDL dies. In order to make the determination will this chapter firstly present the approach used for the determination, along with a discussion of which requirements a die design has to meet in order to be considered as suitable. After the approach have been described, different CDL designs, in the proximity of the closest fit design described in 5.2.2, are tested using different scenarios, from which the results are evaluated in accordance with the specified requirements, hence a suitable CDL design for the testing and implementation at DENEX are chosen.

6.1 Determination approach

In the following section will the approach for determining the final CDL design be presented. Firstly by presenting the requirements for a suitable design along with the assumptions made for the determination process, and secondly by introducing the approach for choosing the final design.

6.1.1 Design requirements and assumptions

In order to determine a suitable design for the test and implementation of the CDL design to the ironing process at DENEX is it necessary to elaborate on which requirements the design have to fulfil in order to be considered as suitable. If considering that the scope of the project is to test the effects that a CDL design has on the ironing process, then the desired outcome is to determine a CDL design that produces cartridge cases similar to those produced with the conventional design, which represents the outcome of an in praxis functional design, but with an increased stability in regards to the presence of small die tilt.

In section 5.2 is it observed that the CDL radius have an effect on the strains in the cartridge case, and thereby influences both the cartridge case height and wall thickness. For the design evaluation is it assumed that comparing the strains, between the cartridge cases simulated using the CDL design with those simulated using the conventional die design can be used as an indication for which CDL design that would provide the cartridge cases that have the closest resemblance to those produced with the conventional die design.

From observations made in the production at DENEX is it evident that the current ironing process can be considered as borderline stable, since the cartridge cases tend to snap, see figure 6.1 after a certain run period, due to tool wear which results in a rougher contact surface and thereby increases friction, which results in larger strains in the cartridge cases. By considering this observation is it decided to introduce a criterion to the strain evaluation, where the strain for the cartridge cases simulated using the CDL design are not allowed to have higher strains than for the conventional design, since this might cause the process to become unstable.



Figure 6.1. Cartridge case snap due to tool wear

Though the comparison of the strains are considered as the governing criteria for choosing a CDL design is it still necessary to inspect other aspects of the design, in order to assure that it is not introducing any destabilizing effects. The inspected effects are the punch force, with focus on the impact with the cartridge cases, and the contract pressure between the cartridge case and the die. A full overview of the results gathered for the different designs can be seen in appendix D.

For determining which CDL design to use for the implementation at DENEX is it assumed that a suitable design can be found by using the same CDL radius for all the dies. This is due to the design period has a limited time frame, since the chosen design have to be manufactured and tested in the production.

In section 5.2.2 the CDL designs, used for the investigation of the CDL designs effects on the ironing process, is compared to the conventional design in regards to how implementing the design in general affects the ironing process. From this comparison is it found that the CDL design that provides the closest fit the conventional design, is the design using a die land radius of $r_{cdl} = 10.34\text{mm}$. For the investigation of which CDL design to use for the test and implementation is it assumed that the results from the comparison can be used as an indication for where in the CDL dies design space the further investigations should be conducted. The following design determination will thereby consider the implementation of the CDL radii listed in table 6.1.

$$r_{cdl} = [9\text{mm} \quad 11\text{mm} \quad 13\text{mm}]$$

Table 6.1. Considered design space for the design determination

6.1.2 Investigation approach

For the determination of which CDL design to use for the test and implementation, three die design are established for each of the five dies used in the ironing process of 5.56mm NATO cartridge cases, hence three independent iron model are constructed, each representing a design for one of the considered CDL radii in table 6.1.

By evaluating the results obtained by from the three considered CDL designs in regards to the results obtained by performing a full ironing sequence using the conventional design, the CDL radius for the final design is determined, based on the requirements specified in section 6.1.1. Thereby is the different design firstly evaluated in regards to the strains in the cartridge case after each draw, whereafter the punch force and the contact pressure for the dies are inspected in order to ensure that they does not deviate, from those obtained by the conventional design, in a way that would affect the process stability adversely.

After determining the final design for CDL dies, is the chosen design tested in regards to its ability to stabilize the ironing process when introducing a small die tilt. The test of the designs stabilizing effects is, as in section 5.3, performed by introducing a 0.20° and 0.40° die tilt do the dies. The considered scenarios are conducted by introduced the same tilt angle and direction to all the dies in the setup. The dies performance is evaluated both in regards to the punch displacement and the skewness of the cartridge cases height.

6.2 Evaluation of strains

For the evaluation of the strains in the cartridge cases, when simulating a complete ironing sequence for the regarded designs, the strains are displayed for the cartridge cases after completing the draw at each station, see section 6.2.1, 6.2.1 and 6.2.1. The evaluation is performed by firstly presenting the strains monitored after each draw, followed by a discussion where it is concluded which design that will chosen for the implementation.

6.2.1 Station 1

By extrating the cartridge cases after completing the draw at station 1 are the following results obtained, see figure 6.2, 6.3, 6.4 and 6.5. Note that the fringe range have been fixed to: $[0.15 \leq \varepsilon \leq 1.2]$.

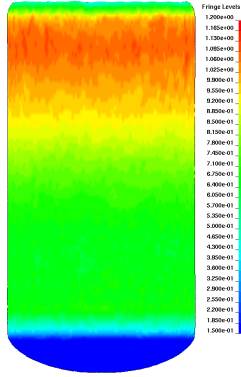


Figure 6.2. Effective plastic strain - Station 1
- 0.00° die tilt - Conventional die design

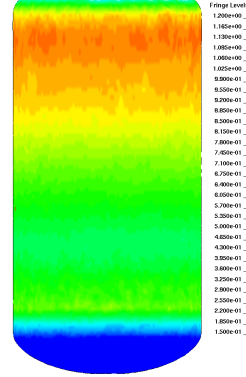


Figure 6.3. Effective plastic strain - Station 1
- 0.00° die tilt - $r_{cdl} = 9\text{mm}$

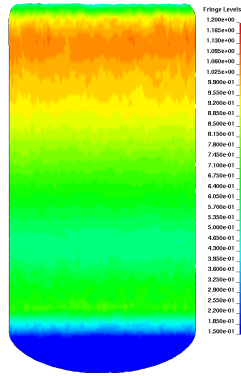


Figure 6.4. Effective plastic strain - Station 1
- 0.00° die tilt - $r_{cdl} = 11\text{mm}$

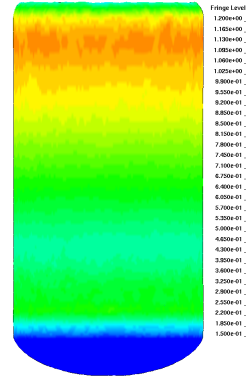


Figure 6.5. Effective plastic strain - Station 1
- 0.00° die tilt - $r_{cdl} = 13\text{mm}$

6.2.2 Station 2

By extrating the cartridge cases after completing the draw at station 2 are the following results obtained, see figure 6.6, 6.7, 6.8 and 6.9. Note that the fringe range have been fixed to: $[0.5 \leq \varepsilon \leq 2.0]$.

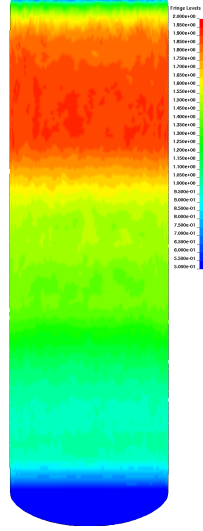


Figure 6.6. Effective plastic strain - Station 2
- 0.00° die tilt - Conventional die design

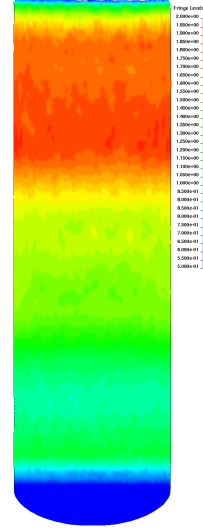


Figure 6.7. Effective plastic strain - Station 2
- 0.00° die tilt - $r_{cdl} = 9\text{mm}$

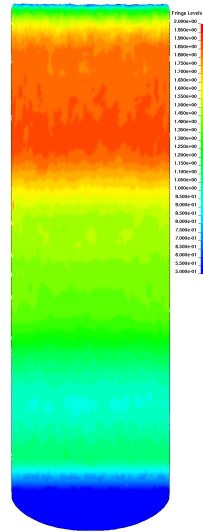


Figure 6.8. Effective plastic strain - Station 2
- 0.00° die tilt - $r_{cdl} = 11\text{mm}$

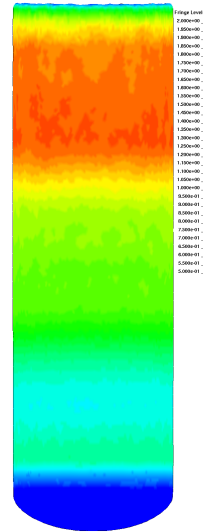


Figure 6.9. Effective plastic strain - Station 2
- 0.00° die tilt - $r_{cdl} = 13\text{mm}$

6.2.3 Station 3

By extrating the cartridge cases after completing the draw at station 3 are the following results obtained, see figure 6.10, 6.11, 6.12 and 6.13. Note that the fringe range have been fixed to: $[0.5 \leq \varepsilon \leq 2.6]$.

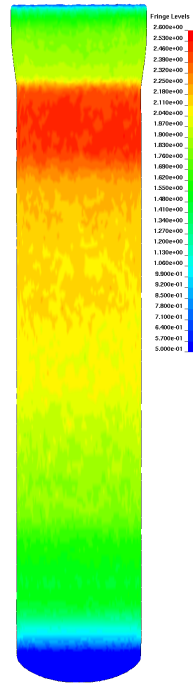


Figure 6.10. Effective plastic strain - Station 3 - 0.00° die tilt - Conventional die design

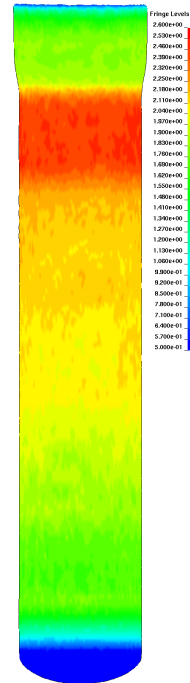


Figure 6.11. Effective plastic strain - Station 3 - 0.00° die tilt - $r_{cdl} = 9\text{mm}$

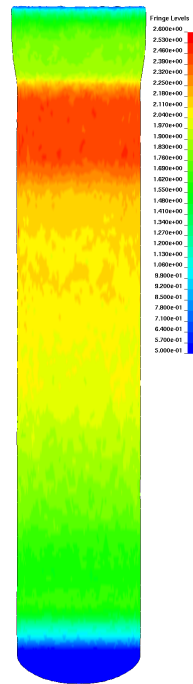


Figure 6.12. Effective plastic strain - Station 3 - 0.00° die tilt - $r_{cdl} = 11\text{mm}$

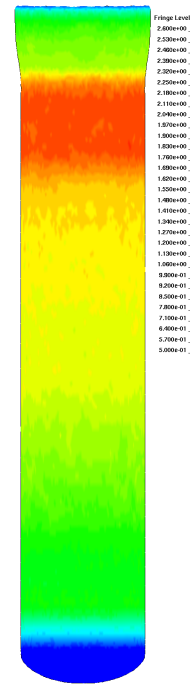


Figure 6.13. Effective plastic strain - Station 3 - 0.00° die tilt - $r_{cdl} = 13\text{mm}$

6.2.4 Discussion and determination of CDL design

When visually inspecting the results shown in section 6.2.1, 6.2.1 and 6.2.1, can it be seen that the strains in the cartridge cases for the CDL designs have slightly smaller strains compared to those simulated using the conventional design. Likewise can it be seen, for both station 1, 2 and 3, that the strains are decreasing with an increasing die land radius, as observed in section 5.2. When considering the requirement for a suitable CDL design, see section 6.1, the most suitable design would be $r_{cdl} = 9\text{mm}$, since the cartridge cases obtained by using this design provides the closet fit to the conventional design without having higher strains.

Though the design using $r_{cdl} = 9\text{mm}$ is considered to be the most suitable design according to the requirement, is it observed that the cartridge cases produced by this design generally have a higher level of strain, without having higher maximum strains than for the cartridge cases produced by the conventional design. If instead considering the cartridge cases simulated using $r_{cdl} = 11\text{mm}$, can it be seen that the strains generally are lower, than for the conventional design, for the entire cartridge case. Furthermore is it deemed that the difference in the results between the different designs can be considered as being minor, hence none of the design is assumed to perform notable better than the others. It is thereby decided to choose the design using $r_{cdl} = 11\text{mm}$ for the test and implementation in the production at DENEX.

6.3 Inspection of process stability

In this section is the punch force and the contact pressure between the dies and the cartridge case inspected in regards to identifying if the choice of CDL design effects the process stability adversely. Due to the assumption made in section 6.2.4, stating that the different designs is assumed to perform equally, are the results for all of the considered design shown in order to asses if the assumption is reasonable.

In order to make the inspection, will the data for punch force and the contact pressure firstly be presented, whereafter the results and observation are regarded in a combined discussion.

6.3.1 Punch force

By monitoring the punch force for the different die designs are the results on figure 6.14, 6.15 and 6.16 obtained.

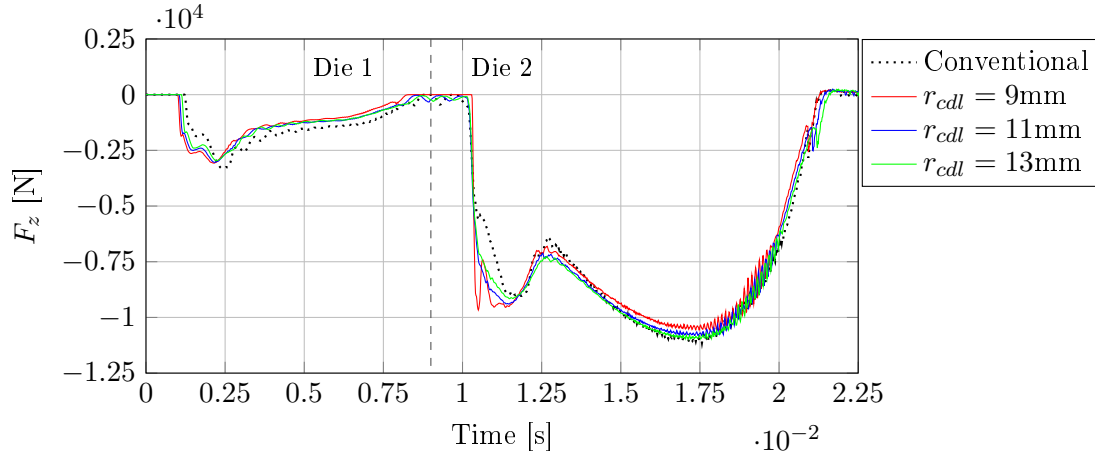


Figure 6.14. F_z - Station 1 - Punch - 0.00° die tilt

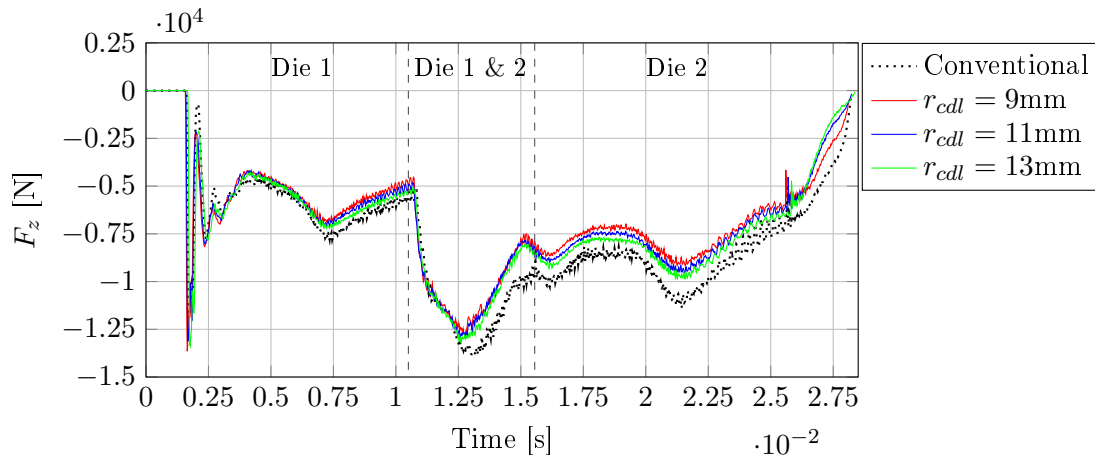


Figure 6.15. F_z - Station 2 - Punch - 0.00° die tilt

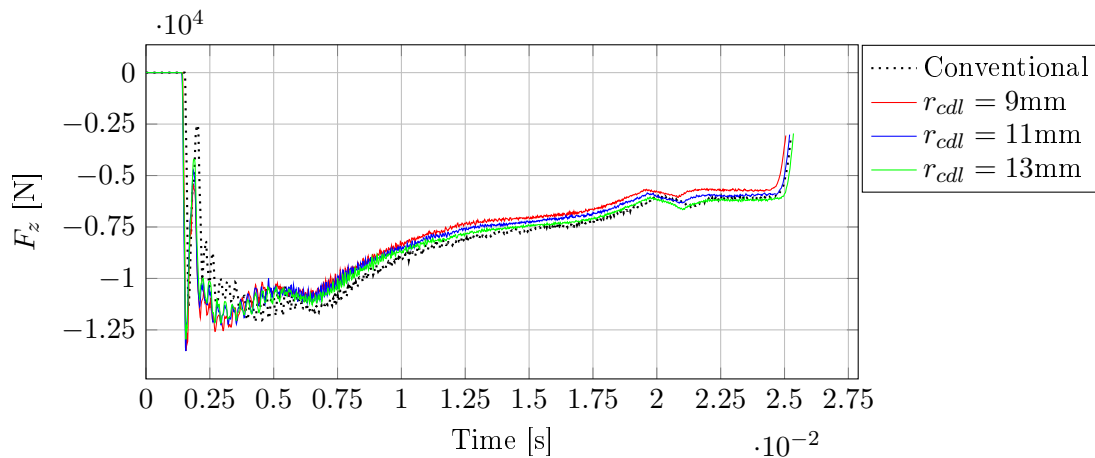


Figure 6.16. F_z - Station 3 - Punch - 0.00° die tilt

6.3.2 Contact pressure

By monitoring the maximum contact pressure for the different die designs the results shown in figure 6.17, 6.18 and 6.19 obtained.

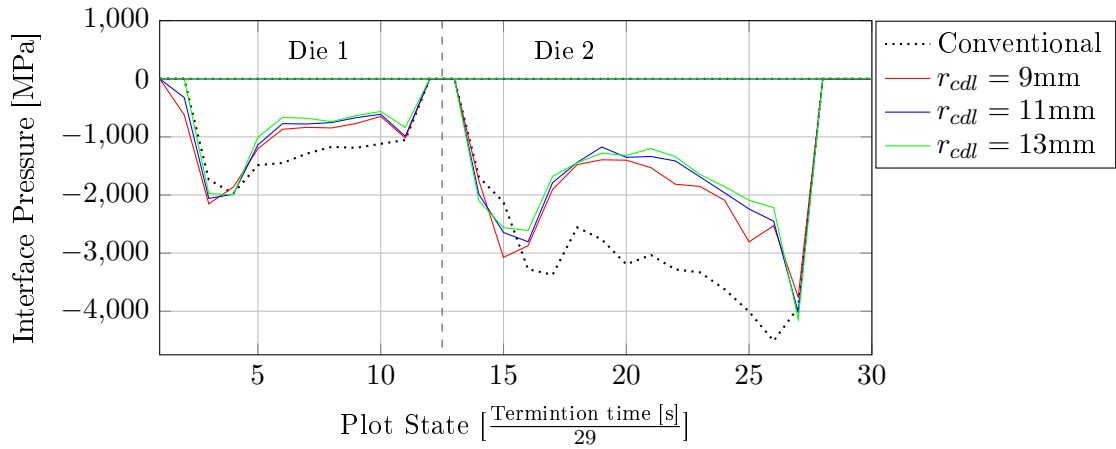


Figure 6.17. Maximum interface pressure - Station 1 - Die 1 and 2 x^- - 0.00° die tilt

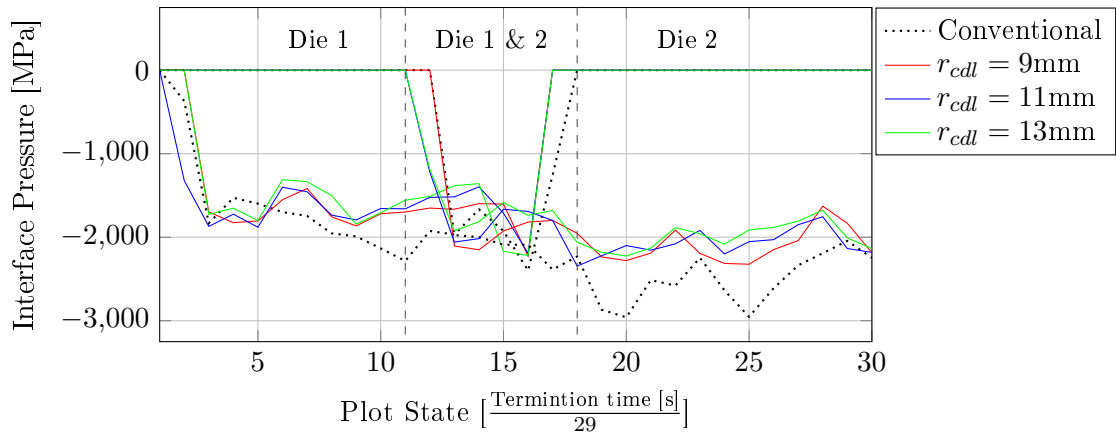


Figure 6.18. Maximum interface pressure - Station 2 - Die 1 and 2 x^- - 0.00° die tilt

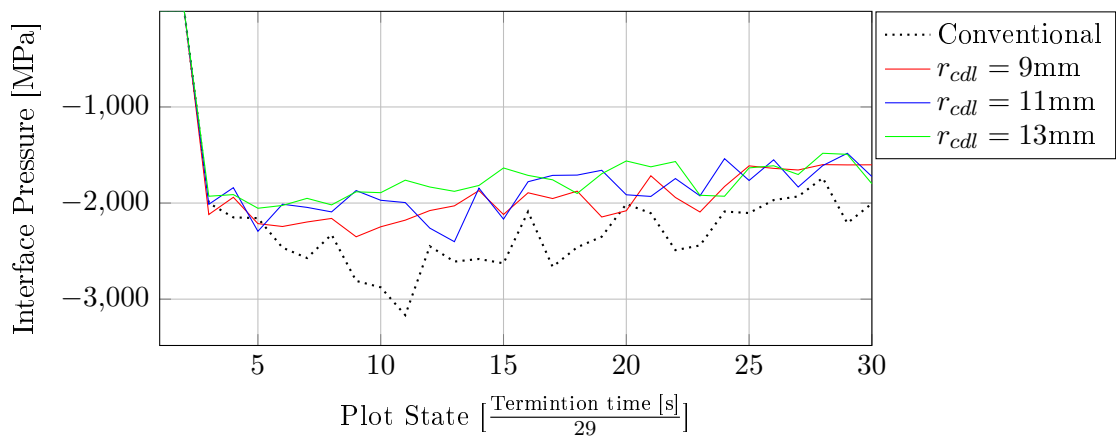


Figure 6.19. Maximum interface pressure - Station 3 - Die 1 x^- - 0.00° die tilt

6.3.3 Discussion of observations

When observing the punch force for the different designs, see figure 6.14, 6.15 and 6.16, it can be seen that the punch force for the CDL designs is similar to the punch force monitored for the conventional design, only with a slightly smaller magnitude. Furthermore, when observing the punch force at the cartridge cases impact with the dies, it can be seen that the force peaks have a magnitude in the same area as for the conventional design. It can likewise be observed that only a small difference is present between the punch force for the different CDL designs. Based on these observations on the punch force, it is assessed that there is no indication of that the CDL designs introduce stability issues in regards to a raise in the punch force, or a considerable higher force during cartridge impact with the dies. It is likewise observed that the different CDL designs perform equally, as assumed in section 6.2.4.

In regards to the monitored maximum contact pressure, see figure 6.17, 6.18, and 6.19, it is observed that using the CDL design results in a lower contact pressure than the conventional design, and that using the different CDL radii results in approximately the same pressure. When observing the pressure at the different dies throughout the stations, it can be seen that the largest reduction in contact pressure, compared to the conventional die design, is for die 2 at station 1, where the maximum pressure is reduced with approximately 1500MPa during the draw, whereas the other dies in the process are subjected to a reduction in the area of 500MPa. From these observations, it is thereby concluded that the considered CDL design does not represent a stability issue in regards to wear of the dies. It has to be noted that this conclusion is based on the assumption made in section 5.2, where it is assumed that the maximum contact pressure can be used as a measurement for the dies wear performance.

6.4 Design performance when introducing a small die tilt

After determining which design to use in the test and implementation of the CDL design to the ironing process of 5.56mm NATO cartridge cases, is the final investigation, before realizing the design, to test if the design provides the assumed stabilizing effect on a small die tilt. In order to conduct the test, two scenarios are considered where a 0.20° and a 0.40° tilt at the y-axis are introduced to all the dies in the setup.

For evaluating the CDL designs performance in regards to the die tilts, the punch displacement in the x-direction is measured, see figure 6.20 to 6.25, thereby monitoring the designs ability to keep the process stable when subjected to a die tilt.

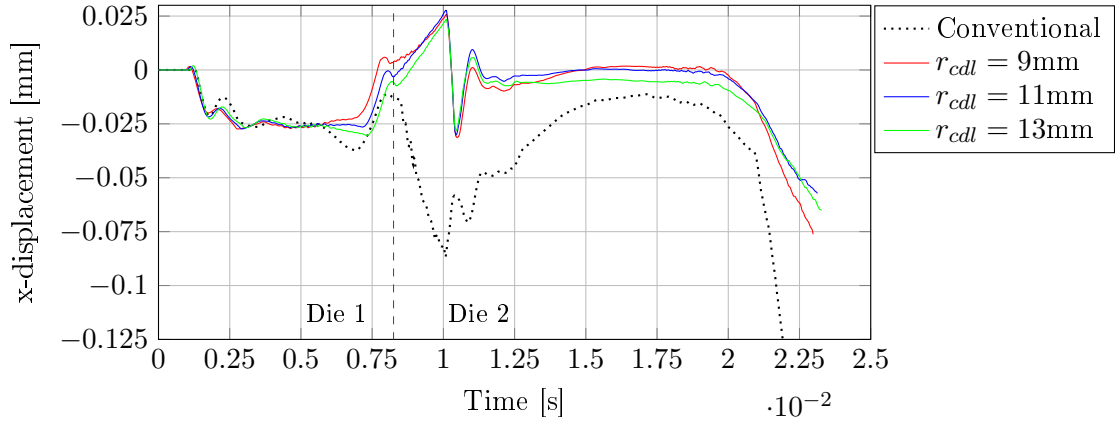


Figure 6.20. x-displacement - Station 1 - Punch - 0.20° die tilt

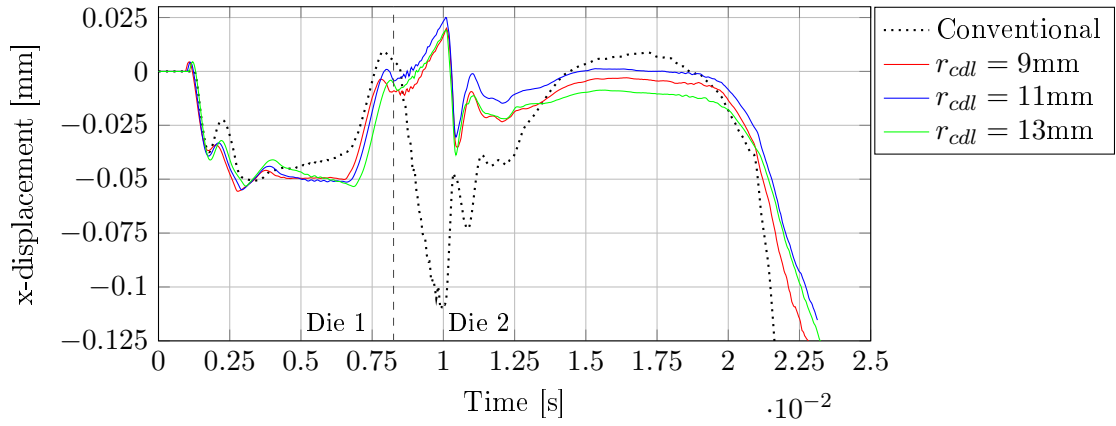


Figure 6.21. x-displacement - Station 1 - Punch - 0.40° die tilt

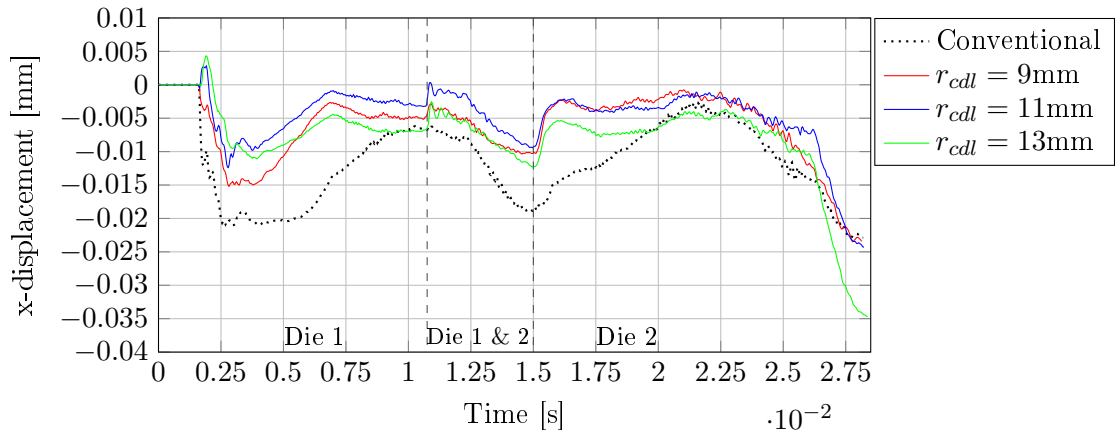


Figure 6.22. x-displacement - Station 2 - Punch - 0.20° die tilt

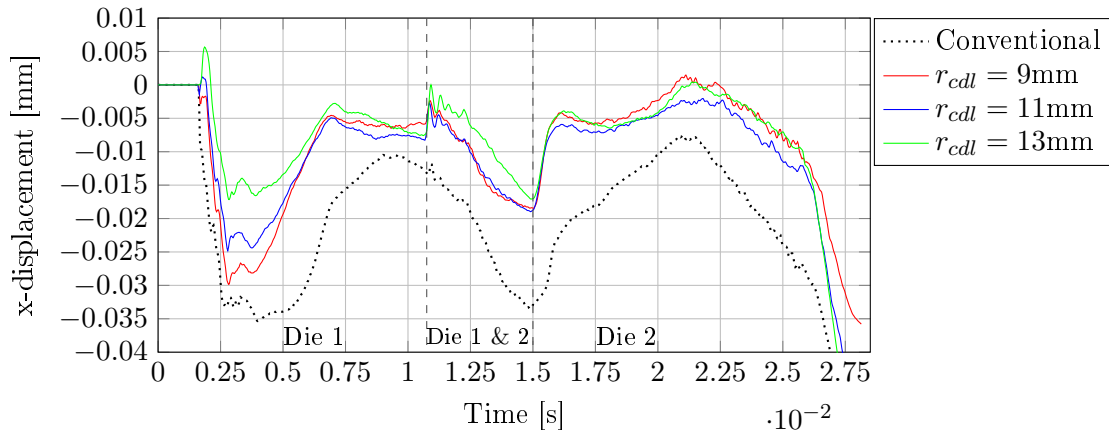


Figure 6.23. x-displacement - Station 2 - Punch - 0.40° die tilt

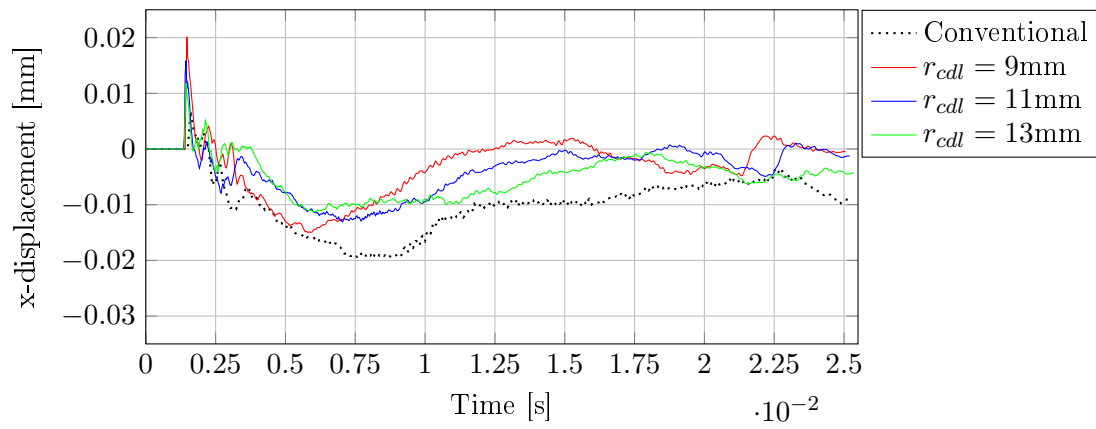


Figure 6.24. x-displacement - Station 3 - Punch - 0.20° die tilt

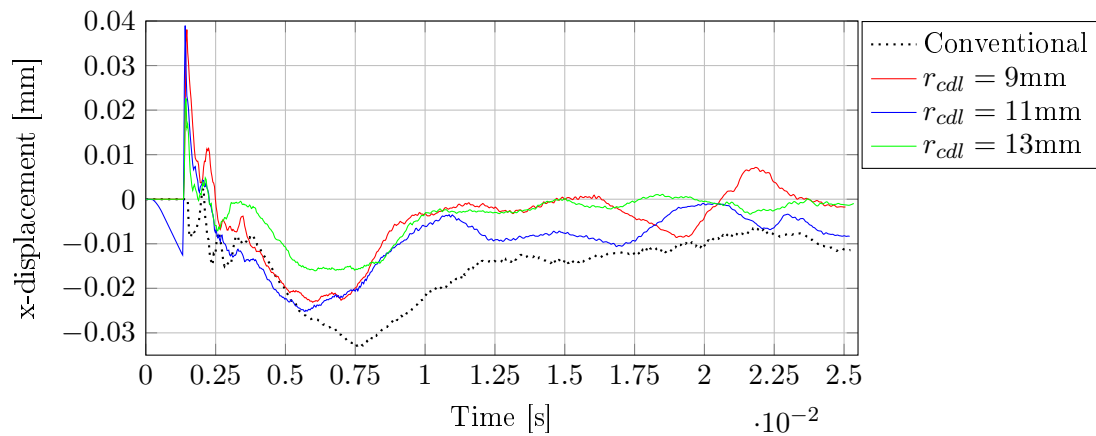


Figure 6.25. x-displacement - Station 3 - Punch - 0.40° die tilt

From the data presented in figure 6.20 to 6.25 can it be seen that the process is subjected to less punch displacement when using the CDL die design, than when using the CDL design i.e a cartridge case with a more uniform wall thickness is obtained. Though the CDL design is able to reduce the punch displacement compared to the conventional design, is it still subjected to disturbances. When observing the punch displacement for the different scenarios can it likewise be seen the that the major part of the punch displacement are inflected when the cartridge case enter the respective dies. This behaviour is, as observed in section 5.2, due to that the considered ironing process are performing a reduction of the cartridge cases inner diameter along with the wall thickness reduction, which provides the cartridge case with both translational and rotational freedom at impact with the dies. Besides introducing disturbance to the punch displacement, does this condition also introduce asymmetry to the cartridge case bottom. This effect is displayed at figure 6.26 where the bottom profile for the final cartridge case from the three CDL designs are displayed in comparison to the bottom profile for a cartridge case simulated using the conventional design without die tilt.

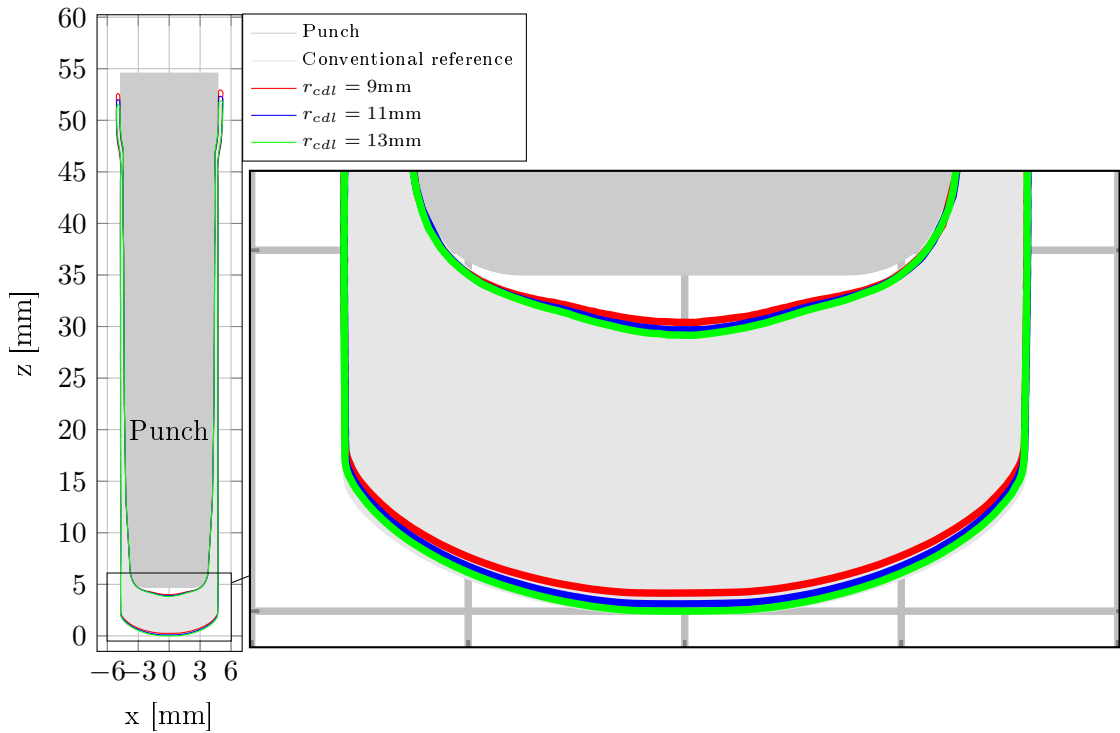


Figure 6.26. Cartridge bottom profile - Station 3 - 0.40° die tilt

When considering the skewness in the cartridge cases height, see table 6.2 and 6.3, can it be seen that the CDL design only have a stabilizing effect on the skewness for the scenario using a 0.40° die tilt, though the CDL design is shown to have a more centred punch displacement during the draw for both tilt scenarios, see figure 6.20 to 6.25. This observation is assumed to be a consequence of having the reduction of the inner cartridge case diameter included in the ironing process, which results in a misalignment of the cartridge case when introducing a die tilt.

| 0.20° die tilt | | | |
|-------------------------|-----------------|-----------|-----------|
| Die design | Δh [mm] | | |
| | Station 1 | Station 2 | Station 3 |
| Conventional design | 0.2707 | 0.1535 | 0.1200 |
| $r_{cdl} = 9\text{mm}$ | 0.1376 | 0.1676 | 0.1549 |
| $r_{cdl} = 11\text{mm}$ | 0.1165 | 0.2325 | 0.2137 |
| $r_{cdl} = 13\text{mm}$ | 0.1131 | 0.2201 | 0.2058 |

Table 6.2. Height difference - 0.20° die tilt

| 0.40° die tilt | | | |
|-------------------------|-----------------|-----------|-----------|
| Die design | Δh [mm] | | |
| | Station 1 | Station 2 | Station 3 |
| Conventional | 0.4692 | 0.5024 | 0.4115 |
| $r_{cdl} = 9\text{mm}$ | 0.2149 | 0.3630 | 0.3459 |
| $r_{cdl} = 11\text{mm}$ | 0.1999 | 0.3950 | 0.3428 |
| $r_{cdl} = 13\text{mm}$ | 0.1954 | 0.4688 | 0.4054 |

Table 6.3. Height difference - 0.40° die tilt

Based on the observation above is it concluded that introducing the CDL design to the ironing process have a stabilizing effect on the ironing process of 5.56mm NATO cartridge cases when introducing a small die tilt. It is likewise observed that presence of a reduction of the cartridge cases inner diameter at each ironing station is a major contributor to the presence of a skewness of the cartridge case height, hence the stabilizing effect of the CDL design is a more centred punch travel, thereby producing cartridge cases with a more uniform wall thickness distribution.

It is thereby deemed that introducing the CDL design to the ironing process will result in a more stable process, hence the CDL design will be implemented and tested in the production at DENEX. As stated in section 6.2 is the chosen CDL design for the implementation $r_{cdl} = 11\text{mm}$, hence technical documentation for the design have been produced, which can be found in appendix A. Note that the drawings presented in this report are displayed without specifying tolerances, surface finish etc. due to confidentiality.

Evaluation of die implementation 7

This chapter regards the implementation of the CDL design, concluded in chapter 6, to the ironing process of 5.56mm NATO cartridge cases. The chapter will firstly concern the implementation of the CDL dies to the process, and afterwards an evaluations of the designs performance.

7.1 Process implementation of the CDL design

Based on the design chosen in chapter 6, and the drawings presented in appendix A, the dies shown on figure 7.1 were manufactured, and mounted in the ironing machine at DENEX, where both the mounting and operation of the machine were performed by one of DENEX's experienced operators.

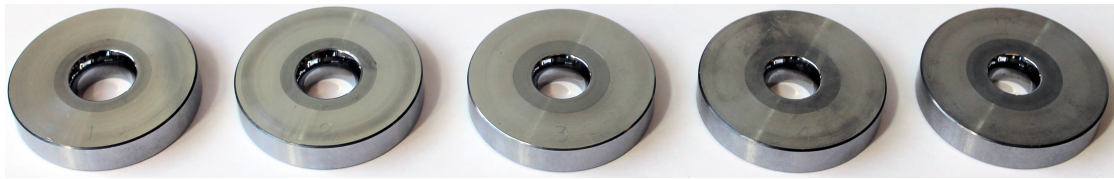


Figure 7.1. Manufactured CDL dies

When running the ironing process with the CDL dies, the cartridge cases shown on figure 7.2 were obtained, when performing the draws using the ironing machine in operator mode i.e each punch stroke is initiated by the operator.



Figure 7.2. Cartridge cases produced by the CDL dies

When switching to performing the ironing sequence as a continuous operation, the cartridge case began to snap during the 3rd draw i.e station 3, see figure 6.1. It has to be noted that approximately 5-10 cartridge cases could be produced before a snap occurred, and that the machine automatically stops when registering a defect cartridge case, hence it is not known if the failure is inflicted by running continuously, since it was not possible to determine if the subsequent cartridge case would snap.



Figure 7.3. Cartridge case snap during the 3rd draw

Since a snap of the cartridge cases, for the conventional design, is known to be a result of a insufficient surface finish of the dies was the CDL dies dismantled, subjected to further polishing, and remounted in the setup. When restarting the test with the further polished dies, the cartridge cases continued to snap, hence the test was terminated, and it was concluded that implementing the considered CDL design to the ironing process did not result in a stable process.

7.2 Discussion of the CDL dies performance

As stated in section 7.1 did the implementation of the CDL design to the ironing process of 5.56mm NATO cartridge cases not conclude a stable process i.e the cartridge cases tended to snap during the third draw. This section will thereby concern the observations made both during the test of the dies, and observations made on the cartridge cases produced by the CDL design, in order to determine possible causes for the designs instability.

If considering the effects causing a cup to snap during an ironing process, then this is a result of transferring a higher load through the cup wall than it can withstand without introducing necking and subsequently fracture. When considering the cartridge cases that did not snap during the third draw, a starting tendency for necking was observed in the same area as were the snap was observed, see figure 7.4. Note that this observation is made both on the cartridge cases produced during the operator mode and the continuous production, hence all the cartridges are on the verge of fracture i.e only a small disturbance in the process conditions is needed to trigger a fracture.

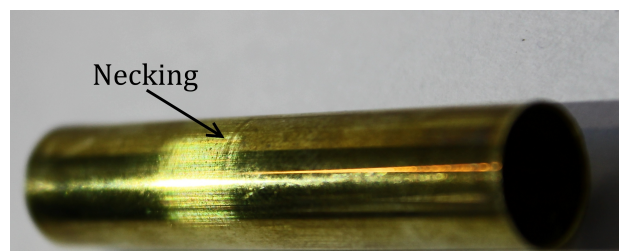


Figure 7.4. Necking in the cartridge cases produced by the CDL dies

As stated above, are both the observed necking and fracture a result of transmitting higher forces through the cartridge cases wall, than the material can withstand i.e the punch force transmitted through the punch nose is too high. If considering the punch force and its components, see equation 5.1 and figure 5.8, then the needed punch force is the sum of the force transmitted at the punch nose and the friction force between the punch and the cartridge case, hence a higher force at the punch nose is a result of either a lower friction force or if a higher punch force is needed, assuming that only one of them is subjected to changes.

If firstly considering the increased force transmitted through the punch nose as a result of a lower friction force i.e. the needed punch force has not changed, then the cause for this would either be a reduced friction between the cartridge case and the punch or decreased radial forces on the punch. Since both the CDL dies and the conventional dies use the same punch is a change in friction neglected, hence only a change in the radial forces on the punch remains as a factor.

If secondly considering an increased force transmitted through the punch nose as a result of an increase in the needed punch force, while noting that the CDL and conventional design have the same reduction ratios, then the increase in needed punch force can be a result of having a higher friction between the CDL dies and the cartridge case than for the conventional dies. When making a visual inspection of the cartridge case produced by the CDL dies and the conventional dies, see figure 7.5 and 7.6, can it be seen that the surface of the cartridge cases produced by the CDL dies are significantly more worn than those produced by the conventional design. Note that the displayed cartridge cases both have been submerged in an acid solution in order to enhance the visibility of the surface condition, and that both the same solution and submergence duration were used.



Figure 7.5. Surface finish of cartridge cases produced by the CDL dies



Figure 7.6. Surface finish of cartridge cases produced by the conventional dies

Due to the more worn surface on the cartridge cases produced by the CDL dies, it is assumed that the CDL dies are subjected to different friction conditions than the conventional dies, thereby causing either the necking or fracture of the cartridge cases during the third draw.

Conclusion 8

In this project has an investigation, of the influence an implementation of a die design with a circular die land, CDL, have to the ironing process of 5.56mm NATO cartridge cases, been conducted. The concept of using CDL design is proposed in [Dancert, 2005], where it is shown to have a stabilizing effect on ironing processes when subjected to the presence of a small die tilt, which is caused by inaccurate machining or mounting of the dies. In order to conduct the investigation is the project conducted in collaboration with DENEX, who have contributed to the project by providing technical information about the process, and by manufacturing and implementing a set of CDL dies for ironing of 5.56mm NATO cartridge cases.

In order to conduct the above described investigation have the following problem statements been regarded in the project:

1. **Which effects does the implementation of a circular die land design have on the ironing process of 5.56mm NATO cartridge cases?**
2. **What would be a suitable die design for the test and implementation of the circular die land design to the process?**
3. **How does the circular die land design perform when implemented to the production setup at DENEX?**

In regards to the first problem statement was it in chapter 3 described why an introduction of a small a die tilt represent a stability issue in ironing processes and that the stability issue is due to that the cup, when using a conventional die design, partially loses contact with the die when introducing a die tilt. It was further describes that this issue would not be present if using a CDL design for the die. Besides describing the stabilizing effects of introducing a CDL design, did chapter 3 also include a determination of the design space for which CDL radii that can be used in the ironing process of 5.56mm NATO cartridge cases, see table 3.4.

In order to make the investigation of the effect a CDL design has on the ironing process of cartridge cases, the LS-Dyna model developed in [Pedersen, 2016] for the ironing process of 7.62mm NATO cartridge cases was modified to represent the ironing process of 5.56mm NATO cartridge cases along with modifications that enabled the investigation of the die tilts influence on the ironing process. The modifications introduced to the LS-Dyna model was described in chapter 4.

For the investigations of the CDL designs influence on the ironing process was a series of simulations conducted for die 2 at ironing station 1. From these simulations was the following observations made when evaluating which effects using different CDL radii, within the dies design space, had on the process, and which of the design that represent the closest fit to the conventional design:

| Evaluated effect | Observed tendency | Closest fit, r_{cdl} |
|-----------------------------------|-------------------|------------------------|
| Strain | ↘ | 10.34mm - 13.89mm |
| Cartridge height, absolute | Mixed | 17.44mm |
| Cartridge height, From punch nose | ↘ | 10.34mm |
| Radial punch force | ↗ | 10.34mm |
| Radial die force | ↗ | 10.34mm |
| Punch force | ↘ | 10.34mm |
| Impact force | ↘ | 10.34mm |
| Contact pressure | ↘ | None |

Table 8.1. The CDL designs influence on the ironing process when increasing the die land radius, and the CDL radius that provides the closet fit to the conventional die design when comparing the effect

Besides evaluating the CDL designs effect on the ironing process, was it during this investigation discovered that the performed reduction of the cartridge cases inner diameter causes instability to the process. The above discussed investigation was presented in chapter 5.

For the second part of the problem statement was an investigation conducted in LS-Dyna for three different CDL designs, each using the same CDL radius for all the dies in the setup. The aim for the investigation was to determine a CDL design to use for the implementation in the production at DENEX. By using a design criterion stating that the most suitable design would be the one where the strains in the cartridge cases had the closest resemblance to the strains in the cartridge cases simulated using the conventional design, it was determined that the design for the implementation should have a CDL radius of $r_{cdl} = 11\text{mm}$. The determination of the die design was presented in chapter 6. Furthermore, when testing the designs performance in regards to the presence of a die tilt, it was concluded that the design had a stabilizing effect, though highly influenced by the previously observed effects of having a reduction of the cartridge cases inner diameter.

In regards to the third problem statement was dies for the chosen die design manufactured and implemented to the ironing process performed at DENEX. It was discovered that the design did not provide conforming cartridge cases since they tended to fracture during the draw at station 3. It was likewise observed that the cartridge cases that did not fracture had a tendency towards necking in the observed fracture zone. Based on observation at the produced cartridge cases was it concluded that a possible cause for the design failure is that the tested CDL design is subjected to different friction conditions than the conventional design.

Perspectives 9

The following chapter contains a reflection on the project content in the form of a discussion on possible directions for future work. The following topics are considered:

- Redesign of the process in order to avoid reduction of the cartridge cases inner diameter
- Investigation of the assumed higher friction for the CDL design
- Investigation of the critical reduction ratio
- Determination of a CDL design were the dies are not constrained to use the same CDL radius

Redesign of the process in order to avoid reduction of the cartridge cases inner diameter:

As discovered in chapter 5 and 6 is one of the major stability issues connected to the ironing process of 5.56mm NATO cartridge cases that a reduction inner diameter is performed at each ironing station. By redesigning the process to exclude this reduction is assumed that a major improvement of both the process stability and cartridge case quality can be obtained.

Investigation of the assumed higher friction for the CDL design:

From the implementation of the CDL design to the ironing process at DENEX is it discovered that the design was not able to produce conforming cartridge cases and that a possible cause for this could be linked to a having a higher friction between the cartridge case and the dies, hence further work have to be conducted in order to determine the cause for the assumed higher friction. Possible directions for this investigation could be:

- Inspect if the dies have been manufactured with the specified surface finish
- Make further investigation concerning the contact pressure between the dies and the cartridge case. As seen at figure 5.19 and 5.20 does the conventional design and the CDL design have different pressure profiles on the die which could be suspected to influence the lubrication during the draw.

Determination of a CDL design were the dies are not constrained to use the same CDL radius:

During the determination of the CDL design for the implementation, was one of the major assumptions that a suitable design could be found when using the same CDL radius for all of the dies in the setup. This assumption was introduced to the determination process due to having a limited time frame for the investigation, hence it is assumed that a better design can be obtained when determining a suitable CDL radius for each of the dies in the setup.

Investigation of the critical reduction ratio:

A topic within the field of ironing that have not been regarded in the project is to investigate if the ironing process of 5.56mm NATO cartridge cases are subjected to instability caused by exceeding the critical reduction ratio. The critical reduction ratio is described in [Danckert, 2005], and is when an ironing process reaches a certain reduction ratio, then the equilibrium between the radial forces can be obtained both by introducing an increased or decreased reduction ratio. This effect can be seen on figure 3.3

List of Figures

| | | |
|------|--|----|
| 1.1 | 5.56mm NATO cartridge | 3 |
| 1.2 | Cartridge terminology..... | 4 |
| 1.3 | Basic ironing setup, based on figure 11.5 and 11.6 in [Avitzur, 1983] | 5 |
| 1.4 | New Lachaussée 702 cartridge case press [New Lachaussée, 2017] | 6 |
| 1.5 | Simplified illustration of the ironing setup for 5.56mm cartridge cases ... | 7 |
| 1.6 | 5.56mm cartridge case specifications..... | 8 |
| 1.7 | Simplified ironing model | 10 |
| 1.8 | Output cartridges for ironing station 1, 2 and 3 | 11 |
| 1.9 | Approach for multi-station ironing simulation | 12 |
| 1.10 | Evaluation of model accuracy | 13 |
| 1.11 | Visual inspection of the manufactured cartridge cases | 14 |
| 1.12 | Eccentric alignment of the cartridge case..... | 14 |
| 1.13 | Die tilt | 14 |
| 1.14 | Results of tilt scenarios | 15 |
| 3.1 | Conventional and CDL die design..... | 19 |
| 3.2 | Radial forces on the die | 20 |
| 3.3 | Radial force as function of reduction ratio [Danckert, 2005, figure 56] | 20 |
| 3.4 | The effect on the radial forces introduced by a small die tilt [Danckert, 2005, figure 56] | 20 |
| 3.5 | Geometric effects of introducing a die tilt | 21 |
| 3.6 | Comparison of conventional and CDL design when introducing a small die tilt | 21 |
| 3.7 | Design of CDL dies..... | 22 |
| 4.1 | Geometric representation of ironing station 1 | 26 |
| 4.2 | Die notation | 26 |
| 5.1 | Effective plastic strain - Station 1 - 0.00° die tilt - Conventional die design | 31 |
| 5.2 | Effective plastic strain - Station 1 - 0.00° die tilt - $r_{cdl} = 6.80mm$ | 31 |
| 5.3 | Effective plastic strain - Station 1 - 0.00° die tilt - $r_{cdl} = 10.34mm$ | 31 |
| 5.4 | Effective plastic strain - Station 1 - 0.00° die tilt - $r_{cdl} = 13.89mm$ | 31 |
| 5.5 | Effective plastic strain - Station 1 - 0.00° die tilt - $r_{cdl} = 17.44mm$ | 31 |
| 5.6 | Effective plastic strain - Station 1 - 0.00° die tilt - $r_{cdl} = 20.98mm$ | 31 |
| 5.7 | F_y - Station 1 - Punch - 0.00° die tilt | 32 |
| 5.8 | Punch force components | 32 |
| 5.9 | F_z - Station 1 - Punch - 0.00° die tilt | 33 |
| 5.10 | F_z - Station 1 - Die 2 x^- - 0.00° die tilt..... | 33 |
| 5.11 | The CDL radius, r_{cdl} , influence on the inlet angle, α | 34 |
| 5.12 | F_x - Station 1 - Die 2 x^- - 0.00° die tilt | 34 |
| 5.13 | Cartridge bottom profile - Station 1 - 0.00° die tilt | 35 |

| | | |
|------|--|----|
| 5.14 | Force distribution at the cartridge case entry to the die | 35 |
| 5.15 | Cartridge height - Station 1 - 0.00° die tilt | 36 |
| 5.16 | Cartridge bottom profile - Station 1 - 0.00° die tilt | 36 |
| 5.17 | Maximum interface pressure - Station 1 - Die 2 x^- - 0.00° die tilt..... | 37 |
| 5.18 | Contact zone for the CDL design | 37 |
| 5.19 | Contact pressure - Station 1 - Die 2 x^- - 0.00° die tilt - Conventional die design | 38 |
| 5.20 | Contact pressure - Station 1 - Die 2 x^- - 0.00° die tilt - $r_{cdl} = 6.80\text{mm}$.. | 38 |
| 5.21 | x-displacement - Station 1 - Punch - 0.20° die tilt..... | 40 |
| 5.22 | x-displacement - Station 1 - Punch - 0.40° die tilt..... | 40 |
| 5.23 | Initial position of the cartridge case for the conventional design - $t = 0\text{s}$ - 0.40° die tilt..... | 41 |
| 5.24 | Initial cartridge rotation due to impact for the conventional design - $t = 0.001\text{s}$ - 0.40° die tilt | 41 |
| 5.25 | Material distribution in the cartridge case top - $t = 0.011\text{s}$ - 0.40° die tilt - Conventional design | 41 |
| 5.26 | Cartridge case height difference, Δh | 42 |
| 6.1 | Cartridge case snap due to tool wear | 44 |
| 6.2 | Effective plastic strain - Station 1 - 0.00° die tilt - Conventional die design | 46 |
| 6.3 | Effective plastic strain - Station 1 - 0.00° die tilt - $r_{cdl} = 9\text{mm}$ | 46 |
| 6.4 | Effective plastic strain - Station 1 - 0.00° die tilt - $r_{cdl} = 11\text{mm}$ | 46 |
| 6.5 | Effective plastic strain - Station 1 - 0.00° die tilt - $r_{cdl} = 13\text{mm}$ | 46 |
| 6.6 | Effective plastic strain - Station 2 - 0.00° die tilt - Conventional die design | 47 |
| 6.7 | Effective plastic strain - Station 2 - 0.00° die tilt - $r_{cdl} = 9\text{mm}$ | 47 |
| 6.8 | Effective plastic strain - Station 2 - 0.00° die tilt - $r_{cdl} = 11\text{mm}$ | 47 |
| 6.9 | Effective plastic strain - Station 2 - 0.00° die tilt - $r_{cdl} = 13\text{mm}$ | 47 |
| 6.10 | Effective plastic strain - Station 3 - 0.00° die tilt - Conventional die design | 48 |
| 6.11 | Effective plastic strain - Station 3 - 0.00° die tilt - $r_{cdl} = 9\text{mm}$ | 48 |
| 6.12 | Effective plastic strain - Station 3 - 0.00° die tilt - $r_{cdl} = 11\text{mm}$ | 48 |
| 6.13 | Effective plastic strain - Station 3 - 0.00° die tilt - $r_{cdl} = 13\text{mm}$ | 48 |
| 6.14 | F_z - Station 1 - Punch - 0.00° die tilt | 50 |
| 6.15 | F_z - Station 2 - Punch - 0.00° die tilt | 50 |
| 6.16 | F_z - Station 3 - Punch - 0.00° die tilt | 50 |
| 6.17 | Maximum interface pressure - Station 1 - Die 1 and 2 x^- - 0.00° die tilt. | 51 |
| 6.18 | Maximum interface pressure - Station 2 - Die 1 and 2 x^- - 0.00° die tilt. | 51 |
| 6.19 | Maximum interface pressure - Station 3 - Die 1 x^- - 0.00° die tilt..... | 51 |
| 6.20 | x-displacement - Station 1 - Punch - 0.20° die tilt..... | 53 |
| 6.21 | x-displacement - Station 1 - Punch - 0.40° die tilt..... | 53 |
| 6.22 | x-displacement - Station 2 - Punch - 0.20° die tilt..... | 53 |
| 6.23 | x-displacement - Station 2 - Punch - 0.40° die tilt..... | 54 |
| 6.24 | x-displacement - Station 3 - Punch - 0.20° die tilt..... | 54 |
| 6.25 | x-displacement - Station 3 - Punch - 0.40° die tilt..... | 54 |
| 6.26 | Cartridge bottom profile - Station 3 - 0.40° die tilt | 55 |
| 7.1 | Manufactured CDL dies | 57 |
| 7.2 | Cartridge cases produced by the CDL dies..... | 57 |

| | | |
|-----|---|----|
| 7.3 | Cartridge case snap during the 3 rd draw | 58 |
| 7.4 | Necking in the cartridge cases produced by the CDL dies | 58 |
| 7.5 | Surface finish of cartridge cases produced by the CDL dies..... | 59 |
| 7.6 | Surface finish of cartridge cases produced by the conventional dies | 59 |

List of Tables

| | | |
|-----|--|----|
| 1.1 | 5.56mm cartridge case specifications | 8 |
| 1.2 | Model parameters and settings | 10 |
| 3.1 | Geometric effects of introducing a small die tilt | 21 |
| 3.2 | Minimum die land radii | 23 |
| 3.3 | Maximum die land radii | 23 |
| 3.4 | Design space for the CDL dies die land radius | 24 |
| 4.1 | Applied constraints | 27 |
| 5.1 | Implemented CDL radii | 30 |
| 5.2 | The CDL designs effect on the ironing process when increasing the CDL radius, r_{cdl} | 38 |
| 5.3 | CDL designs resemblance to the conventional design | 39 |
| 5.4 | Cartridge case height difference | 42 |
| 6.1 | Considered design space for the design determination | 44 |
| 6.2 | Height difference - 0.20° die tilt | 56 |
| 6.3 | Height difference - 0.40° die tilt | 56 |
| 8.1 | The CDL designs influence on the ironing process when increasing the die land radius, and the CDL radius that provides the closet fit to the conventional die design when comparing the effect | 62 |

Bibliography

- Adamic et al., 2008.** D. Adamic, M. Stefanovic, M. Plancak and S. Aleksandrovic. *Analysis of change of total ironing force and friction on punch at ironing.* Journal for Technology of Platicity, 33, 23–37, 2008.
- Avitzur, 1983.** Betzalel Avitzur. *Handbook of metal-forming processes.* John Wiley and Sons, Inc., first edition, 1983. ISBN 0-471-03474-6.
- Danckert, 2005.** Joachim Danckert. *Analysis of deep drawing, ironing and backward can extrusion.* Department of production, AAU, 2005.
- New Lachaussee, 2017.** *New Lachaussee.*
http://www.lachaussee.com/en_US/ammunition-munitions/l, 2017. Downloaded d. 20-04-2017.
- Pedersen, 2016.** Jakob Bengtson Pedersen. *Process modelling of cartridge case ironing,* 2016. Student report.

Process stabilization of cartridge case ironing

AN INVESTIGATION OF THE STABILIZING EFFECTS INTRODUCED BY USING A CIRCULAR
DIE LAND IN CARTRIDGE CASE IRONING

By

JAKOB B. PEDERSEN



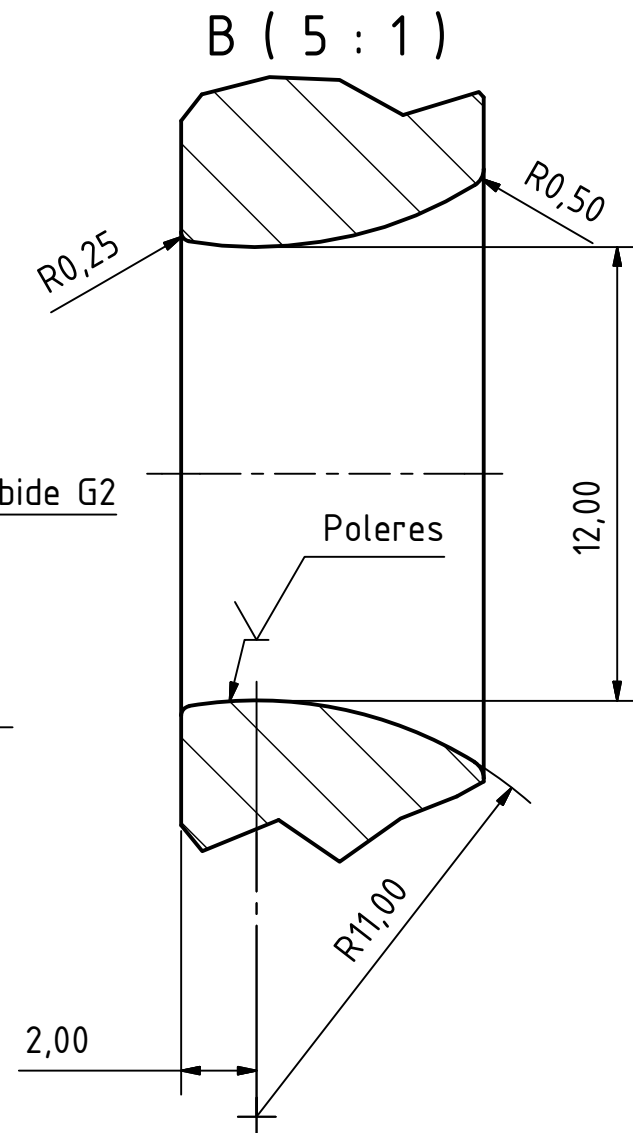
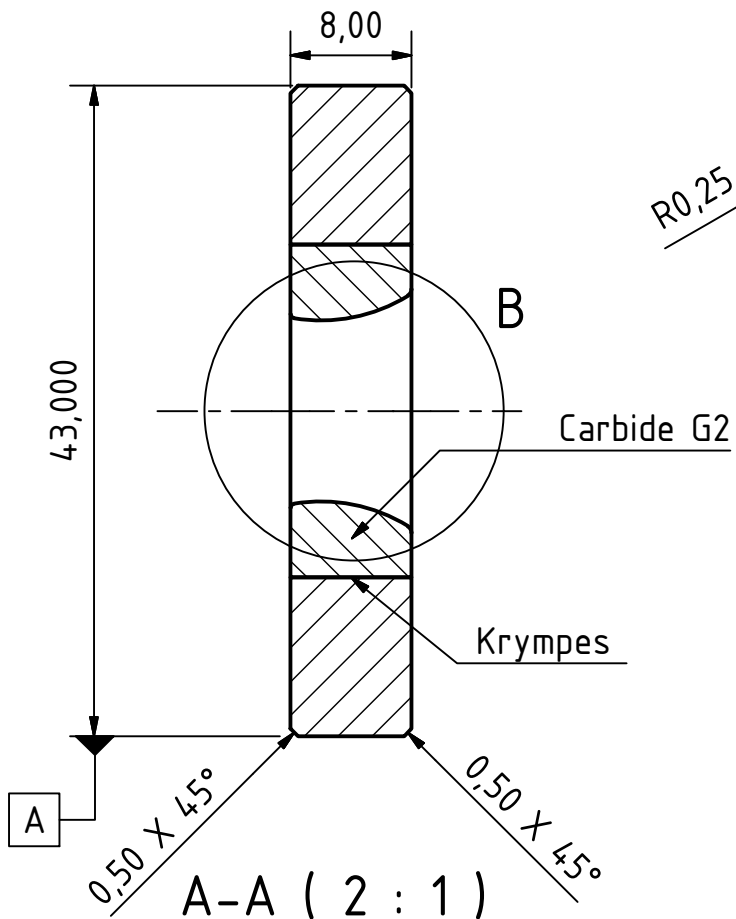
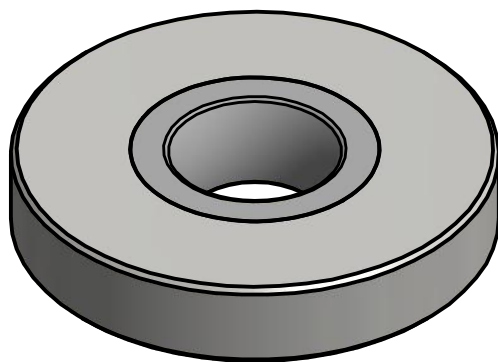
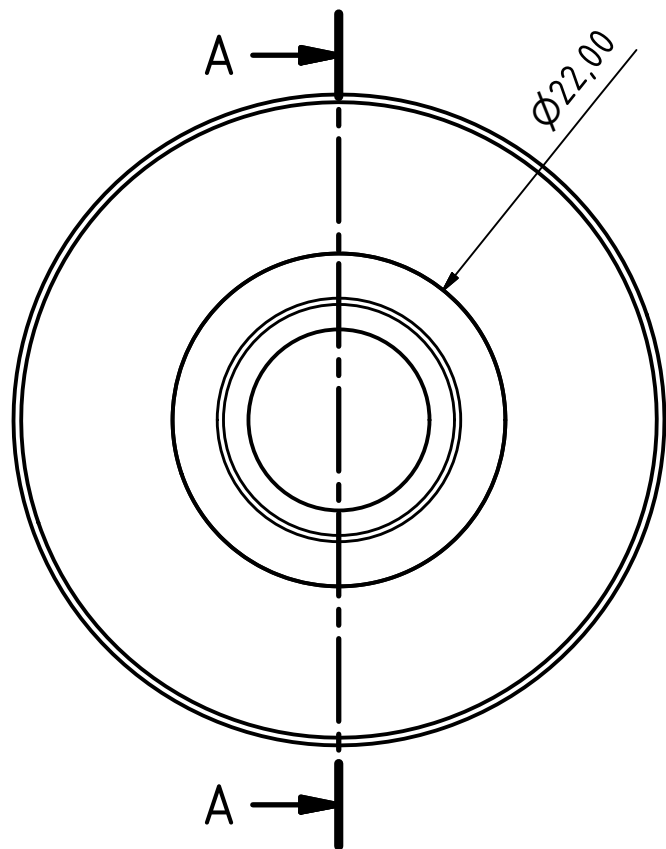
AALBORG UNIVERSITY
STUDENT REPORT

APPENDIX

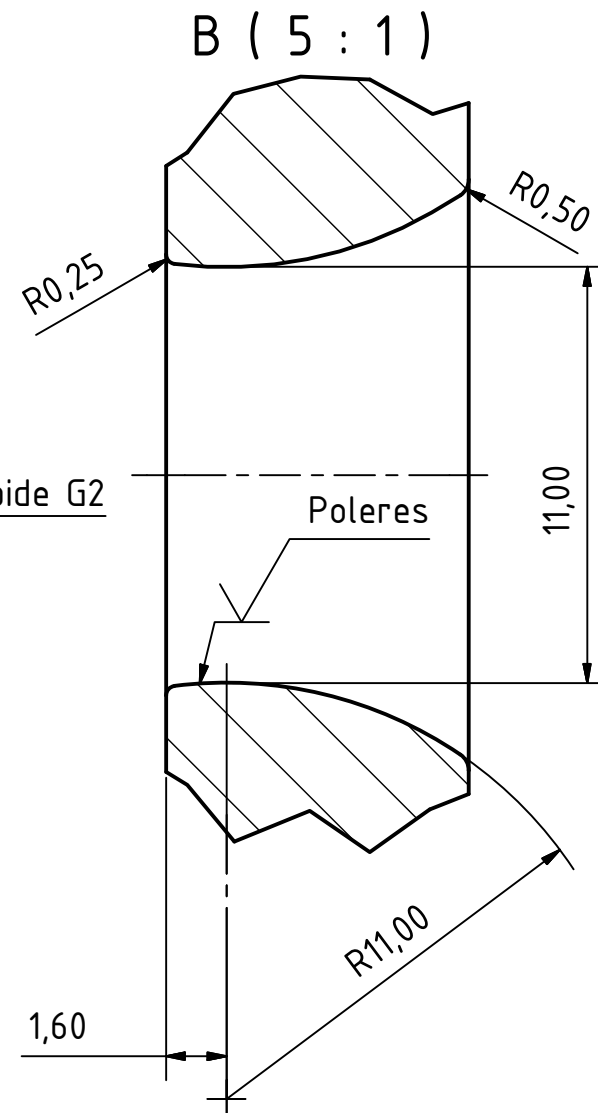
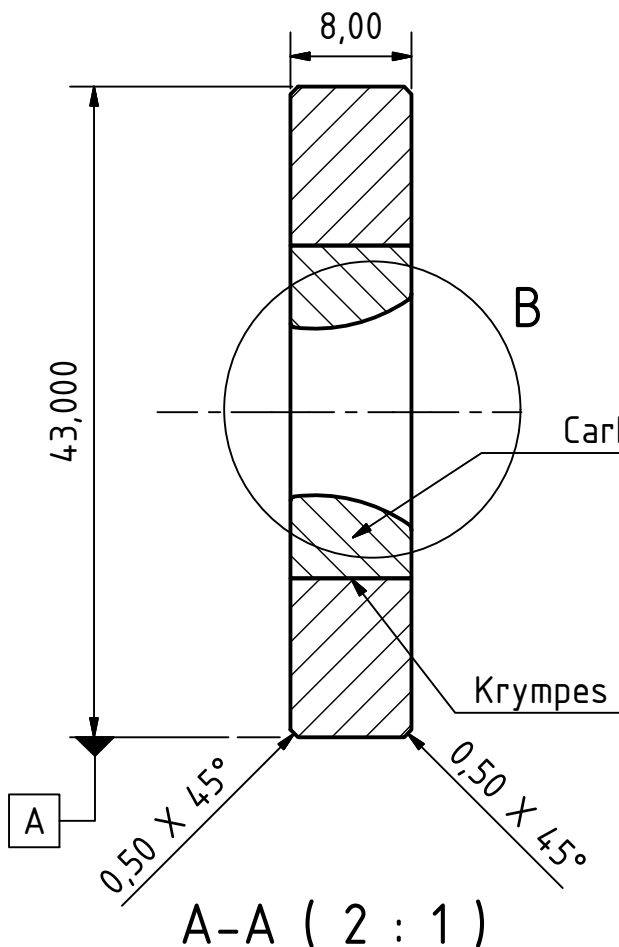
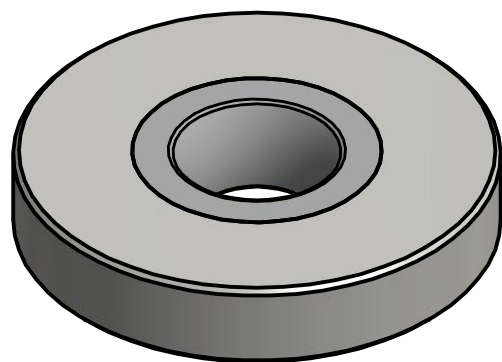
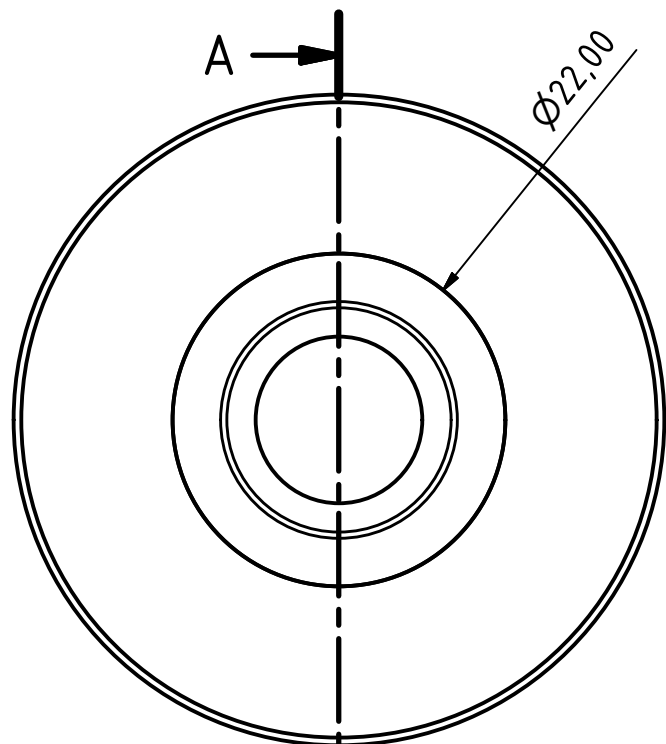
Table of content

| | |
|--|-----|
| Appendix A: Drawings | 5 |
| Appendix B: Reading guide for chapter C and D | 11 |
| Appendix C: Initial investigation of CDL effects | 21 |
| Appendix D: Determination of final CDL radius | 43 |
| Appendix E: LS-Dyna model | 129 |

Drawings A

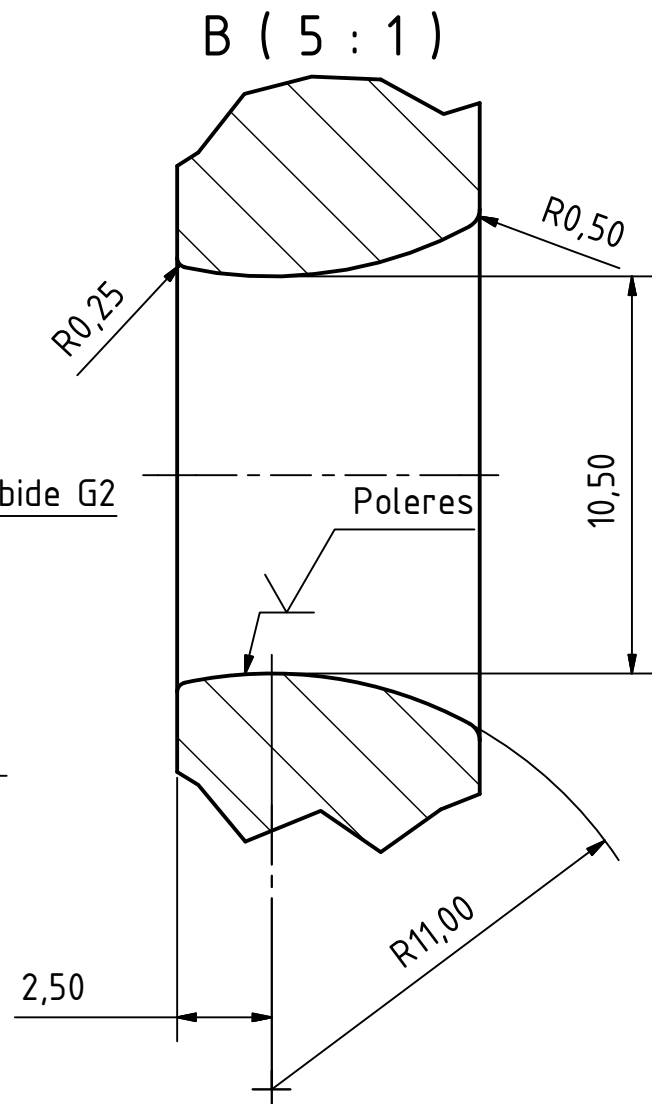
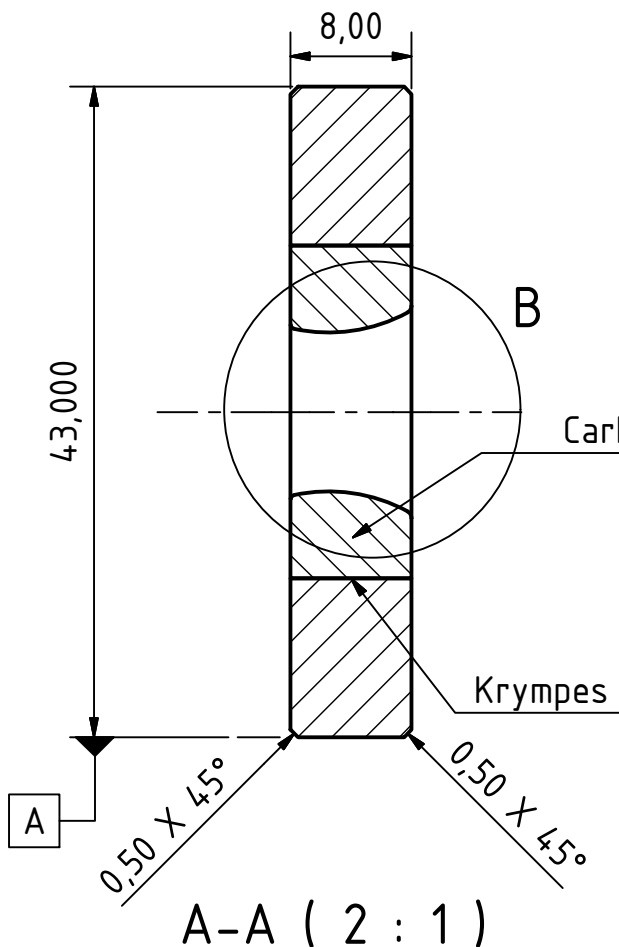
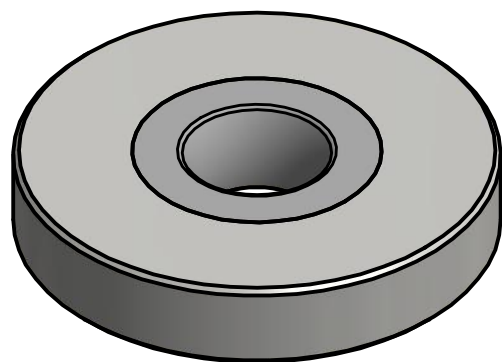
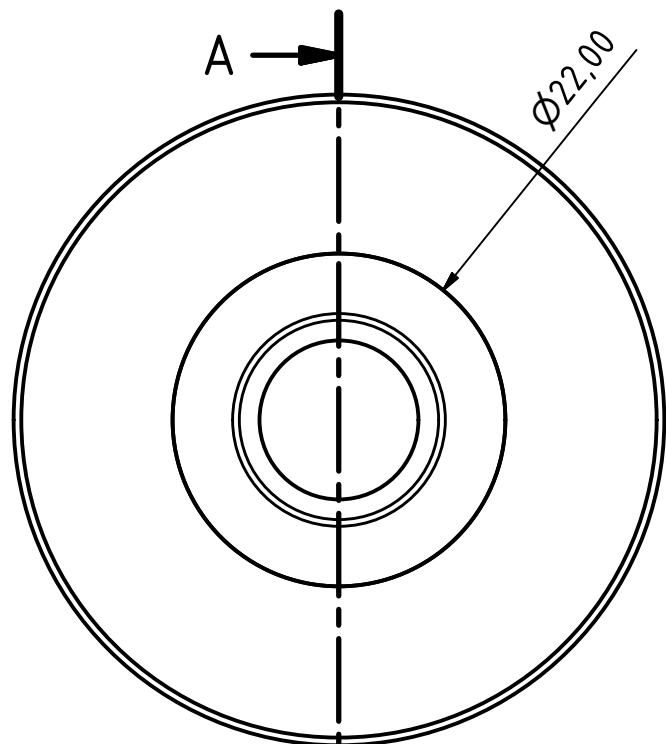


| | | | | | | | |
|-------------------------------|---------|------|------|-----------------|---------|--|--|
| Material: | | | | Name: | | | |
| Surface treatment: | | | | 1. Strækmatrice | | | |
| Work Standard: DS/EN ISO 1302 | | | | Station 2 + 8 | | | |
| Allowance: ISO 2798-m | | | | 5,56mm | | | |
| State | Changes | Date | Name | Part No.: | 0000001 | | |
| | | | | | 1 | | |
| | | | | | A4 | | |

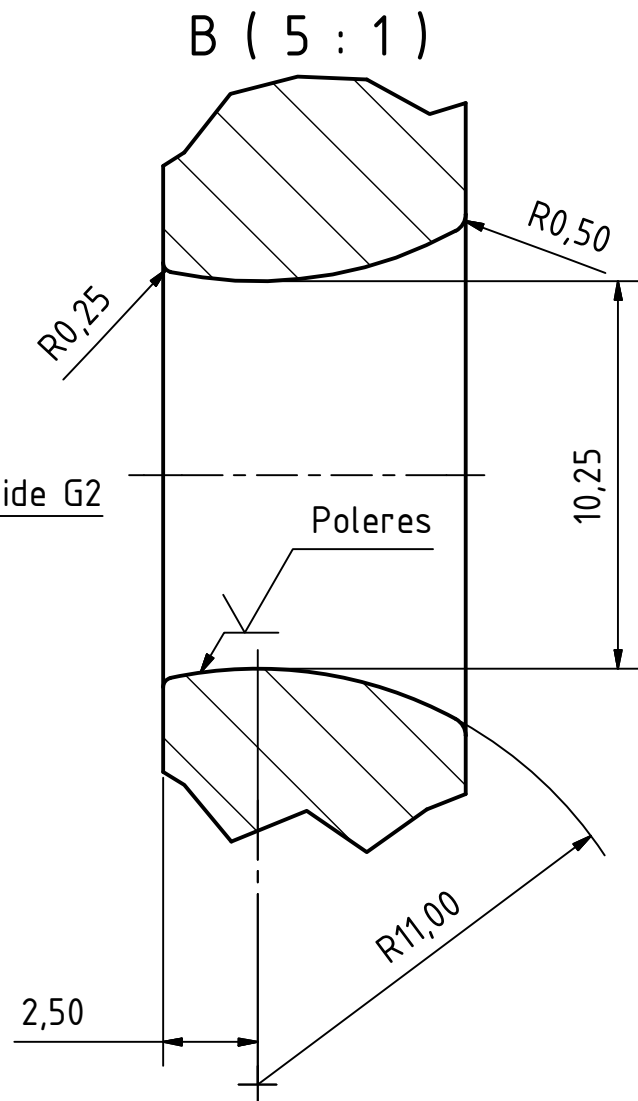
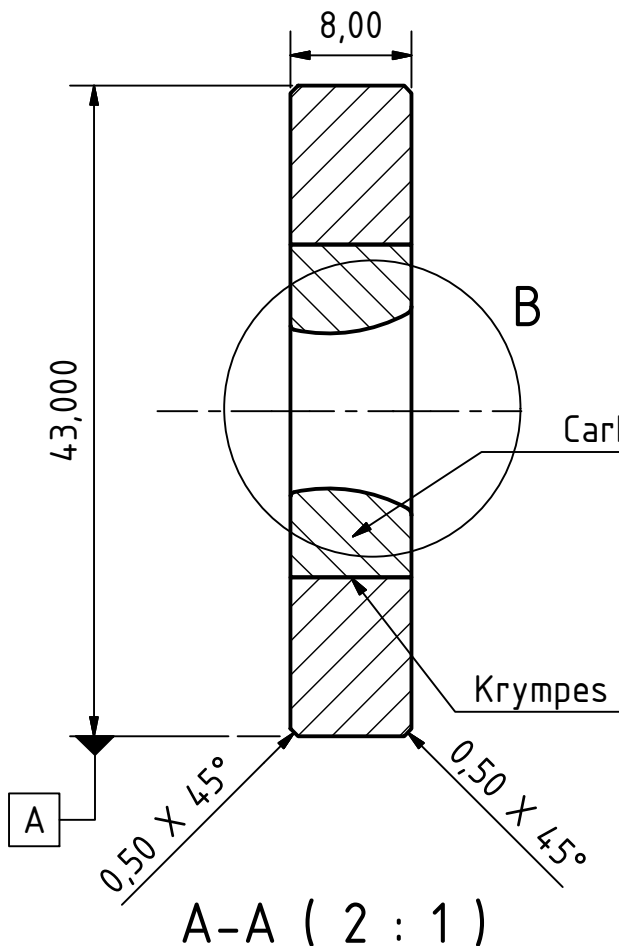
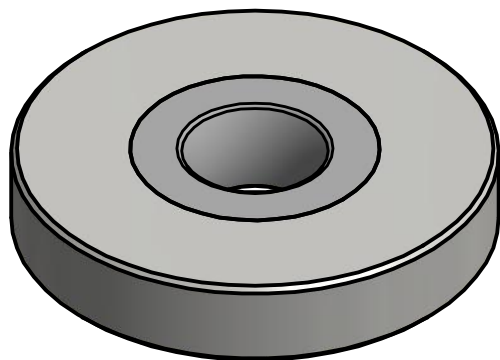
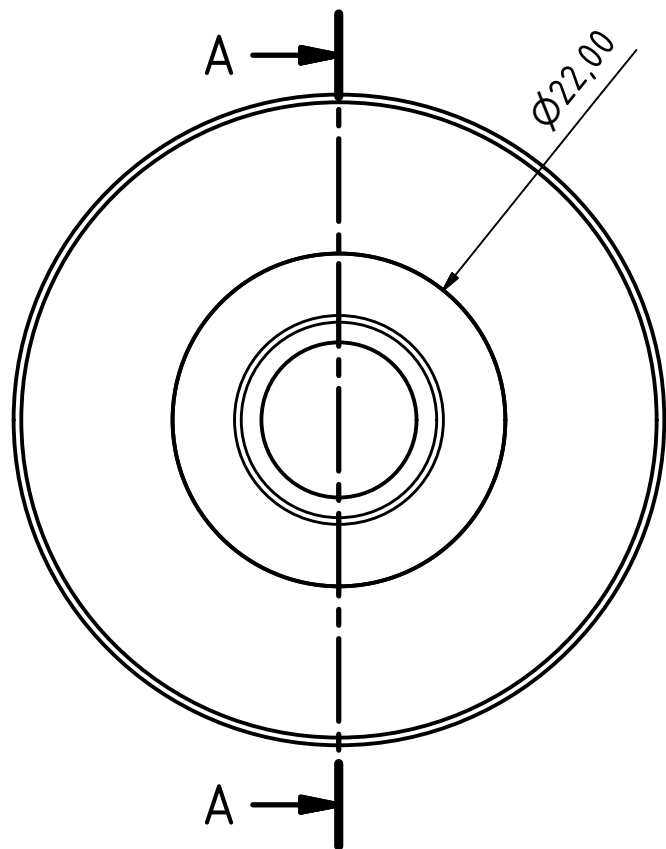


| | | | |
|-------|---------|------|------|
| | | | |
| State | Changes | Date | Name |

| | | | | | |
|-------------------------------|--|--|-------------------|--|--|
| Material: | | | Name: | | |
| Surface treatment: | | | 2. Strækmatrice | | |
| Work Standard: DS/EN ISO 1302 | | | Station 2 + 8 | | |
| Allowance: | | | 5,56mm | | |
| ISO 2798-m | | | Part No.: 0000002 | | |
| Drawn | | | 1 | | |
| Checked | | | A4 | | |

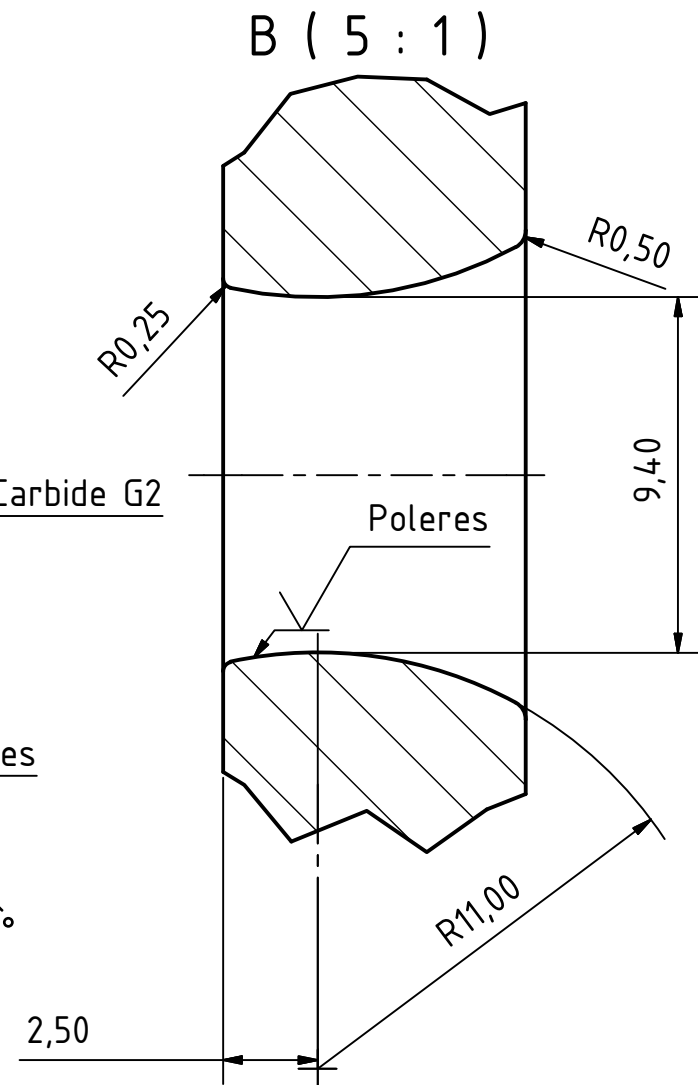
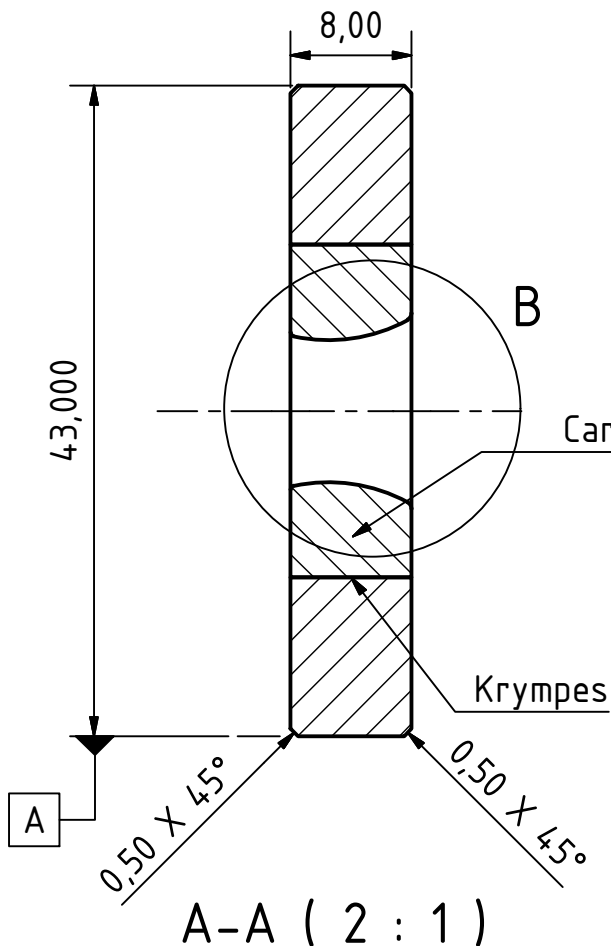
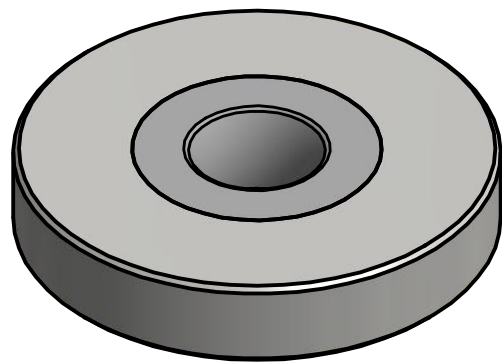
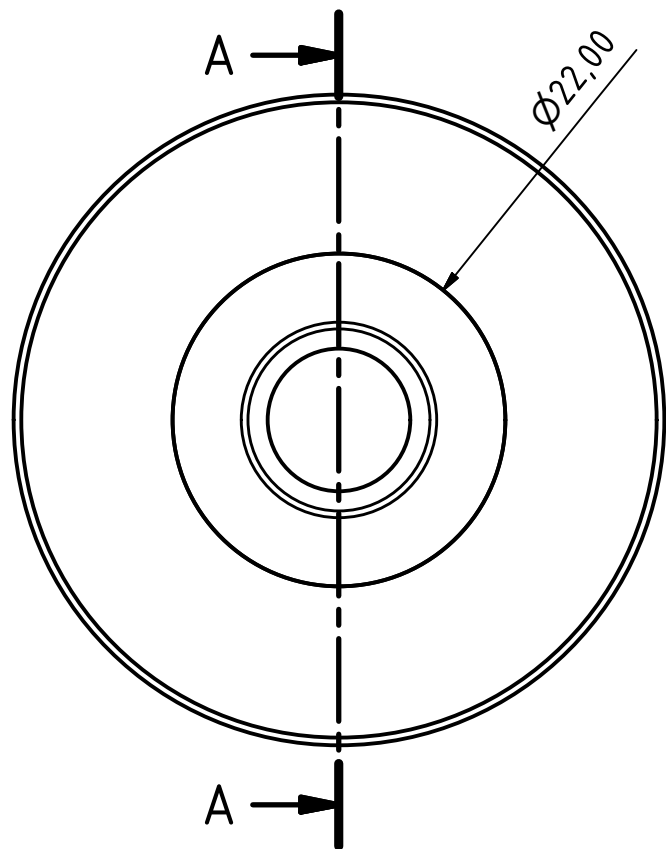


| | | | | | | | |
|-------------------------------|--|--|--|-----------------|--|--|--|
| Material: | | | | Name: | | | |
| Surface treatment: | | | | 3. Strækmatrice | | | |
| Work Standard: DS/EN ISO 1302 | | | | Station 3 + 9 | | | |
| Allowance: | | | | 5,56mm | | | |
| ISO 2798-m | | | | Part No.: | | | |
| Drawn | | | | 0000003 | | | |
| Checked | | | | 1 | | | |
| State | | | | A4 | | | |



| | | | |
|-------|---------|------|------|
| | | | |
| State | Changes | Date | Name |

| | | | | | |
|-------------------------------|---------|------------|------|---|----|
| Material: | | | | Name: 4. Strækmatrice Station 3 + 9 5,56mm | |
| Surface treatment: | | | | | |
| Work Standard: DS/EN ISO 1302 | | Date | Name | Part No.: 0000004 | 1 |
| Allowance: ISO 2798-m | Drawn | 23/03/2017 | JBP | | A4 |
| | Checked | | | | |



| | | | | | | | |
|-------------------------------|--|--|--|-----------------|--|--|--|
| Material: | | | | Name: | | | |
| Surface treatment: | | | | 5. Strækmatrice | | | |
| Work Standard: DS/EN ISO 1302 | | | | Station 4 + 10 | | | |
| Allowance: | | | | 5,56mm | | | |
| ISO 2798-m | | | | Part No.: | | | |
| Drawn | | | | 0000005 | | | |
| Checked | | | | 1 | | | |
| State | | | | A4 | | | |

Reading guide for chapter C and D

B

This chapter serves as a reading guide for chapter C and D, thereby presenting the structure behind how the data in the respective chapters are presented, and how these data are obtained and processed. The description of which simulations and investigations the data are representing is presented in the individual chapters.

B.1 Data structure

The structure for how the data is presented, follows the same approach throughout the concerned chapters, and is illustrated below at figure B.1.

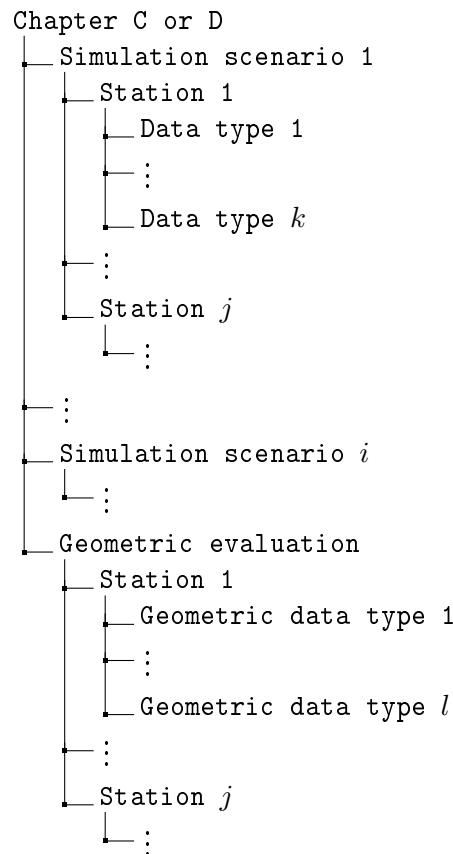


Figure B.1. Data structure for chapter C and D

From figure B.1 it can be seen that each of the concerned chapters are divided into range of sub-levels. The first level of the sub-levels specifies either the simulation scenario which

is investigated or contains a geometric evaluation of the results gathered from all the investigated scenarios. The second level specifies which ironing station the data is gathered from. The third level specifies the type of data which is presented. A description of the different data types can be found in section B.3 and B.4.

B.2 Die notation

Throughout the concerned chapters, data is presented for both forces and pressures between the cartridge case and the individual tools in the ironing setup i.e. the dies and the punch. Since each station in the setup consists of multiple dies, and that each die is modelled in two parts, the following notation is introduced:

- Die 1 x^+ : Top right die at figure B.2
- Die 1 x^- : Top left die at figure B.2
- Die 2 x^+ : Bottom right die at figure B.2
- Die 2 x^- : Bottom left die at figure B.2

The terminology of x^- and x^+ describes on which side of the models global x origin the part is positioned i.e. x^- is positioned at the left side, and x^+ on the right side in regards to the orientation seen on figure B.2. It have to be noted that the term of die 1 and 2 are local names, and thereby depended on which ironing station they are regarded in relation to.

B.3 Data Types

The results that are presented for each of the stations in chapter C and D, covers a series of different data types:

- Effective Plastic strain
- Resultant force
- x-forces
- z-forces
- Maximum interface pressure

In the following the methods for collecting and processing the data are described.

B.3.1 Effective plastic strain

The effective plastic strain results are gathered from the last state of the simulation, by dumping an image displaying the effective plastic strain distribution, **fringe 7** in LS-PrePost, for the cartridge. At figure B.3 an example of this is shown:

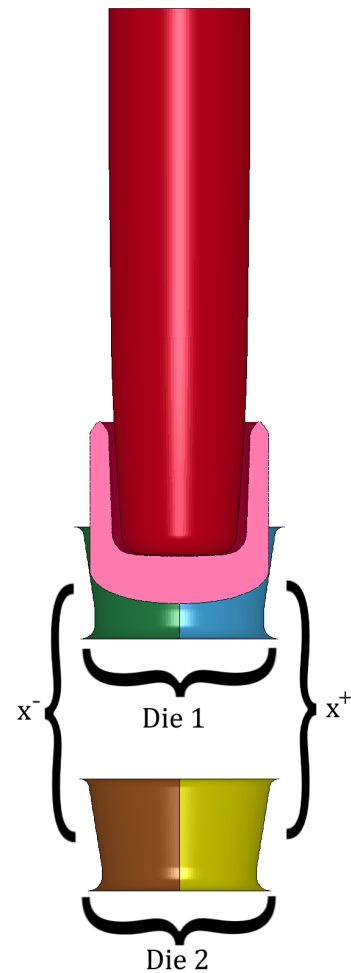


Figure B.2. Die notation

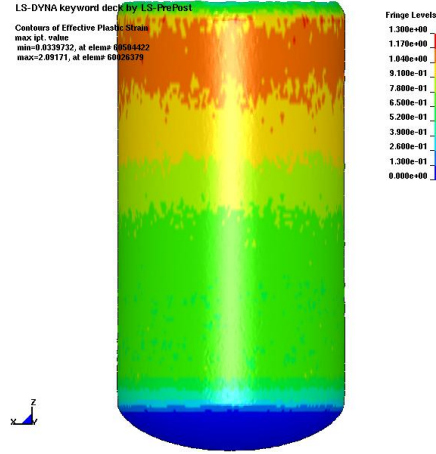


Figure B.3. Example of effective plastic strain plot

It have to be noted that the cartridges have been rotated 180° around the z-axis compared to the orientation at figure B.2 i.e. the x^+ side is now positioned to the left at the image, and vice versa. Furthermore, it has to be noted that the range of the legend has been fixed in order to ensure visual comparability between the results. The following fringe ranges have been used:

| | ε_{min} | ε_{max} |
|-----------|---------------------|---------------------|
| Station 1 | 0 | 1.3 |
| Station 2 | 0 | 2.0 |
| Station 3 | 0 | 3.0 |

Table B.1. Applied effective plastic strain ranges

B.3.2 Force data

Throughout chapter C and D are the contact forces between the cartridge and the tools displayed in the form of the resultant contact force F_{res} , and its components in the x and z-direction, F_x and F_z . These information is gathered from the **rcforc** ascii file produced by LS-Dyna, through LS-PrePost, where the forces for the considered contact pairs can be saved as a xy-pair, specifying the force in regards to elapsed simulation time. When writing the data from LS-Dyna, a dump frequency of 0.000015s is used e.g. a simulation with a termination time of 0.02s will result in a data file with 1333 samples.

Along with presenting the x and z-forces for the dies, the force difference are likewise presented between the x^+ and x^- die parts in order to display how the die tilt affects the force balance. For the forces in the x direction, the difference, ΔF_x , is calculated by adding the x-force for the x^+ die part with the x-force for the x^- die part. For the z-force the difference, ΔF_z is obtained by subtracting the z-force for the x^+ die part from the z-force for the x^- die part. When visualizing the data for ΔF_x and ΔF_z it was observed that the data was subjected to severe oscillation, which makes it difficult to determine tendencies when comparing the results for different die designs. At figure B.4 an example of these oscillations are shown for die 2 at station 2 when comparing ΔF_z for the conventional die design with CDL designs using $r = 9mm$, $r = 11mm$ and $r = 13mm$ in a 0.20° tilt scenario, see section D.2.2.

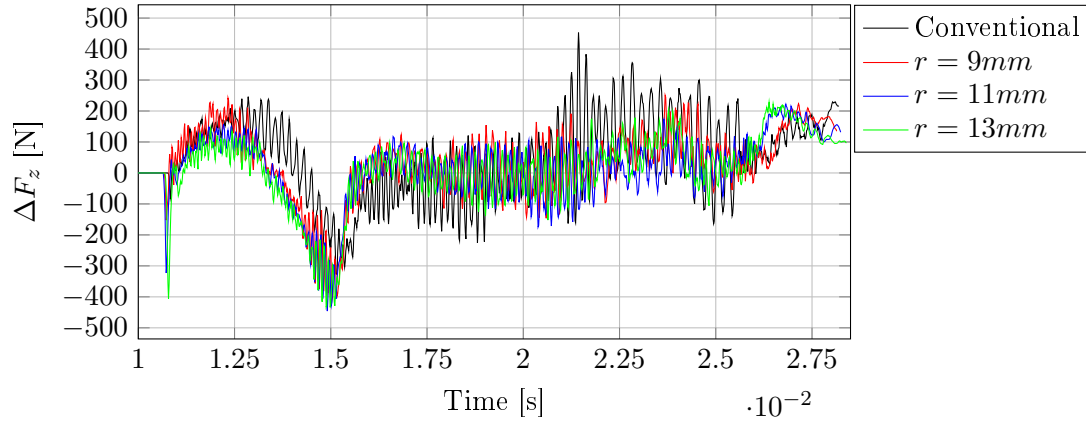


Figure B.4. ΔF_z - Station 2 - Die 2 - 0.20° die tilt - unfiltered

As seen on figure B.4 the oscillations makes it difficult to compare the results and derive tendencies associated with the use of different die designs. In order to ease the comparison and identification of tendencies in the data, a filter is applied. For filtering the data Matlabs smooth function is used, using a lowess (LOcally WEighted Scatterplot Smoothing) filter with a span of 0.01%. By applying the filter to the ΔF_z data for the conventional die design shown on figure B.4, the results shown on figure B.5 are obtained, and likewise on figure B.6 when applying the filter to all the the data presented at figure B.4.

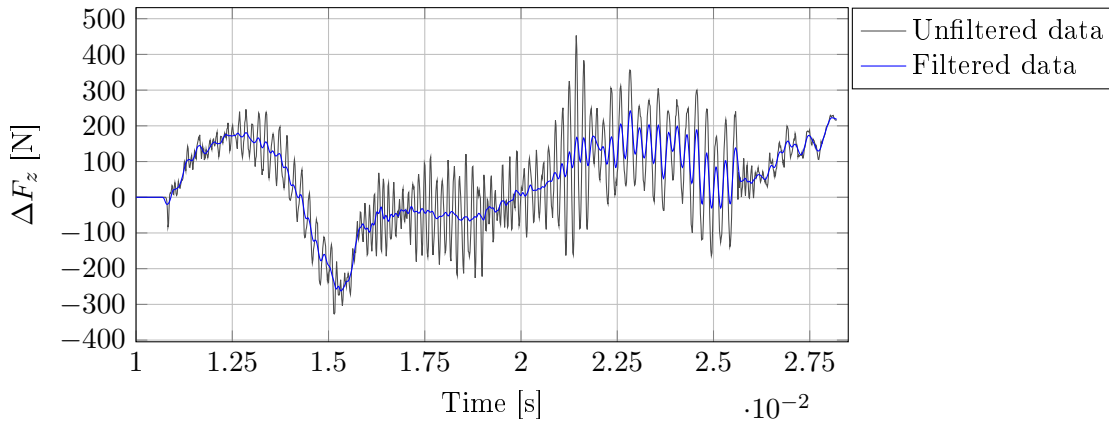


Figure B.5. ΔF_z - Station 2 - Conventional die 2 - 0.20° die tilt

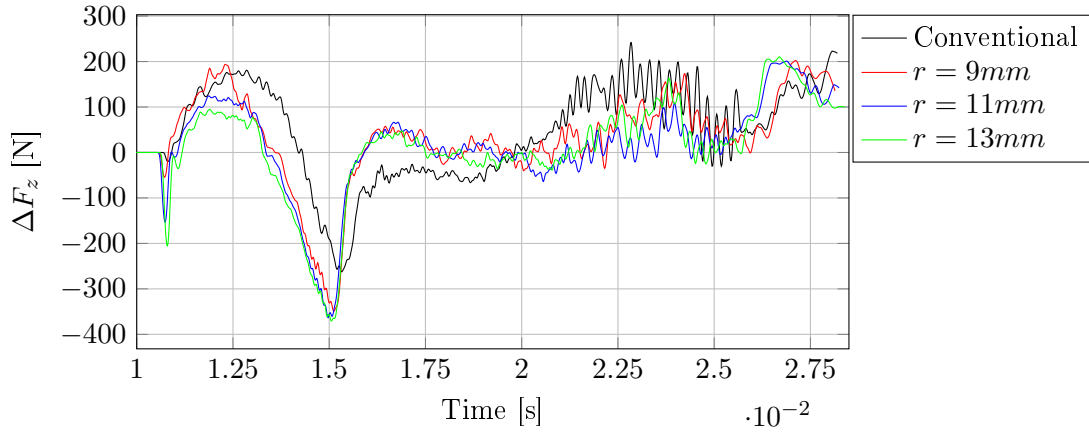


Figure B.6. ΔF_z - Station 2 - Die 2 - 0.20° die tilt - filtered

At figure B.5 and B.6 it can be seen that applying the filter to the data reduces the oscillations, and thereby makes it easier to distinguished and identify tendencies in the data when comparing data from multiple simulations. It have to be noted that smoothing a signal is a trade-off between data smoothness and peak information. This can be seen at figure B.4 and B.6 at ≈ 0.011 s, where the force peaks reaches a magnitude upto ≈ -400 N, whereas it for the filtered data is reduced to a magnitude upto ≈ -200 N. Since the purpose of displaying the x and z force difference between the die parts is to observe the force balance, it is deemed that a loss of peak information is acceptable, as long as the general outline of the data profile is preserved.

B.3.3 Maximum interface pressure

For the means of collecting the maximum interface pressure, the LS-Dyna `intfor` option is used, which writes a binary database that can be processed by LS-PrePost. The interface pressure can be visualized for the contact between the cartridge case and the tools in LS-PrePost by using the `fringe 1` option, see figure B.7.

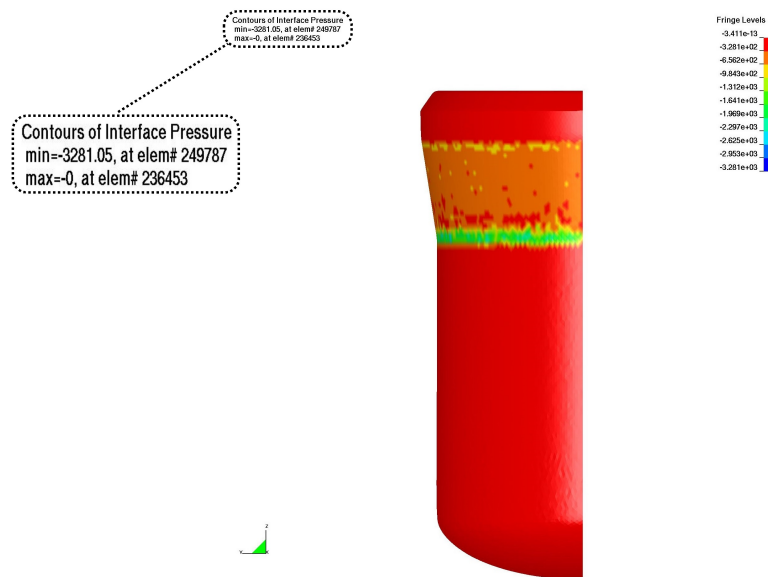


Figure B.7. Interface pressure - Station 1 - Conventional die 2 x^+ - 0.00° die tilt

In order to get a measurement for the interface pressure, that does not rely on visual inspection, the maximum interface pressure is used, which is displayed in the top left corner of the screen, see figure B.7. Note that the pressures are displayed as being negative, which is due to the cartridge case being defined as the slave surface in the contact definition i.e. the pressure appears as negative instead of positive.

For the means of collecting the information of the maximum pressure for each state in the simulation, LS-PrePost does not provide a direct solution for collecting the data besides to manually note the maximum pressure for each state in the simulation i.e. each simulation of a ironing station consist of 30 states, and the maximum pressure have to be gathered for the contact between the cartridge case and the individual die parts, which results in 120 pressure readings. The solution for gathering the data without manually inspect each time state for all the simulations, were to make LS-PrePost write an image for each time state, and afterwards process the images using Matlabs *optical character recognition* (OCR) feature for collect the maximum pressure at each image. At figure B.8 an example of the maximum pressure for the contact between the cartridge case and die 2 x^+ , see figure B.7, is shown.

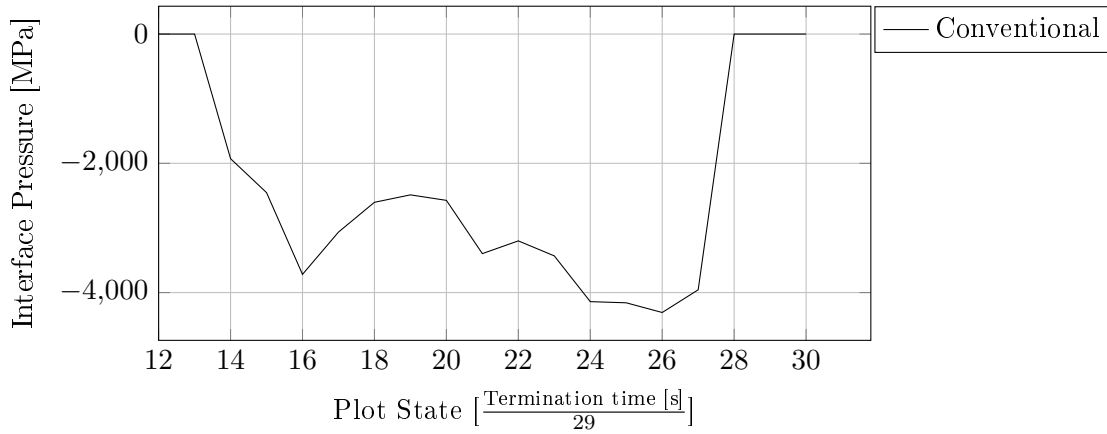


Figure B.8. Maximum interface pressure - Station 1 - Die 2 x^+ - 0.00° die tilt

It have to be noted that the pressures are not directly display as a function of time, but as function of the plot state. This is due to that the dump frequency for the `intfor` database is define as $\frac{\text{Termination time[s]}}{29}$, which yields 30 states per simulation. Since the simulations termination time is defined as a problem depend variable in the model, see [Pedersen, 2016, page 31-32], the termination times are not exactly the same when comparing the pressures from different simulations. This means that the elapsed simulation time at a given state is not exactly the same when comparing the results from different simulations, which have to be taken into consideration when evaluating the results.

B.4 Geometric data Types

The results that are presented for the geometric evaluation of the simulations covers the following areas:

- Punch displacement

- Cartridge height
- Projected cartridge height
- Cartridge bottom profile

In the following, the methods for collecting and processing the data are described.

B.4.1 Punch displacement

For the means of monitoring deflection of the punch, and thereby if there is a difference in the cartridge case wall thickness, the x-displacement of the punch is monitored. This is done by using LS-PrePost for measuring the x-displacement of one of the nodes in the punch.

B.4.2 Cartridge height

For the purpose of evaluating the stabilizing effects of implementing the CDL design to the dies, the cartridge case height are measured. This is done by evaluating the position of the nodes composing the cartridge case. By searching for the node with highest z-coordinate within the search area, β , for each search increment, ω , see figure B.9 and B.10, a angular representation of the cartridge case height can be obtained.

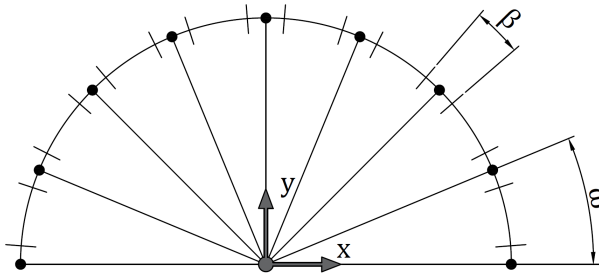


Figure B.9. Polar representation of the cartridge case height

Where:

| | |
|--|-------------|
| β | 3.8° |
| ω | 4° |
| No. measurements, $\frac{180^\circ}{\omega} + 1$ | 46 |

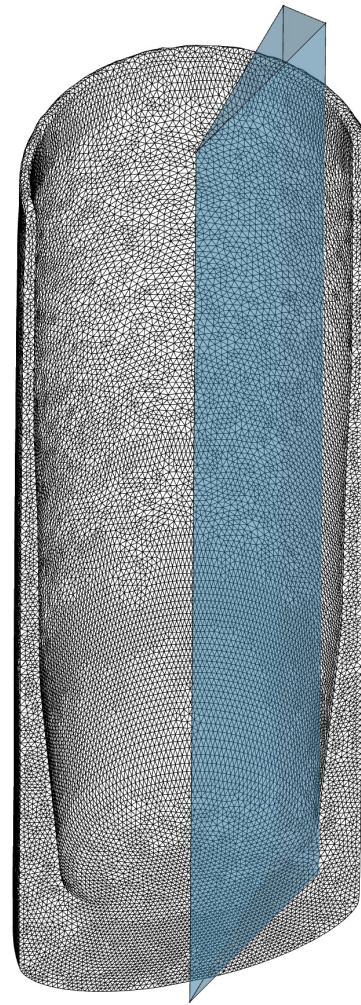


Figure B.10. Visualization of search area

As an example for the polar representation of the cartridge case height, figure B.11 shows the height after the first draw, when using the conventional die design with 0.20° die tilt.

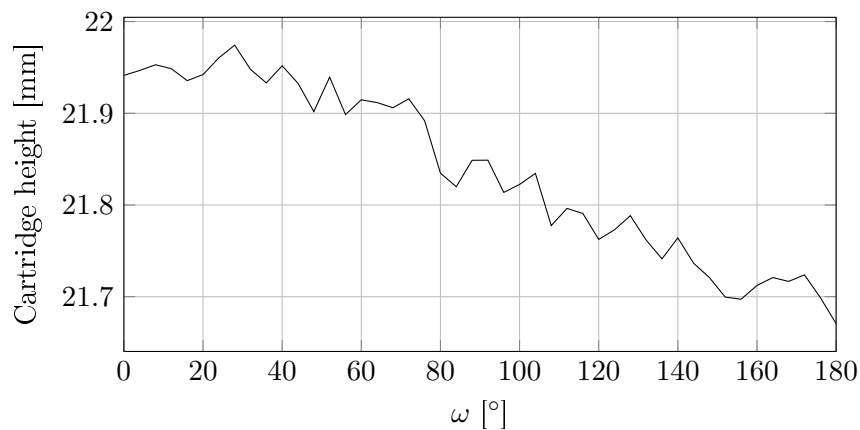


Figure B.11. Cartridge height - Station 1 - Conventional die design - 0.20° die tilt

B.4.3 Projected cartridge height

Another approach for visualizing the cartridge case height is to make a projection of the angular representation to the y-normal plane, see figure B.12 and B.13.

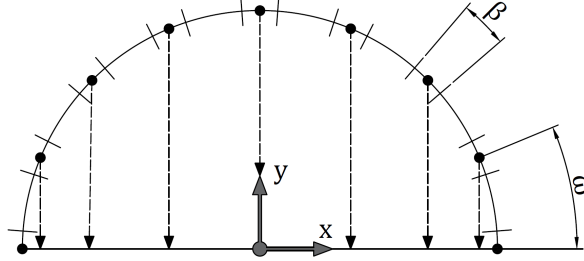


Figure B.12. Height projection to the y-normal plane

By using this transformation, a more linear representation of the cartridge case height is obtained, which is more similar to how the height is visually perceived. Furthermore, the more linear representation makes it possible to make a linear approximation of the height, and thereby use the slope as an measurement for the skewness of the cartridge case, see figure B.14. For determining the linear approximation of the height, Matlab's `fit` command is used, with the `'poly1'` as input option. For the example provided at figure B.14 the fit is described with the following approximation:

$$h(x) = 0.0255 \cdot x + 21.8350 \quad (\text{B.1})$$

With a r^2 value of:

$$r^2 = 0.9613 \quad (\text{B.2})$$

It have to be noted that when presenting the projected cartridge height, it is done in the form of Δh , and not as the absolute height as for the angular representation.

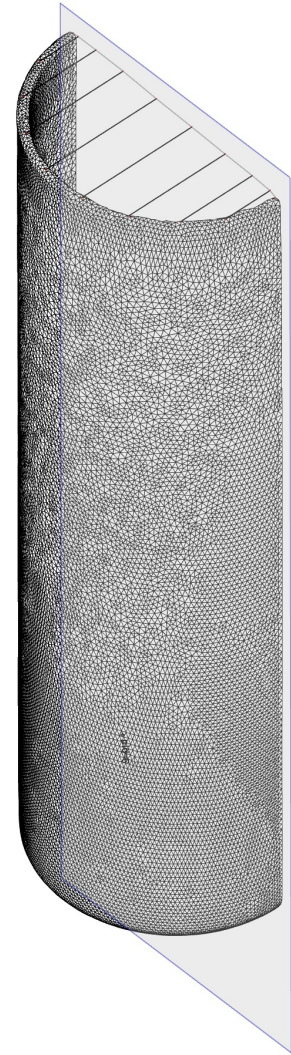


Figure B.13. Projection of cartridge case height to the y-normal plane

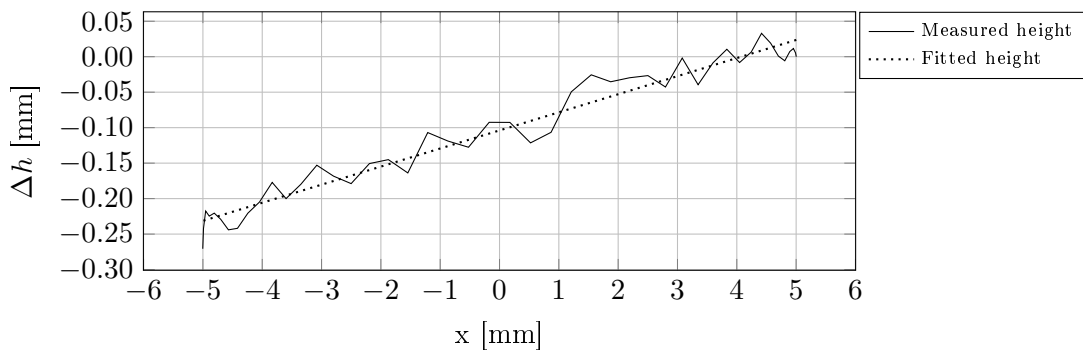


Figure B.14. Projected cartridge height difference - Station 1 - Conventional die design - 0.20° die tilt

B.4.4 Bottom profile

During the simulations, investigating the effects of implementing the CDL design to the dies, it was discovered that the use of different CDL radii's resulted in geometric changes in the cartridge case bottom. These changes was observed in the form of changes in thickness and both the inner an outer curvature of the bottom. In order to visualize these changes, the nodes intersected the symmetry plane is collected, see figure B.15, and processed through Matlab's `boundary` function, which outputs the nodes composing the outer edge of the processed 2D pointcloud, see figure B.16.

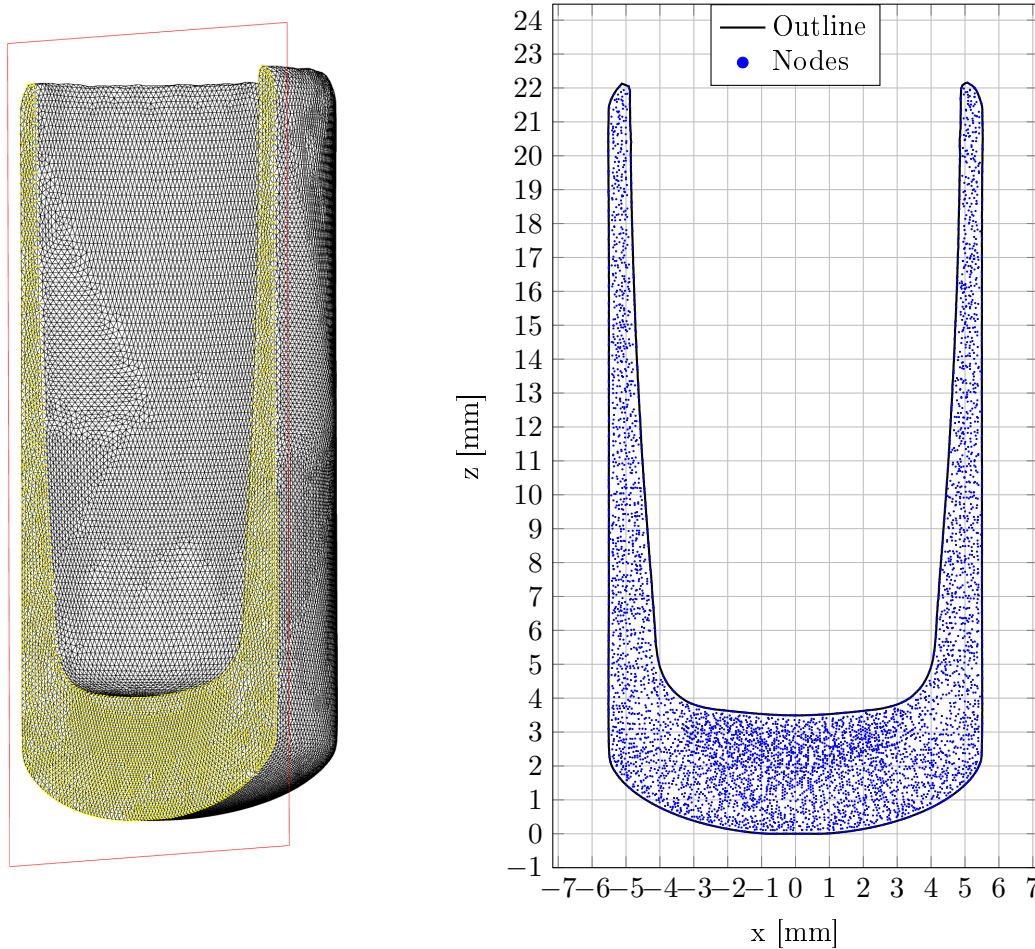


Figure B.15. Nodes intersection the symmetry plane **Figure B.16.** Cartridge bottom profile - Station 1 - 0.00° die tilt

It have to noted that nodes in a distance up to 0.3mm from the symmetry plane are included in order to get enough information to construct the boundary. Furthermore, when the outline is presented in chapter C and D, it is only the lower 6mm of the cartridge case that is present, since this is the area where the different die deigns introduces a visual effect on the cartridge case geometry.

Initial investigation of CDL effects



Chapter content:

| | | |
|---------|---|----|
| C.1 | 0.00° die tilt | 22 |
| C.1.1 | Station 1 | 22 |
| C.1.1.1 | Effective plastic strain | 22 |
| C.1.1.2 | Resultant forces | 23 |
| C.1.1.3 | x-forces | 24 |
| C.1.1.4 | z-forces | 25 |
| C.1.1.5 | Interface pressure | 26 |
| C.2 | 0.20° die tilt | 27 |
| C.2.1 | Station 1 | 27 |
| C.2.1.1 | Effective plastic strain | 27 |
| C.2.1.2 | Resultant forces | 28 |
| C.2.1.3 | x-forces | 29 |
| C.2.1.4 | z-forces | 30 |
| C.2.1.5 | Interface pressure | 31 |
| C.3 | 0.40° die tilt | 32 |
| C.3.1 | Station 1 | 32 |
| C.3.1.1 | Effective plastic strain | 32 |
| C.3.1.2 | Resultant forces | 33 |
| C.3.1.3 | x-forces | 34 |
| C.3.1.4 | z-forces | 35 |
| C.3.1.5 | Interface pressure | 36 |
| C.4 | Geometric evaluation | 37 |
| C.4.1 | Station 1 | 37 |
| C.4.1.1 | Punch displacement | 37 |
| C.4.1.2 | Cartridge height | 38 |
| C.4.1.3 | Projected cartridge height difference | 39 |
| C.4.1.4 | Cartridge bottom profile | 40 |
| C.4.2 | Height difference | 41 |
| C.4.3 | Line fitting parameters | 41 |

C.1 0.00° die tilt

C.1.1 Station 1

C.1.1.1 Effective plastic strain

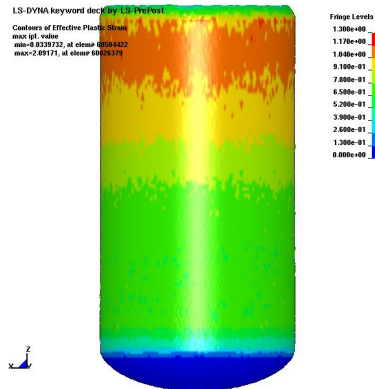


Figure C.1. Effective plastic strain - Station 1
- 0.00° die tilt - Conventional die design

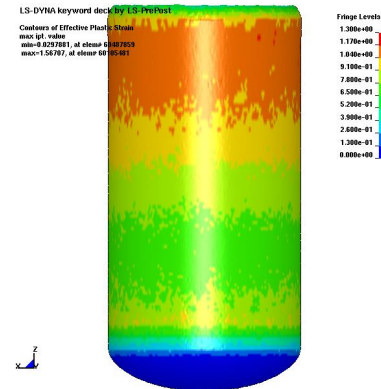


Figure C.2. Effective plastic strain - Station 1
- 0.00° die tilt - $r = 6.80\text{mm}$

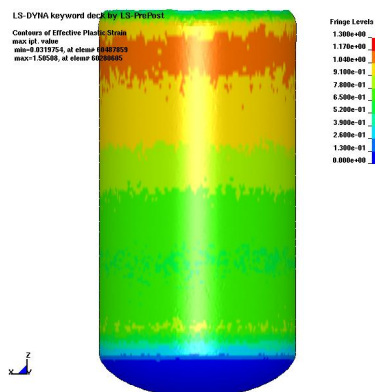


Figure C.3. Effective plastic strain - Station 1
- 0.00° die tilt - $r = 10.34\text{mm}$

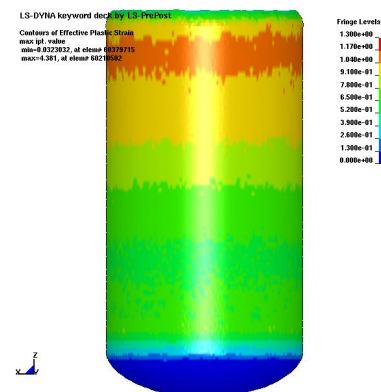


Figure C.4. Effective plastic strain - Station 1
- 0.00° die tilt - $r = 13.89\text{mm}$

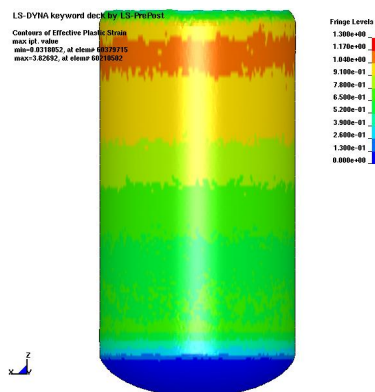


Figure C.5. Effective plastic strain - Station 1
- 0.00° die tilt - $r = 17.44\text{mm}$

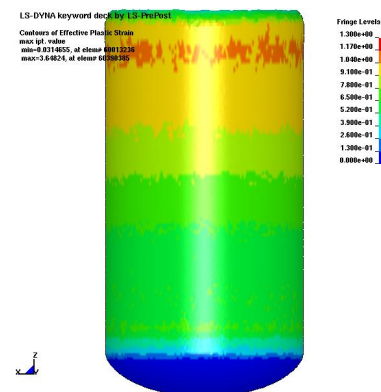
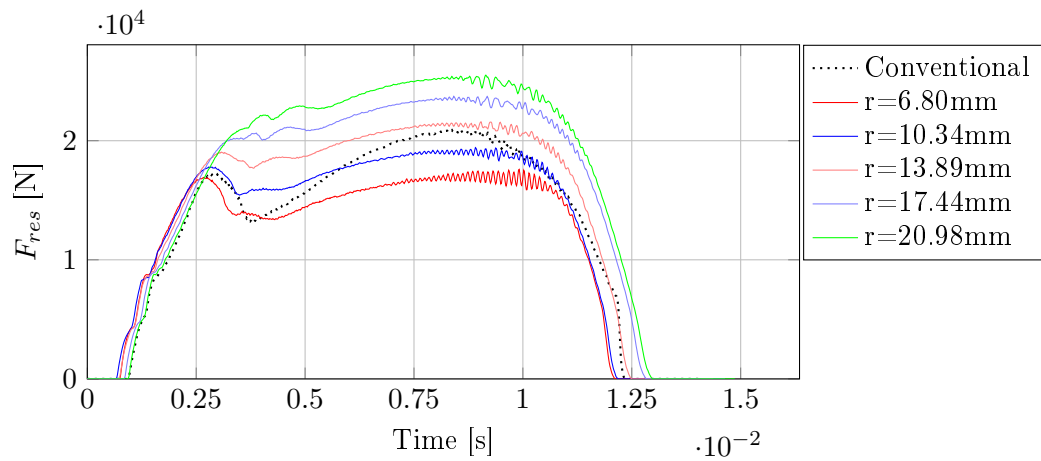
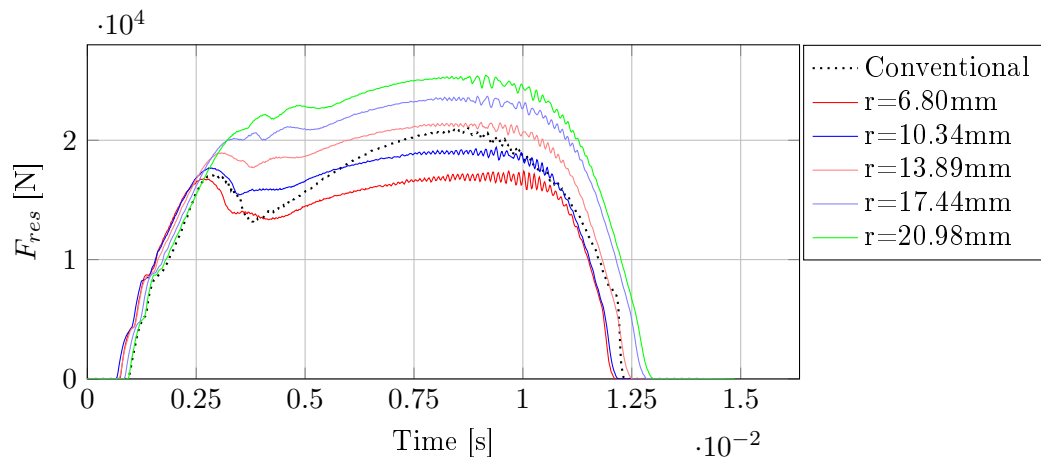
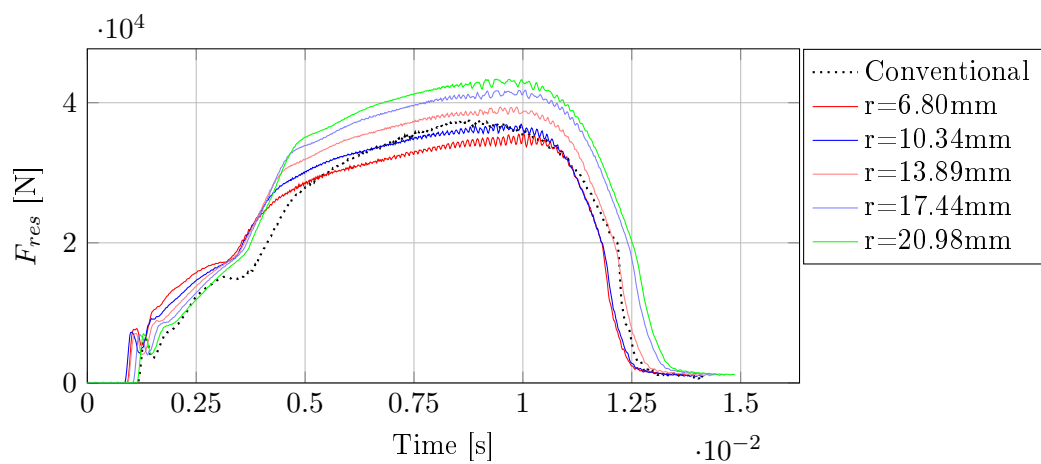


Figure C.6. Effective plastic strain - Station 1
- 0.00° die tilt - $r = 20.98\text{mm}$

C.1.1.2 Resultant forces

Figure C.7. F_{res} - Station 1 - Die 2 x^+ - 0.00° die tiltFigure C.8. F_{res} - Station 1 - Die 2 x^- - 0.00° die tiltFigure C.9. F_{res} - Station 1 - Punch - 0.00° die tilt

C.1.1.3 x-forces

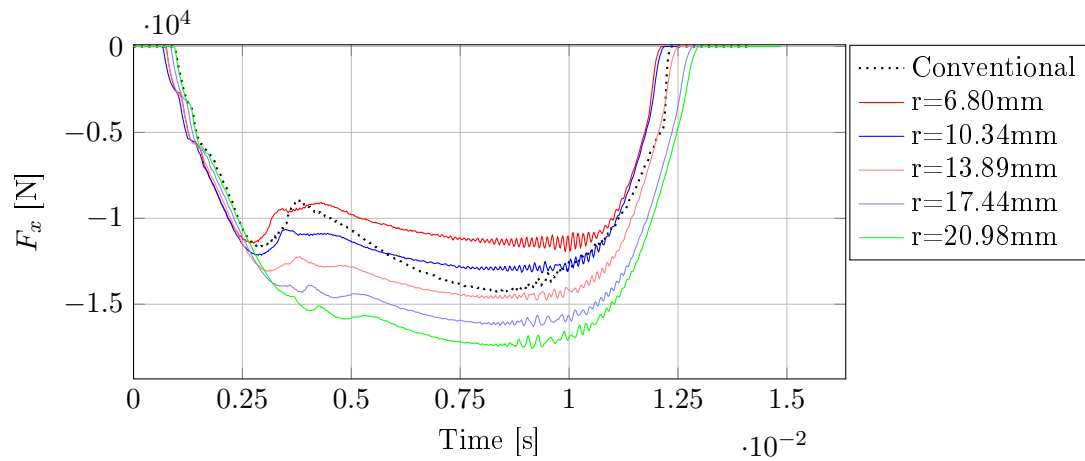


Figure C.10. F_x - Station 1 - Die 2 x^+ - 0.00° die tilt

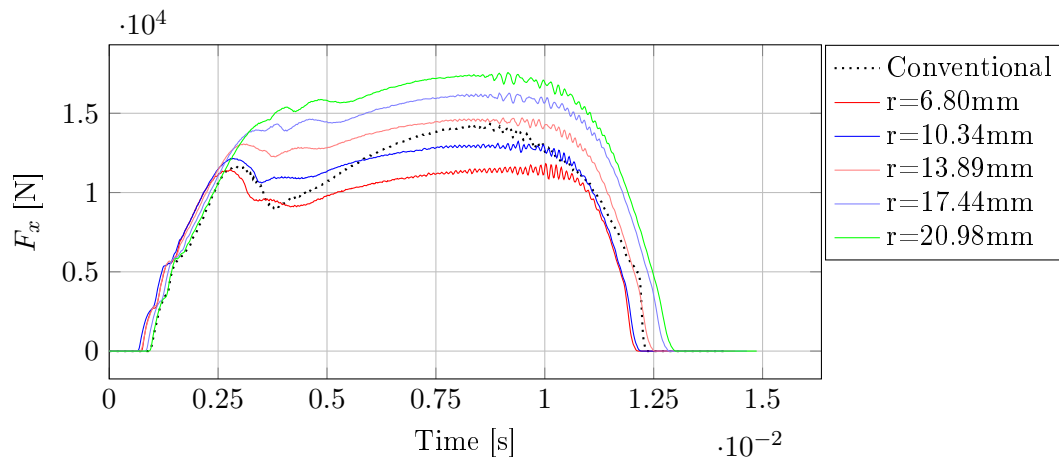


Figure C.11. F_x - Station 1 - Die 2 x^- - 0.00° die tilt

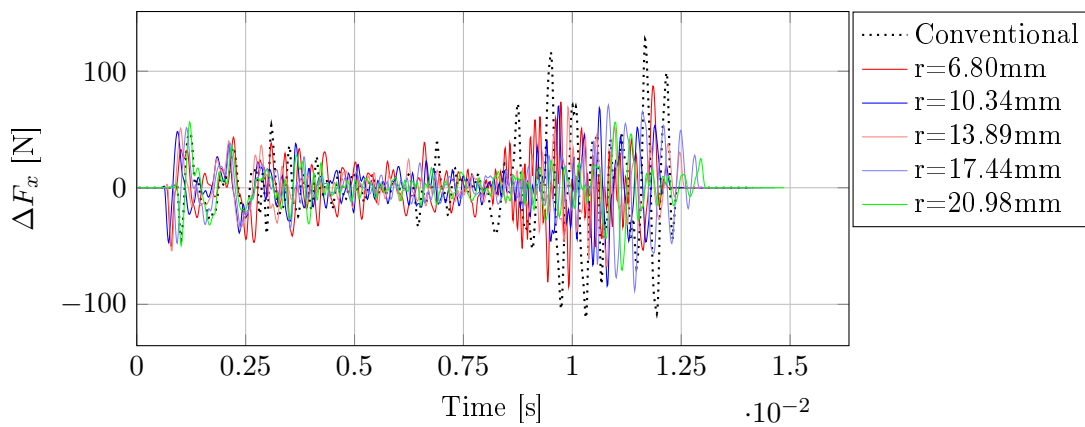


Figure C.12. ΔF_x - Station 1 - Die 2 - 0.00° die tilt

C.1.1.4 z-forces

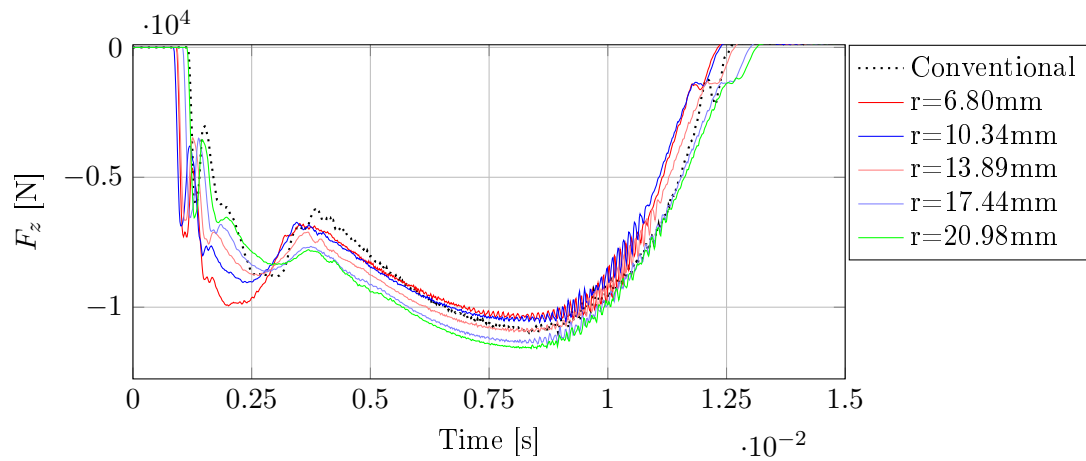


Figure C.13. F_z - Station 1 - Punch - 0.00° die tilt

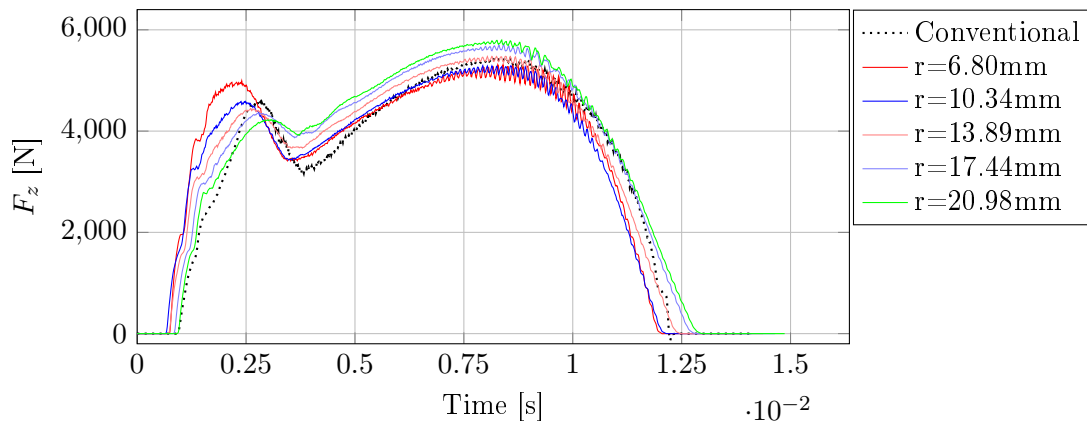


Figure C.14. F_z - Station 1 - Die 2 x^+ - 0.00° die tilt

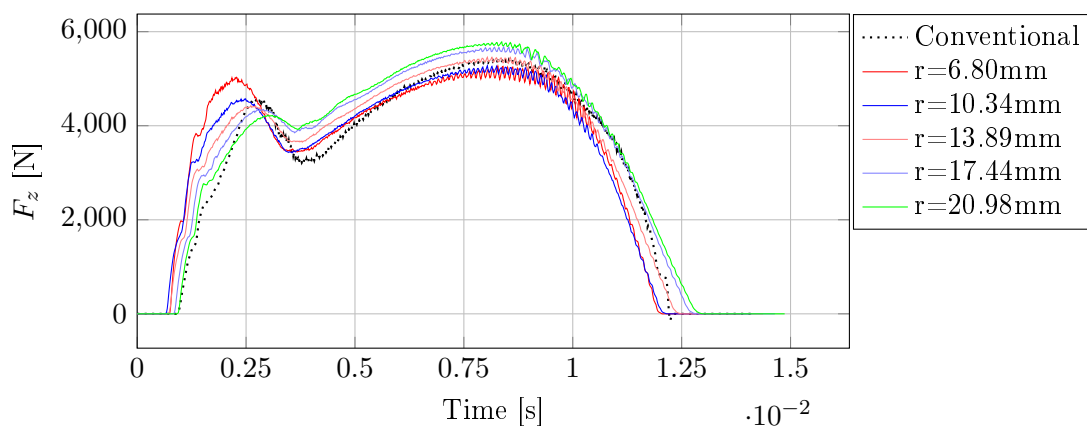


Figure C.15. F_z - Station 1 - Die 2 x^- - 0.00° die tilt

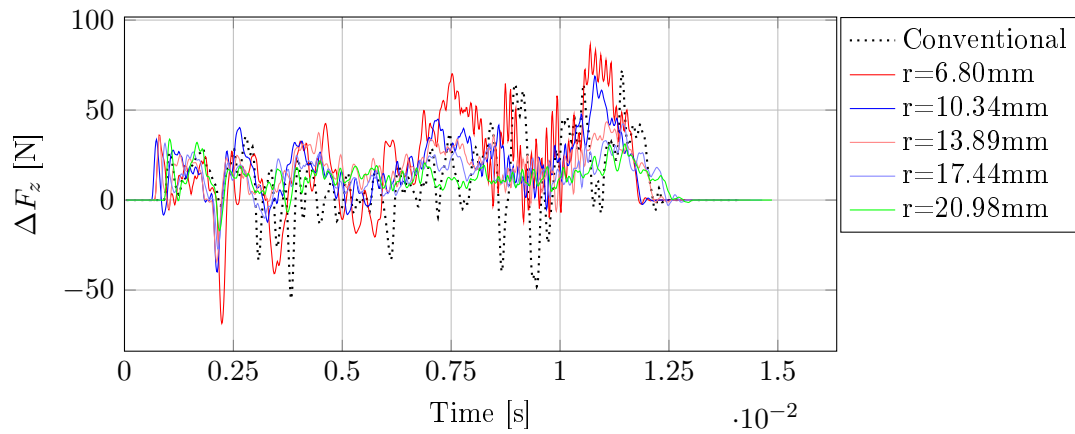


Figure C.16. ΔF_z - Station 1 - Die 2 - 0.00° die tilt

C.1.1.5 Interface pressure

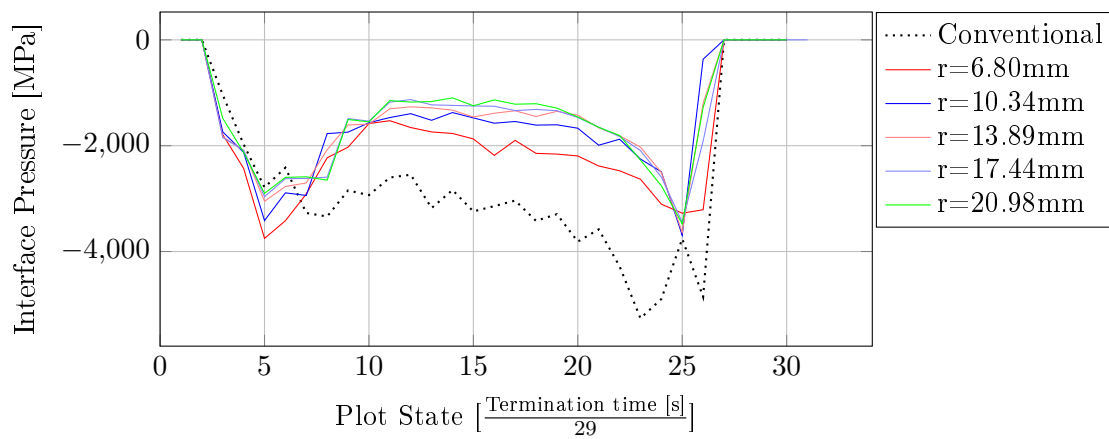


Figure C.17. Maximum interface pressure - Station 1 - Die 2 x^+ - 0.00° die tilt

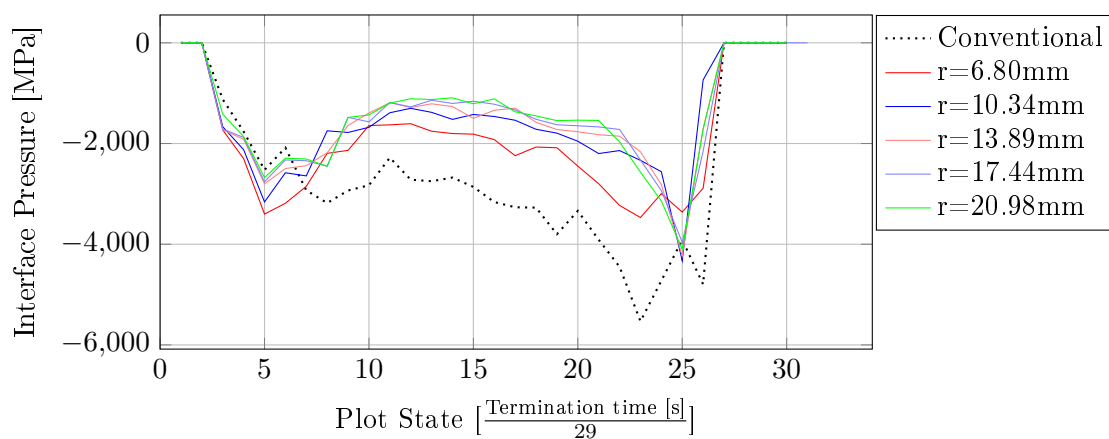


Figure C.18. Maximum interface pressure - Station 1 - Die 2 x^- - 0.00° die tilt

C.2 0.20° die tilt

C.2.1 Station 1

C.2.1.1 Effective plastic strain

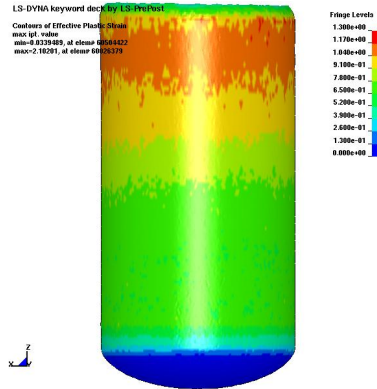


Figure C.19. Effective plastic strain - Station 1 - 0.20° die tilt - Conventional die design

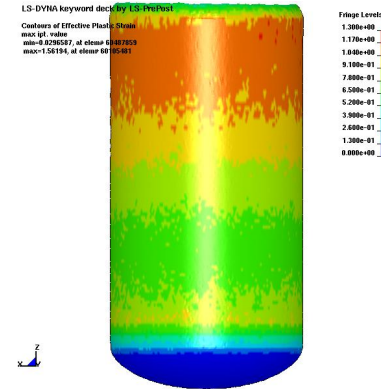


Figure C.20. Effective plastic strain - Station 1 - 0.20° die tilt - $r = 6.80mm$

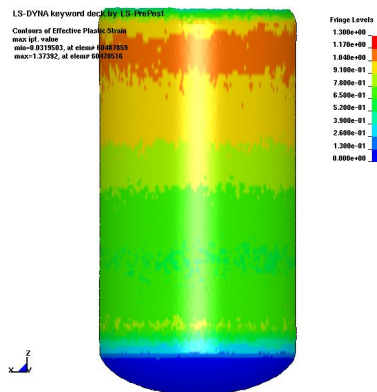


Figure C.21. Effective plastic strain - Station 1 - 0.20° die tilt - $r = 10.34mm$

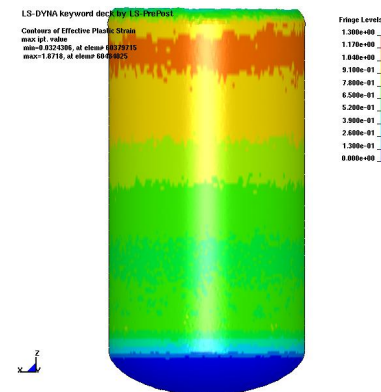


Figure C.22. Effective plastic strain - Station 1 - 0.20° die tilt - $r = 13.89mm$

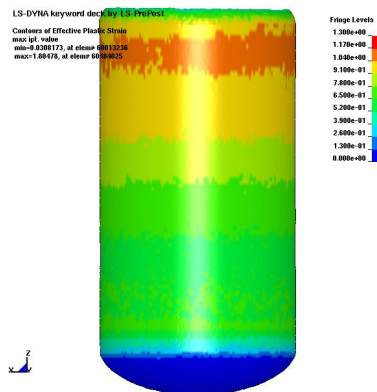


Figure C.23. Effective plastic strain - Station 1 - 0.20° die tilt - $r = 17.44mm$

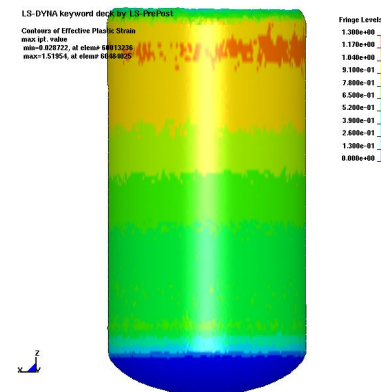


Figure C.24. Effective plastic strain - Station 1 - 0.20° die tilt - $r = 20.98mm$

C.2.1.2 Resultant forces

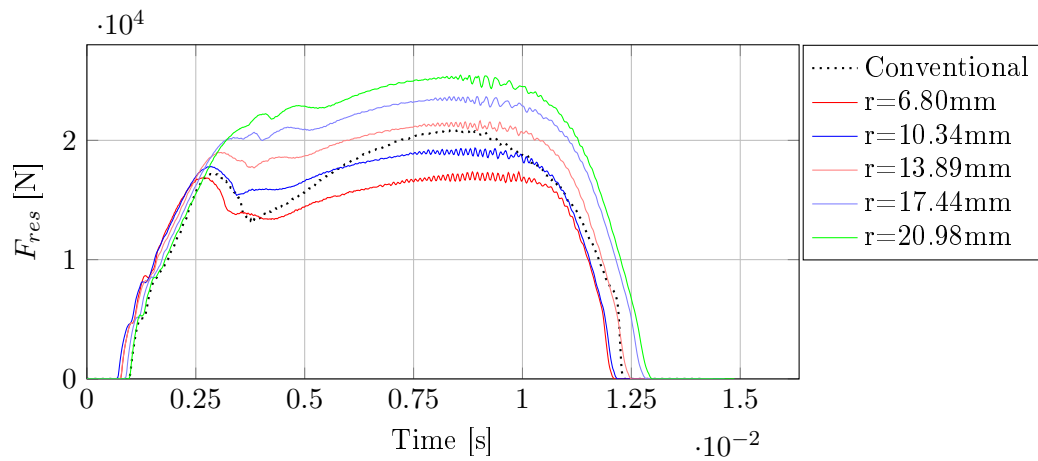


Figure C.25. F_{res} - Station 1 - Die 2 x^+ - 0.20° die tilt

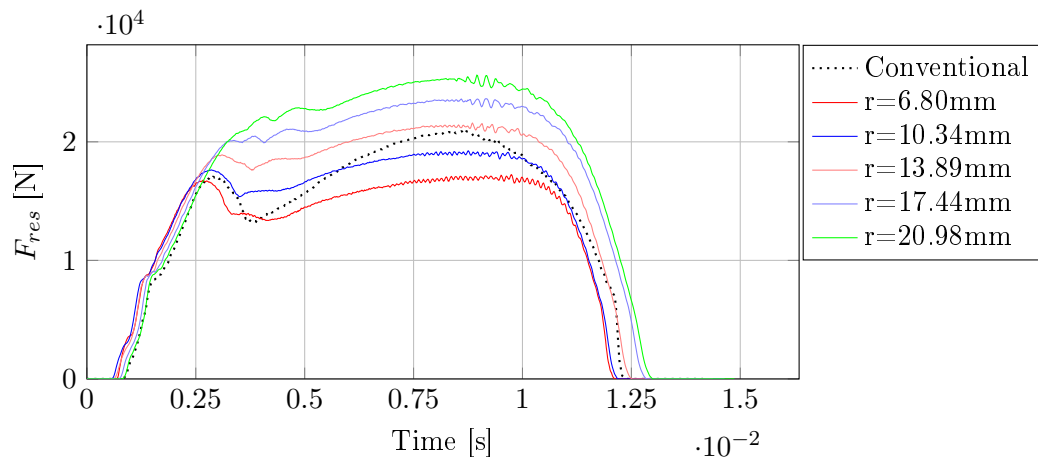


Figure C.26. F_{res} - Station 1 - Die 2 x^- - 0.20° die tilt

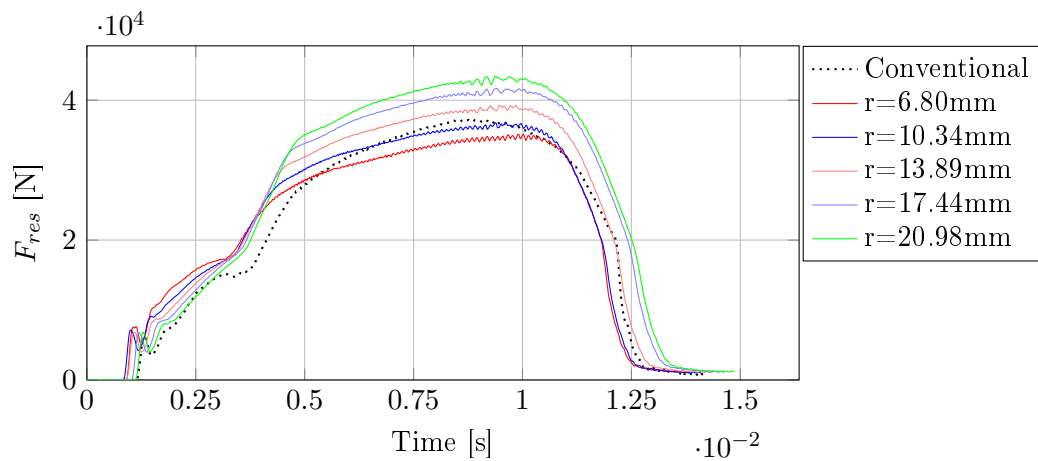
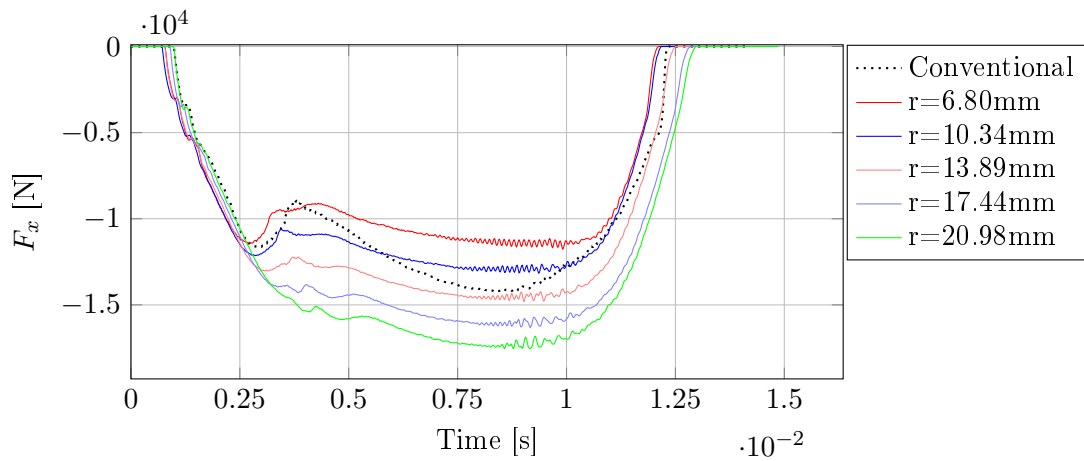
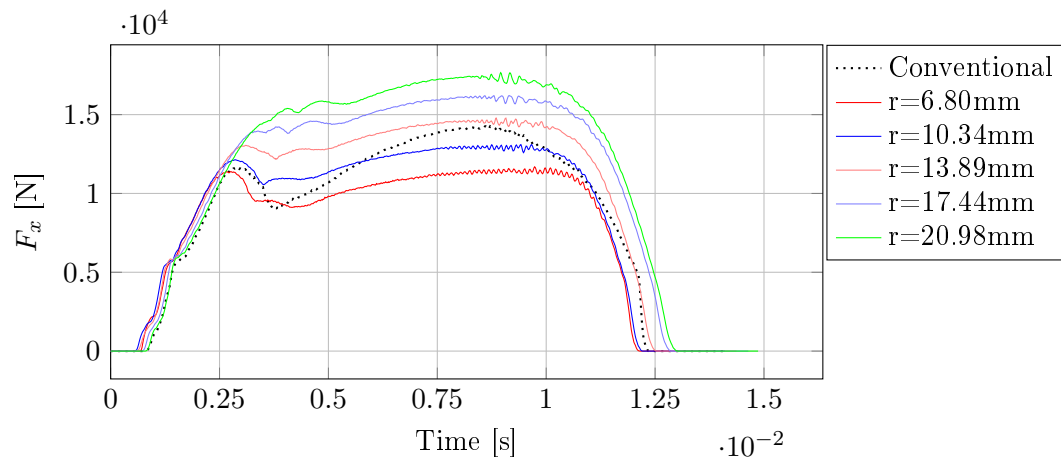
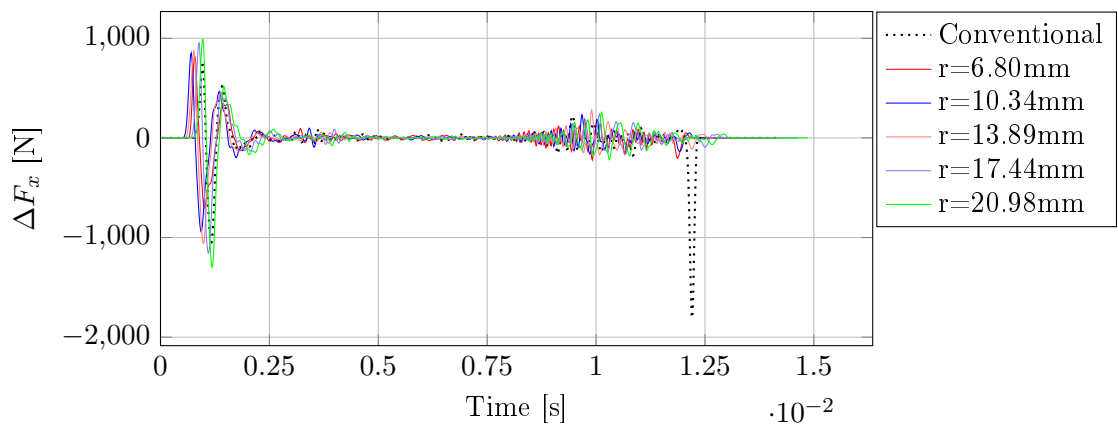


Figure C.27. F_{res} - Station 1 - Punch - 0.20° die tilt

C.2.1.3 x-forces

Figure C.28. F_x - Station 1 - Die 2 x^+ - 0.20° die tiltFigure C.29. F_x - Station 1 - Die 2 x^- - 0.20° die tiltFigure C.30. ΔF_x - Station 1 - Die 2 - 0.20° die tilt

C.2.1.4 z-forces

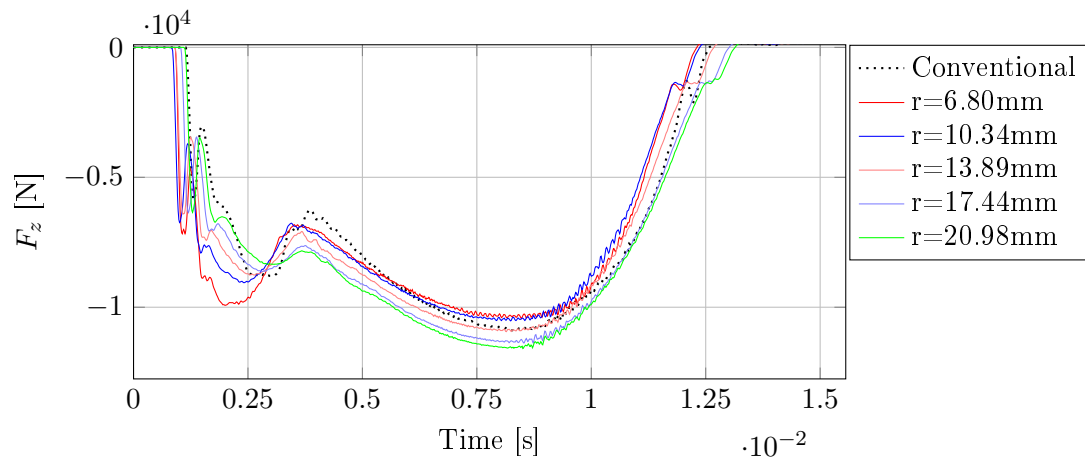


Figure C.31. F_z - Station 1 - Punch - 0.20° die tilt

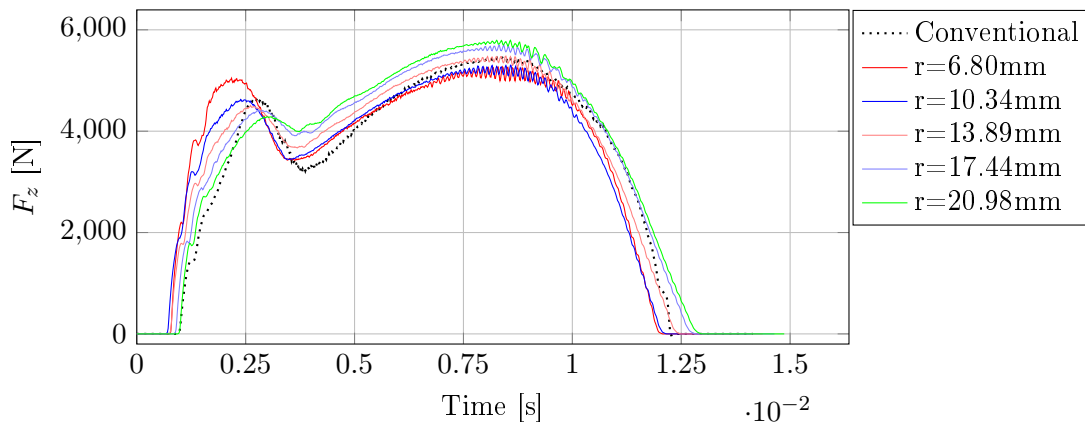


Figure C.32. F_z - Station 1 - Die 2 x^+ - 0.20° die tilt

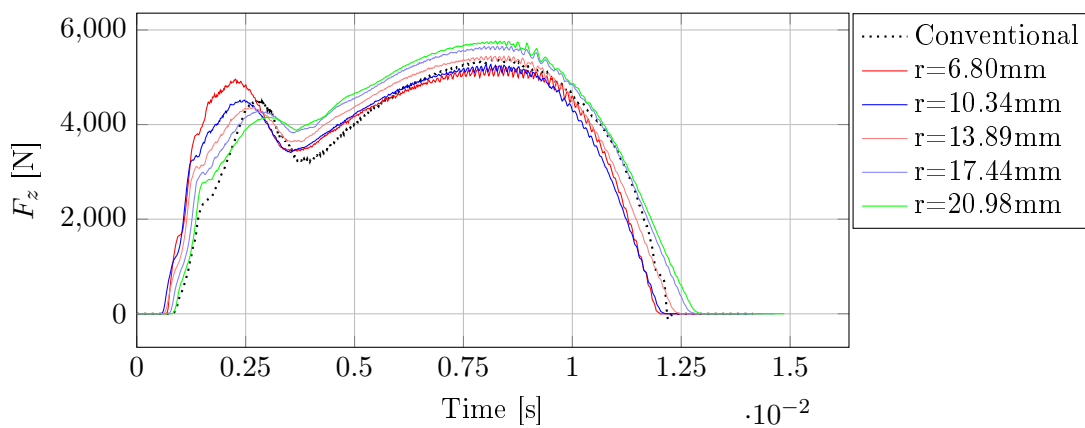


Figure C.33. F_z - Station 1 - Die 2 x^- - 0.20° die tilt

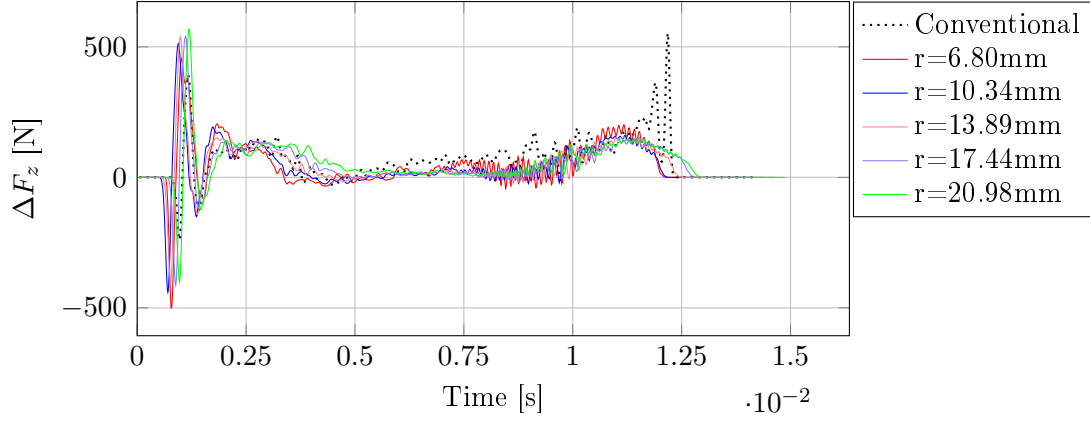


Figure C.34. ΔF_z - Station 1 - Die 2 - 0.20° die tilt

C.2.1.5 Interface pressure

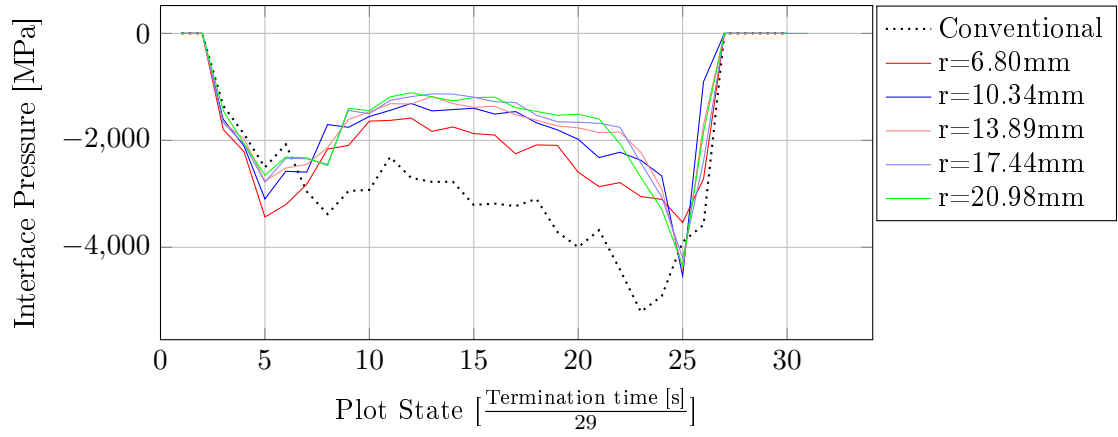


Figure C.35. Maximum interface pressure - Station 1 - Die 2 x^- - 0.20° die tilt

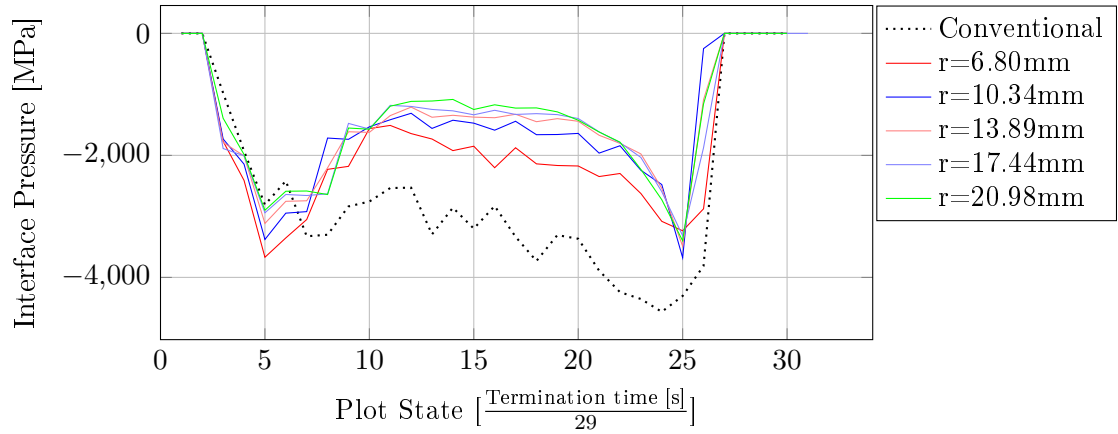


Figure C.36. Maximum interface pressure - Station 1 - Die 2 x^+ - 0.20° die tilt

C.3 0.40° die tilt

C.3.1 Station 1

C.3.1.1 Effective plastic strain

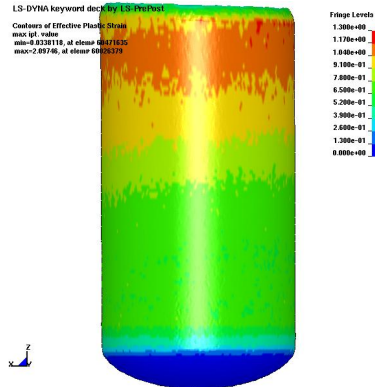


Figure C.37. Effective plastic strain - Station 1 - 0.40° die tilt - Conventional die design

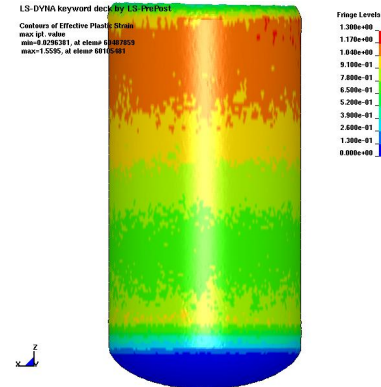


Figure C.38. Effective plastic strain - Station 1 - 0.40° die tilt - $r = 6.80mm$

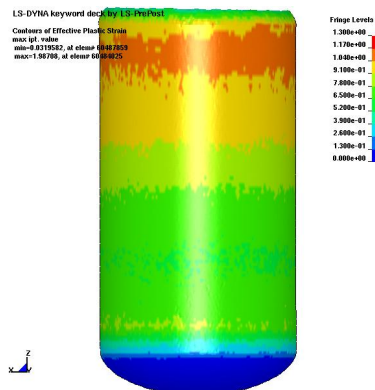


Figure C.39. Effective plastic strain - Station 1 - 0.40° die tilt - $r = 10.34mm$

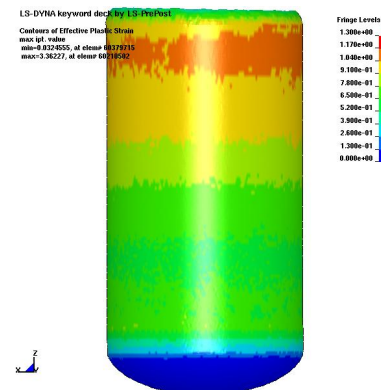


Figure C.40. Effective plastic strain - Station 1 - 0.40° die tilt - $r = 13.89mm$

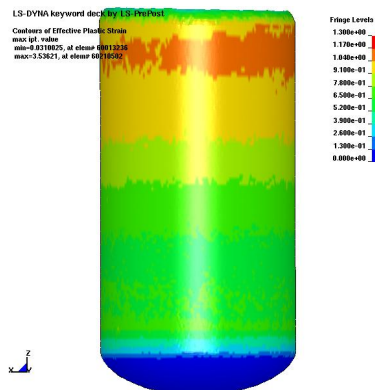


Figure C.41. Effective plastic strain - Station 1 - 0.40° die tilt - $r = 17.44mm$

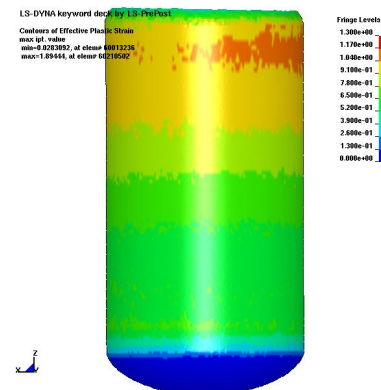
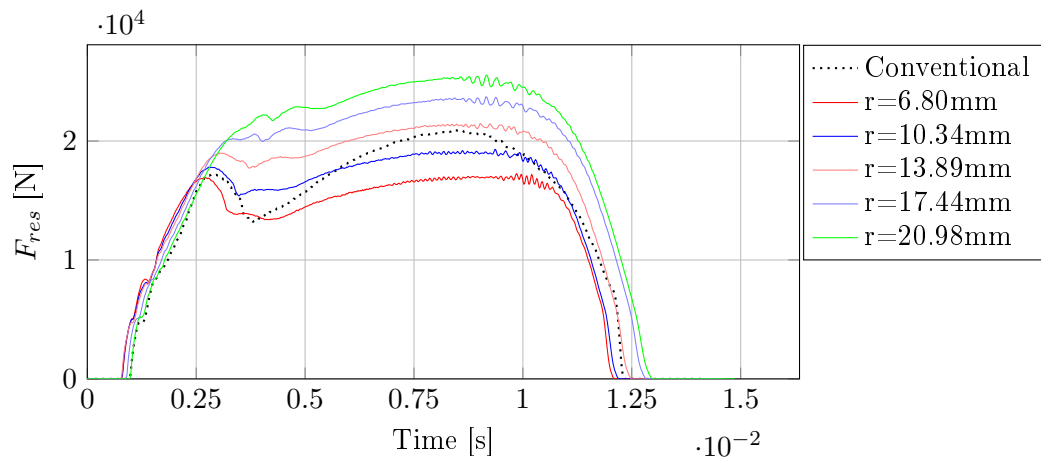
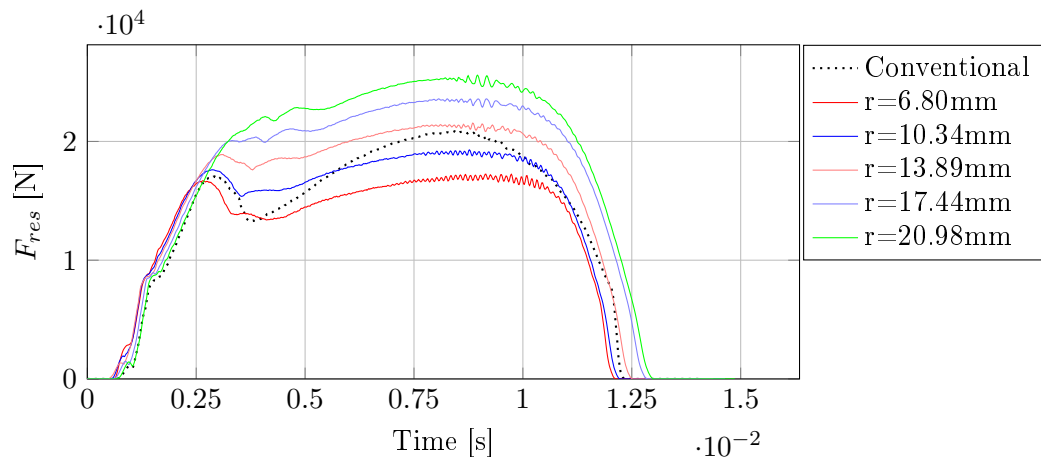
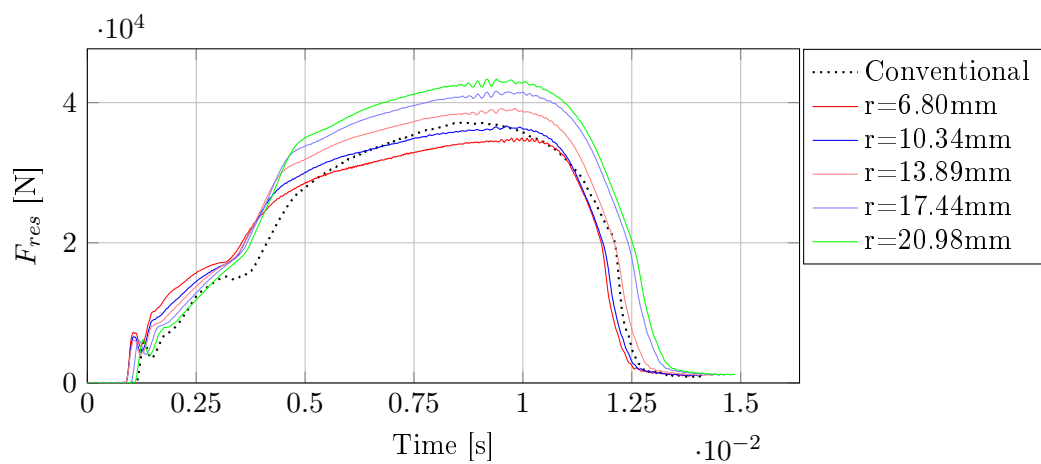


Figure C.42. Effective plastic strain - Station 1 - 0.40° die tilt - $r = 20.98mm$

C.3.1.2 Resultant forces

Figure C.43. F_{res} - Station 1 - Die 2 x^+ - 0.40° die tiltFigure C.44. F_{res} - Station 1 - Die 2 x^- - 0.40° die tiltFigure C.45. F_{res} - Station 1 - Punch - 0.40° die tilt

C.3.1.3 x-forces

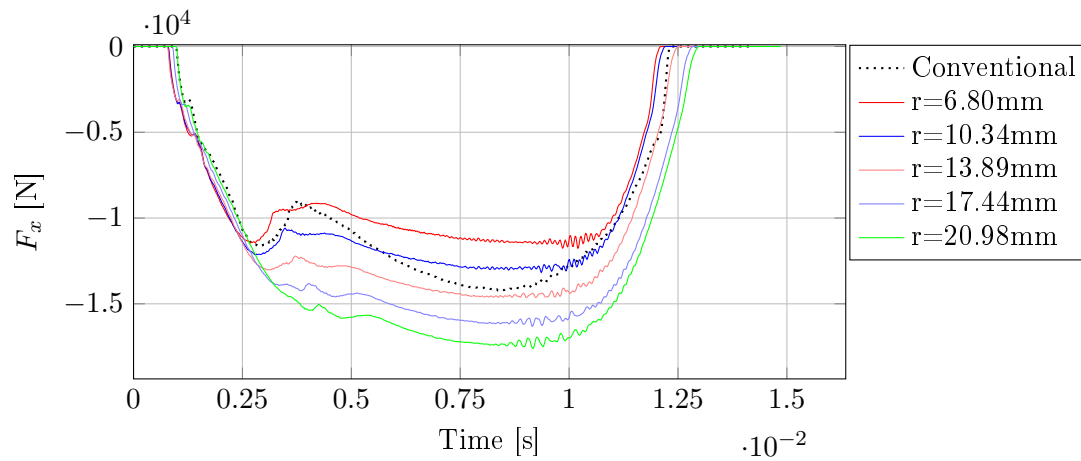


Figure C.46. F_x - Station 1 - Die 2 x^+ - 0.40° die tilt

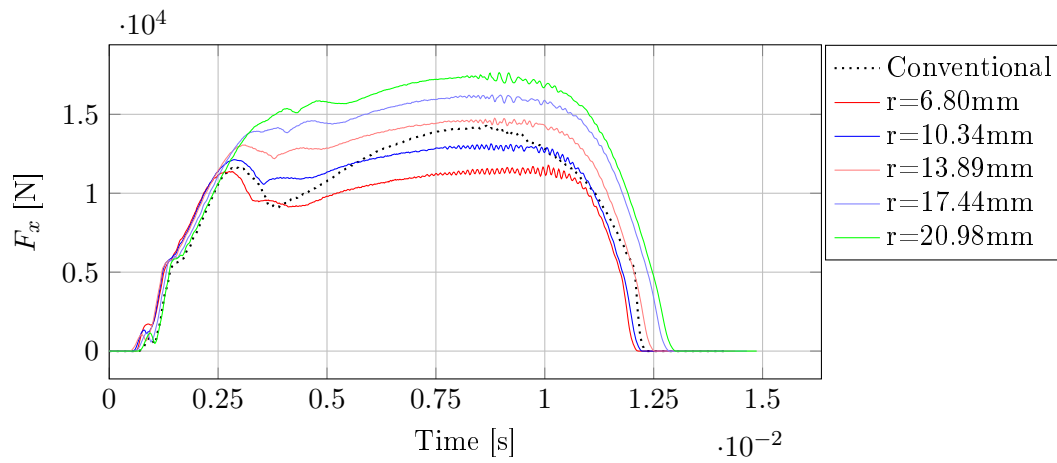


Figure C.47. F_x - Station 1 - Die 2 x^- - 0.40° die tilt

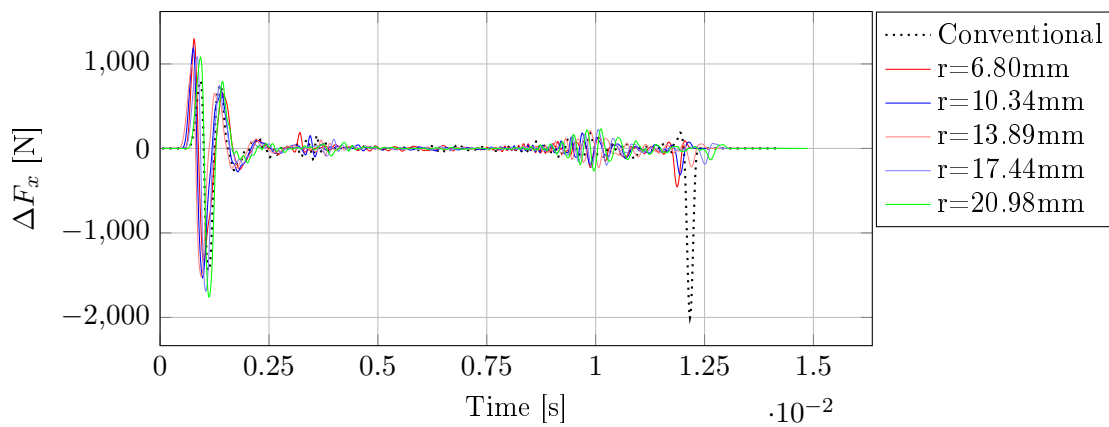
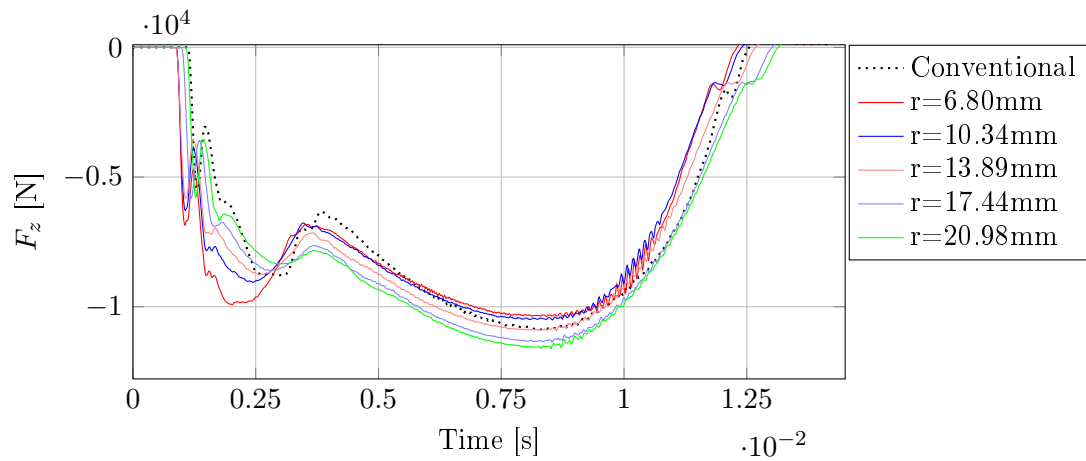
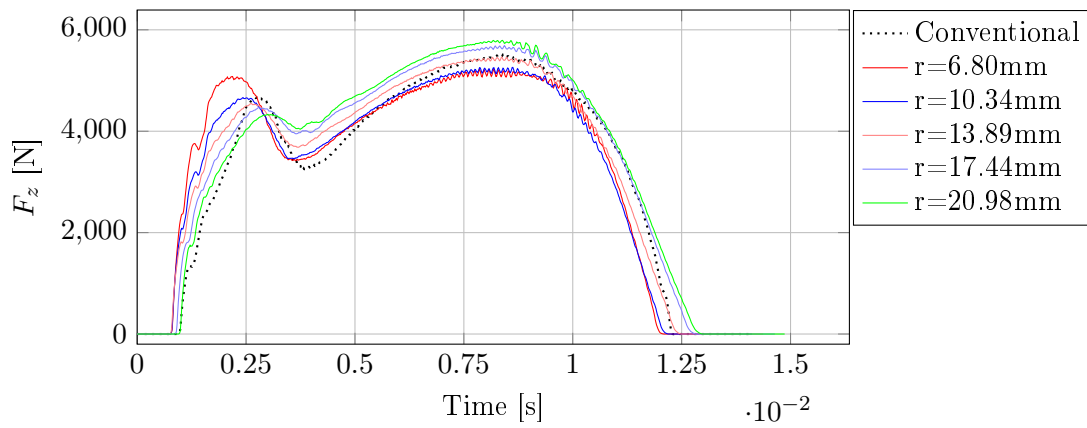
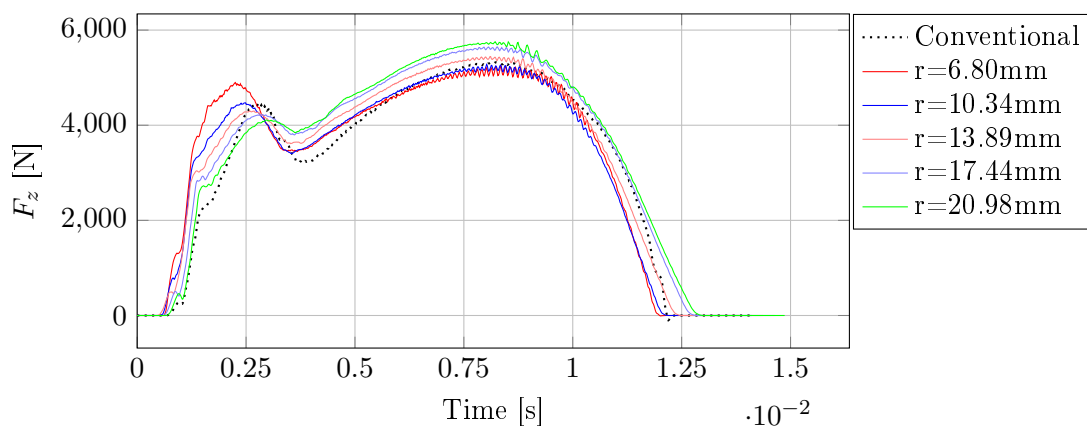


Figure C.48. ΔF_x - Station 1 - Die 2 - 0.40° die tilt

C.3.1.4 z-forces

Figure C.49. F_z - Station 1 - Punch - 0.40° die tiltFigure C.50. F_z - Station 1 - Die 2 x^+ - 0.40° die tiltFigure C.51. F_z - Station 1 - Die 2 x^- - 0.40° die tilt

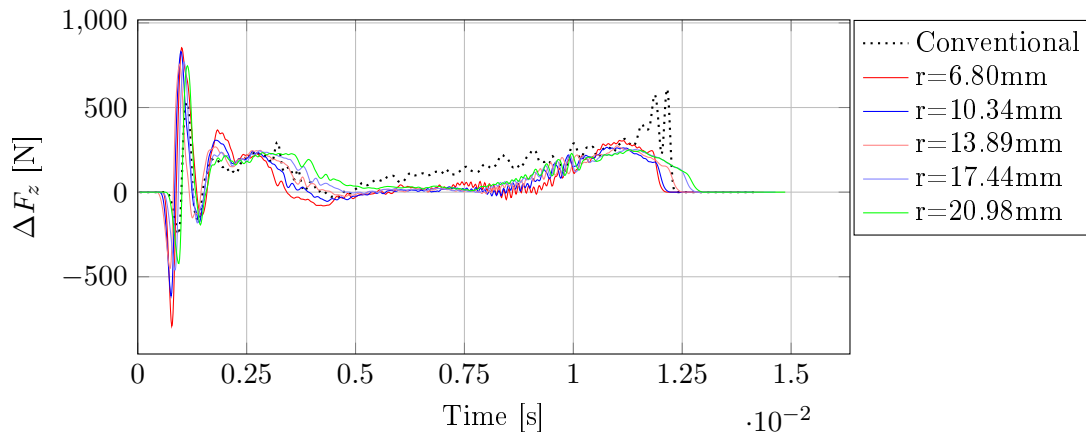


Figure C.52. ΔF_z - Station 1 - Die 2 - 0.40° die tilt

C.3.1.5 Interface pressure

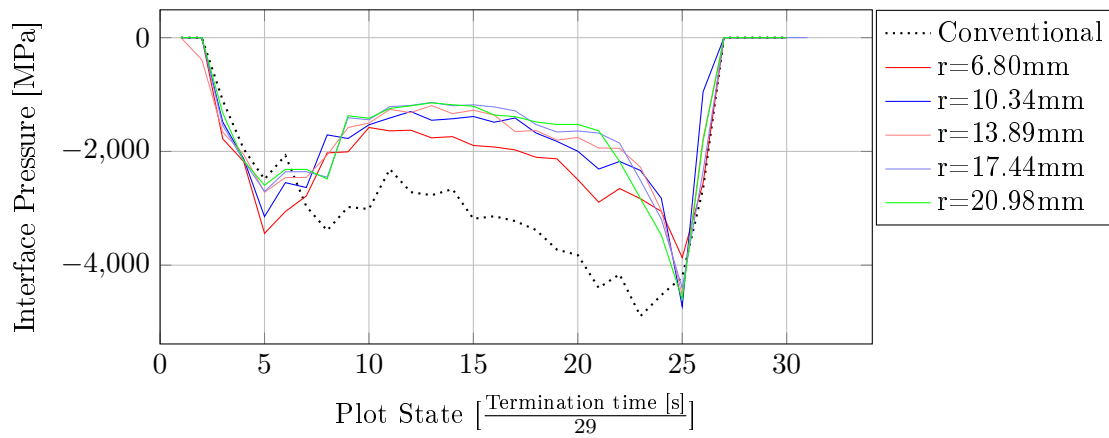


Figure C.53. Maximum interface pressure - Station 1 - Die 2 x^- - 0.40° die tilt

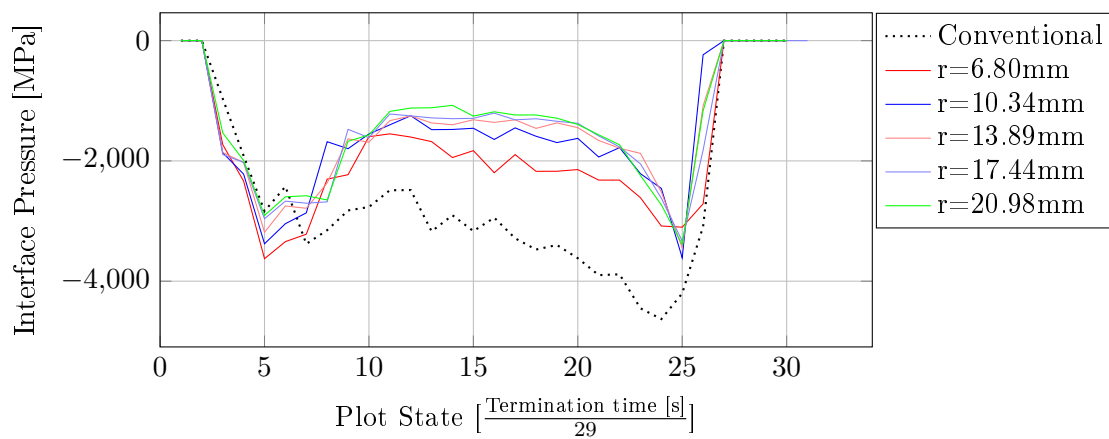


Figure C.54. Maximum interface pressure - Station 1 - Die 2 x^+ - 0.40° die tilt

C.4 Geometric evaluation

C.4.1 Station 1

C.4.1.1 Punch displacement

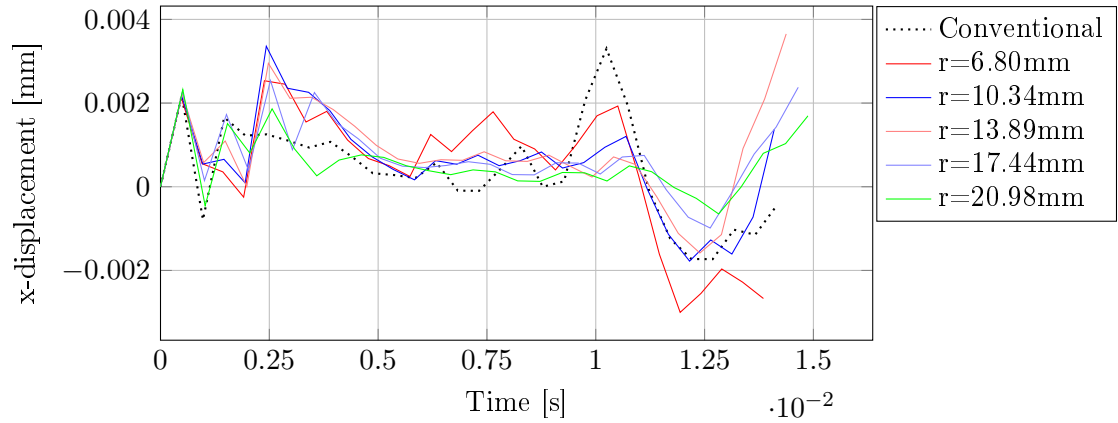


Figure C.55. x-displacement - Station 1 - Punch - 0.00° die tilt

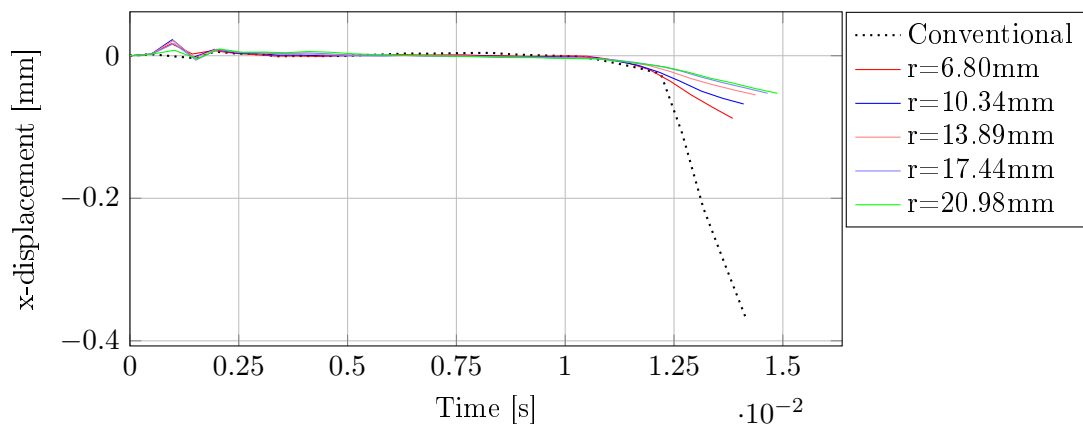


Figure C.56. x-displacement - Station 1 - Punch - 0.20° die tilt

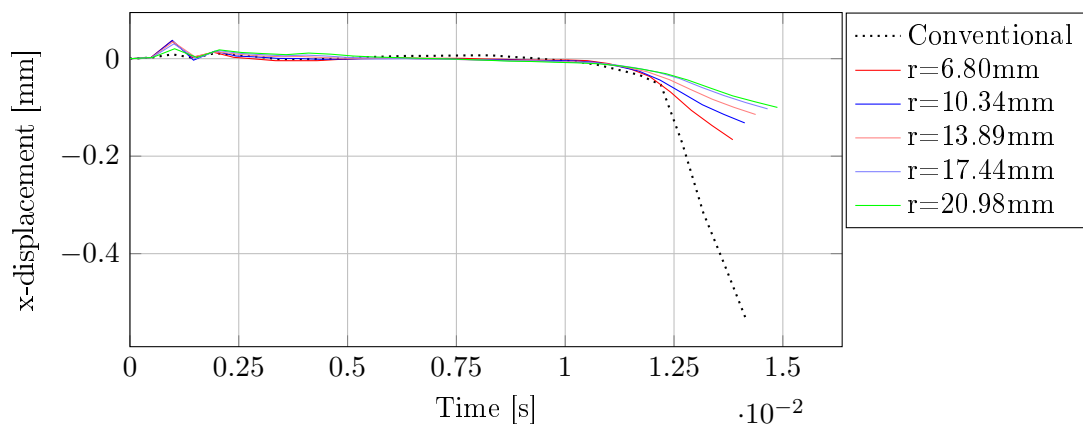


Figure C.57. x-displacement - Station 1 - Punch - 0.40° die tilt

C.4.1.2 Cartridge height

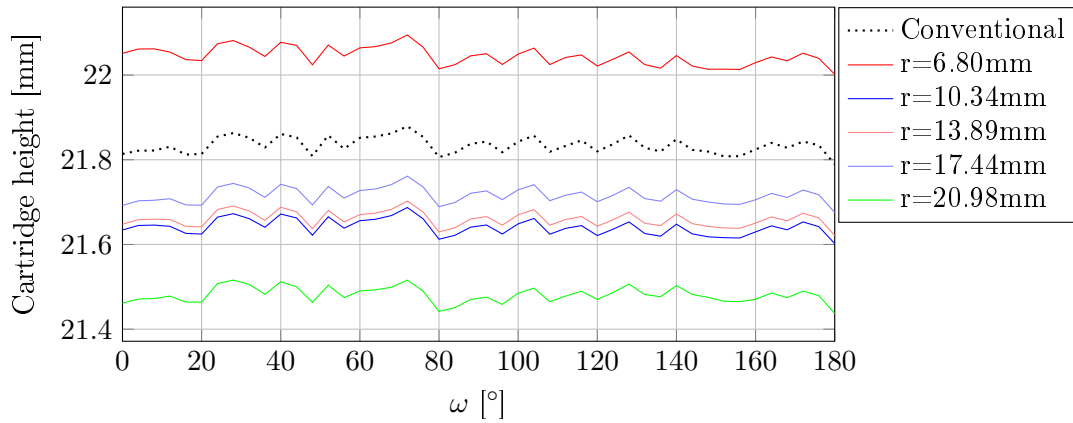


Figure C.58. Cartridge height - Station 1 - 0.00° die tilt

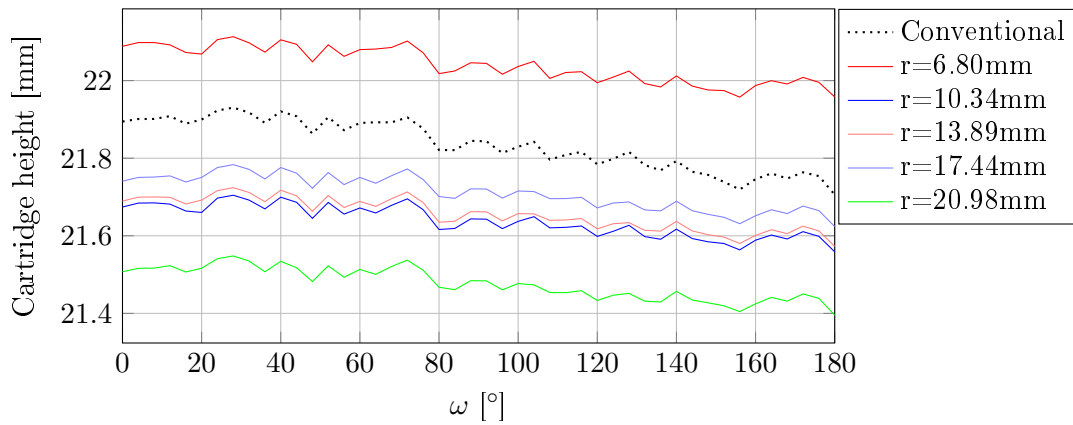


Figure C.59. Cartridge height - Station 1 - 0.20° die tilt

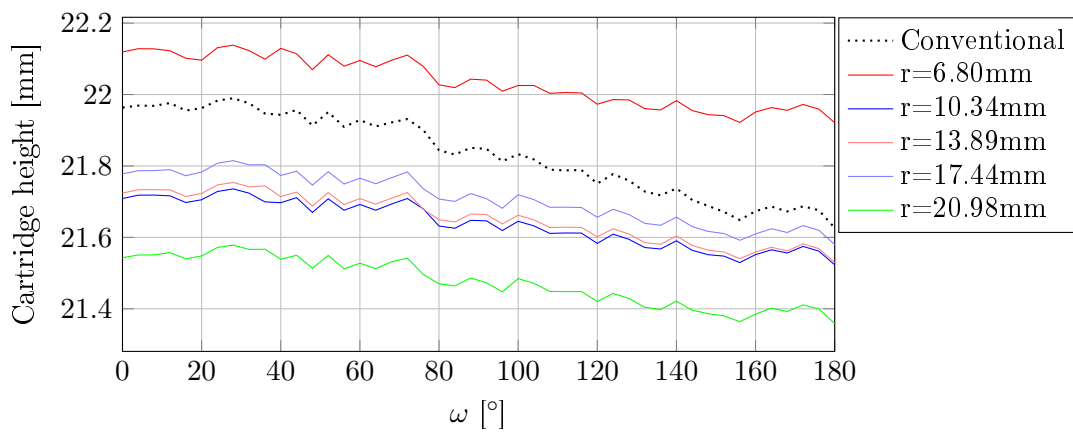


Figure C.60. Cartridge height - Station 1 - 0.40° die tilt

C.4.1.3 Projected cartridge height difference

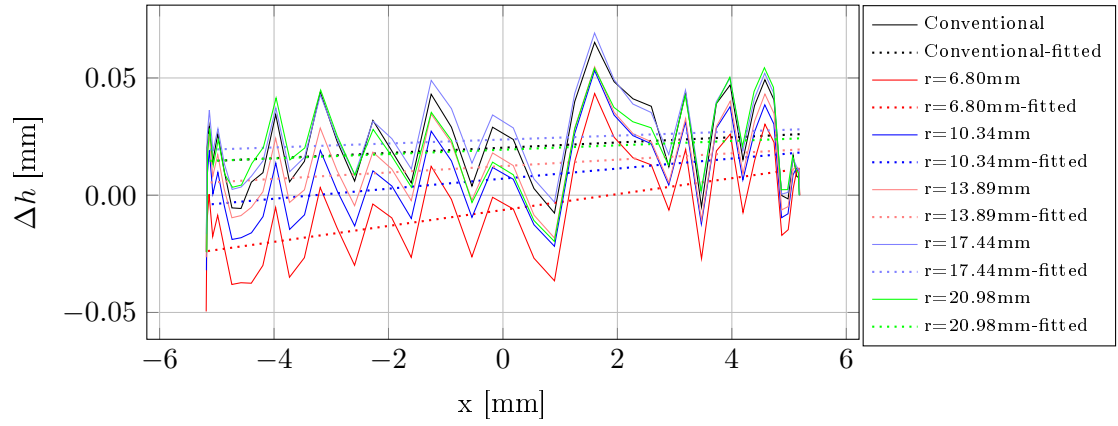


Figure C.61. Projected cartridge height difference - Station 1 - 0.00° die tilt

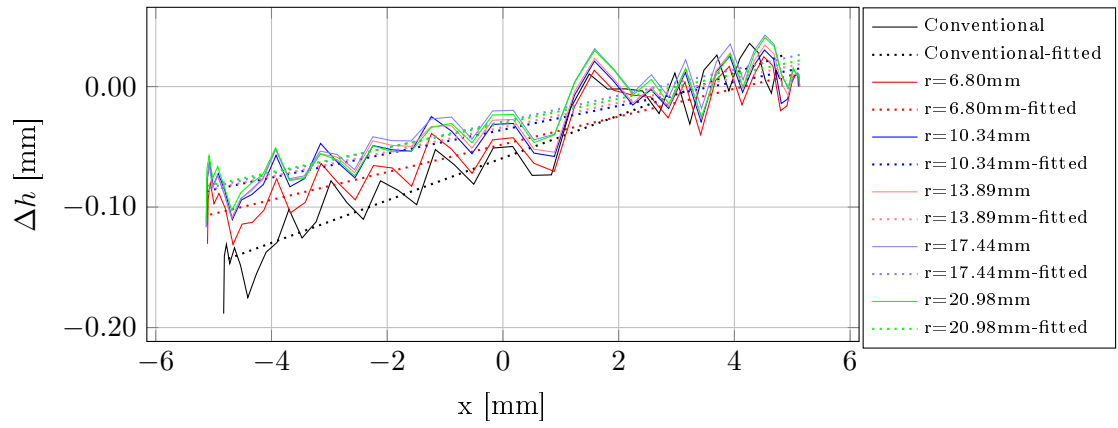


Figure C.62. Projected cartridge height difference - Station 1 - 0.20° die tilt

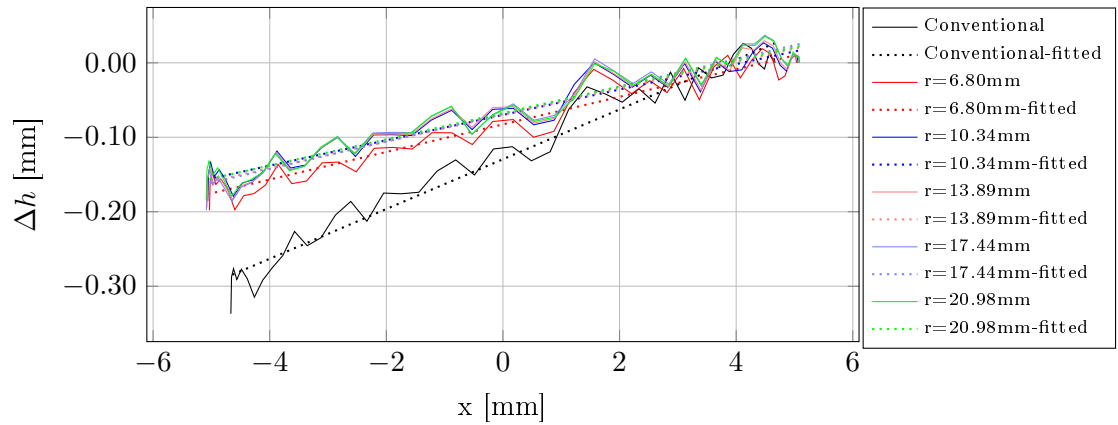


Figure C.63. Projected cartridge height difference - Station 1 - 0.40° die tilt

C.4.1.4 Cartridge bottom profile

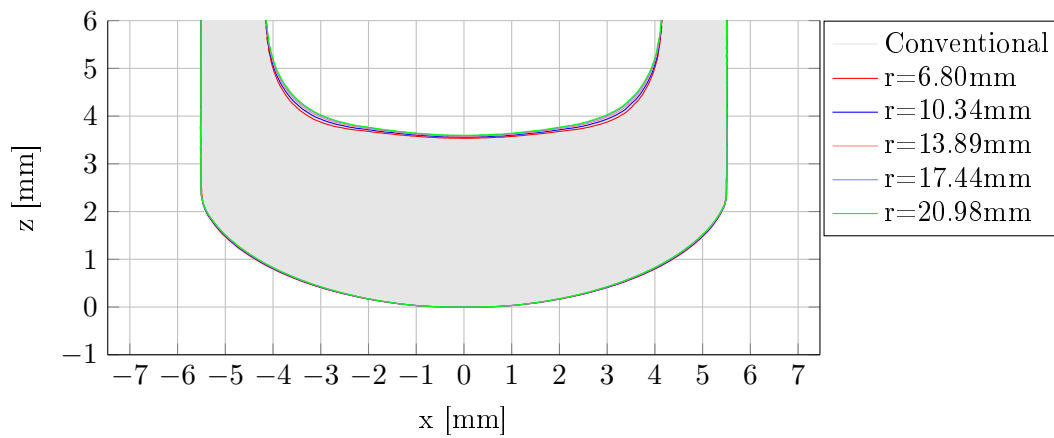


Figure C.64. Cartridge bottom profile - Station 1 - 0.00° die tilt

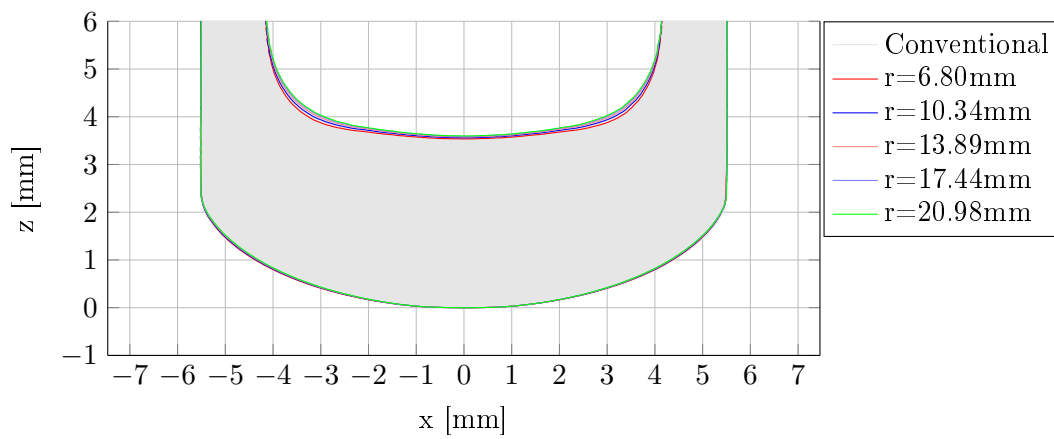


Figure C.65. Cartridge bottom profile - Station 1 - 0.20° die tilt

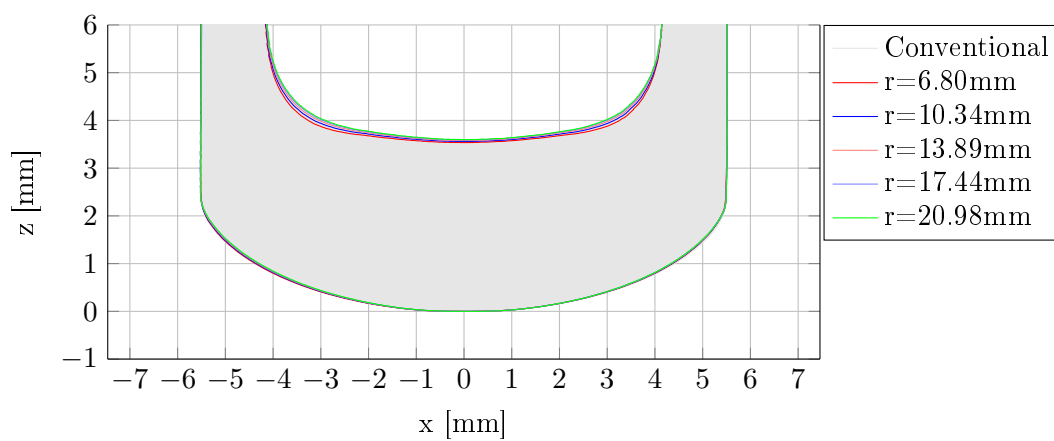


Figure C.66. Cartridge bottom profile - Station 1 - 0.40° die tilt

C.4.2 Height difference

| Station 1 | | | |
|--------------|-----------------|----------------|----------------|
| Die design | Δh [mm] | | |
| | 0.00° die tilt | 0.20° die tilt | 0.40° die tilt |
| Conventional | 0.0242 | 0.1884 | 0.3370 |
| r=6.80mm | 0.0496 | 0.1305 | 0.1980 |
| r=10.34mm | 0.0320 | 0.1155 | 0.1856 |
| r=13.89mm | 0.0265 | 0.1167 | 0.1945 |
| r=17.44mm | 0.0166 | 0.1168 | 0.1980 |
| r=20.98mm | 0.0244 | 0.1120 | 0.1843 |

Table C.1. cartridge case height difference

C.4.3 Line fitting parameters

$$h(x) = p_1 \cdot x + p_2$$

| Station 1 | | | | | | | | | |
|--------------|----------------|---------|--------|----------------|---------|--------|----------------|---------|--------|
| Die design | 0.00° die tilt | | | 0.20° die tilt | | | 0.40° die tilt | | |
| | p_1 | p_2 | r^2 | p_1 | p_2 | r^2 | p_1 | p_2 | r^2 |
| Conventional | 0.0011 | 21.8341 | 0.0461 | 0.0176 | 21.8352 | 0.9054 | 0.0334 | 21.8340 | 0.9664 |
| r=6.80mm | 0.0034 | 22.0449 | 0.3415 | 0.0115 | 22.0405 | 0.8500 | 0.0185 | 22.0365 | 0.9385 |
| r=10.34mm | 0.0021 | 21.6412 | 0.1787 | 0.0099 | 21.6384 | 0.8245 | 0.0170 | 21.6389 | 0.9352 |
| r=13.89mm | 0.0014 | 21.6602 | 0.0828 | 0.0102 | 21.6558 | 0.8451 | 0.0178 | 21.6540 | 0.9384 |
| r=17.44mm | 0.0008 | 21.7159 | 0.0291 | 0.0108 | 21.7117 | 0.8471 | 0.0185 | 21.7092 | 0.9362 |
| r=20.98mm | 0.0009 | 21.4810 | 0.0353 | 0.0102 | 21.4770 | 0.8406 | 0.0176 | 21.4757 | 0.9381 |

Table C.2. Height fit parameters

Determination of final CDL radius



Chapter content:

| | | |
|---------|--------------------------------|----|
| D.1 | 0.00° die tilt | 45 |
| D.1.1 | Station 1 | 45 |
| D.1.1.1 | Effective plastic strain | 45 |
| D.1.1.2 | Resultant forces | 46 |
| D.1.1.3 | x-forces | 47 |
| D.1.1.4 | z-forces | 49 |
| D.1.1.5 | Interface pressure | 52 |
| D.1.2 | Station 2 | 54 |
| D.1.2.1 | Effective plastic strain | 54 |
| D.1.2.2 | Resultant forces | 55 |
| D.1.2.3 | x-forces | 56 |
| D.1.2.4 | z-forces | 58 |
| D.1.2.5 | Interface pressure | 61 |
| D.1.3 | Station 3 | 63 |
| D.1.3.1 | Effective plastic strain | 63 |
| D.1.3.2 | Resultant forces | 64 |
| D.1.3.3 | x-forces | 65 |
| D.1.3.4 | z-forces | 66 |
| D.1.3.5 | Interface pressure | 67 |
| D.2 | 0.20° die tilt | 68 |
| D.2.1 | Station 1 | 68 |
| D.2.1.1 | Effective plastic strain | 68 |
| D.2.1.2 | Resultant forces | 69 |
| D.2.1.3 | x-forces | 70 |
| D.2.1.4 | z-forces | 72 |
| D.2.1.5 | Interface pressure | 75 |
| D.2.2 | Station 2 | 77 |
| D.2.2.1 | Effective plastic strain | 77 |
| D.2.2.2 | Resultant forces | 78 |
| D.2.2.3 | x-forces | 79 |
| D.2.2.4 | z-forces | 81 |
| D.2.2.5 | Interface pressure | 84 |

| | | |
|---------|---|-----|
| D.2.3 | Station 3 | 86 |
| D.2.3.1 | Effective plastic strain | 86 |
| D.2.3.2 | Resultant forces | 87 |
| D.2.3.3 | x-forces | 88 |
| D.2.3.4 | z-forces | 89 |
| D.2.3.5 | Interface pressure | 90 |
| D.3 | 0.40° die tilt | 91 |
| D.3.1 | Station 1 | 91 |
| D.3.1.1 | Effective plastic strain | 91 |
| D.3.1.2 | Resultant forces | 92 |
| D.3.1.3 | x-forces | 93 |
| D.3.1.4 | z-forces | 95 |
| D.3.1.5 | Interface pressure | 98 |
| D.3.2 | Station 2 | 100 |
| D.3.2.1 | Effective plastic strain | 100 |
| D.3.2.2 | Resultant forces | 101 |
| D.3.2.3 | x-forces | 102 |
| D.3.2.4 | z-forces | 104 |
| D.3.2.5 | Interface pressure | 107 |
| D.3.3 | Station 3 | 109 |
| D.3.3.1 | Effective plastic strain | 109 |
| D.3.3.2 | Resultant forces | 110 |
| D.3.3.3 | x-forces | 111 |
| D.3.3.4 | z-forces | 112 |
| D.3.3.5 | Interface pressure | 113 |
| D.4 | Geometric evaluation | 114 |
| D.4.1 | Station 1 | 114 |
| D.4.1.1 | Punch displacement | 114 |
| D.4.1.2 | Cartridge height | 115 |
| D.4.1.3 | Projected cartridge height difference | 116 |
| D.4.1.4 | Cartridge bottom profile | 117 |
| D.4.2 | Station 2 | 118 |
| D.4.2.1 | Punch displacement | 118 |
| D.4.2.2 | Cartridge height | 119 |
| D.4.2.3 | Projected cartridge height difference | 120 |
| D.4.2.4 | Cartridge bottom profile | 121 |
| D.4.3 | Station 3 | 122 |
| D.4.3.1 | Punch displacement | 122 |
| D.4.3.2 | Cartridge height | 123 |
| D.4.3.3 | Projected cartridge height difference | 124 |
| D.4.3.4 | Cartridge bottom profile | 125 |
| D.4.4 | Height difference | 126 |
| D.4.5 | Line fitting parameters | 127 |

D.1 0.00° die tilt

D.1.1 Station 1

D.1.1.1 Effective plastic strain

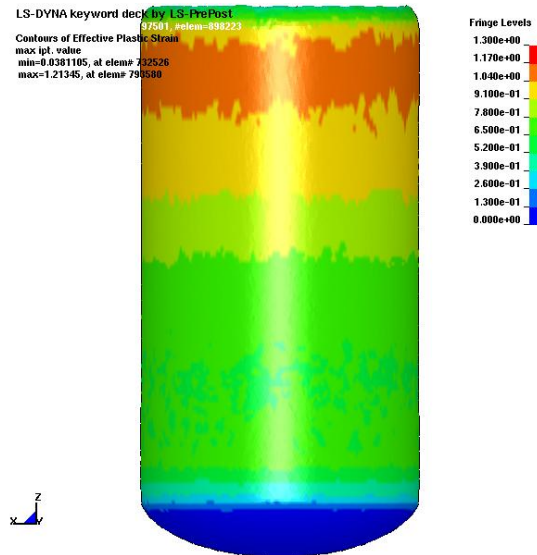


Figure D.1. Effective plastic strain - Station 1
- 0.00° die tilt - Conventional die design

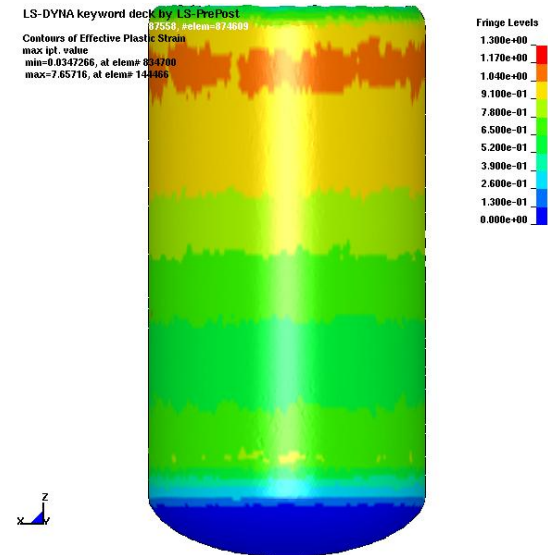


Figure D.2. Effective plastic strain - Station 1
- 0.00° die tilt - $r = 9mm$

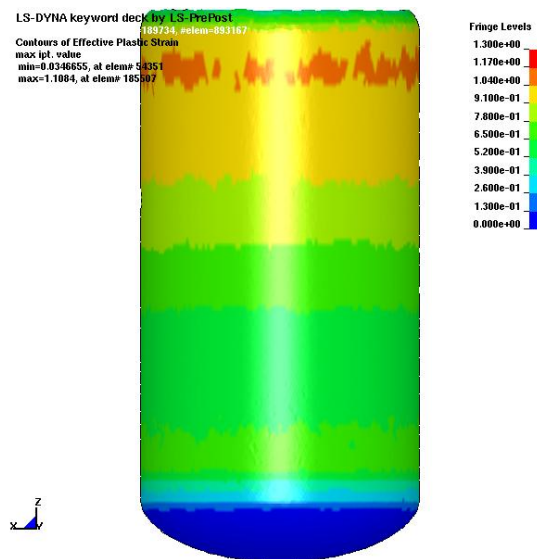


Figure D.3. Effective plastic strain - Station 1
- 0.00° die tilt - $r = 11mm$

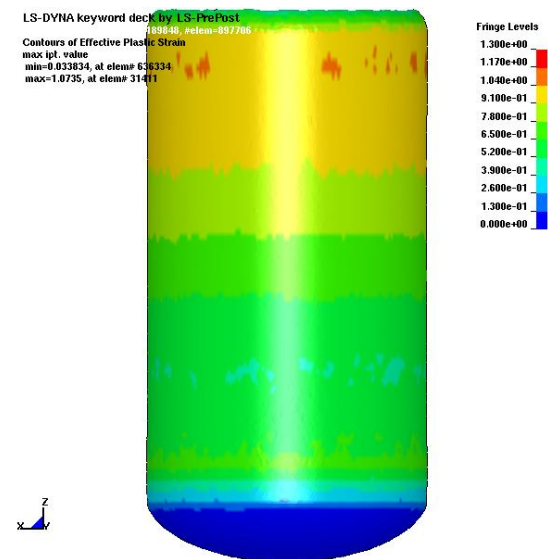


Figure D.4. Effective plastic strain - Station 1
- 0.00° die tilt - $r = 13mm$

D.1.1.2 Resultant forces

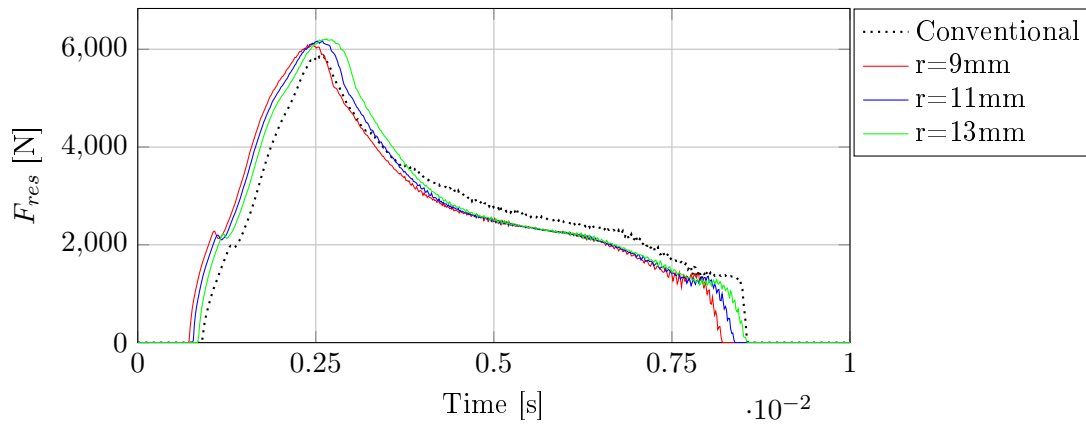


Figure D.5. F_{res} - Station 1 - Die 1 x^+ - 0.00° die tilt

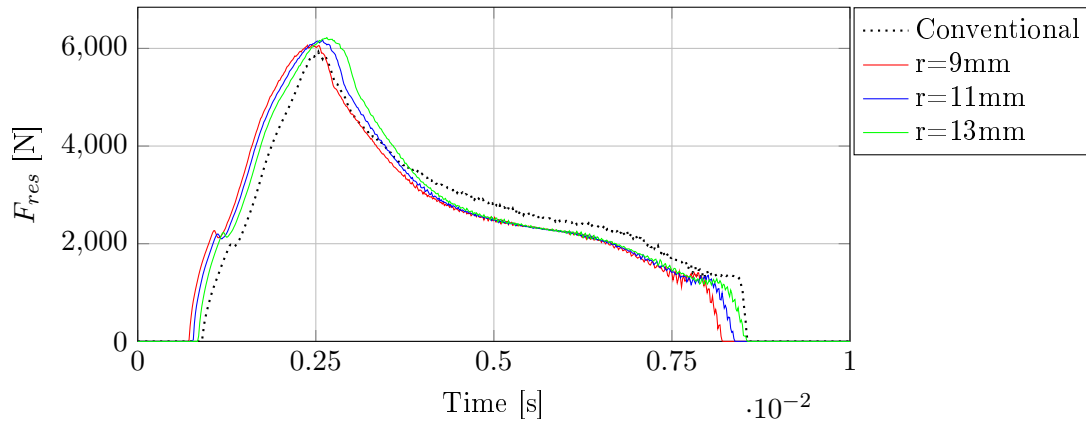


Figure D.6. F_{res} - Station 1 - Die 1 x^- - 0.00° die tilt

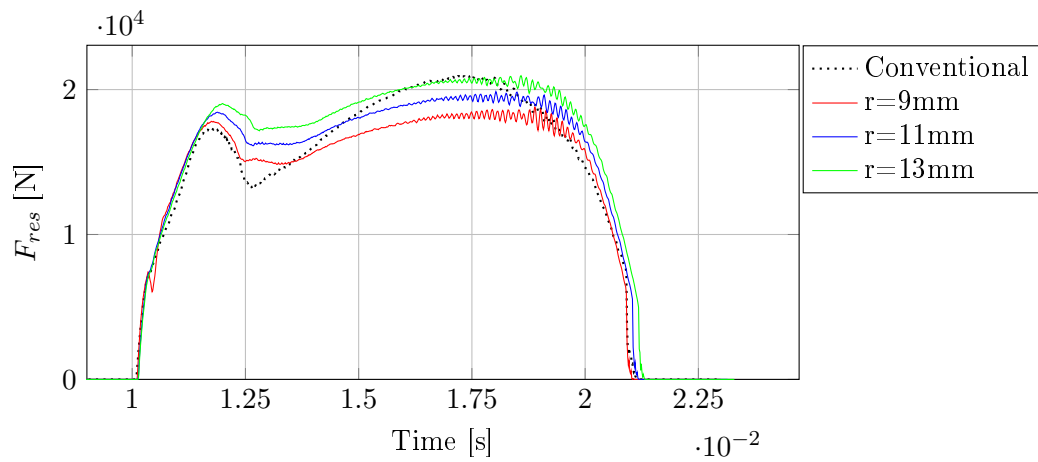


Figure D.7. F_{res} - Station 1 - Die 2 x^+ - 0.00° die tilt

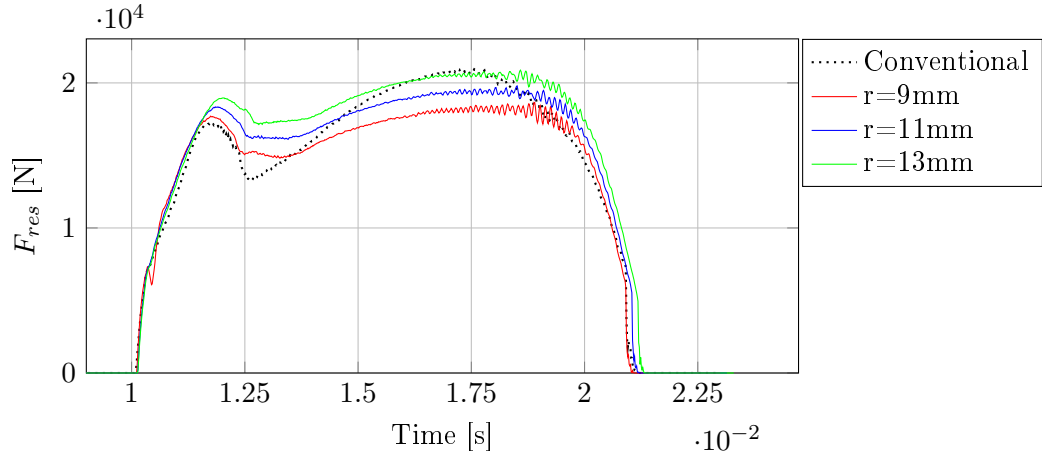


Figure D.8. F_{res} - Station 1 - Die 2 x^- - 0.00° die tilt

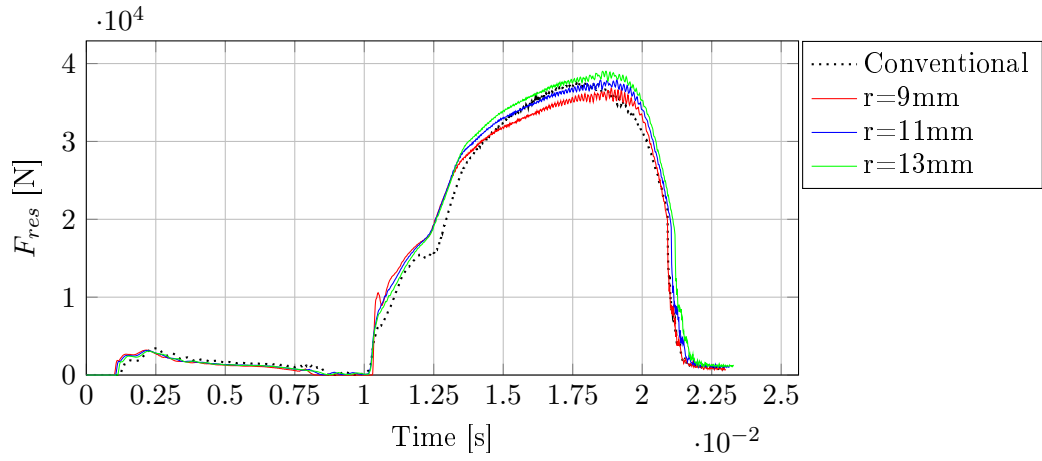


Figure D.9. F_{res} - Station 1 - Punch - 0.00° die tilt

D.1.1.3 x-forces

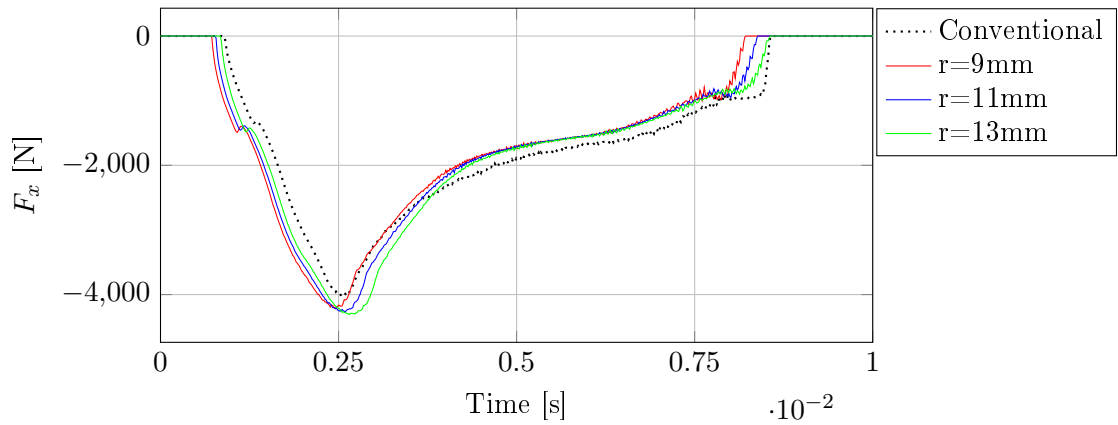


Figure D.10. F_x - Station 1 - Die 1 x^+ - 0.00° die tilt

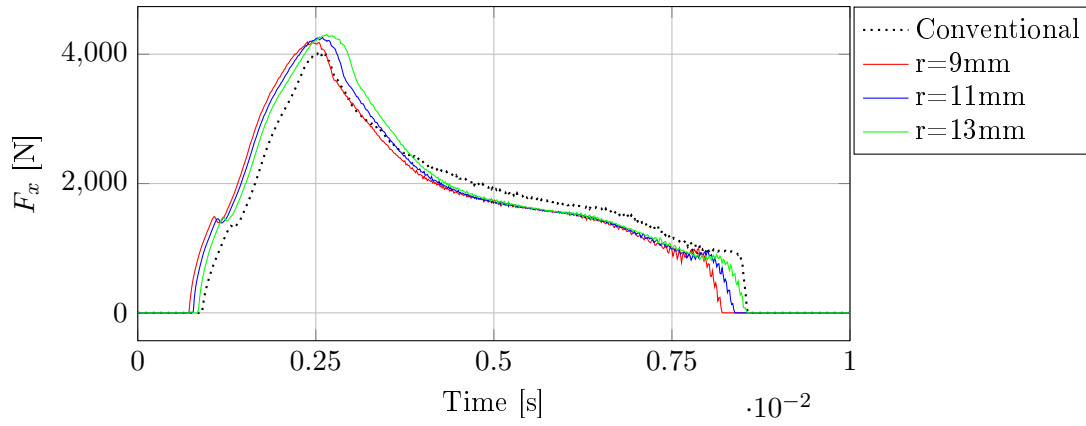


Figure D.11. F_x - Station 1 - Die 1 x^- - 0.00° die tilt

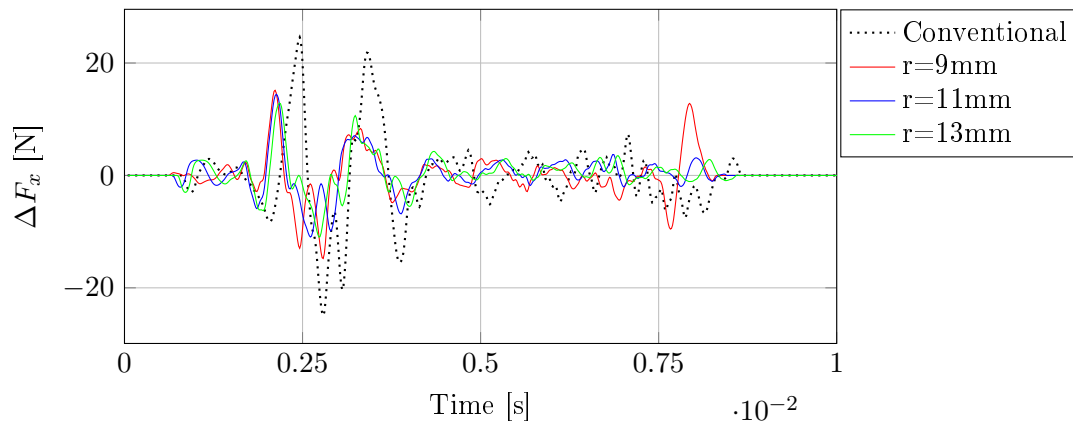


Figure D.12. ΔF_x - Station 1 - Die 1 - 0.00° die tilt

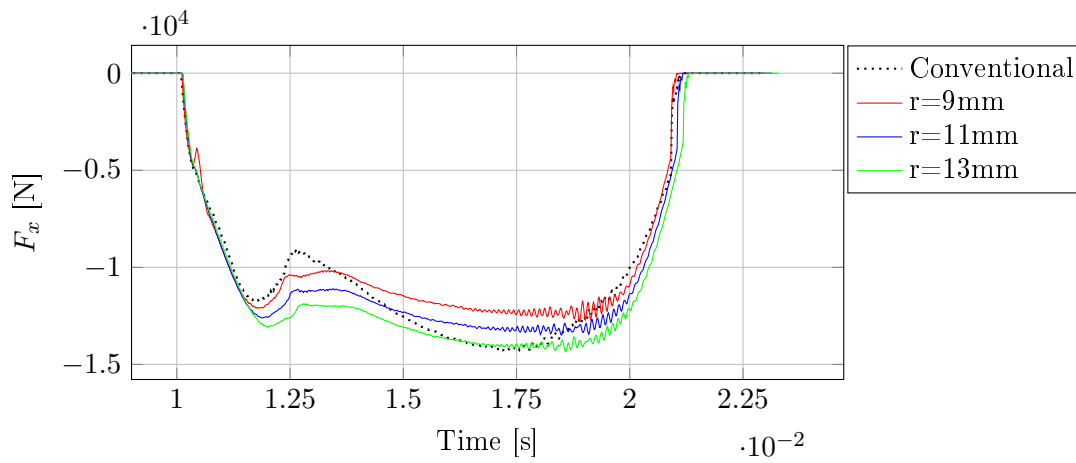


Figure D.13. F_x - Station 1 - Die 2 x^+ - 0.00° die tilt

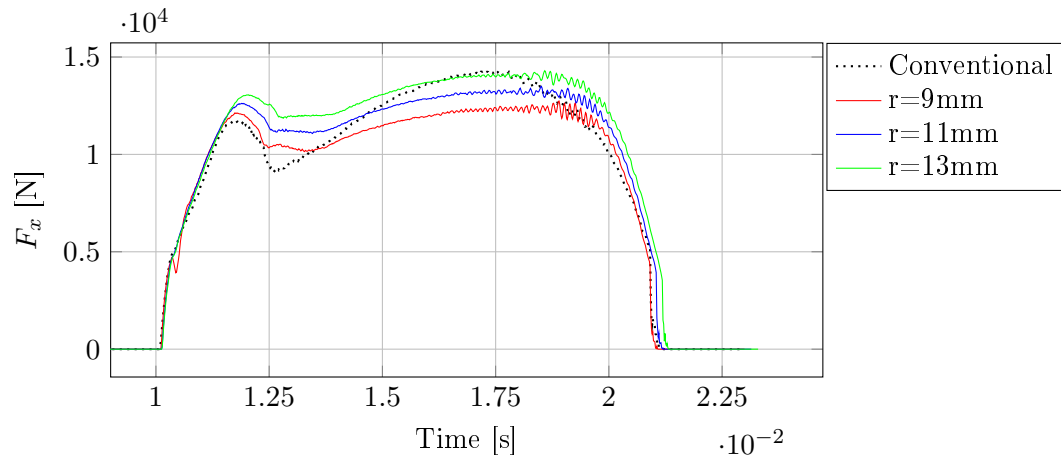


Figure D.14. F_x - Station 1 - Die 2 x^- - 0.00° die tilt

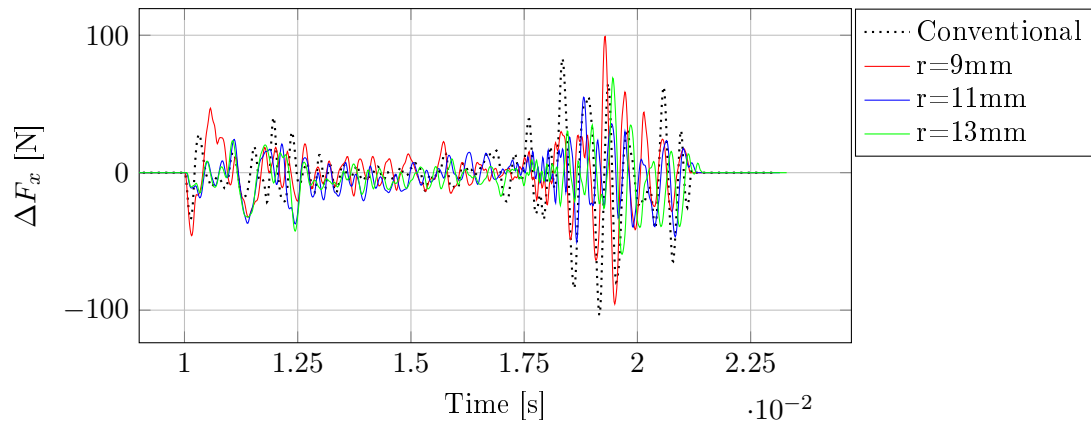


Figure D.15. ΔF_x - Station 1 - Die 2 - 0.00° die tilt

D.1.1.4 z-forces

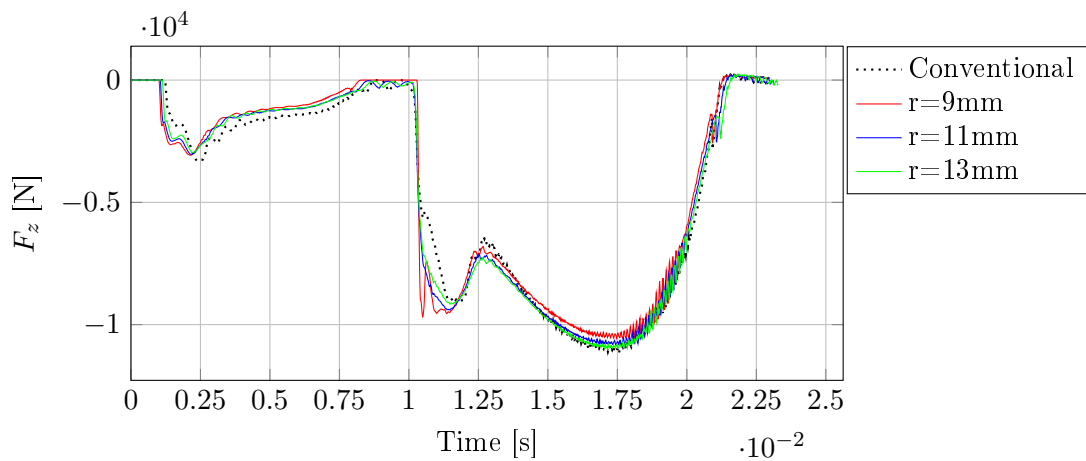


Figure D.16. F_z - Station 1 - Punch - 0.00° die tilt

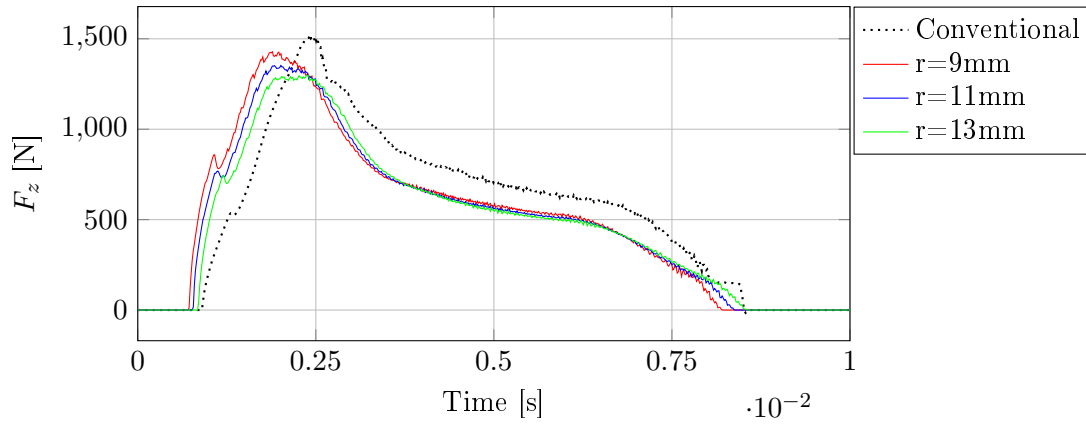


Figure D.17. F_z - Station 1 - Die 1 x^+ - 0.00° die tilt

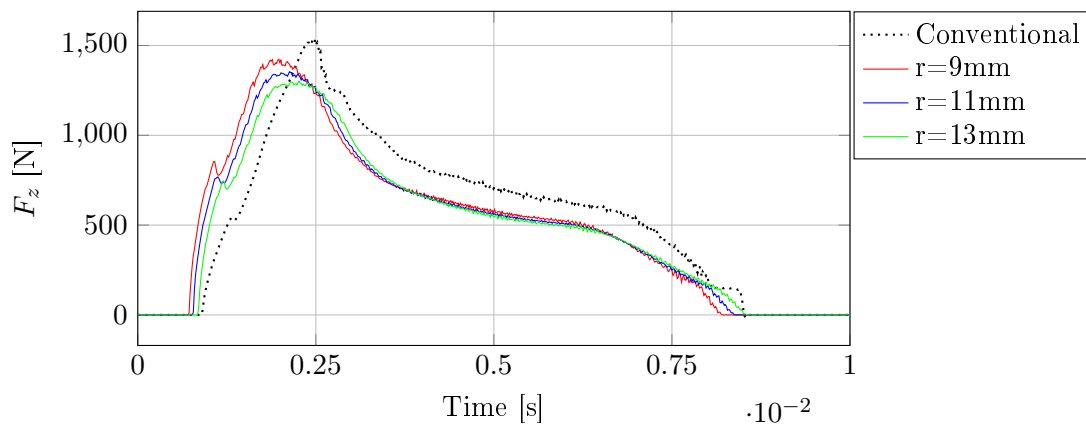


Figure D.18. F_z - Station 1 - Die 1 x^- - 0.00° die tilt

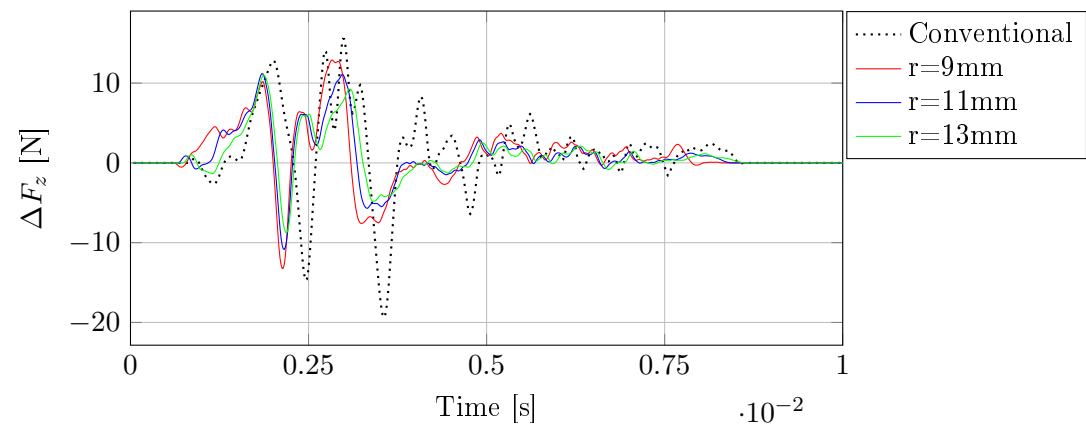


Figure D.19. ΔF_z - Station 1 - Die 1 - 0.00° die tilt

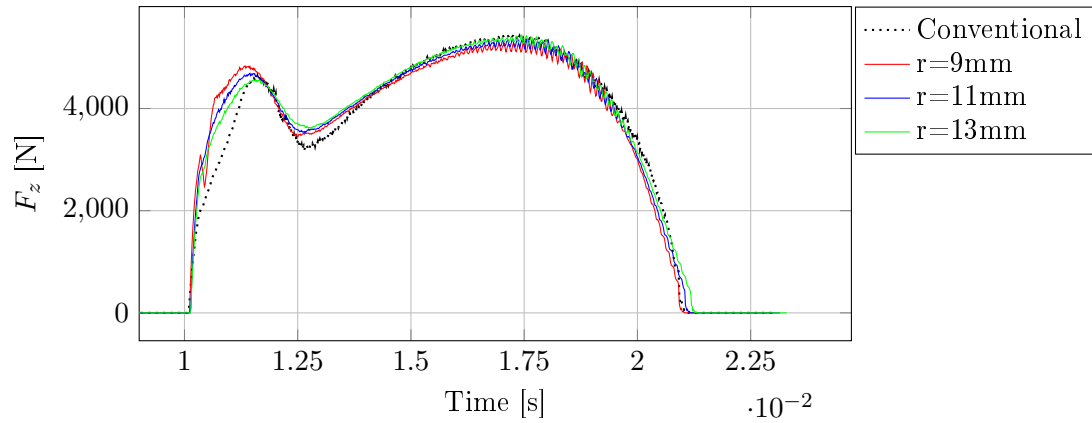


Figure D.20. F_z - Station 1 - Die 2 x^+ - 0.00° die tilt

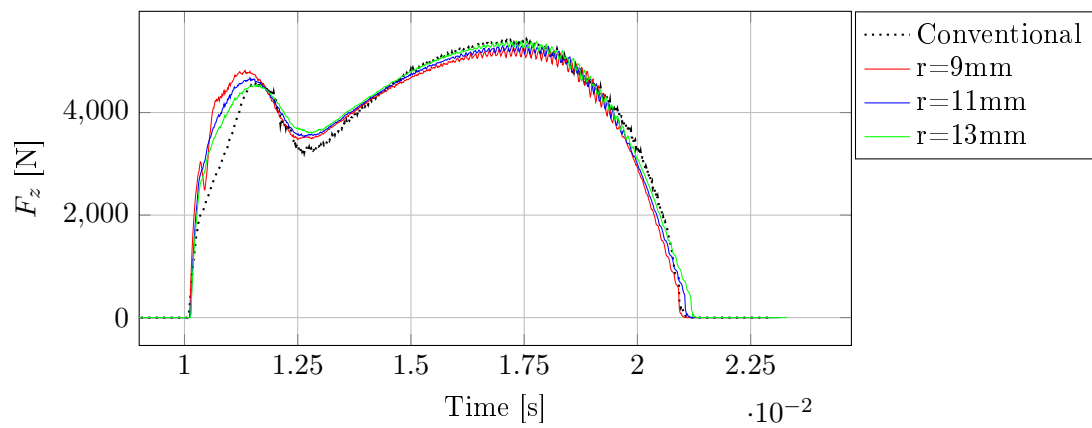


Figure D.21. F_z - Station 1 - Die 2 x^- - 0.00° die tilt

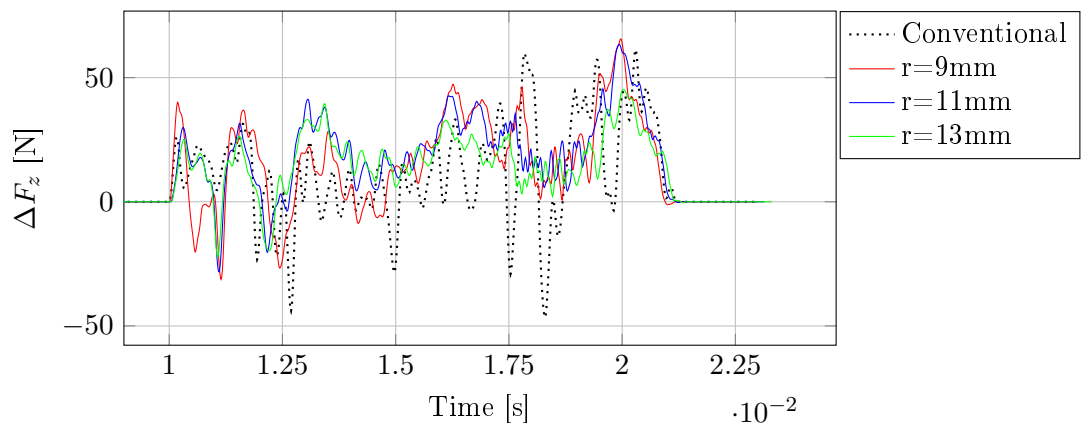


Figure D.22. ΔF_z - Station 1 - Die 2 - 0.00° die tilt

D.1.1.5 Interface pressure

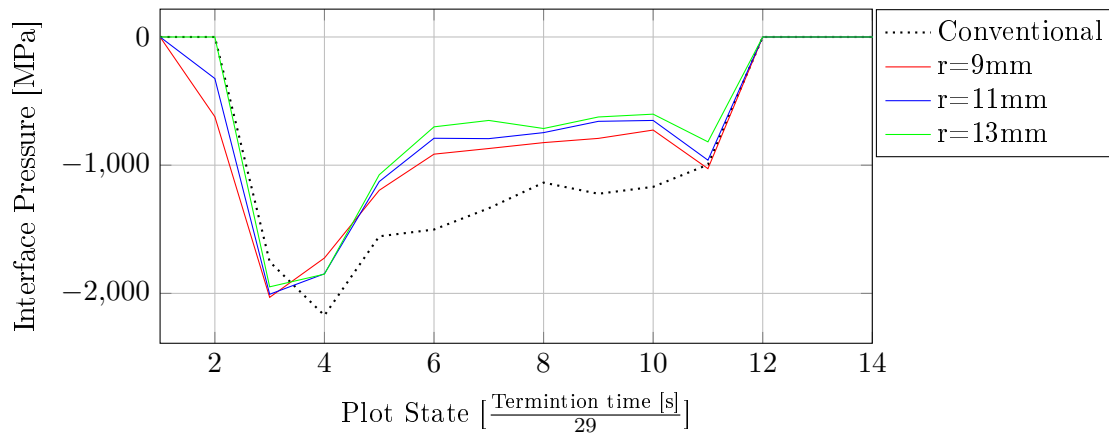


Figure D.23. Maximum interface pressure - Station 1 - Die 1 x^+ - 0.00° die tilt

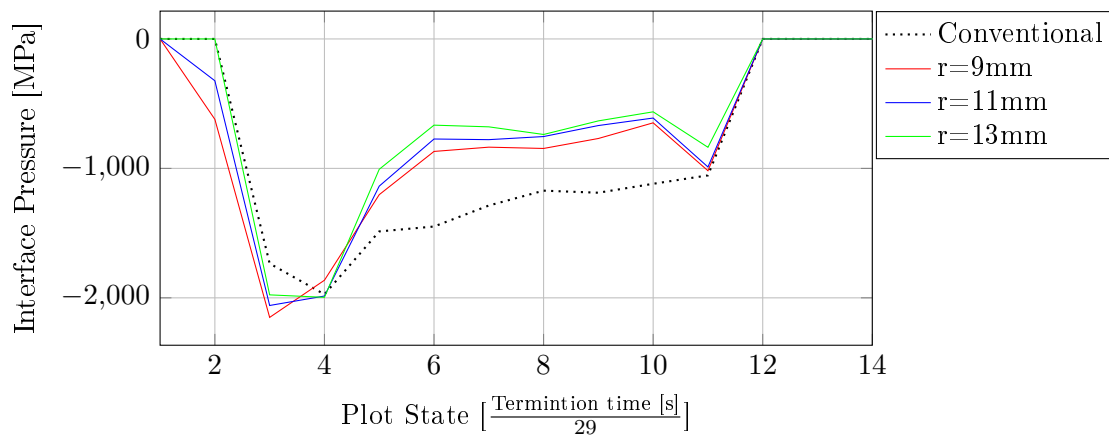


Figure D.24. Maximum interface pressure - Station 1 - Die 1 x^- - 0.00° die tilt

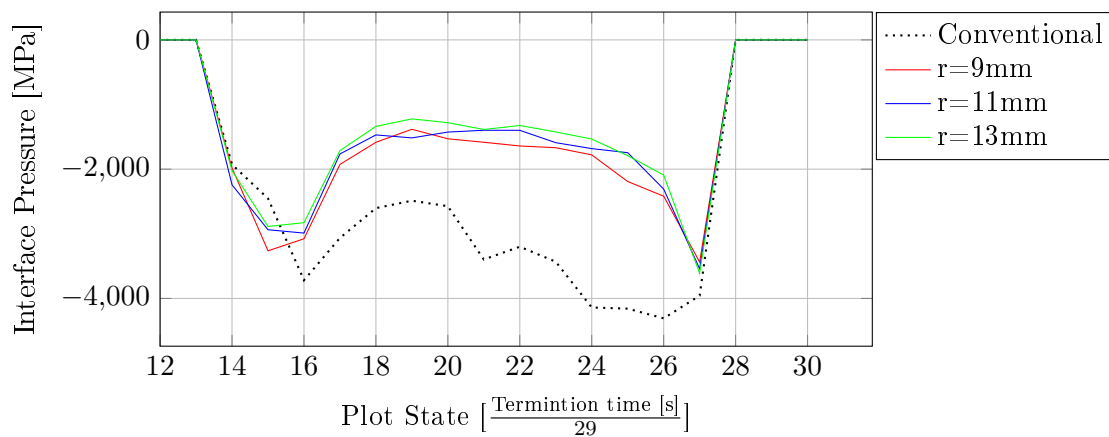


Figure D.25. Maximum interface pressure - Station 1 - Die 2 x^+ - 0.00° die tilt

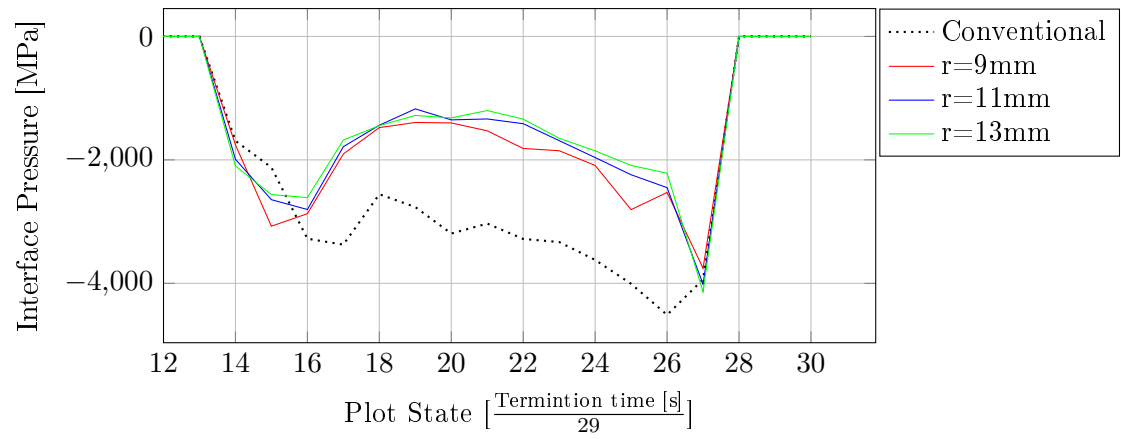


Figure D.26. Maximum interface pressure - Station 1 - Die 2 x^- - 0.00° die tilt

D.1.2 Station 2

D.1.2.1 Effective plastic strain

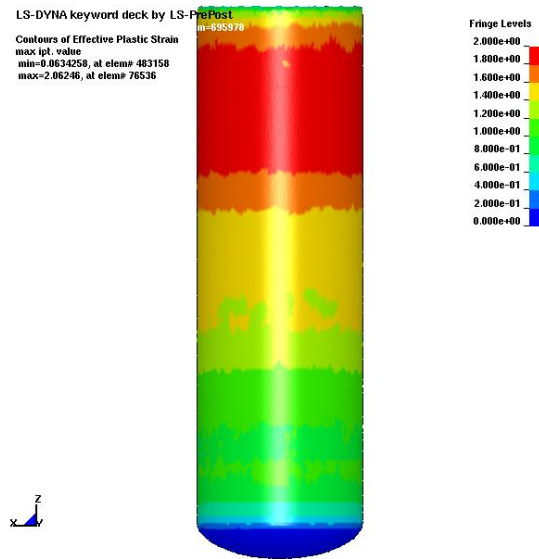


Figure D.27. Effective plastic strain - Station 2 - 0.00° die tilt - Conventional die design

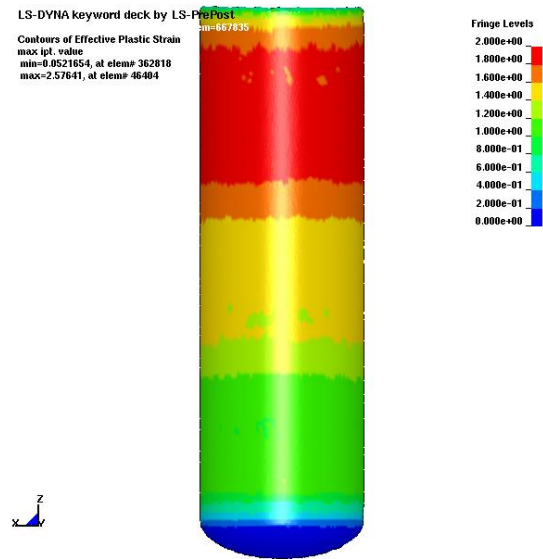


Figure D.28. Effective plastic strain - Station 2 - 0.00° die tilt - $r = 9mm$

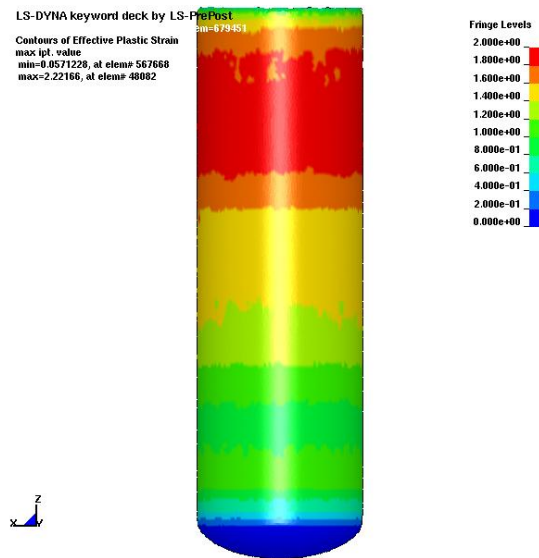


Figure D.29. Effective plastic strain - Station 2 - 0.00° die tilt - $r = 11mm$

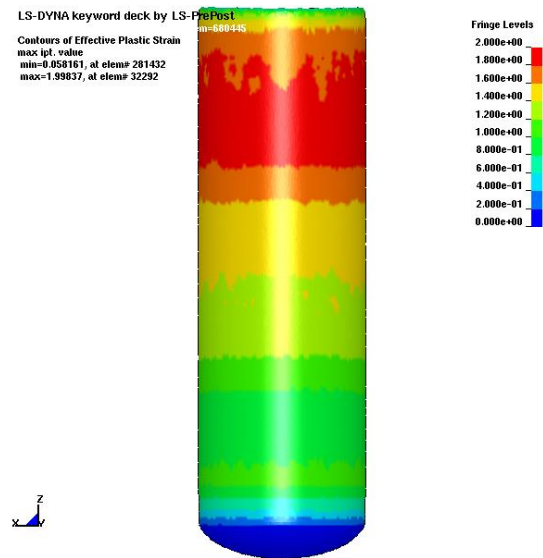


Figure D.30. Effective plastic strain - Station 2 - 0.00° die tilt - $r = 13mm$

D.1.2.2 Resultant forces

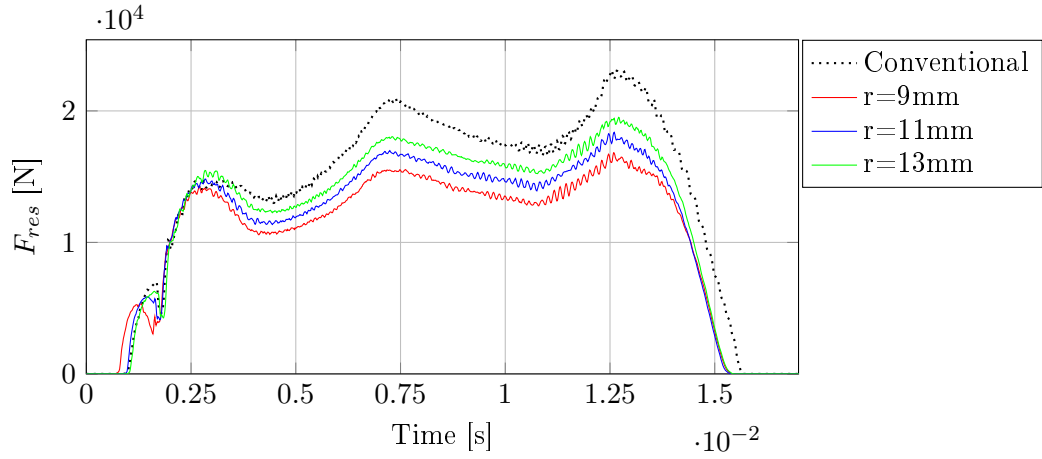


Figure D.31. F_{res} - Station 2 - Die 1 x^+ - 0.00° die tilt

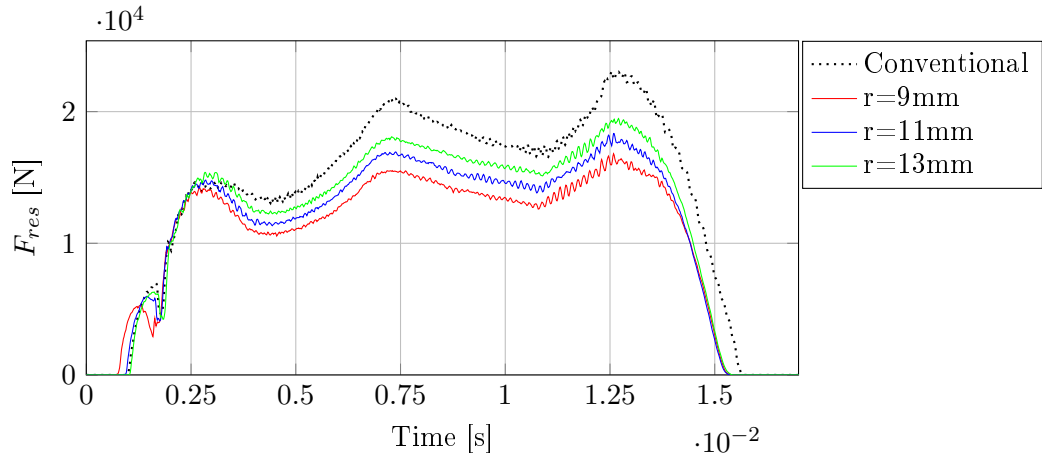


Figure D.32. F_{res} - Station 2 - Die 1 x^- - 0.00° die tilt

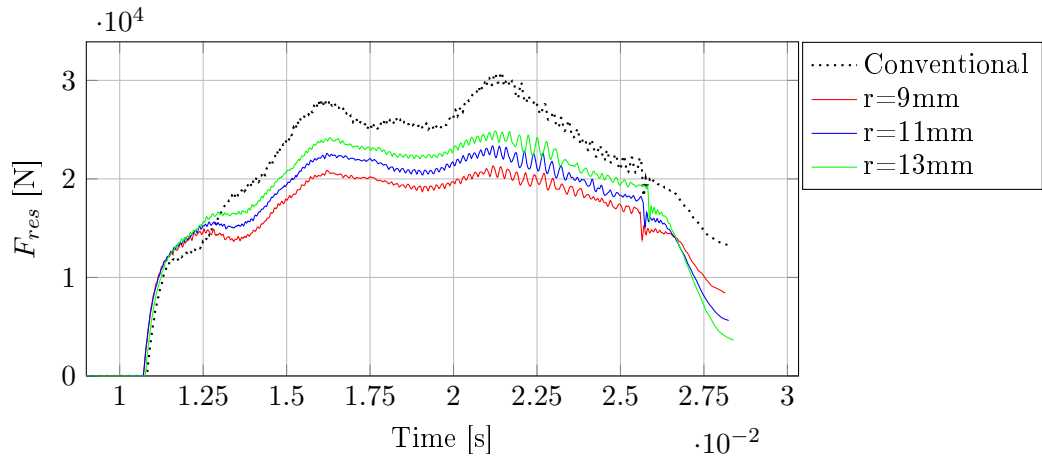


Figure D.33. F_{res} - Station 2 - Die 2 x^+ - 0.00° die tilt

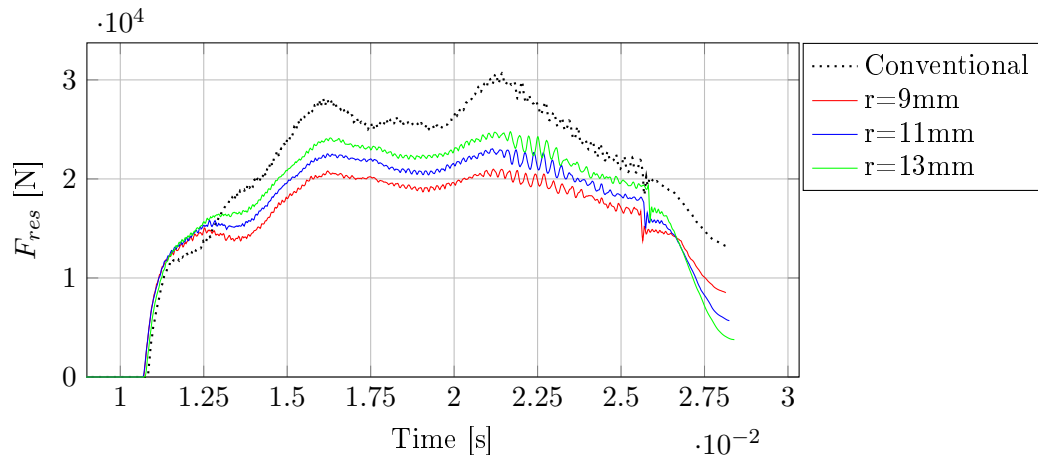


Figure D.34. F_{res} - Station 2 - Die 2 x^- - 0.00° die tilt

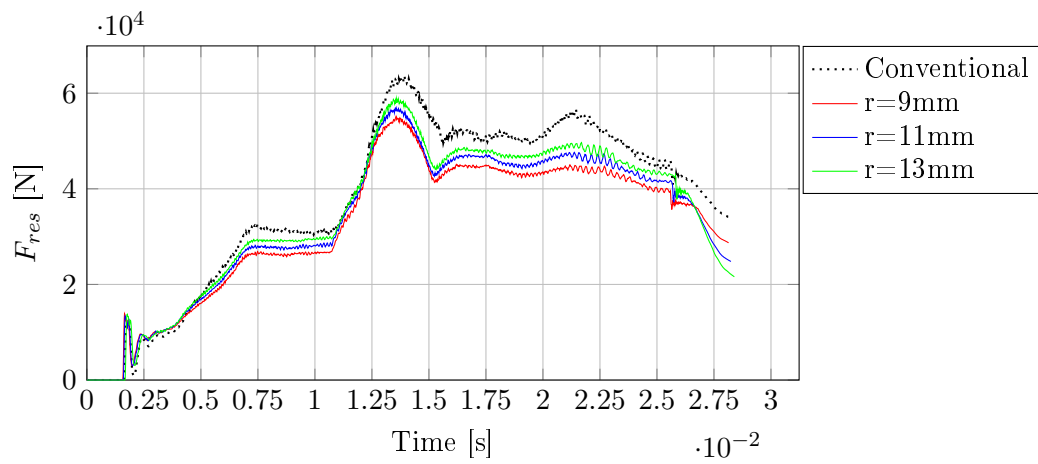


Figure D.35. F_{res} - Station 2 - Punch - 0.00° die tilt

D.1.2.3 x-forces

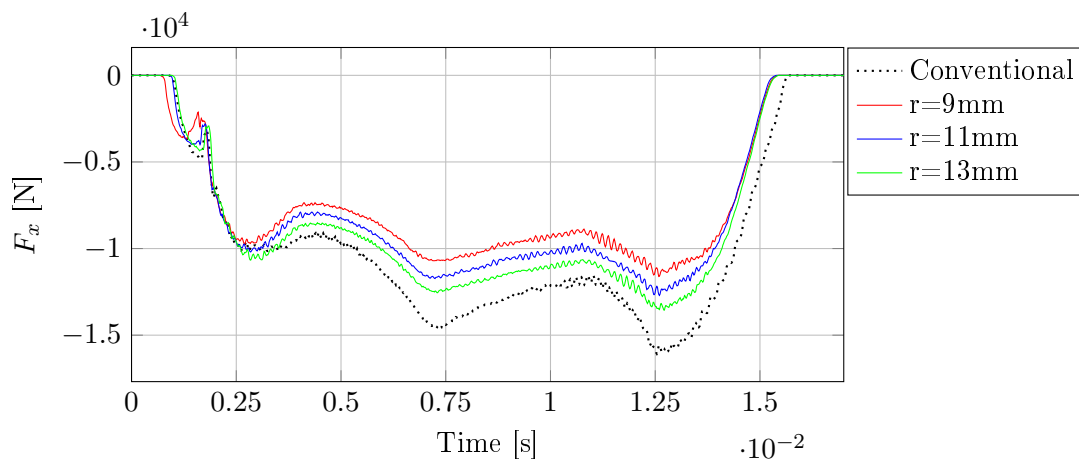


Figure D.36. F_x - Station 2 - Die 1 x^+ - 0.00° die tilt

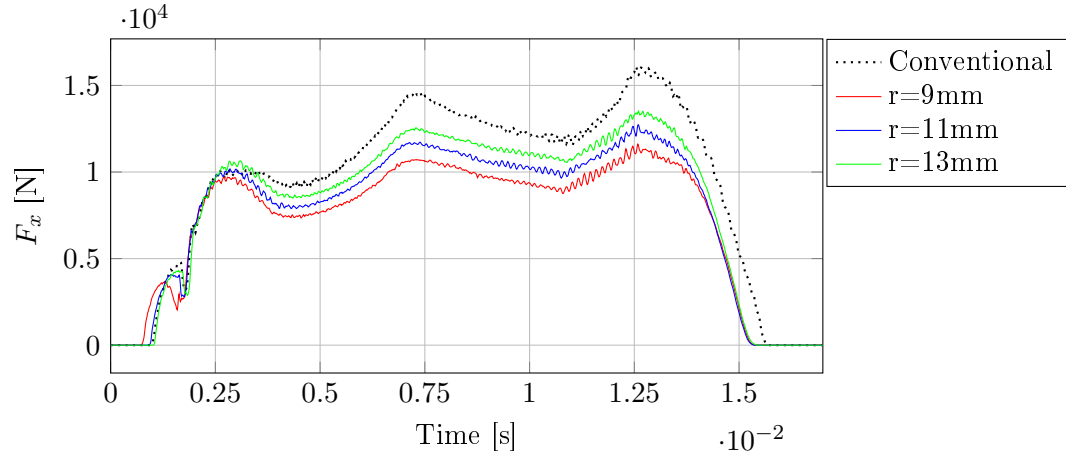


Figure D.37. F_x - Station 2 - Die 1 x^- - 0.00° die tilt

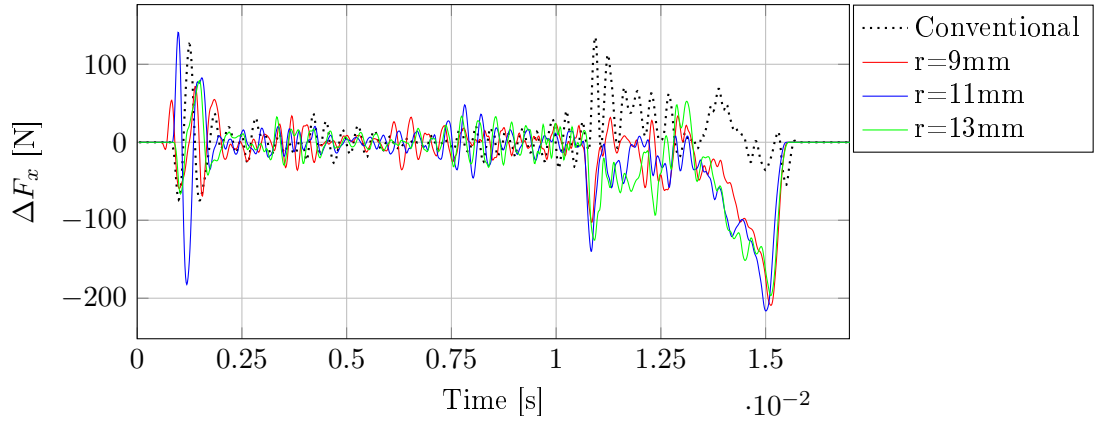


Figure D.38. ΔF_x - Station 2 - Die 1 - 0.00° die tilt

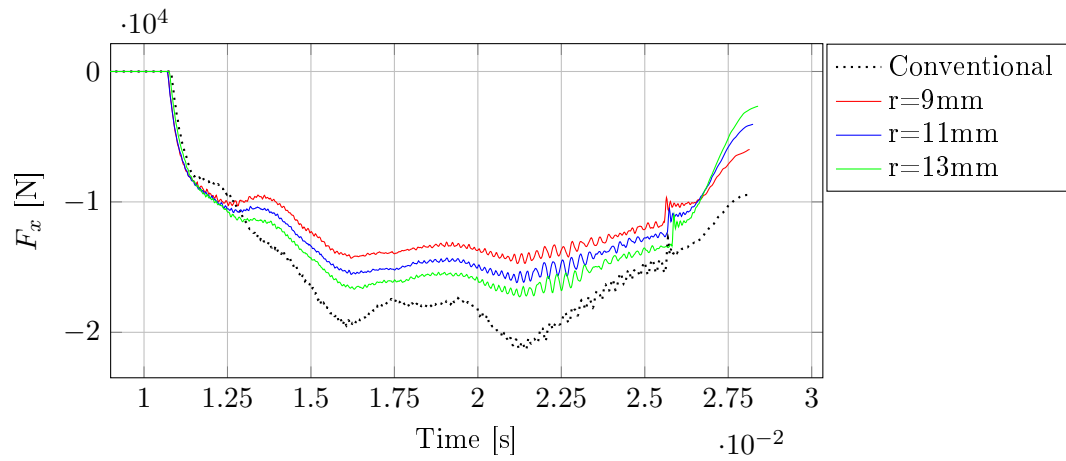


Figure D.39. F_x - Station 2 - Die 2 x^+ - 0.00° die tilt

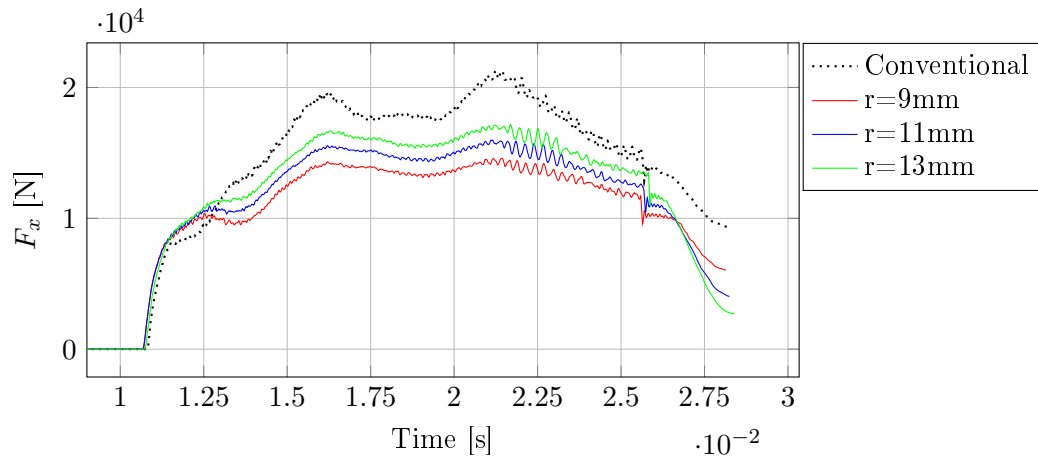


Figure D.40. F_x - Station 2 - Die 2 x^- - 0.00° die tilt

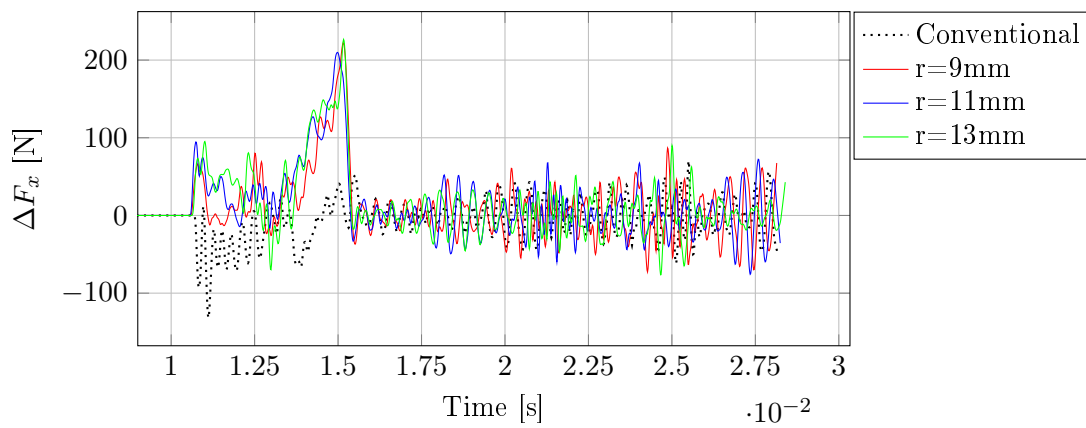


Figure D.41. ΔF_x - Station 2 - Die 2 - 0.00° die tilt

D.1.2.4 z-forces

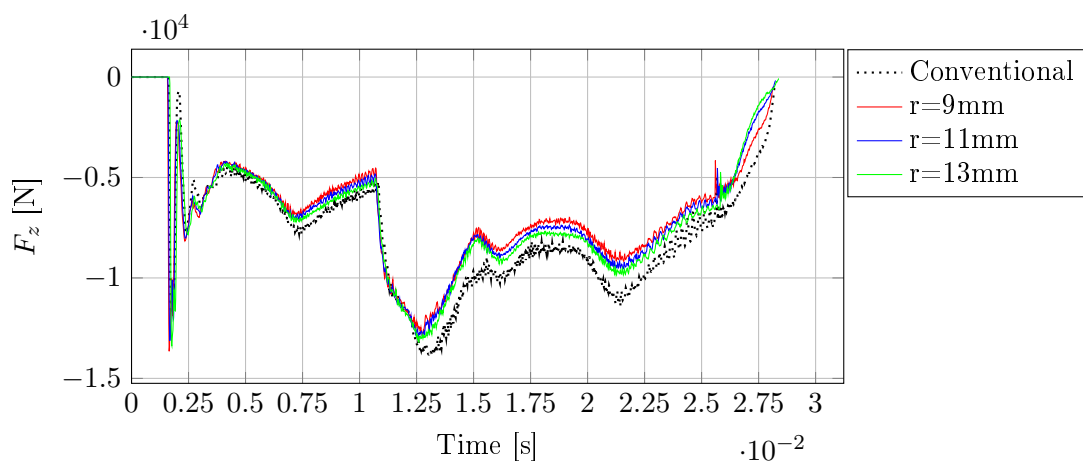


Figure D.42. F_z - Station 2 - Punch - 0.00° die tilt

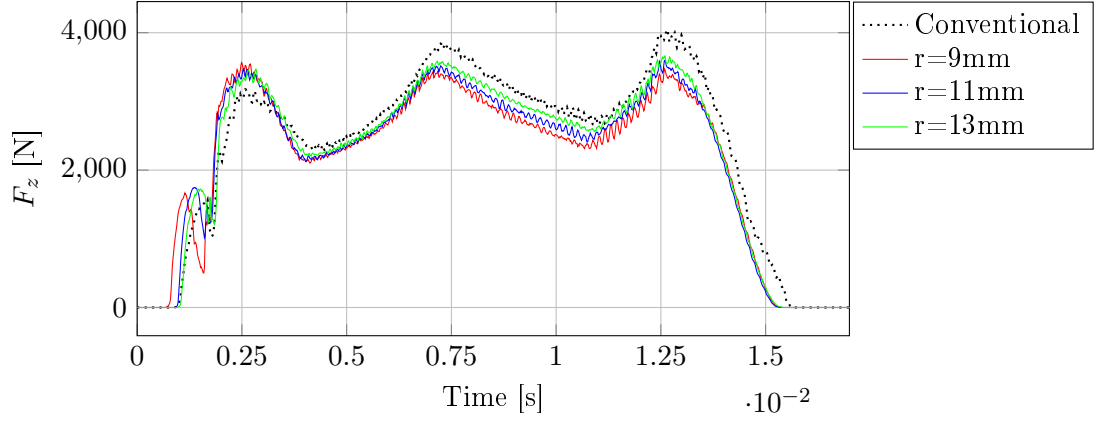


Figure D.43. F_z - Station 2 - Die 1 x^+ - 0.00° die tilt

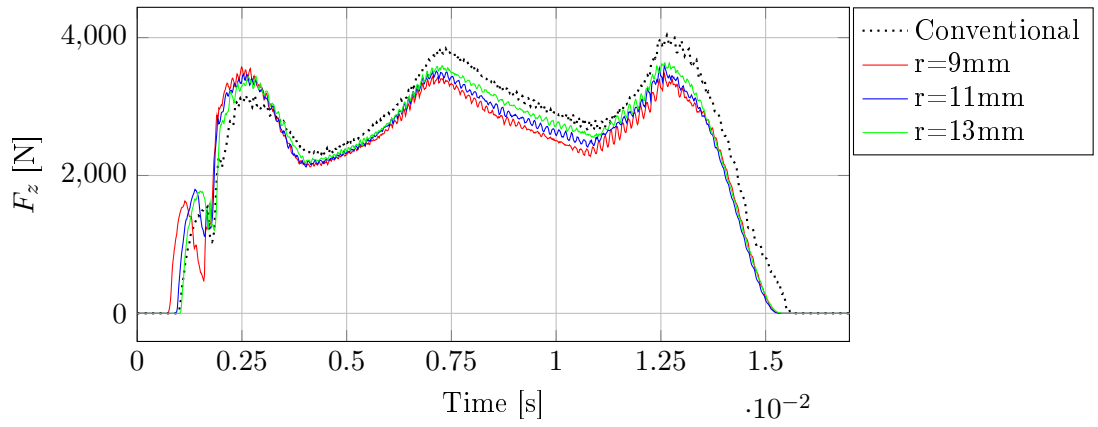


Figure D.44. F_z - Station 2 - Die 1 x^- - 0.00° die tilt

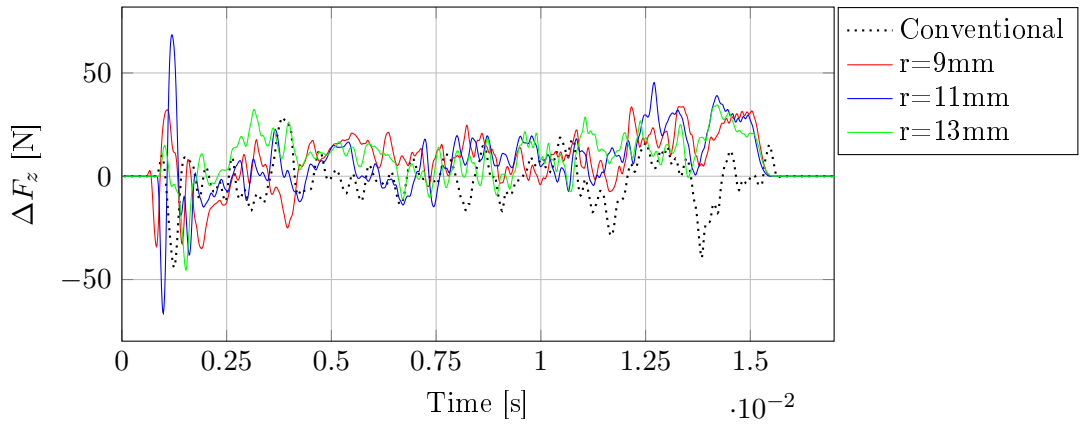


Figure D.45. ΔF_z - Station 2 - Die 1 - 0.00° die tilt

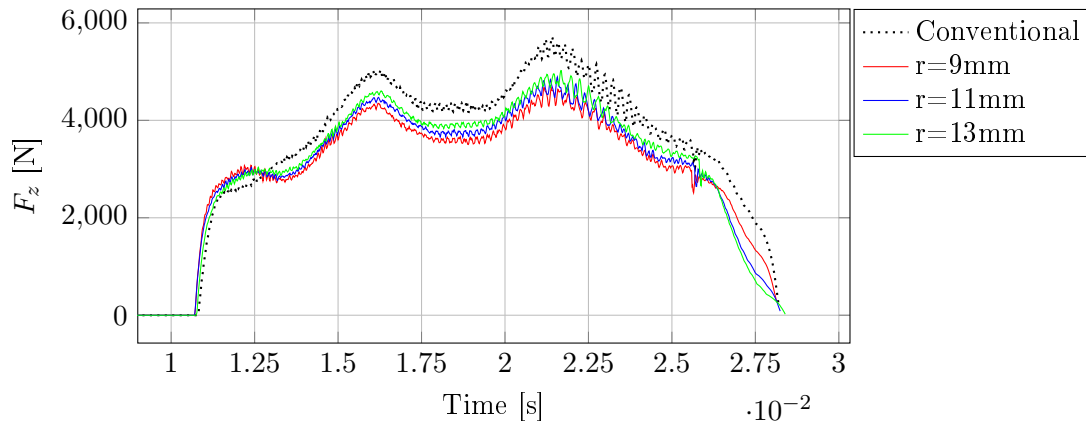


Figure D.46. F_z - Station 2 - Die 2 x^+ - 0.00° die tilt

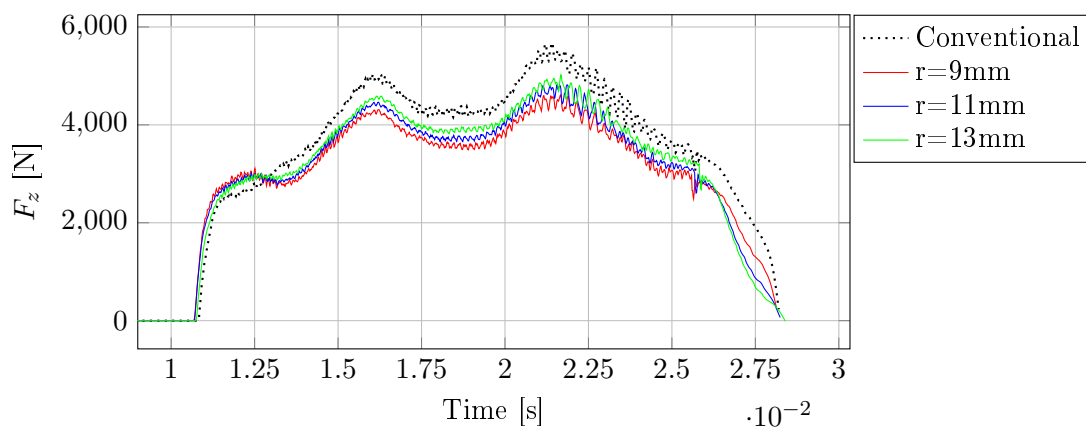


Figure D.47. F_z - Station 2 - Die 2 x^- - 0.00° die tilt

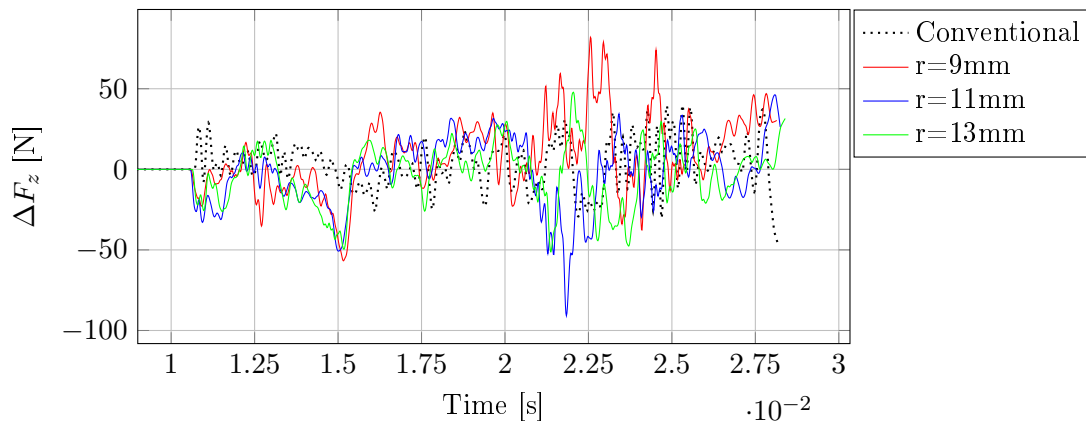


Figure D.48. ΔF_z - Station 2 - Die 2 - 0.00° die tilt

D.1.2.5 Interface pressure

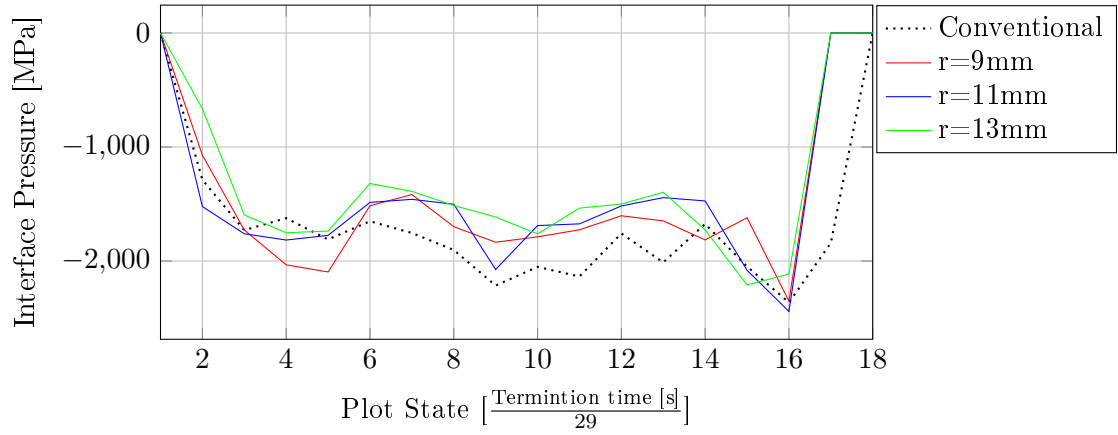


Figure D.49. Maximum interface pressure - Station 2 - Die 1 x^+ - 0.00° die tilt

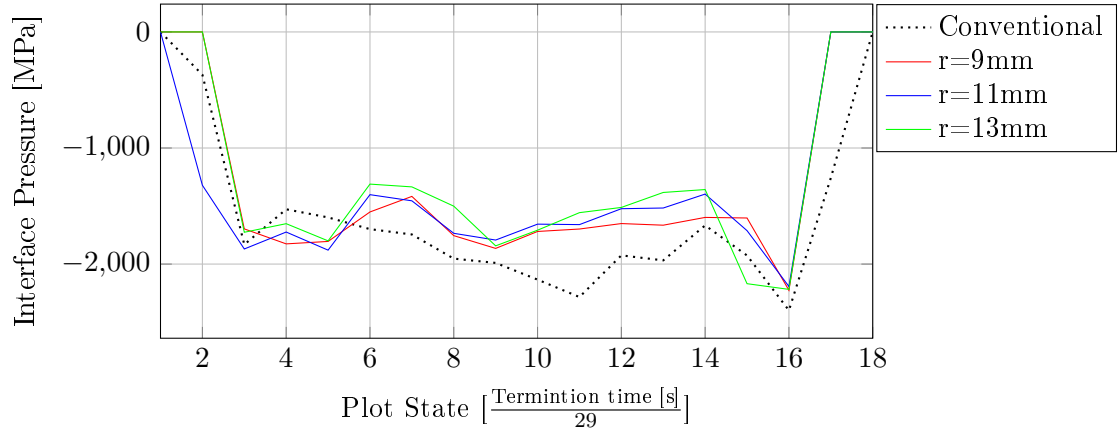


Figure D.50. Maximum interface pressure - Station 2 - Die 1 x^- - 0.00° die tilt

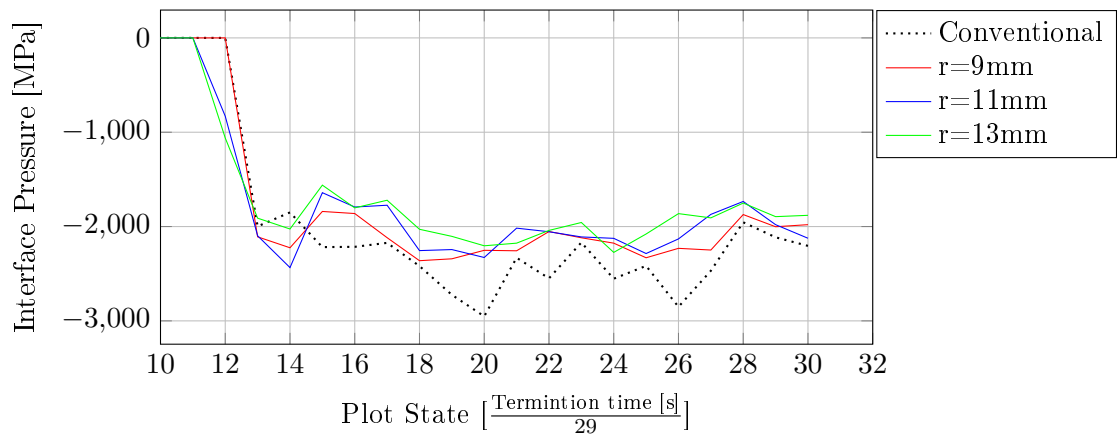


Figure D.51. Maximum interface pressure - Station 2 - Die 2 x^+ - 0.00° die tilt

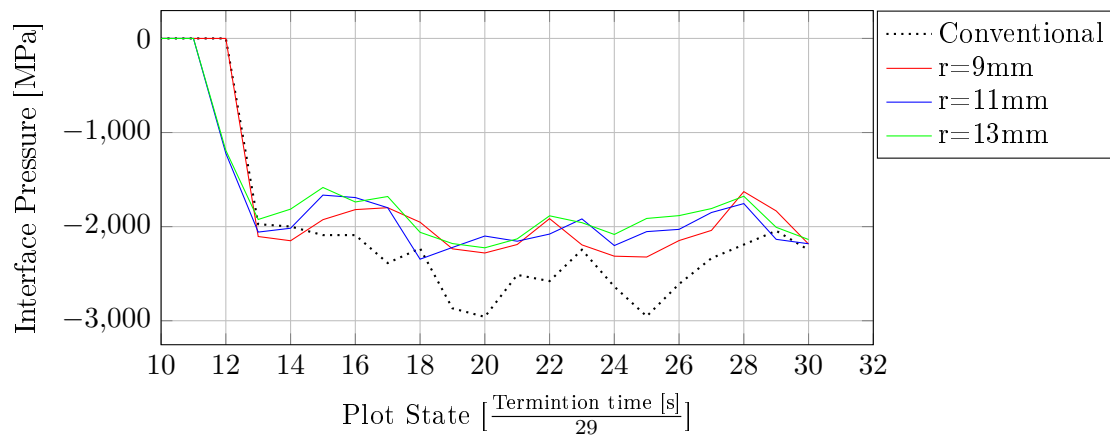


Figure D.52. Maximum interface pressure - Station 2 - Die 2 x^- - 0.00° die tilt

D.1.3 Station 3

D.1.3.1 Effective plastic strain

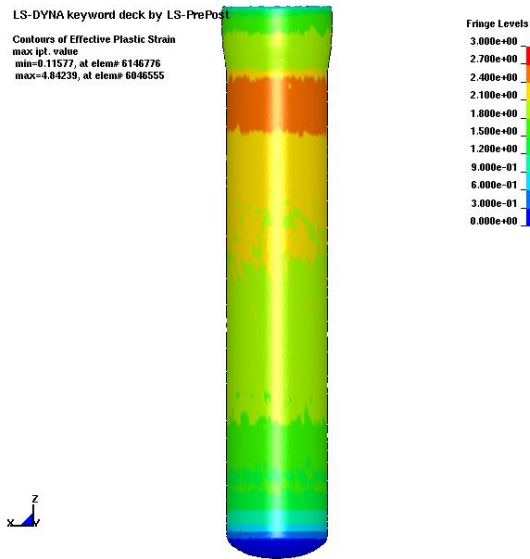


Figure D.53. Effective plastic strain - Station 3 - 0.00° die tilt - Conventional die design

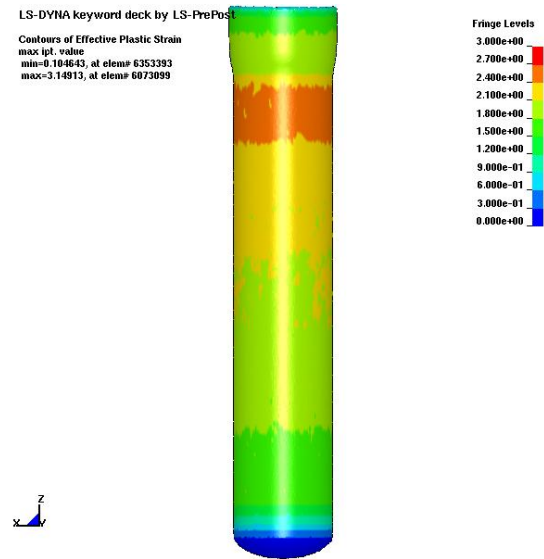


Figure D.54. Effective plastic strain - Station 3 - 0.00° die tilt - $r = 9mm$

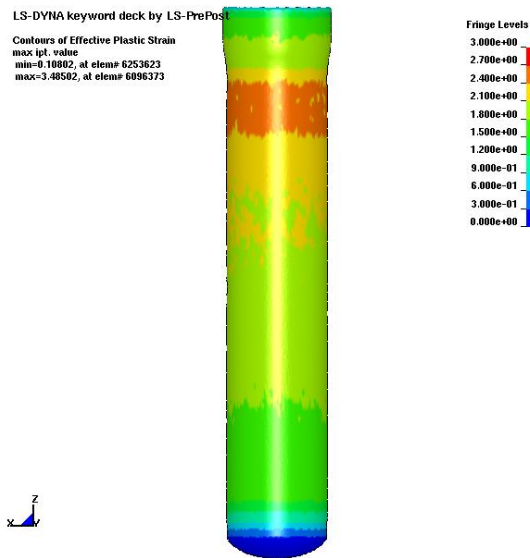


Figure D.55. Effective plastic strain - Station 3 - 0.00° die tilt - $r = 11mm$

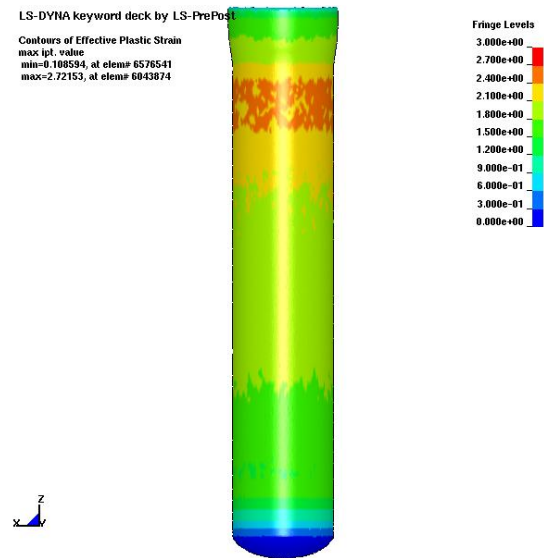


Figure D.56. Effective plastic strain - Station 3 - 0.00° die tilt - $r = 13mm$

D.1.3.2 Resultant forces

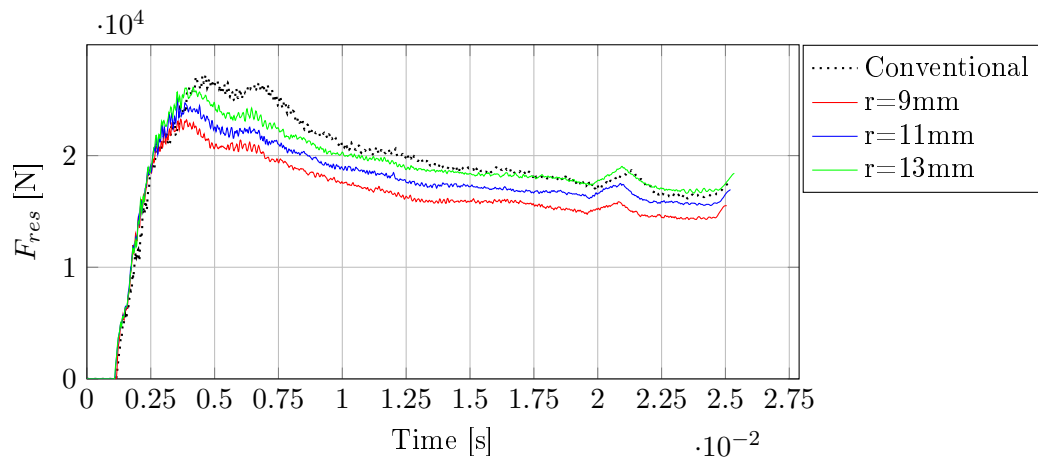


Figure D.57. F_{res} - Station 3 - Die 1 x^+ - 0.00° die tilt

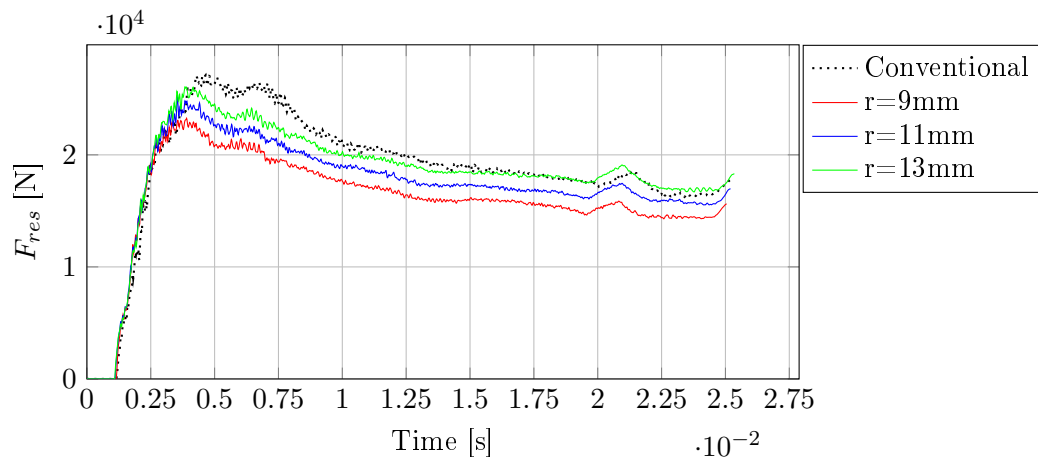


Figure D.58. F_{res} - Station 3 - Die 1 x^- - 0.00° die tilt

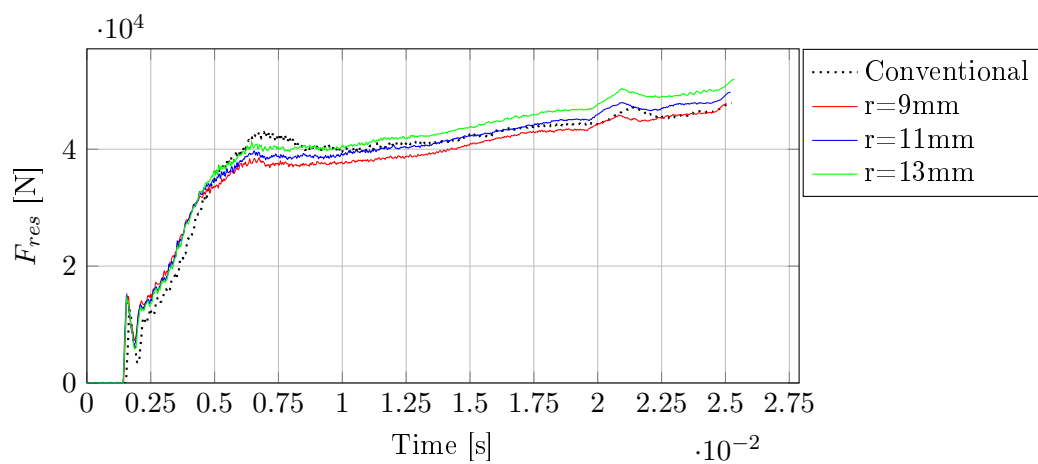


Figure D.59. F_{res} - Station 3 - Punch - 0.00° die tilt

D.1.3.3 x-forces

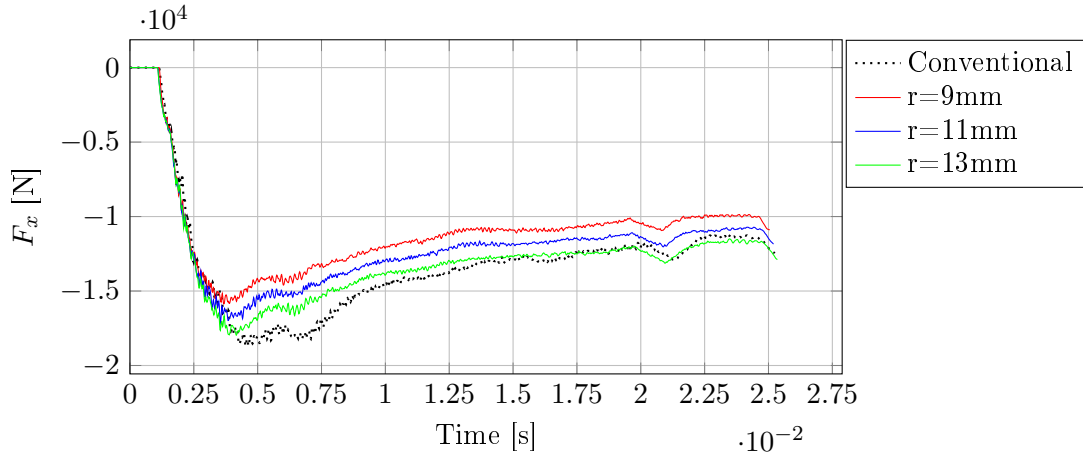


Figure D.60. F_x - Station 3 - Die 1 x^+ - 0.00° die tilt

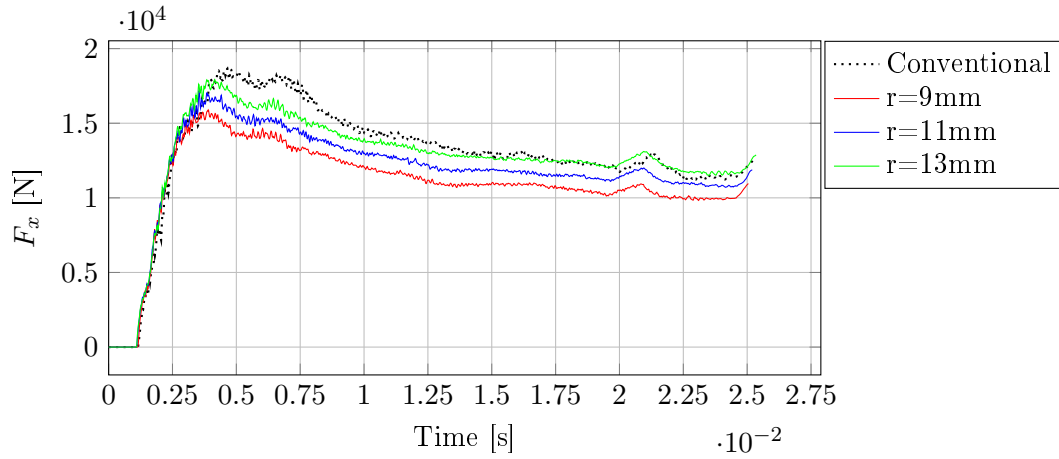


Figure D.61. F_x - Station 3 - Die 1 x^- - 0.00° die tilt

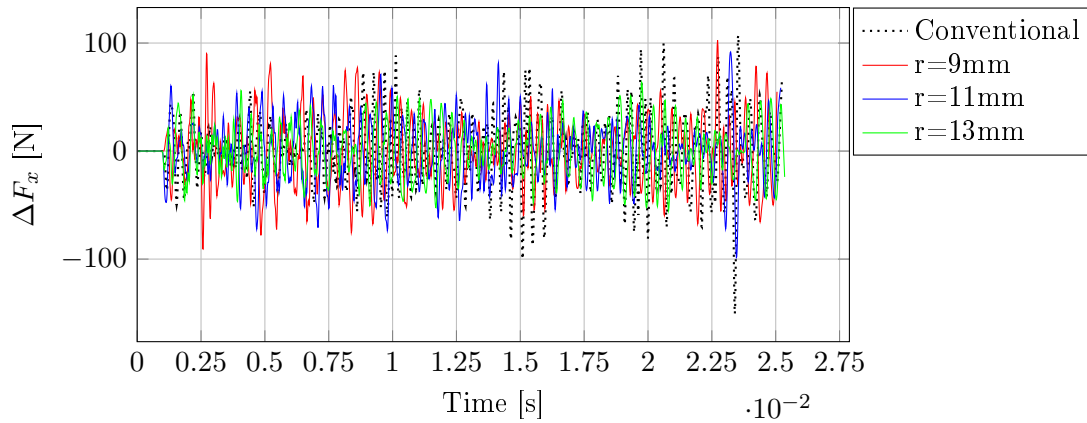


Figure D.62. ΔF_x - Station 3 - Die 1 - 0.00° die tilt

D.1.3.4 z-forces

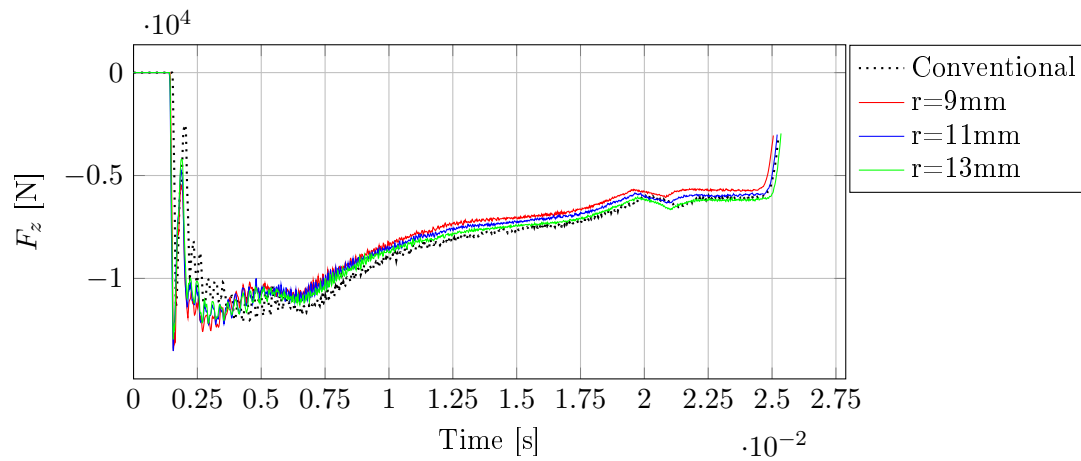


Figure D.63. F_z - Station 3 - Punch - 0.00° die tilt

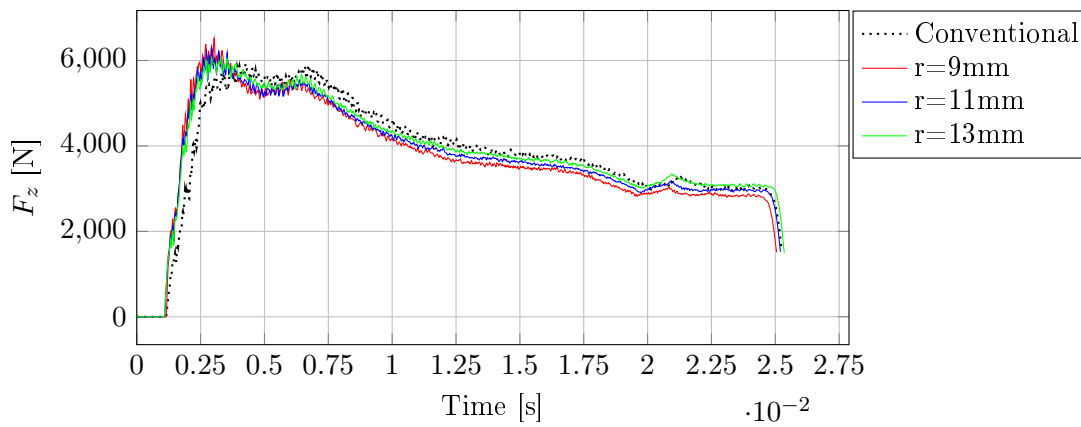


Figure D.64. F_z - Station 3 - Die 1 x^+ - 0.00° die tilt

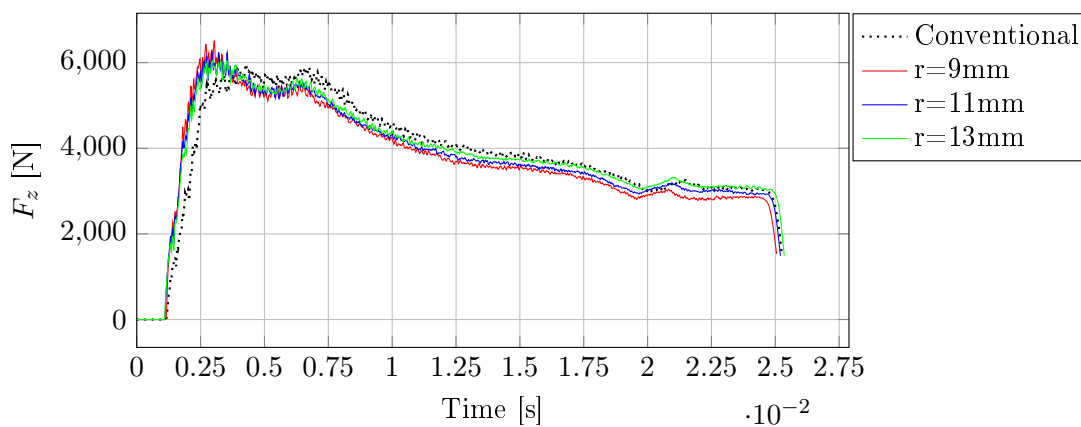


Figure D.65. F_z - Station 3 - Die 1 x^- - 0.00° die tilt

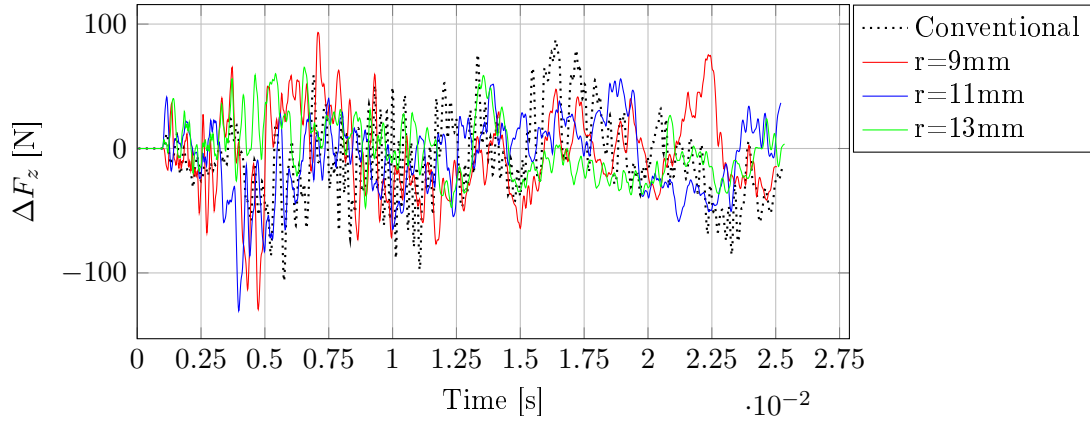


Figure D.66. ΔF_z - Station 3 - Die 1 - 0.00° die tilt

D.1.3.5 Interface pressure

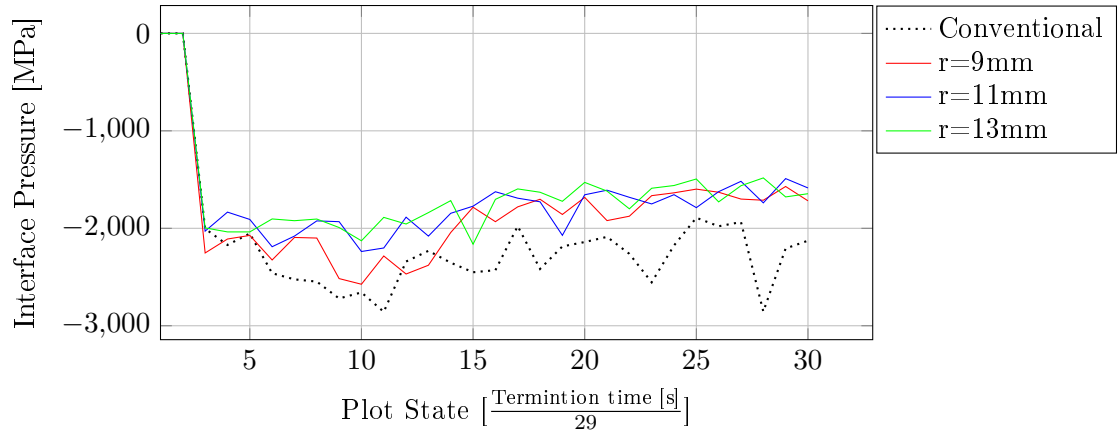


Figure D.67. Maximum interface pressure - Station 3 - Die 1 x^+ - 0.00° die tilt

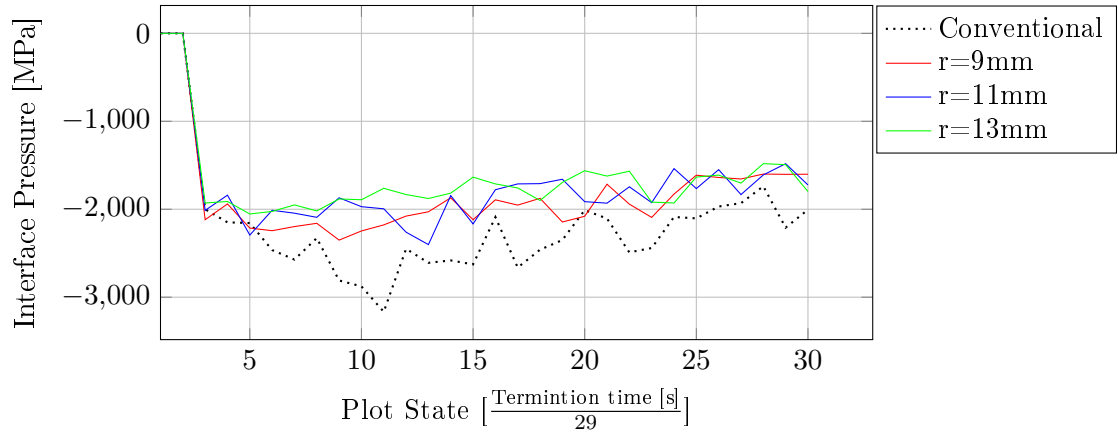


Figure D.68. Maximum interface pressure - Station 3 - Die 1 x^- - 0.00° die tilt

D.2 0.20° die tilt

D.2.1 Station 1

D.2.1.1 Effective plastic strain

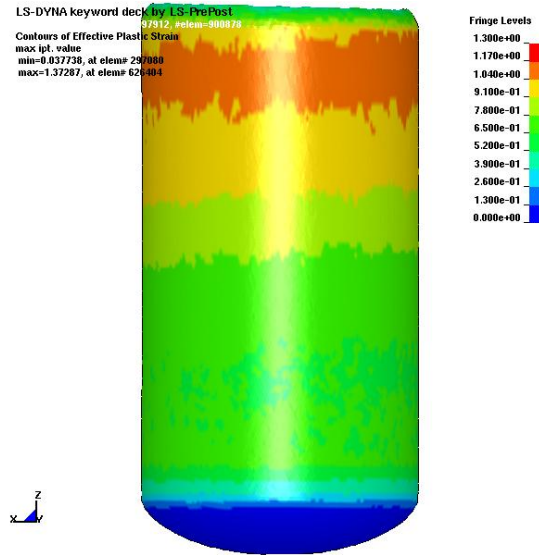


Figure D.69. Effective plastic strain - Station 1 - 0.20° die tilt - Conventional die design

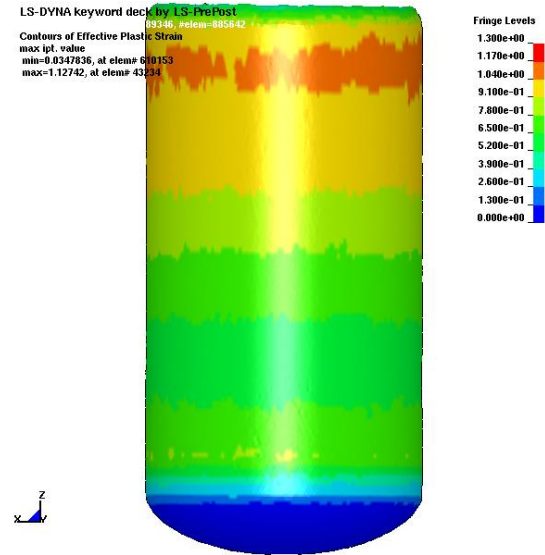


Figure D.70. Effective plastic strain - Station 1 - 0.20° die tilt - $r = 9mm$

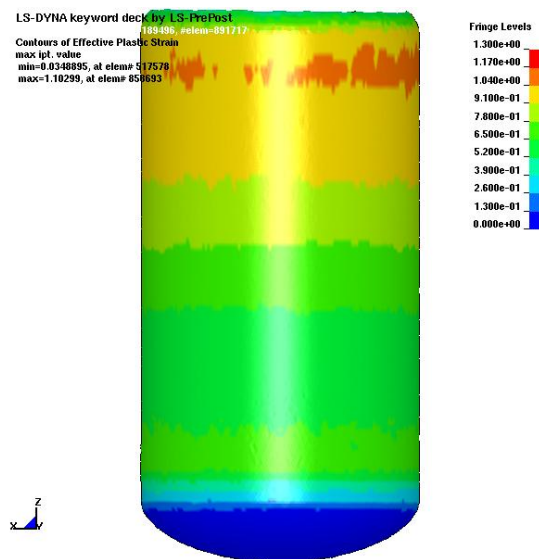


Figure D.71. Effective plastic strain - Station 1 - 0.20° die tilt - $r = 11mm$

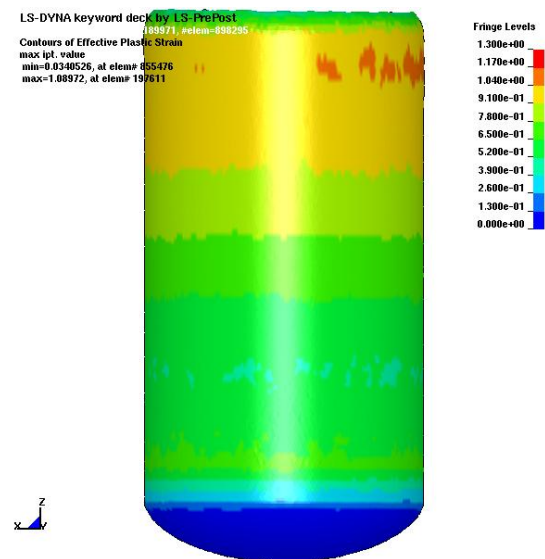


Figure D.72. Effective plastic strain - Station 1 - 0.20° die tilt - $r = 13mm$

D.2.1.2 Resultant forces

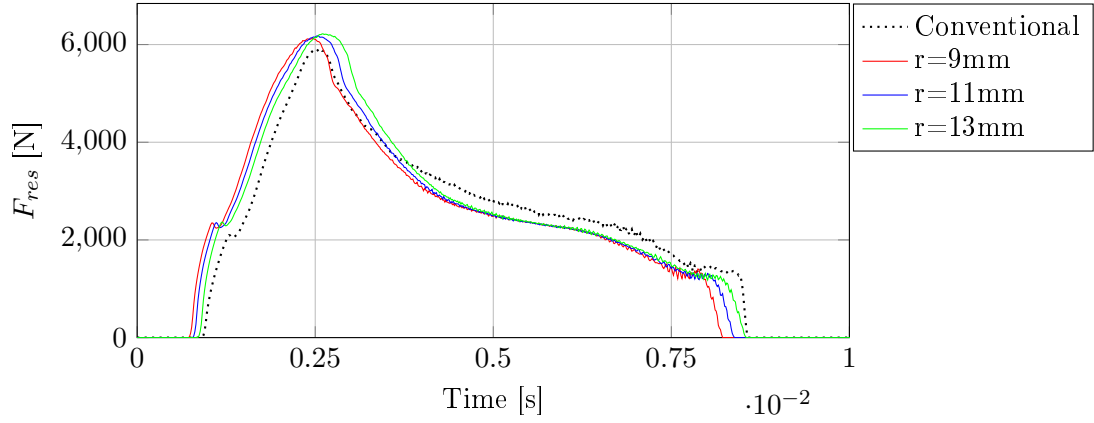


Figure D.73. F_{res} - Station 1 - Die 1 x^+ - 0.20° die tilt

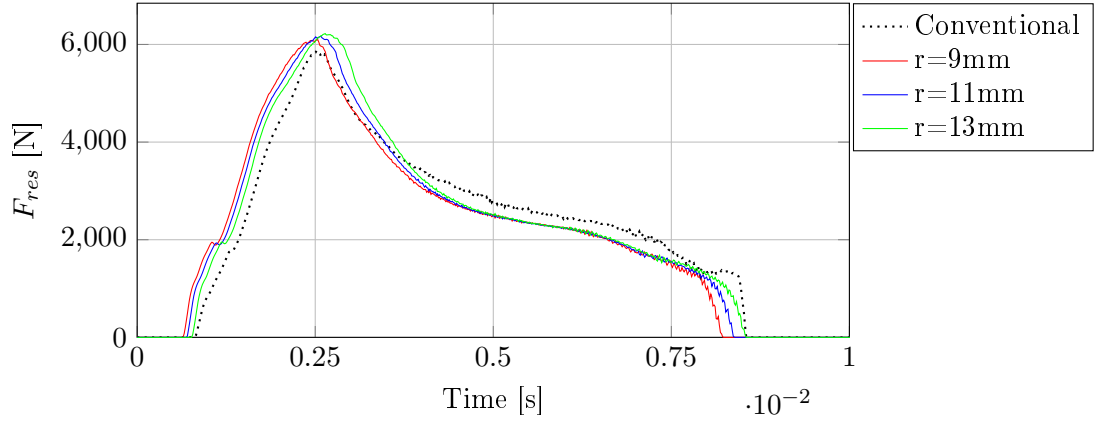


Figure D.74. F_{res} - Station 1 - Die 1 x^- - 0.20° die tilt

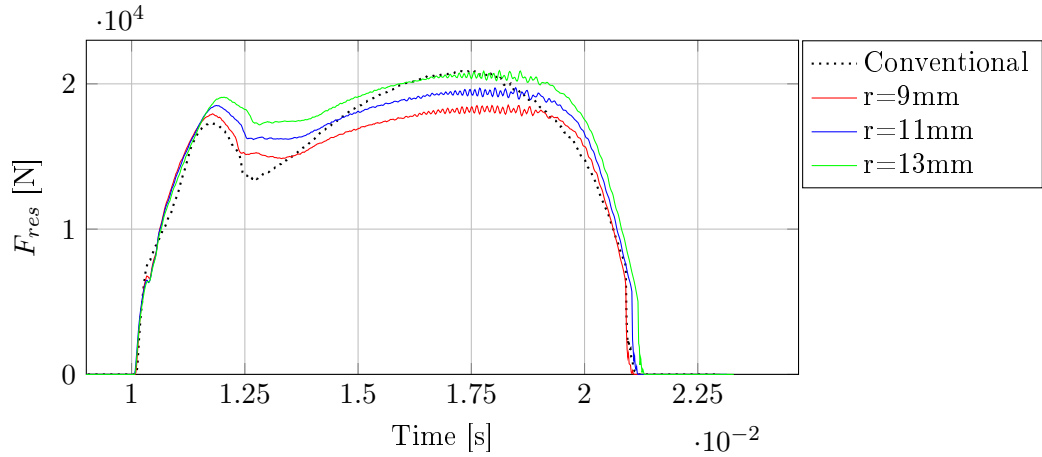


Figure D.75. F_{res} - Station 1 - Die 2 x^+ - 0.20° die tilt

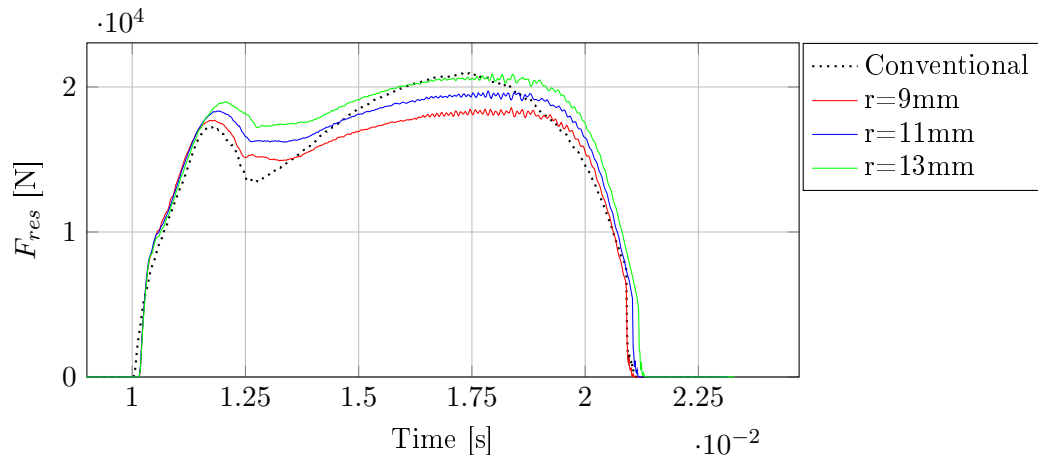


Figure D.76. F_{res} - Station 1 - Die 2 x^- - 0.20° die tilt

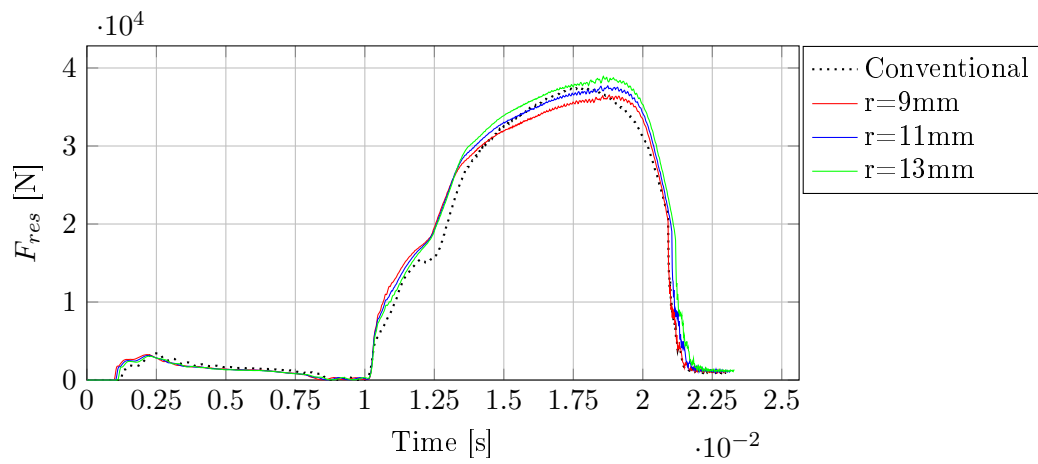


Figure D.77. F_{res} - Station 1 - Punch - 0.20° die tilt

D.2.1.3 x-forces

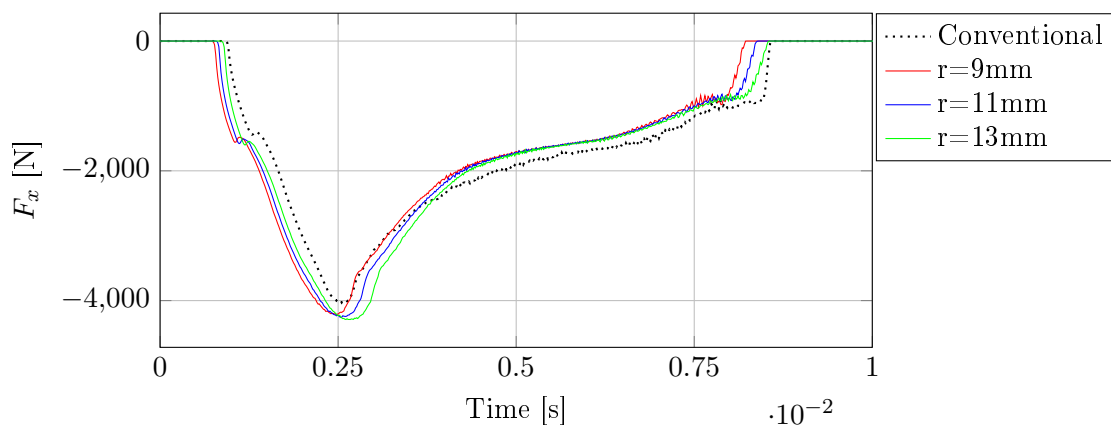


Figure D.78. F_x - Station 1 - Die 1 x^+ - 0.20° die tilt

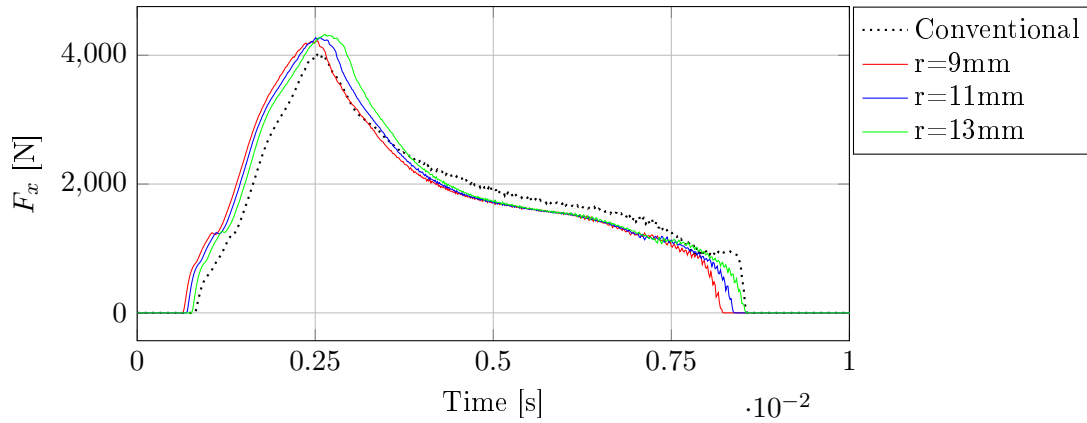


Figure D.79. F_x - Station 1 - Die 1 x^- - 0.20° die tilt

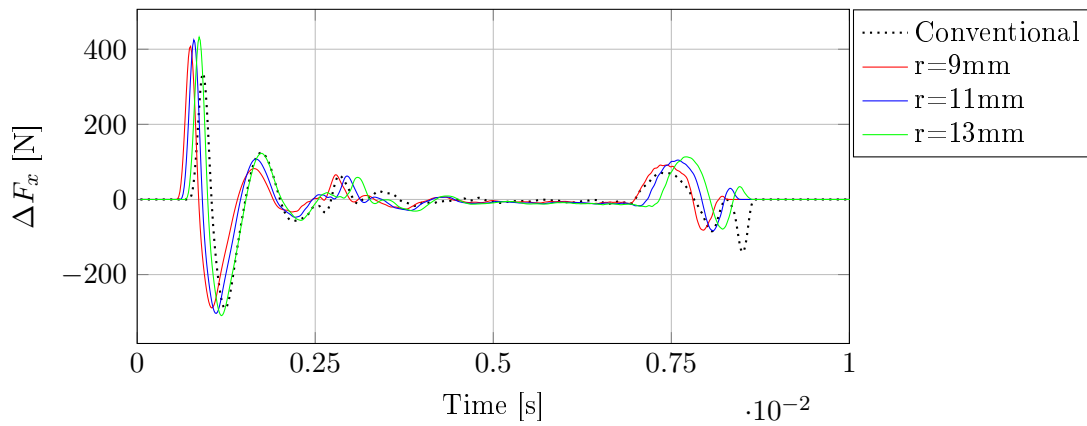


Figure D.80. ΔF_x - Station 1 - Die 1 - 0.20° die tilt

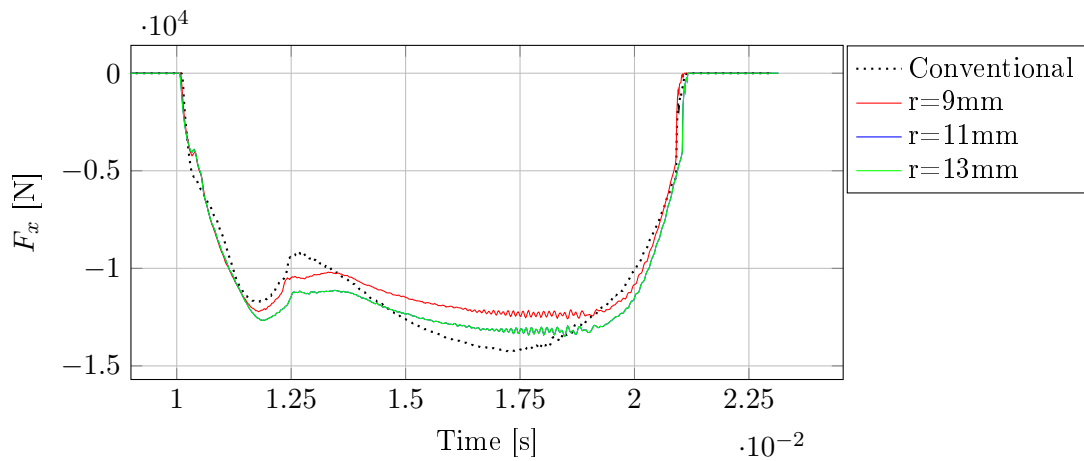


Figure D.81. F_x - Station 1 - Die 2 x^+ - 0.20° die tilt

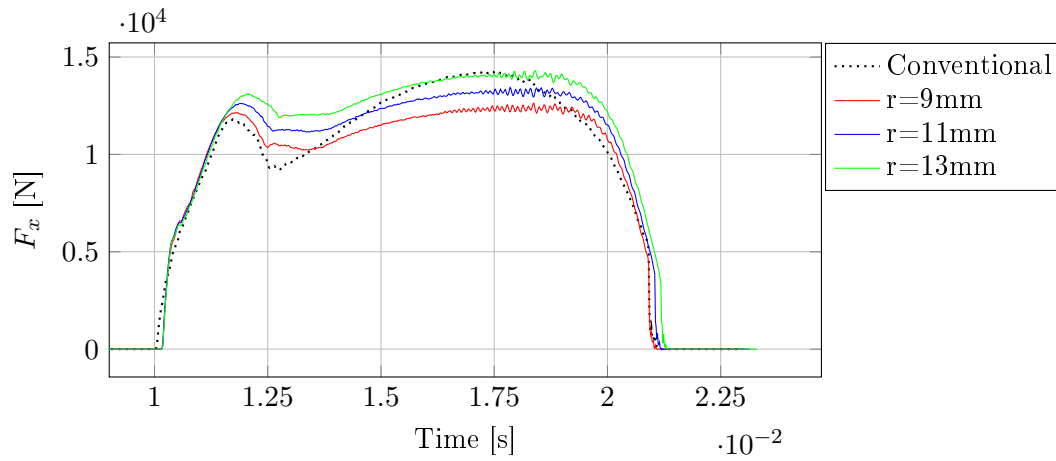


Figure D.82. F_x - Station 1 - Die 2 x^- - 0.20° die tilt

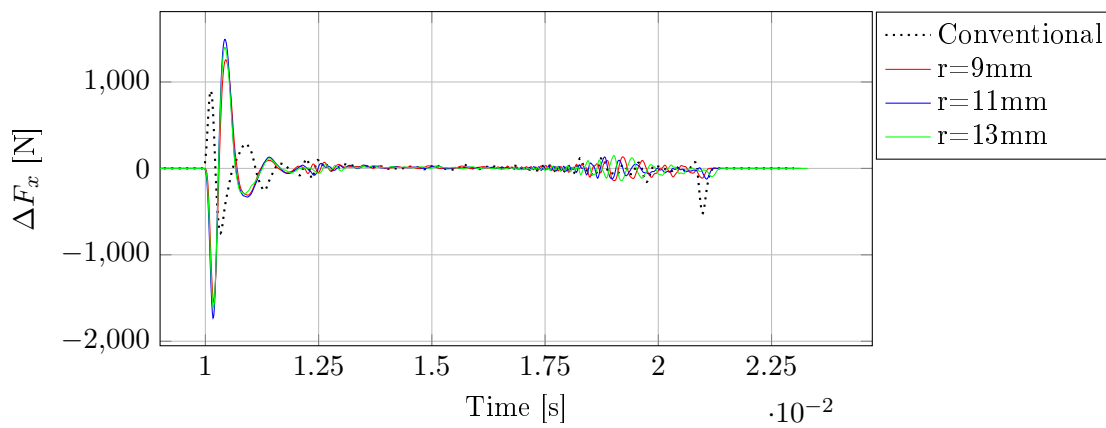


Figure D.83. ΔF_x - Station 1 - Die 2 - 0.20° die tilt

D.2.1.4 z-forces

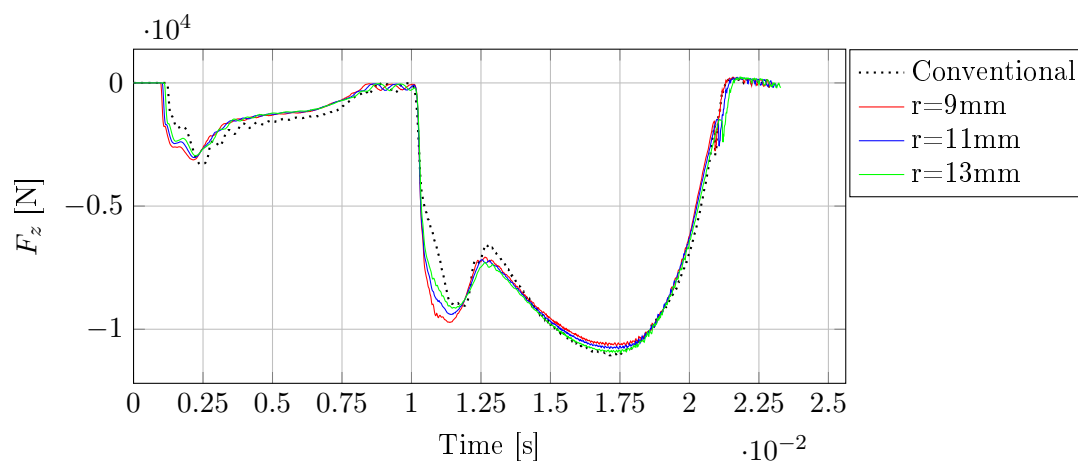


Figure D.84. F_z - Station 1 - Punch - 0.20° die tilt

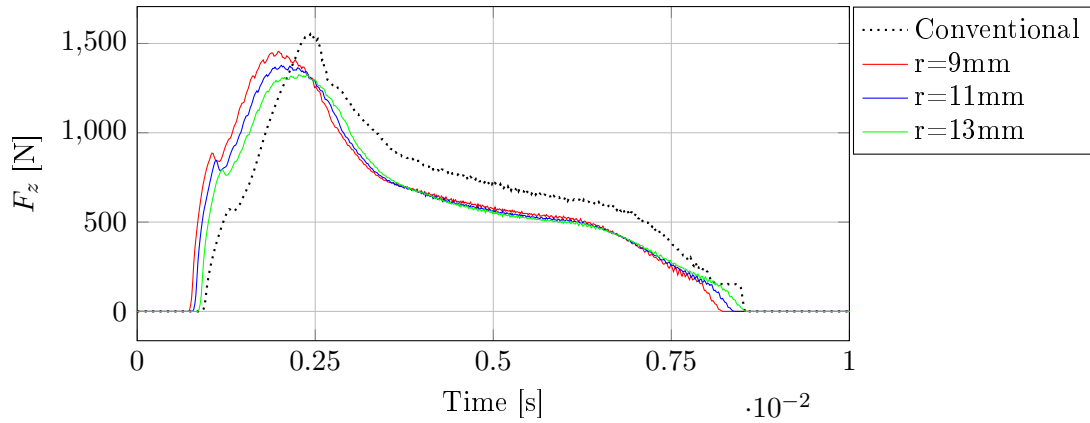


Figure D.85. F_z - Station 1 - Die 1 x^+ - 0.20° die tilt

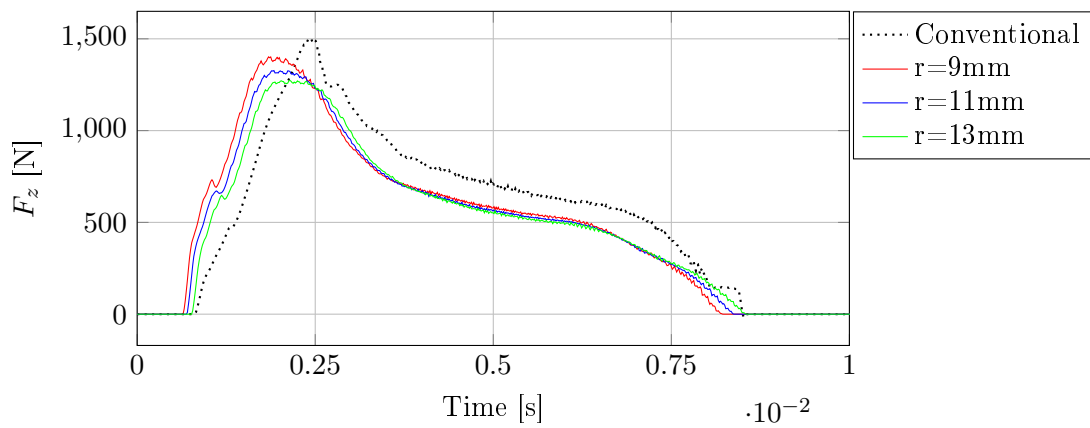


Figure D.86. F_z - Station 1 - Die 1 x^- - 0.20° die tilt

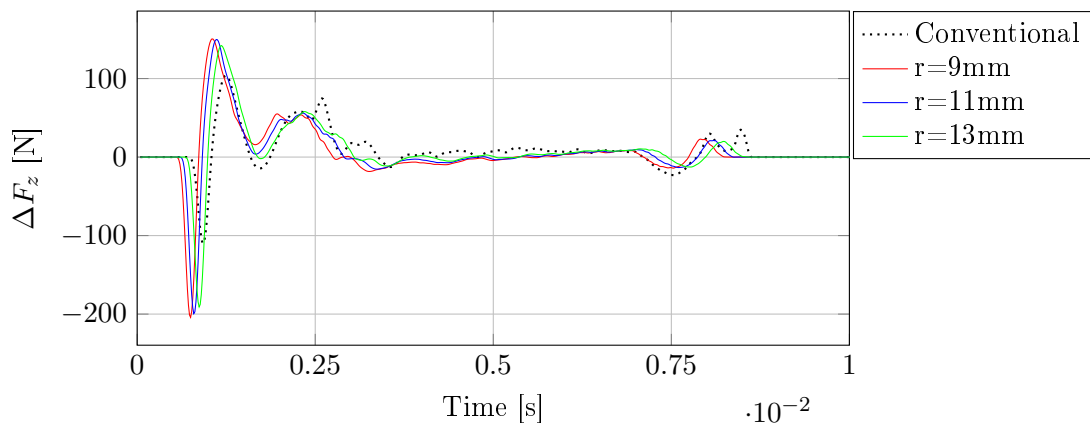


Figure D.87. ΔF_z - Station 1 - Die 1 - 0.20° die tilt

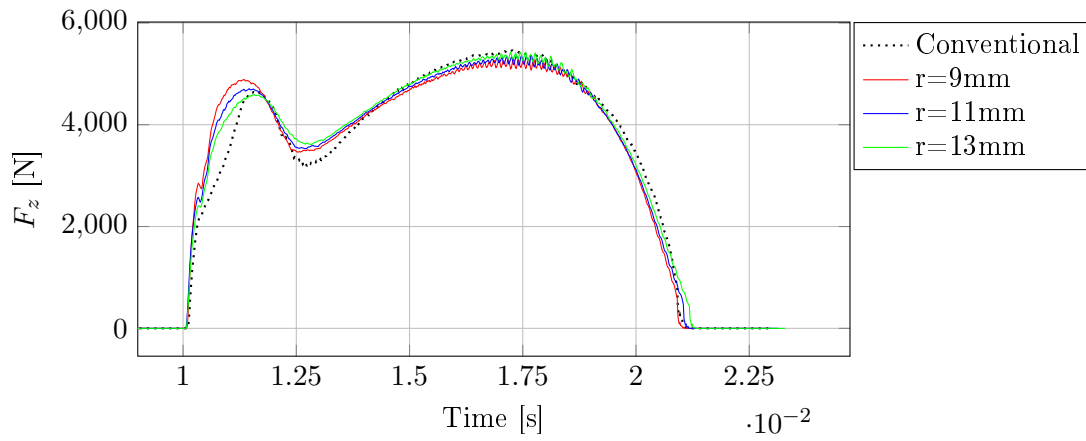


Figure D.88. F_z - Station 1 - Die 2 x^+ - 0.20° die tilt

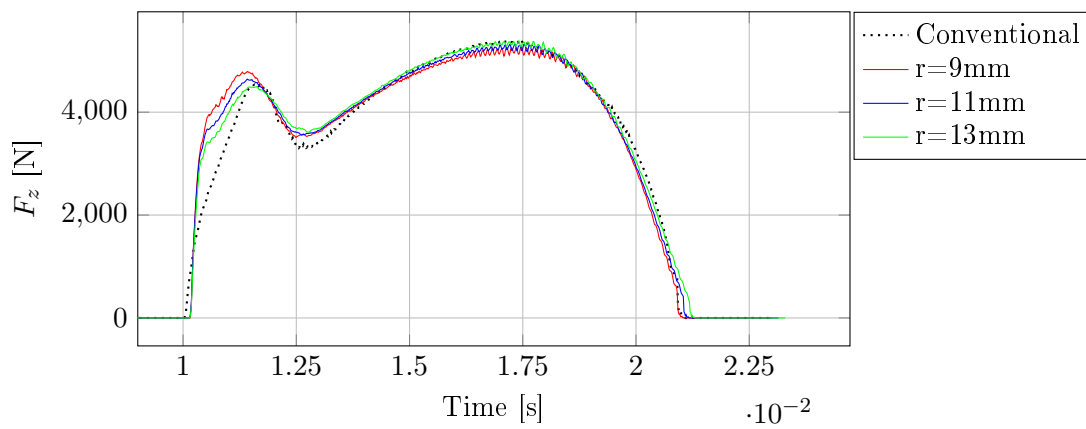


Figure D.89. F_z - Station 1 - Die 2 x^- - 0.20° die tilt

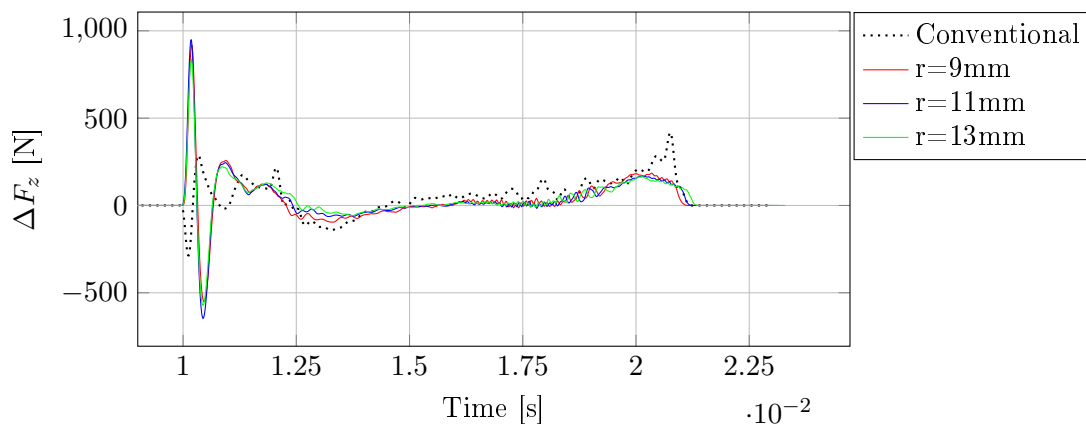


Figure D.90. ΔF_z - Station 1 - Die 2 - 0.20° die tilt

D.2.1.5 Interface pressure

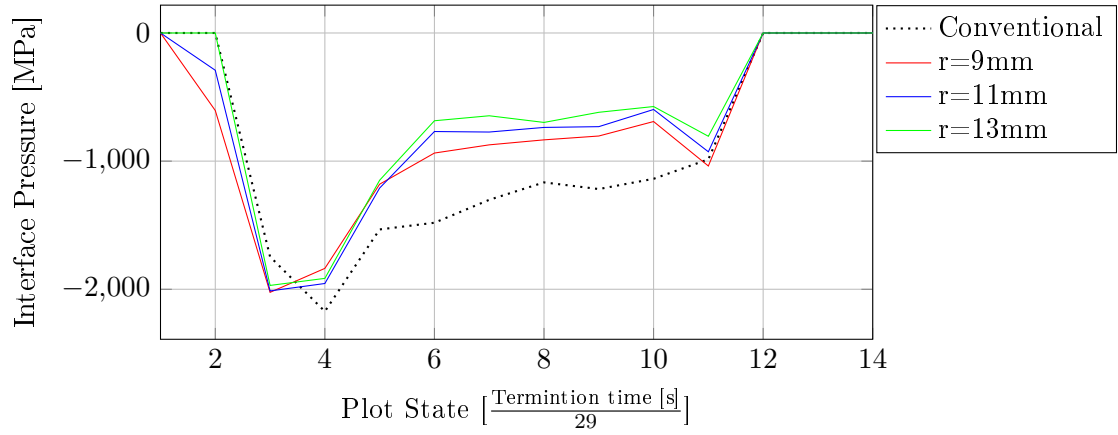


Figure D.91. Maximum interface pressure - Station 1 - Die 1 x^+ - 0.20° die tilt

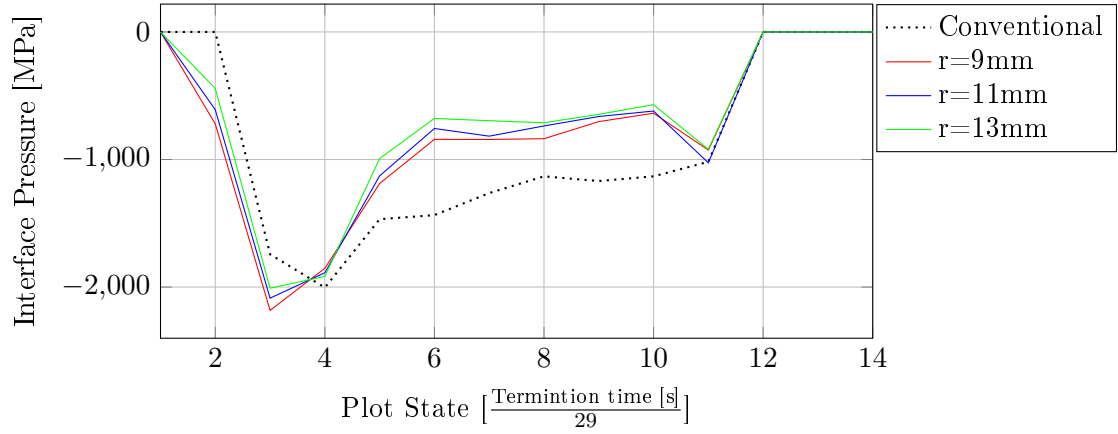


Figure D.92. Maximum interface pressure - Station 1 - Die 1 x^- - 0.20° die tilt

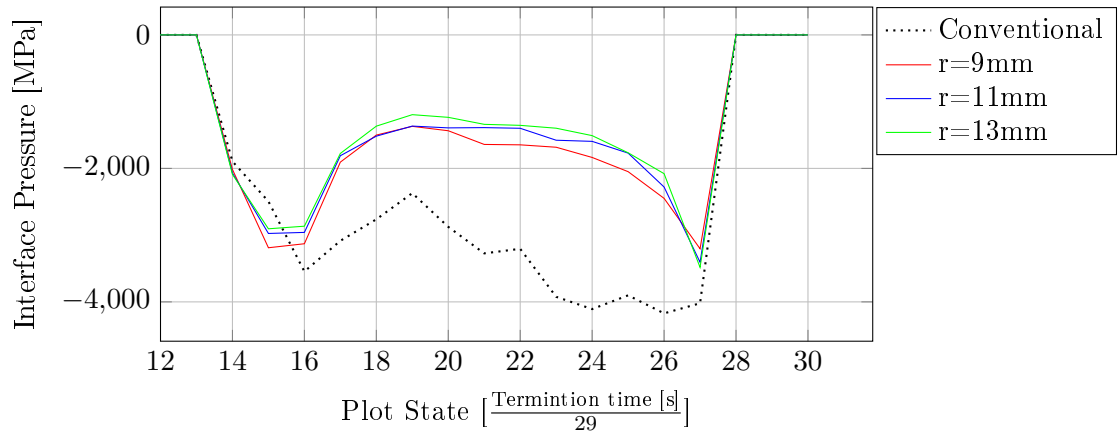


Figure D.93. Maximum interface pressure - Station 1 - Die 2 x^+ - 0.20° die tilt

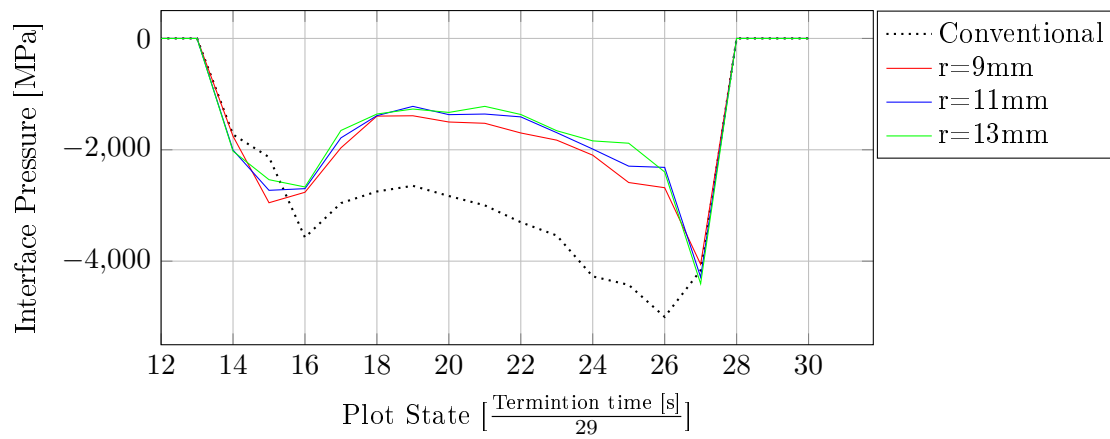


Figure D.94. Maximum interface pressure - Station 1 - Die 2 x^- - 0.20° die tilt

D.2.2 Station 2

D.2.2.1 Effective plastic strain

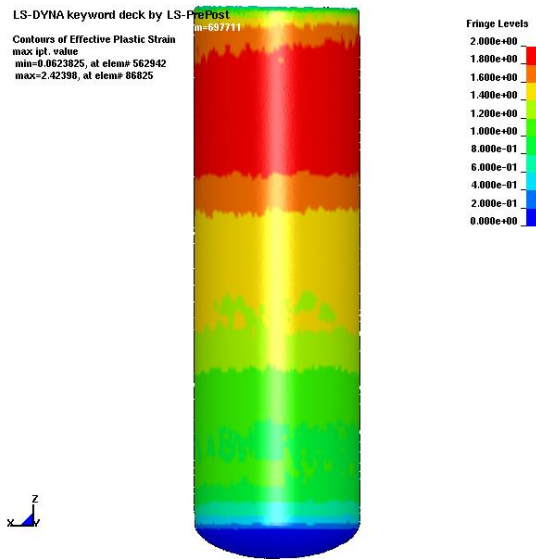


Figure D.95. Effective plastic strain - Station 2 - 0.20° die tilt - Conventional die design

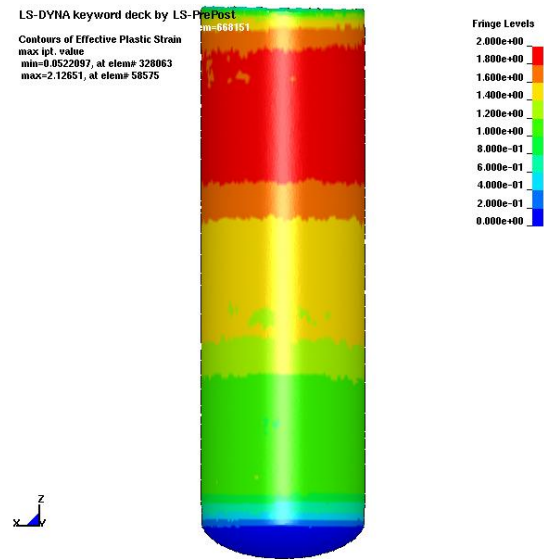


Figure D.96. Effective plastic strain - Station 2 - 0.20° die tilt - $r = 9mm$

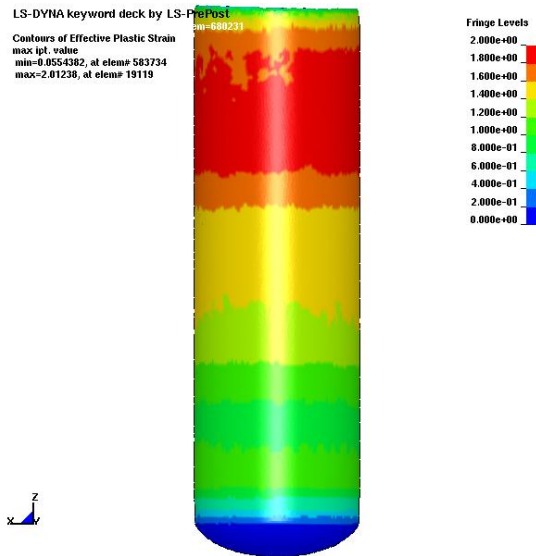


Figure D.97. Effective plastic strain - Station 2 - 0.20° die tilt - $r = 11mm$

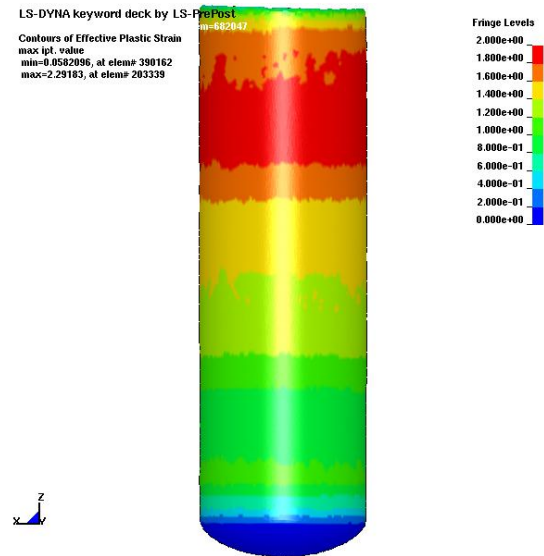


Figure D.98. Effective plastic strain - Station 2 - 0.20° die tilt - $r = 13mm$

D.2.2.2 Resultant forces

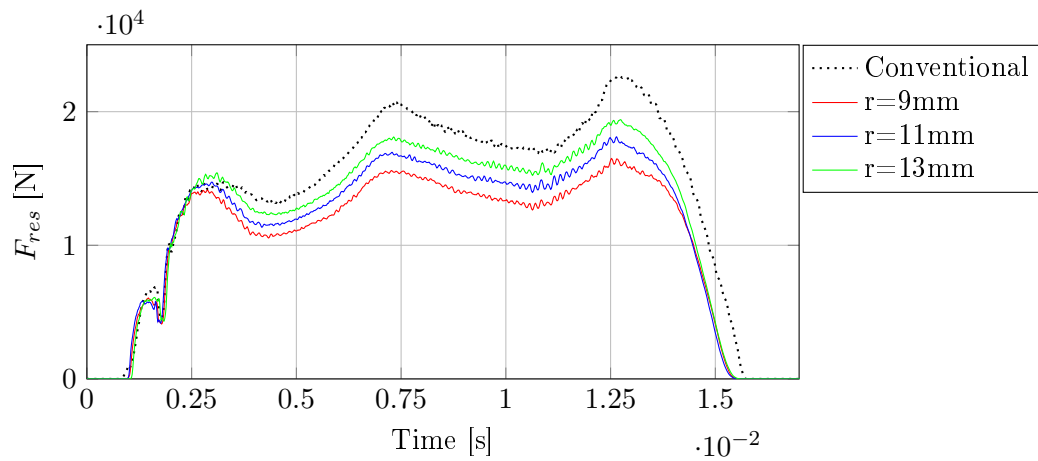


Figure D.99. F_{res} - Station 2 - Die 1 x^+ - 0.20° die tilt

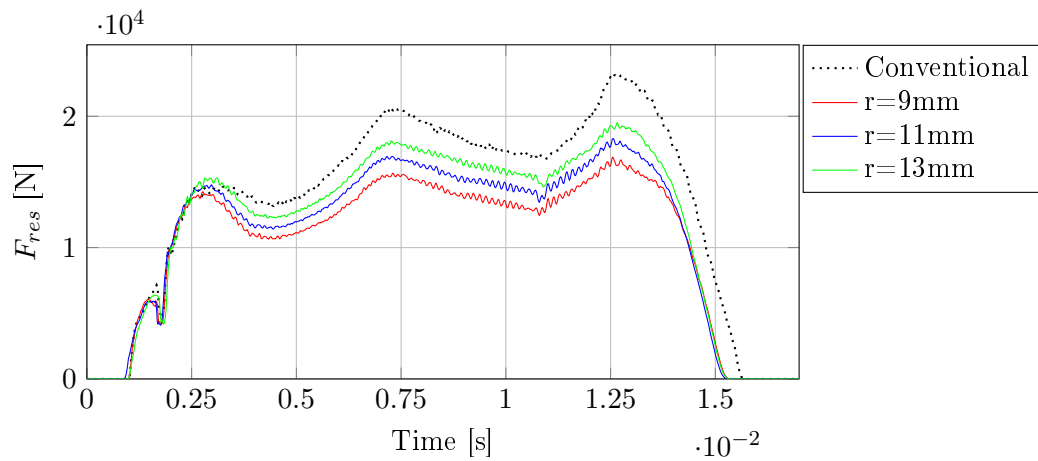


Figure D.100. F_{res} - Station 2 - Die 1 x^- - 0.20° die tilt

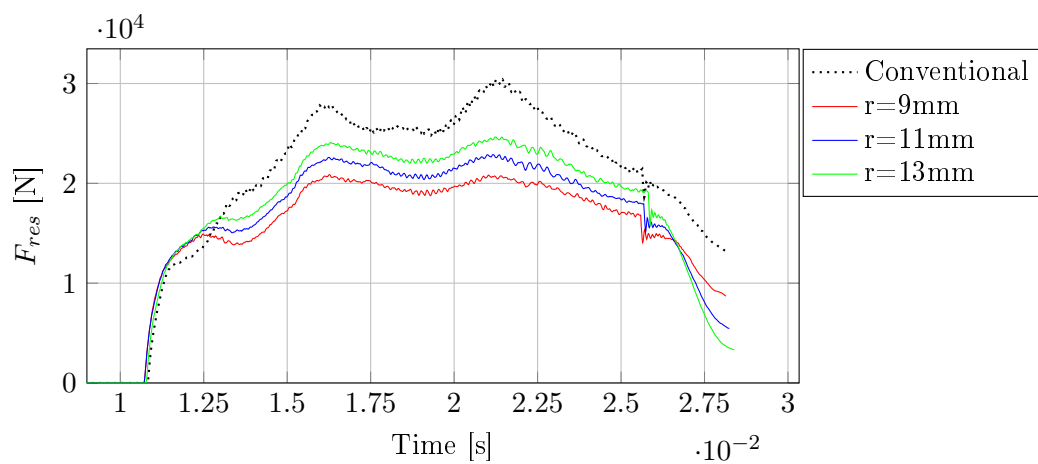


Figure D.101. F_{res} - Station 2 - Die 2 x^+ - 0.20° die tilt

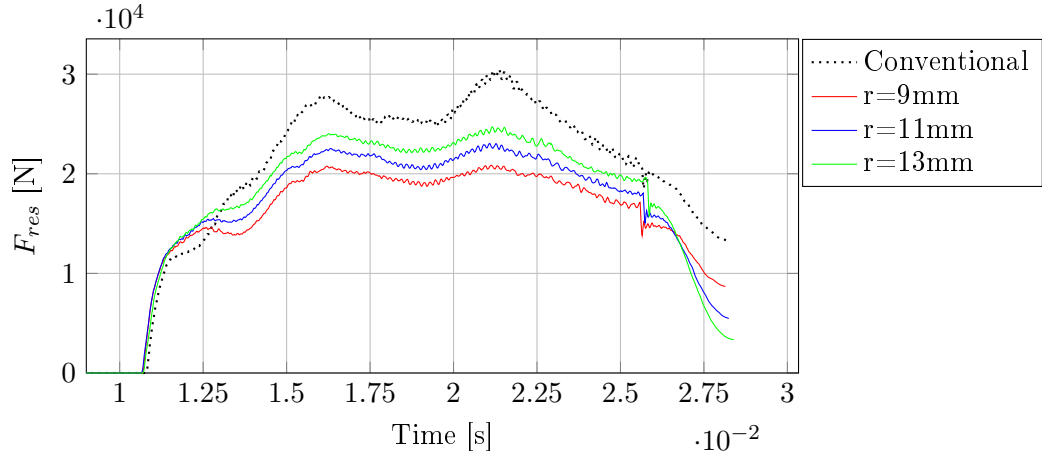


Figure D.102. F_{res} - Station 2 - Die 2 x^- - 0.20° die tilt

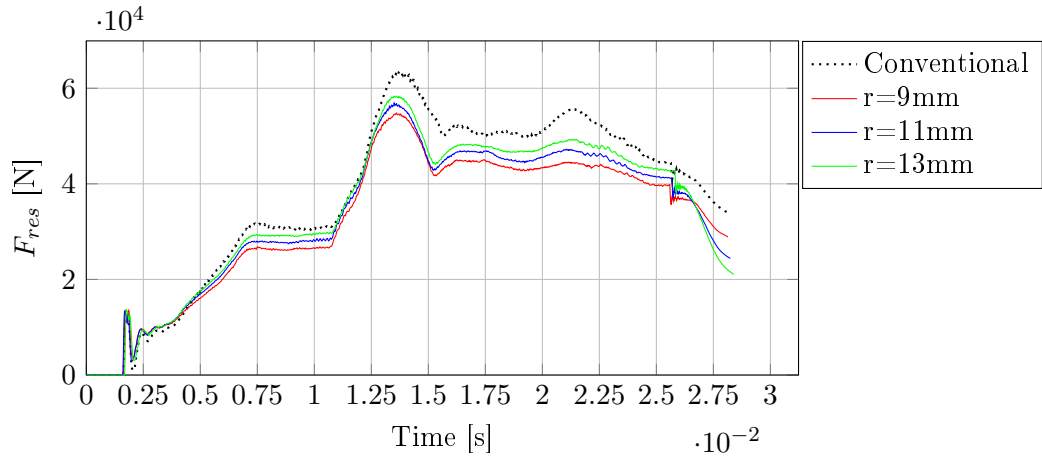


Figure D.103. F_{res} - Station 2 - Punch - 0.20° die tilt

D.2.2.3 x-forces

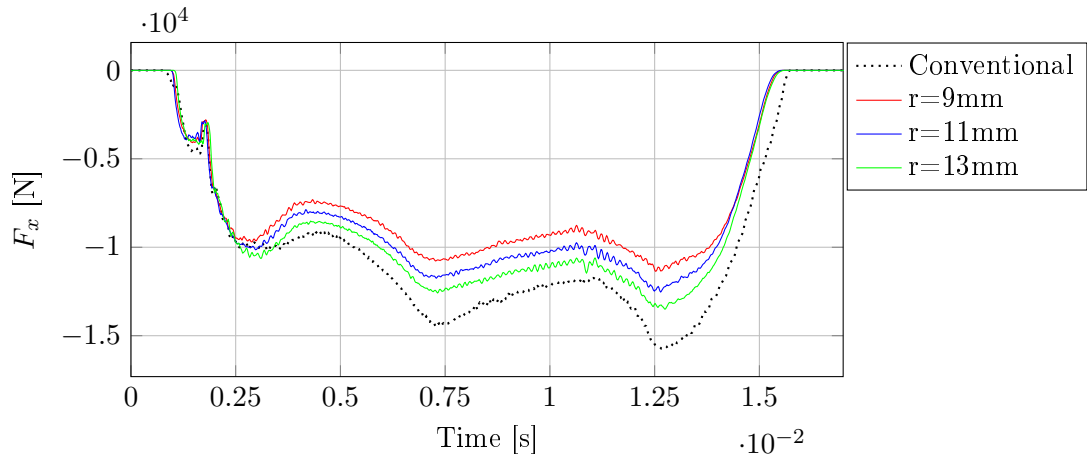


Figure D.104. F_x - Station 2 - Die 1 x^+ - 0.20° die tilt

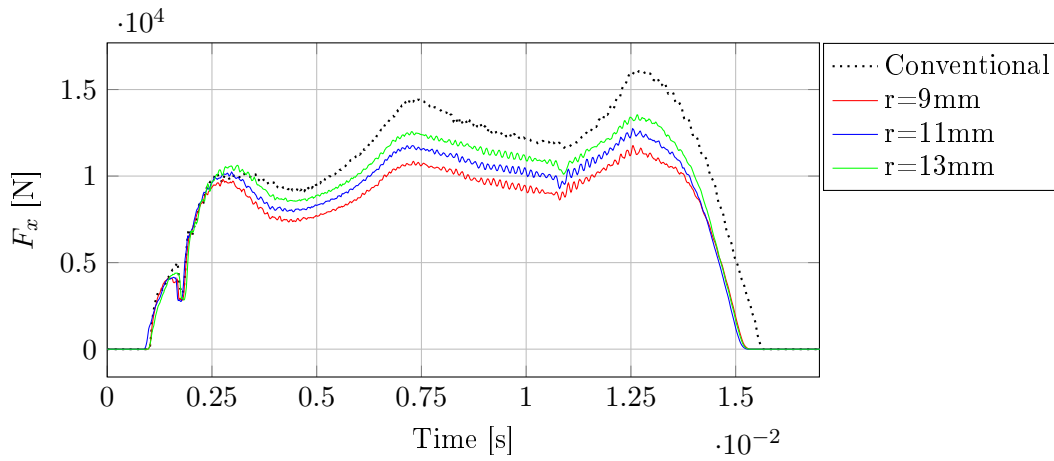


Figure D.105. F_x - Station 2 - Die 1 x^- - 0.20° die tilt

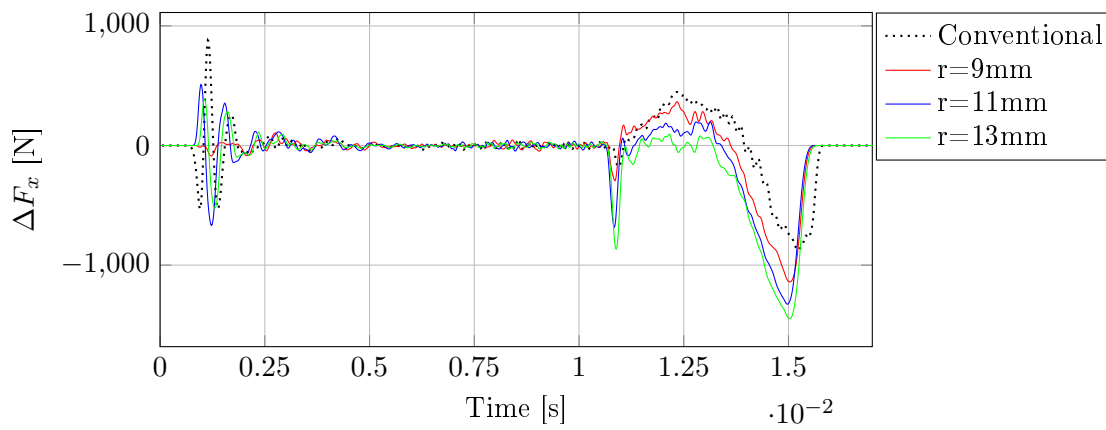


Figure D.106. ΔF_x - Station 2 - Die 1 - 0.20° die tilt

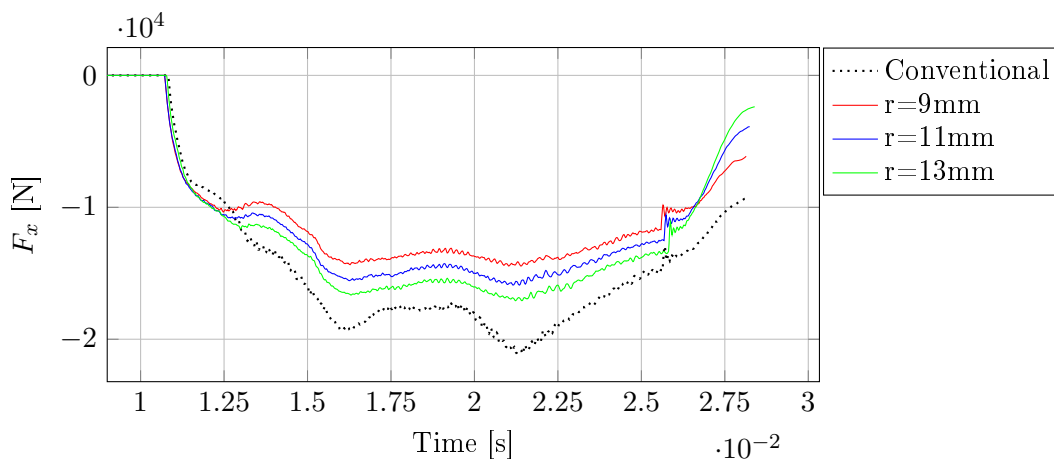


Figure D.107. F_x - Station 2 - Die 2 x^+ - 0.20° die tilt

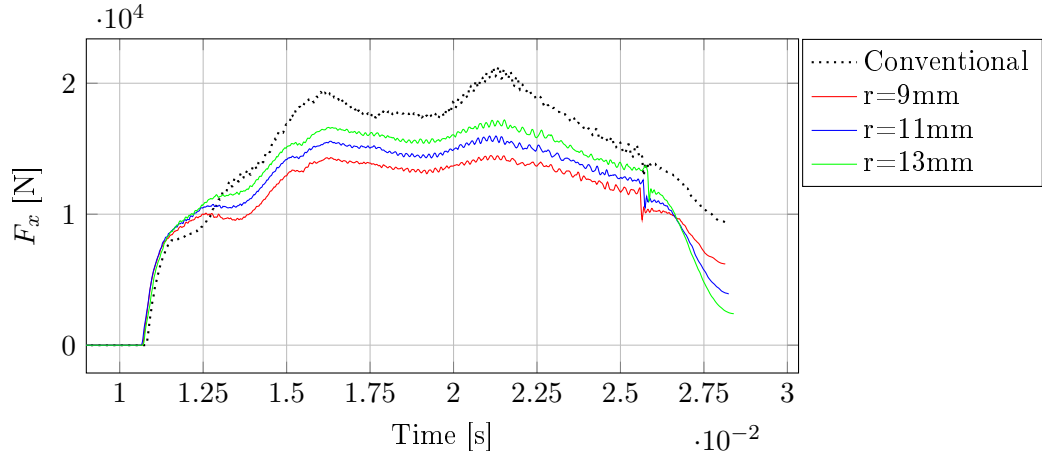


Figure D.108. F_x - Station 2 - Die 2 x^- - 0.20° die tilt

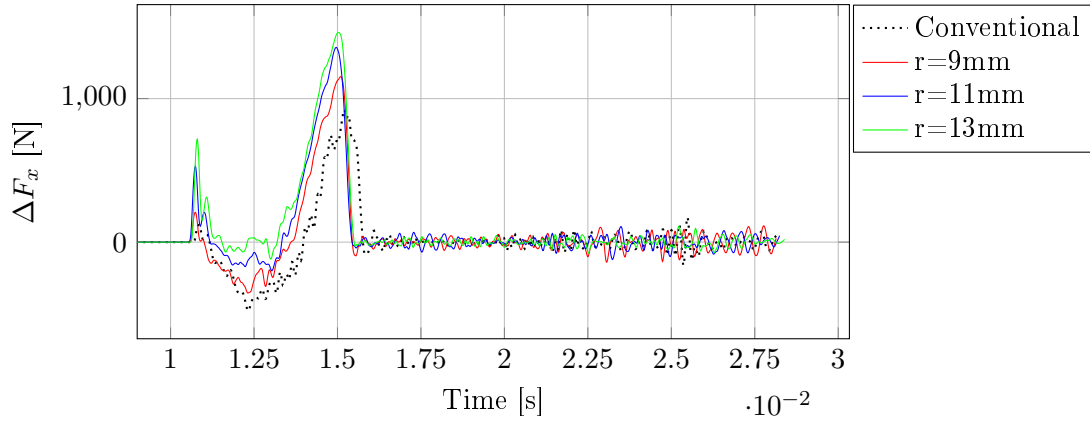


Figure D.109. ΔF_x - Station 2 - Die 2 - 0.20° die tilt

D.2.2.4 z-forces

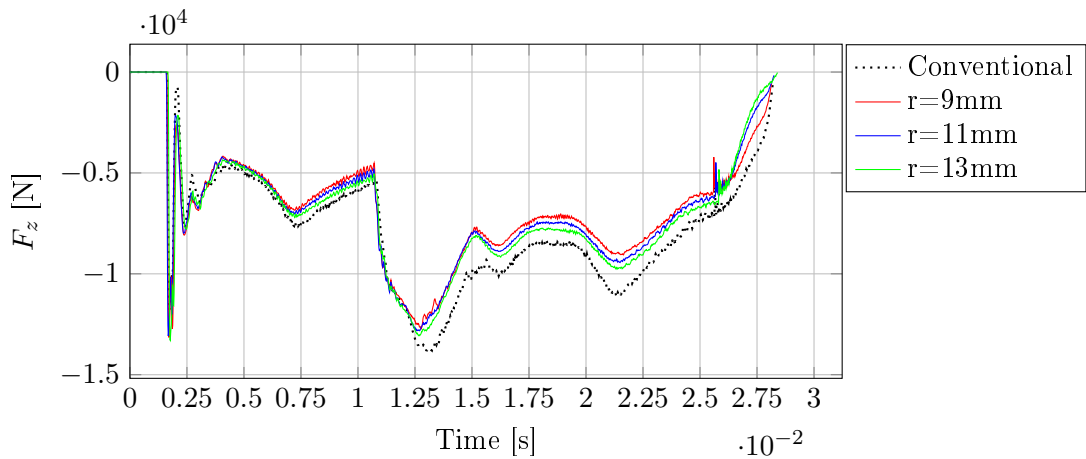


Figure D.110. F_z - Station 2 - Punch - 0.20° die tilt

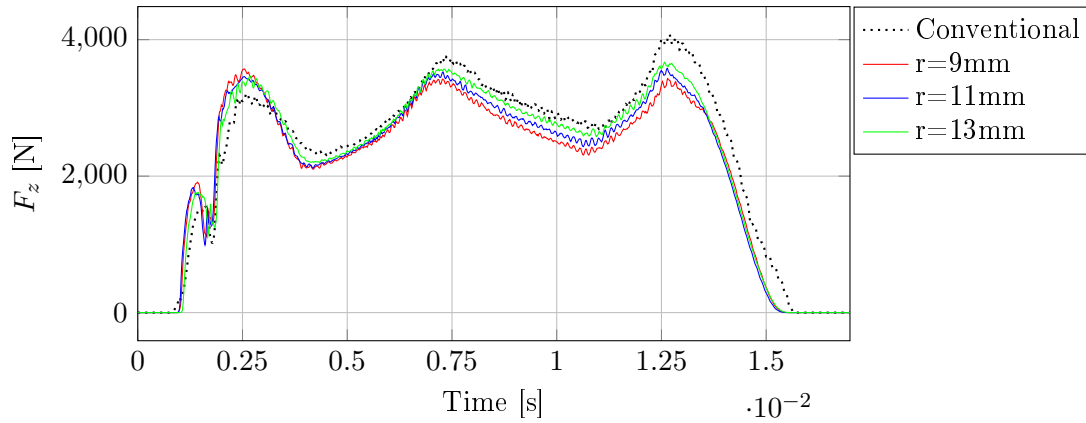


Figure D.111. F_z - Station 2 - Die 1 x^+ - 0.20° die tilt

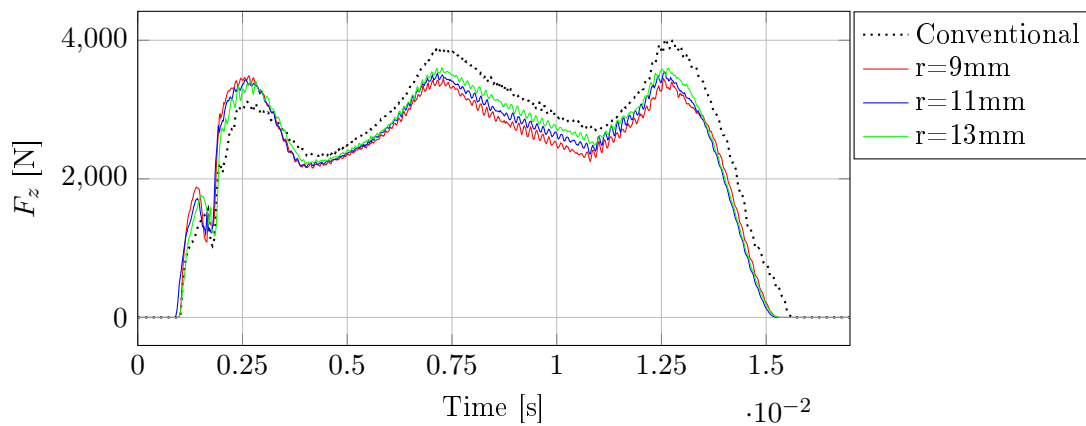


Figure D.112. F_z - Station 2 - Die 1 x^- - 0.20° die tilt

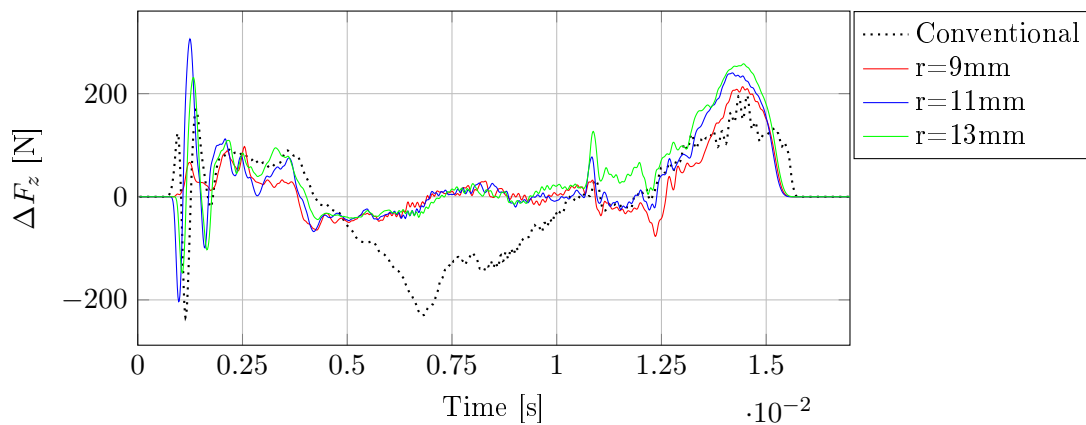


Figure D.113. ΔF_z - Station 2 - Die 1 - 0.20° die tilt

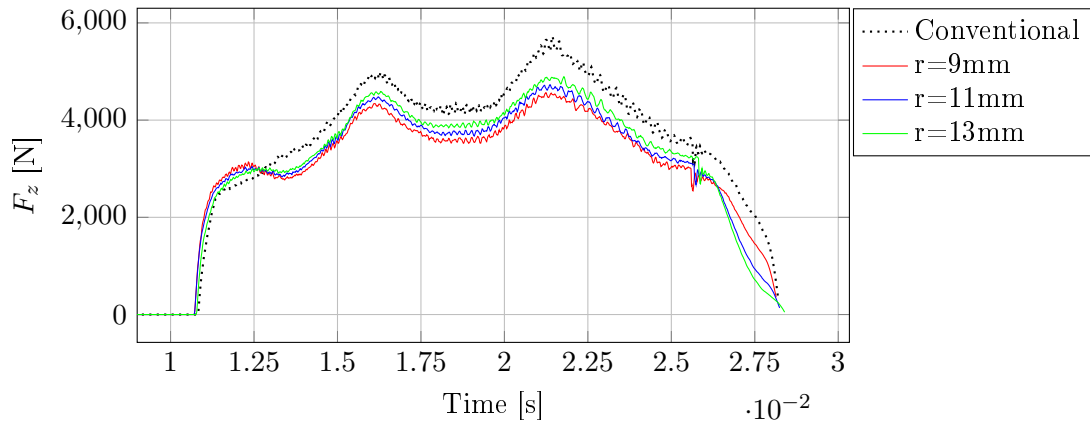


Figure D.114. F_z - Station 2 - Die 2 x^+ - 0.20° die tilt

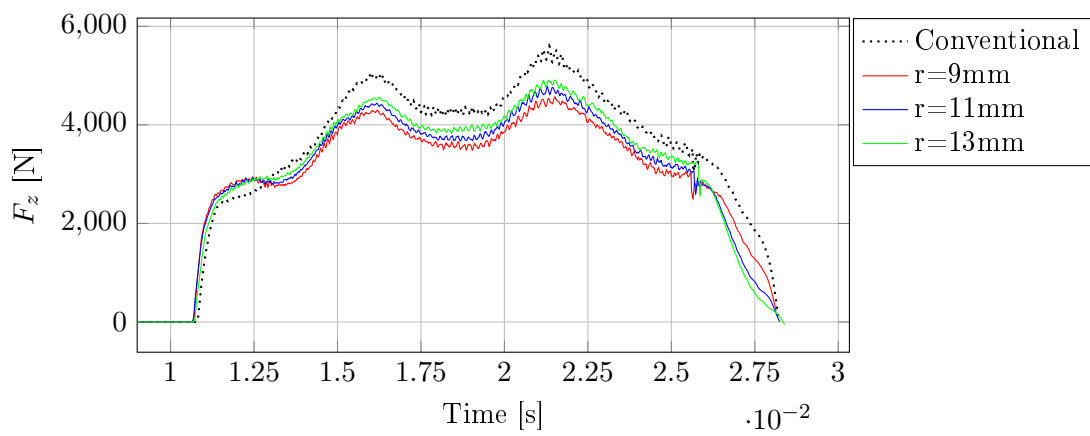


Figure D.115. F_z - Station 2 - Die 2 x^- - 0.20° die tilt

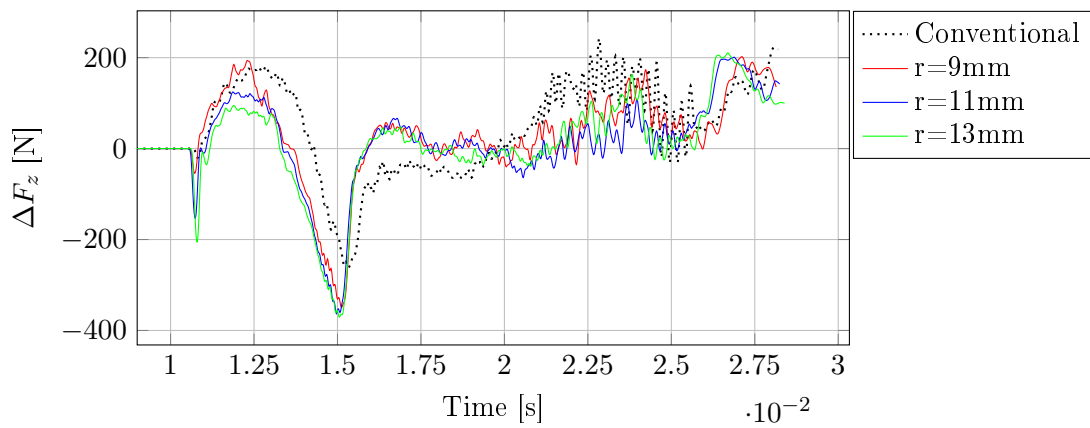


Figure D.116. ΔF_z - Station 2 - Die 2 - 0.20° die tilt

D.2.2.5 Interface pressure

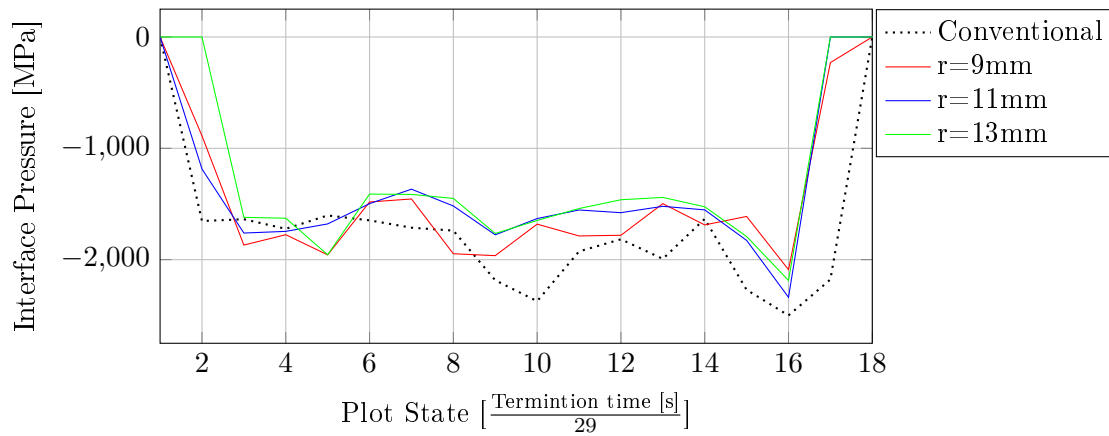


Figure D.117. Maximum interface pressure - Station 2 - Die 1 x^+ - 0.20° die tilt

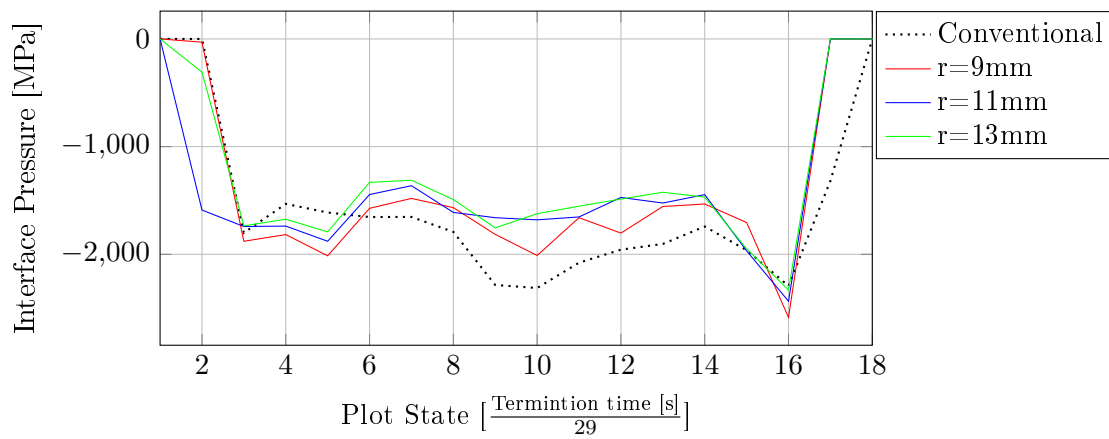


Figure D.118. Maximum interface pressure - Station 2 - Die 1 x^- - 0.20° die tilt

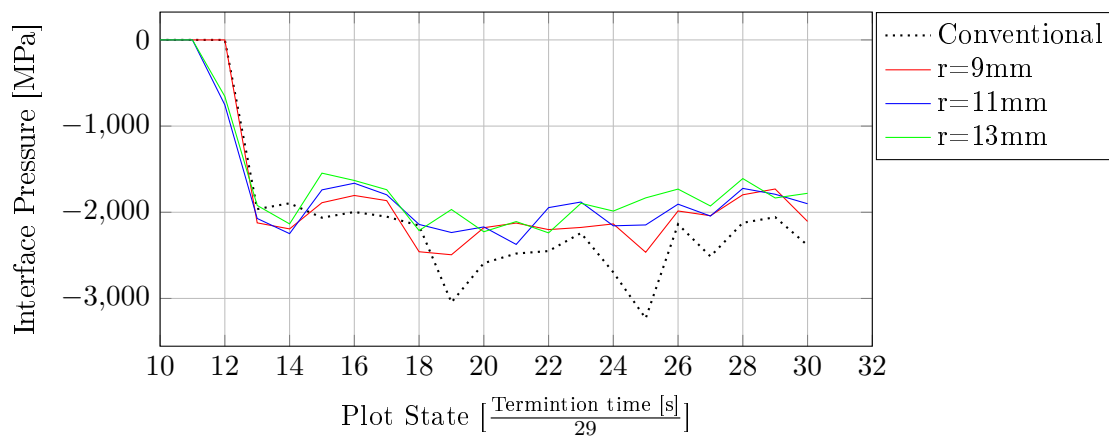


Figure D.119. Maximum interface pressure - Station 2 - Die 2 x^+ - 0.20° die tilt

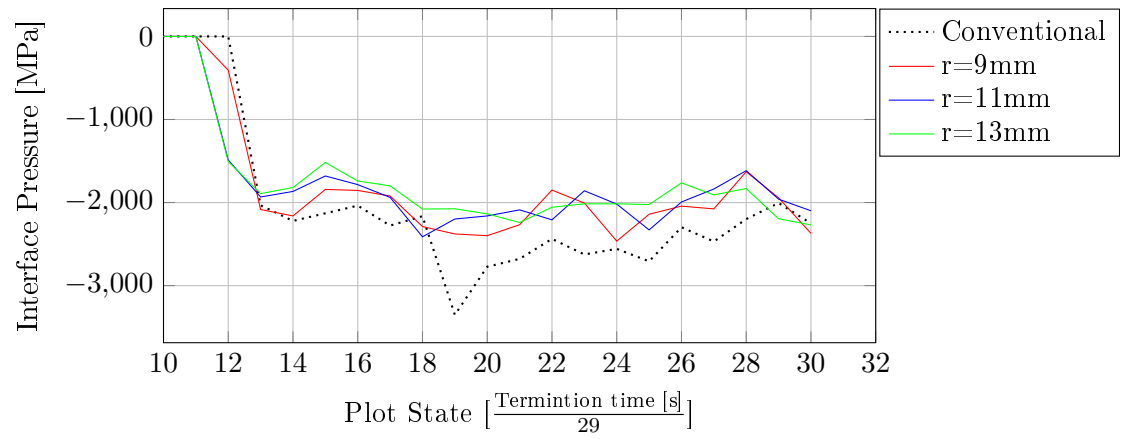


Figure D.120. Maximum interface pressure - Station 2 - Die 2 x^- - 0.20° die tilt

D.2.3 Station 3

D.2.3.1 Effective plastic strain

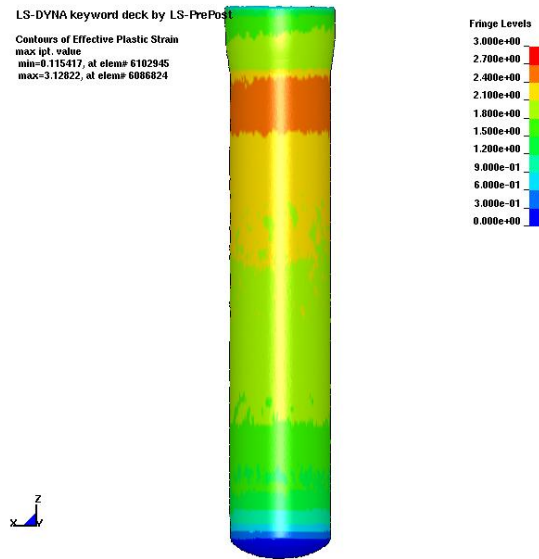


Figure D.121. Effective plastic strain - Station 3 - 0.20° die tilt - Conventional die design

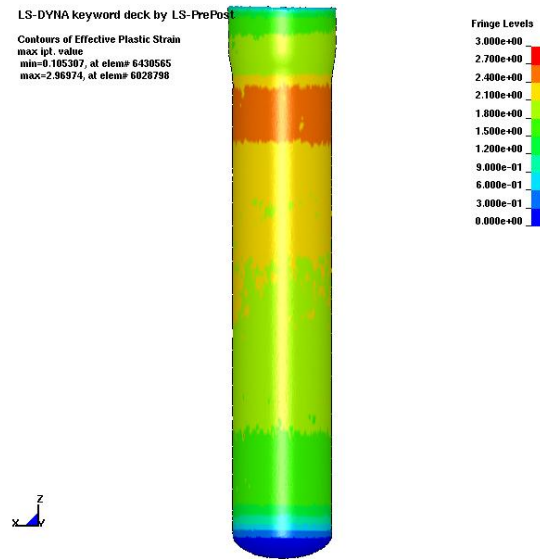


Figure D.122. Effective plastic strain - Station 3 - 0.20° die tilt - $r = 9mm$

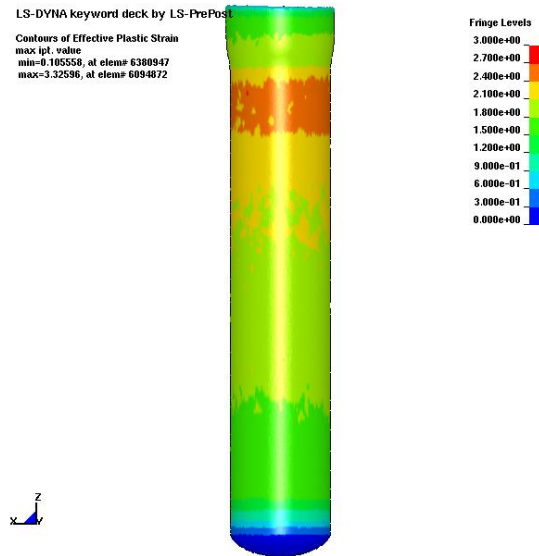


Figure D.123. Effective plastic strain - Station 3 - 0.20° die tilt - $r = 11mm$

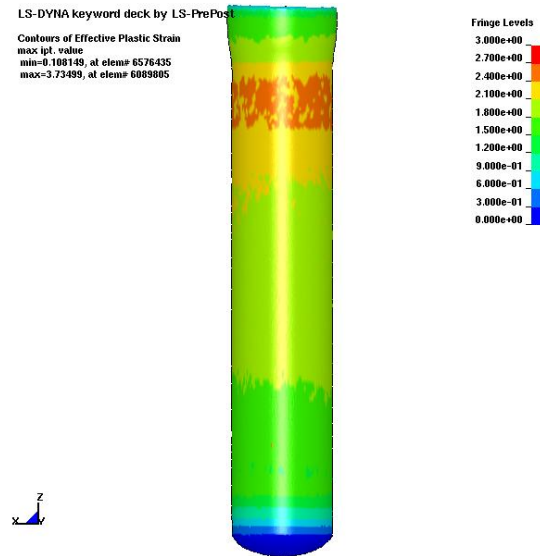


Figure D.124. Effective plastic strain - Station 3 - 0.20° die tilt - $r = 13mm$

D.2.3.2 Resultant forces

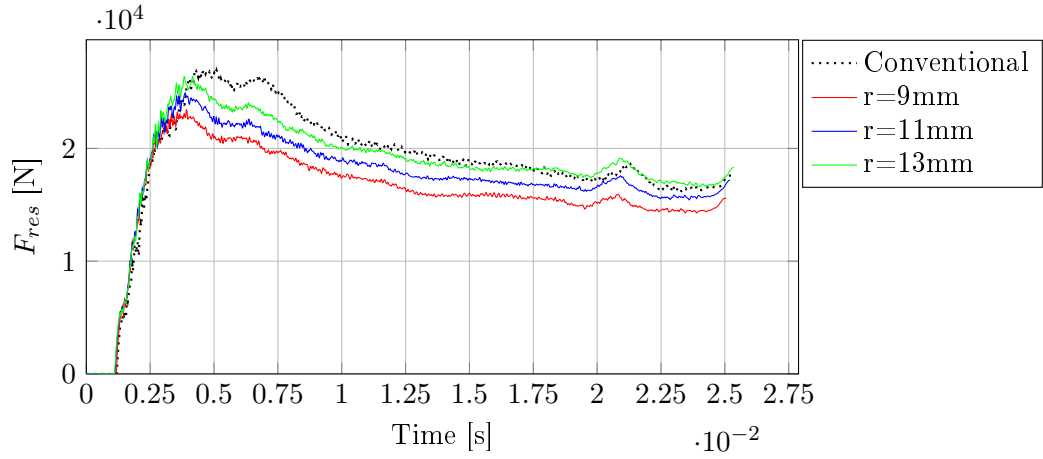


Figure D.125. F_{res} - Station 3 - Die 1 x^+ - 0.20° die tilt

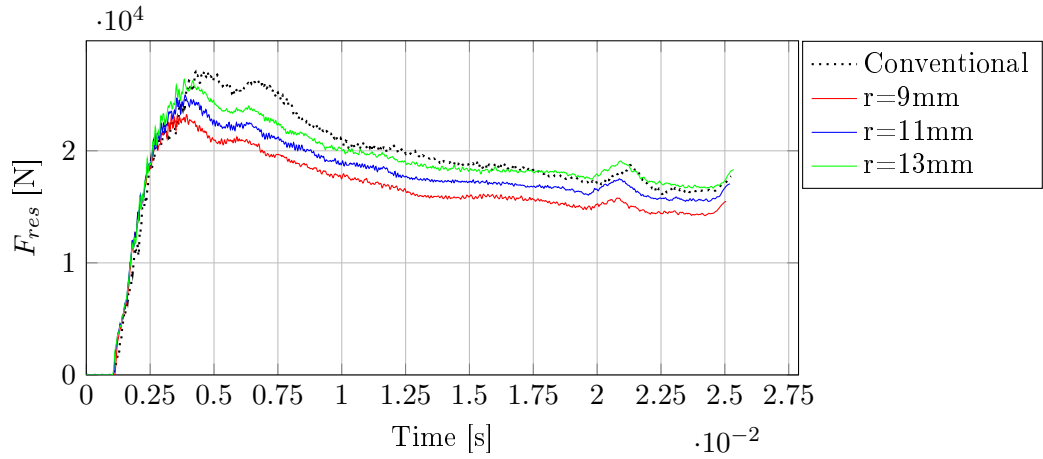


Figure D.126. F_{res} - Station 3 - Die 1 x^- - 0.20° die tilt

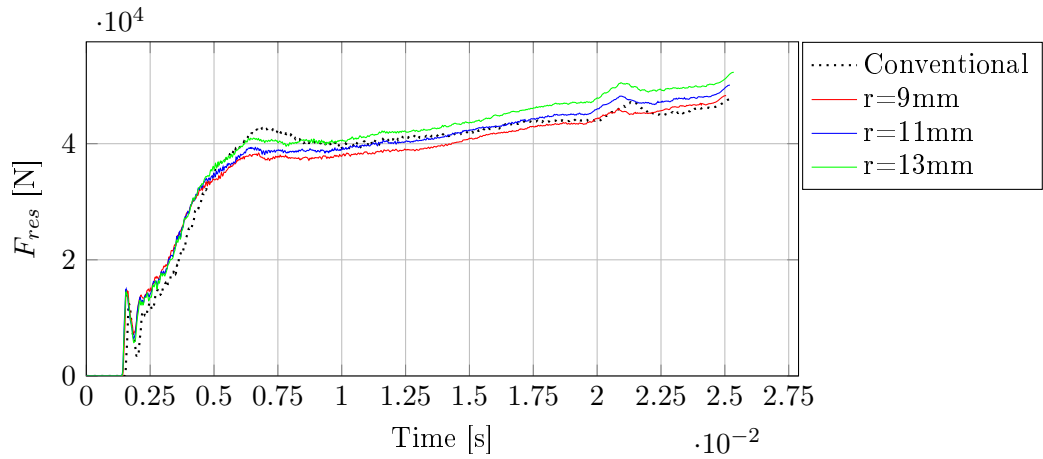


Figure D.127. F_{res} - Station 3 - Punch - 0.20° die tilt

D.2.3.3 x-forces

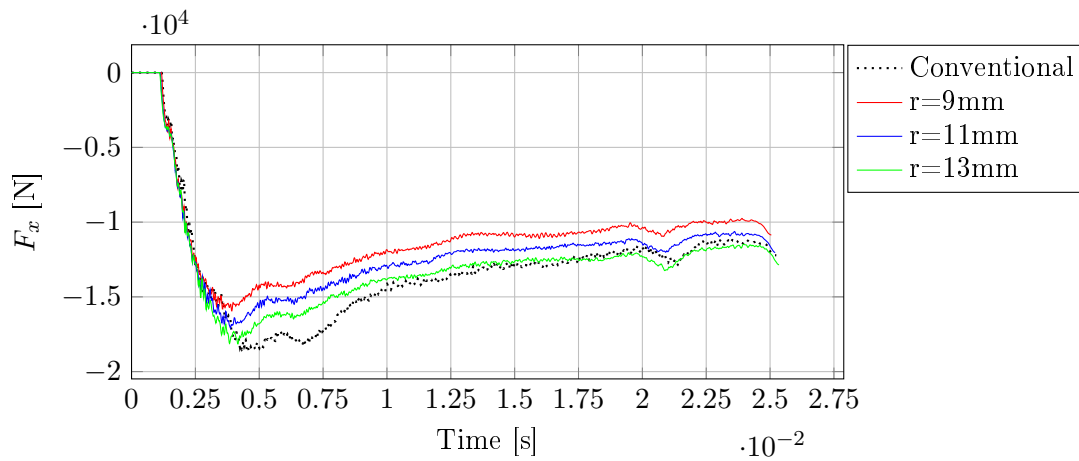


Figure D.128. F_x - Station 3 - Die 1 x^+ - 0.20° die tilt

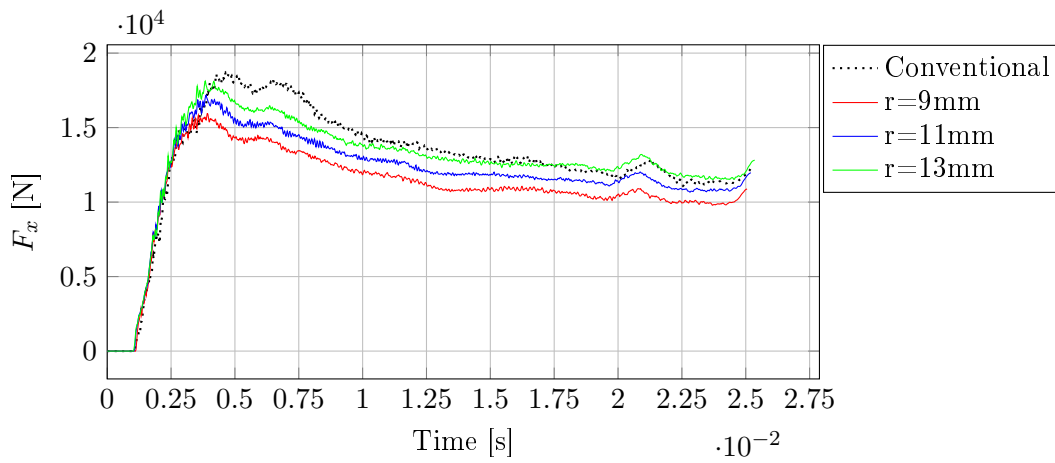


Figure D.129. F_x - Station 3 - Die 1 x^- - 0.20° die tilt

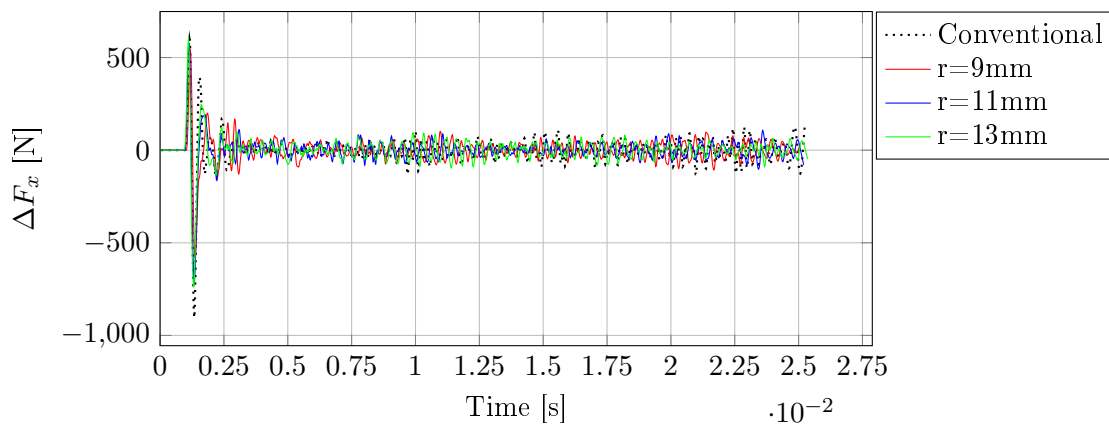
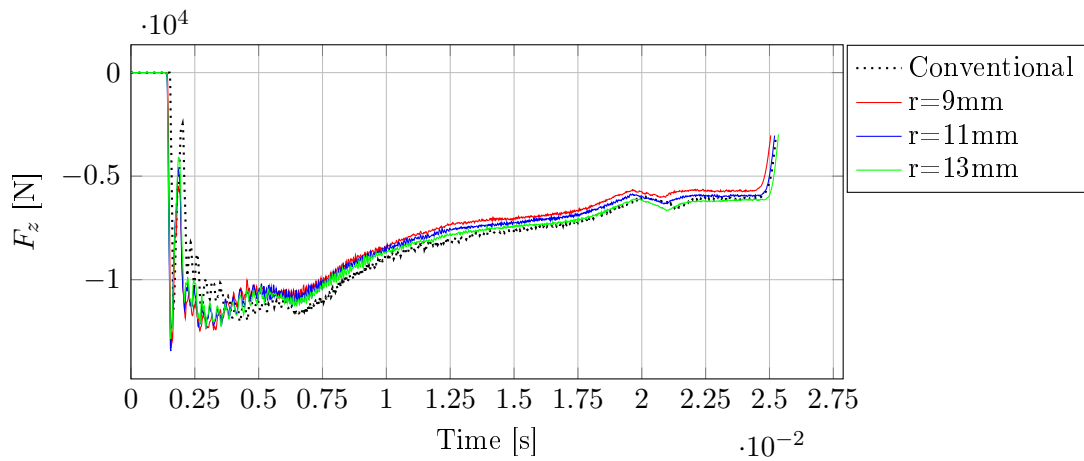
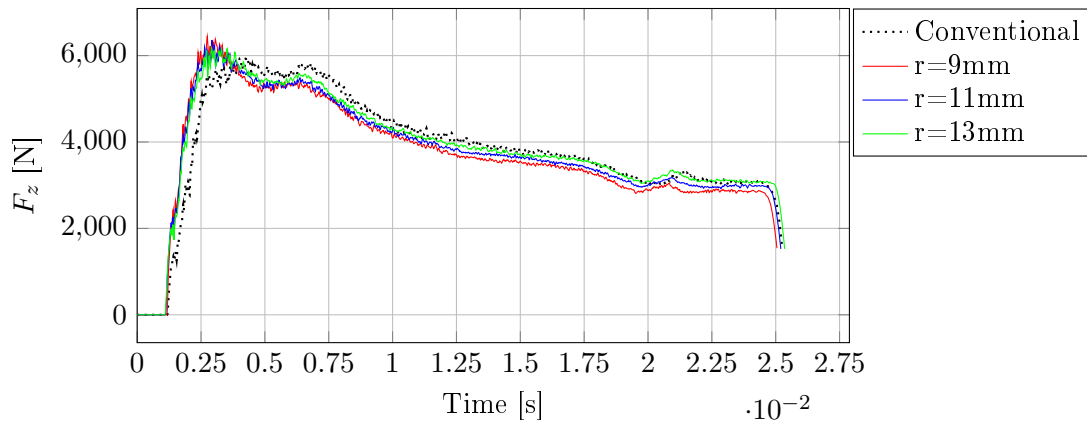
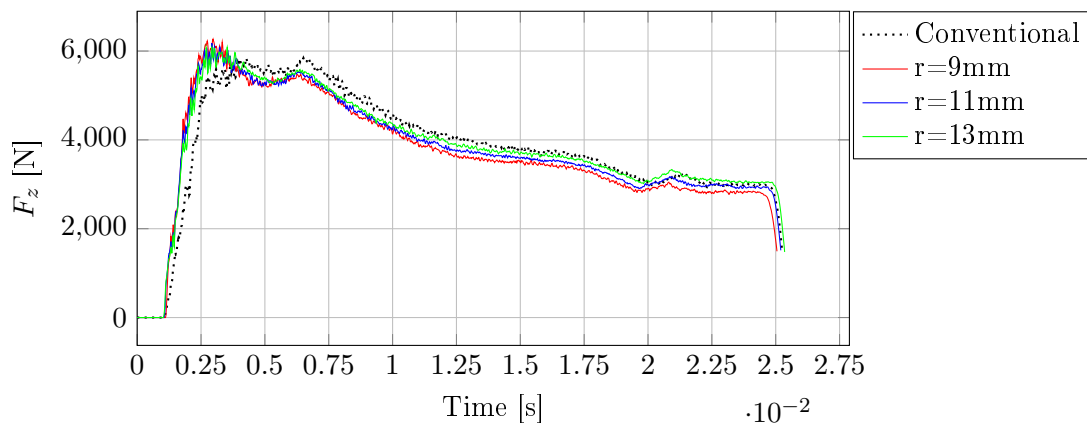


Figure D.130. ΔF_x - Station 3 - Die 1 - 0.20° die tilt

D.2.3.4 z-forces

Figure D.131. F_z - Station 3 - Punch - 0.20° die tiltFigure D.132. F_z - Station 3 - Die 1 x^+ - 0.20° die tiltFigure D.133. F_z - Station 3 - Die 1 x^- - 0.20° die tilt

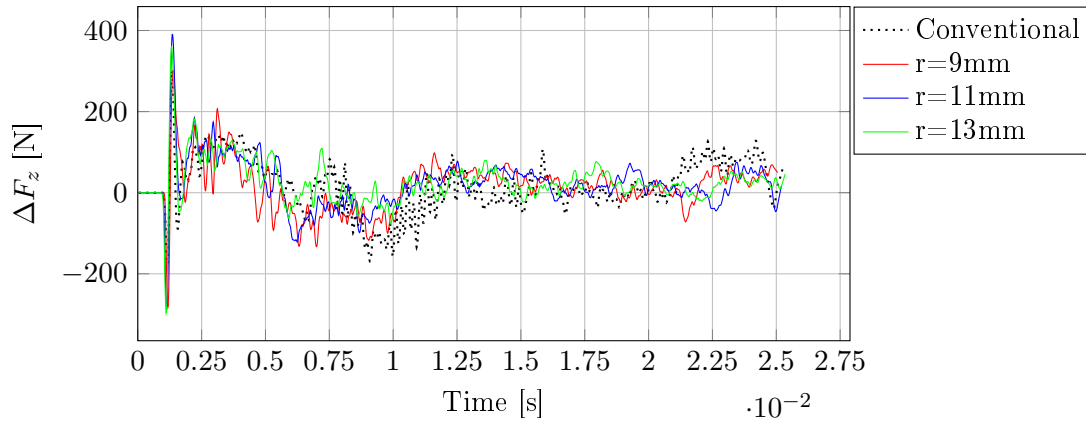


Figure D.134. ΔF_z - Station 3 - Die 1 - 0.20° die tilt

D.2.3.5 Interface pressure

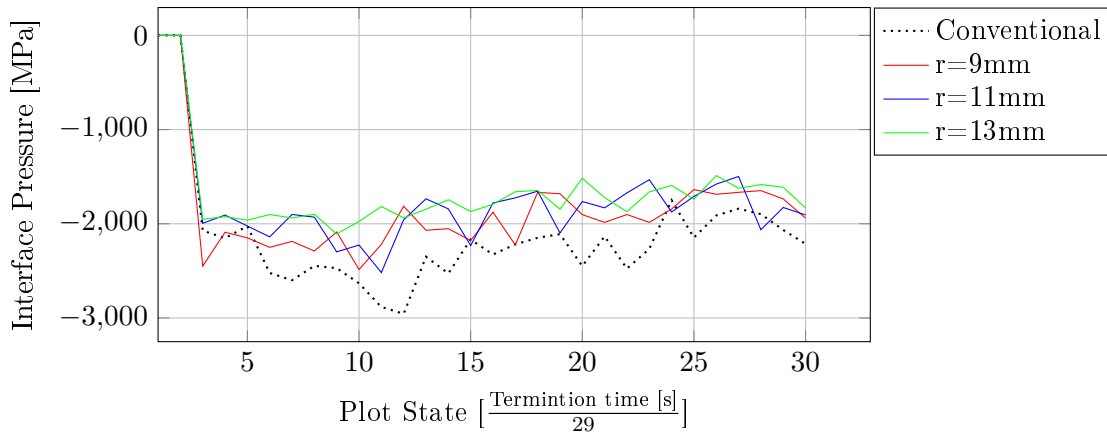


Figure D.135. Maximum interface pressure - Station 3 - Die 1 x^+ - 0.20° die tilt

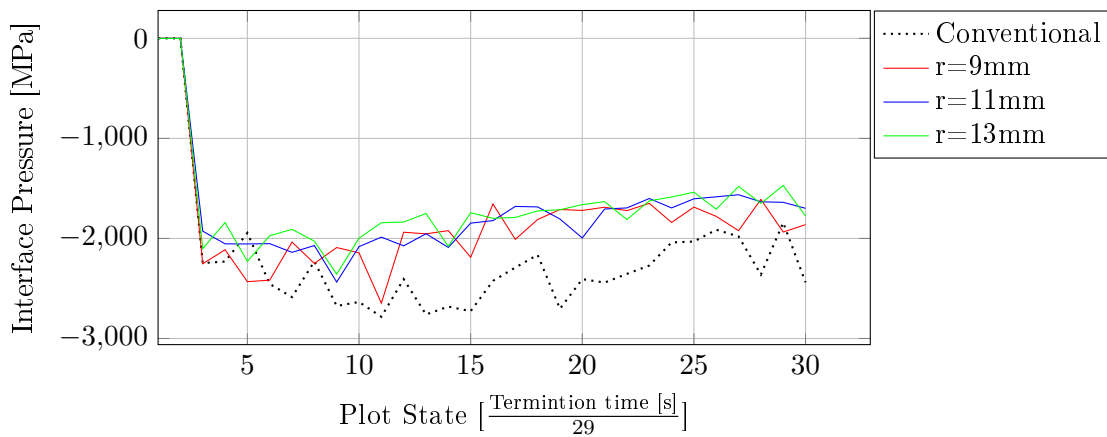


Figure D.136. Maximum interface pressure - Station 3 - Die 1 x^- - 0.20° die tilt

D.3 0.40° die tilt

D.3.1 Station 1

D.3.1.1 Effective plastic strain

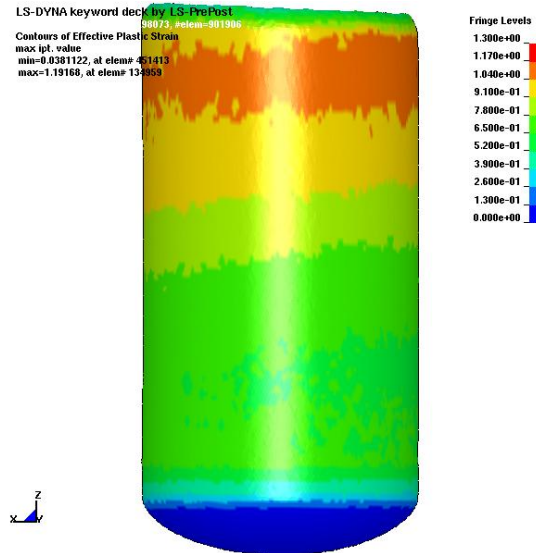


Figure D.137. Effective plastic strain - Station 1 - 0.40° die tilt - Conventional die design

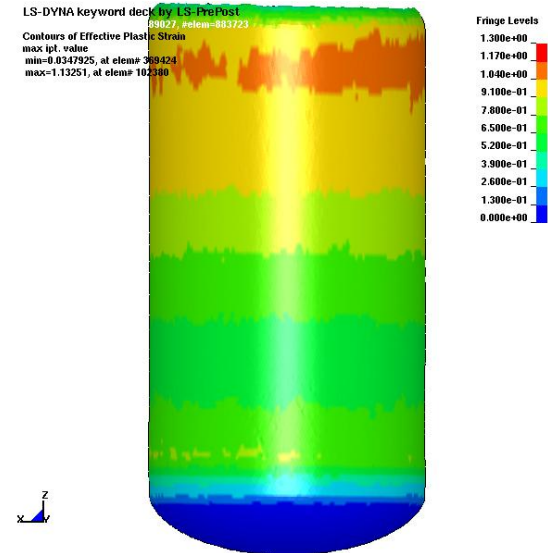


Figure D.138. Effective plastic strain - Station 1 - 0.40° die tilt - $r = 9mm$

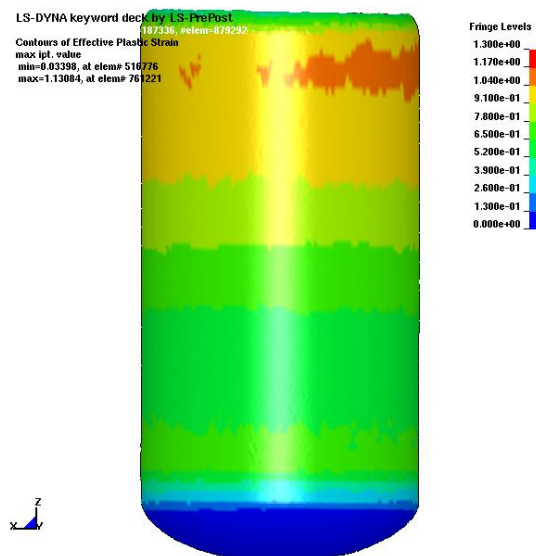


Figure D.139. Effective plastic strain - Station 1 - 0.40° die tilt - $r = 11mm$

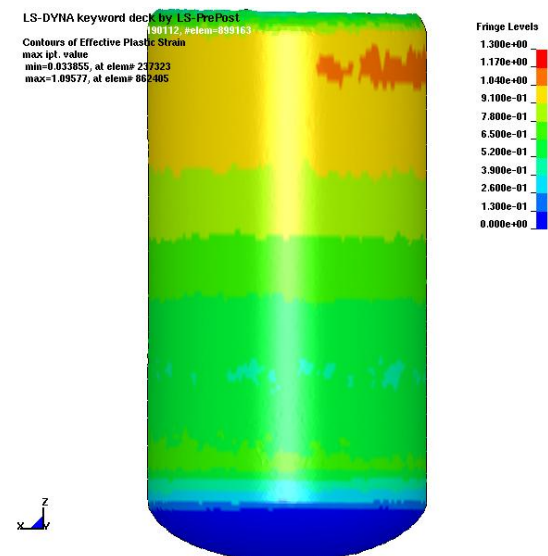


Figure D.140. Effective plastic strain - Station 1 - 0.40° die tilt - $r = 13mm$

D.3.1.2 Resultant forces

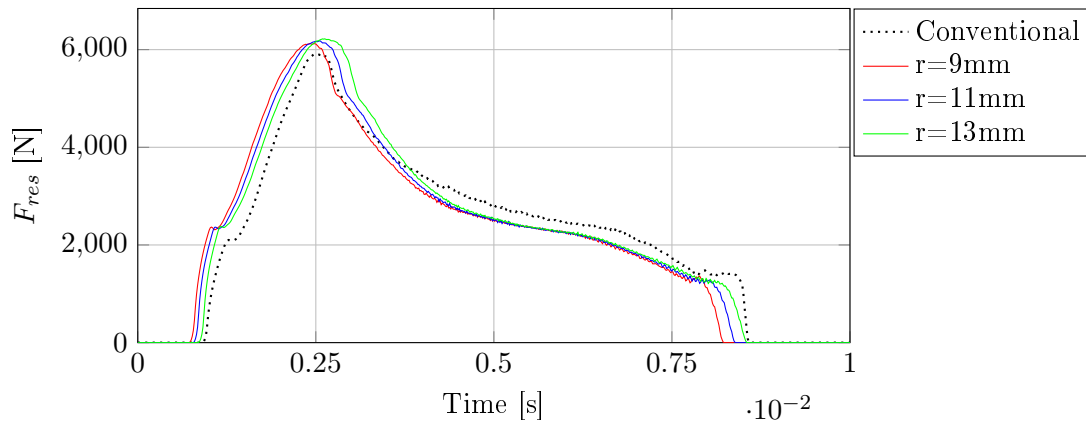


Figure D.141. F_{res} - Station 1 - Die 1 x^+ - 0.40° die tilt

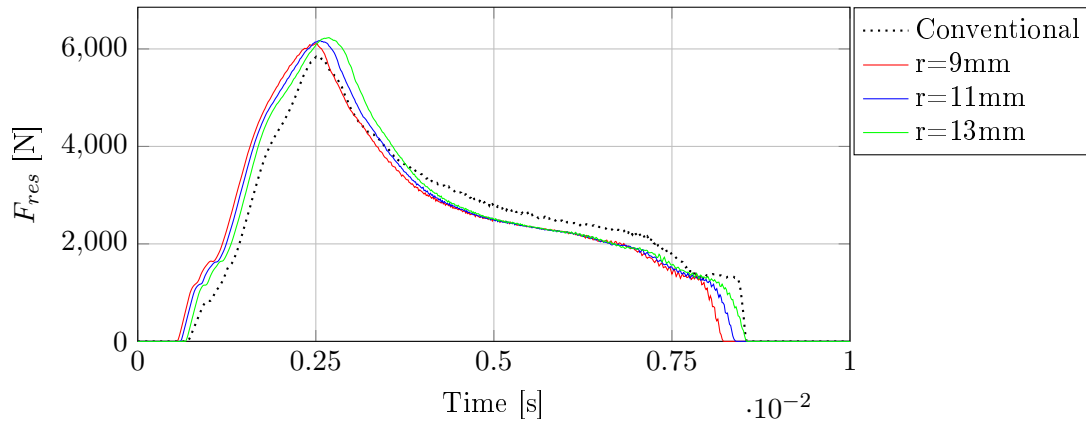


Figure D.142. F_{res} - Station 1 - Die 1 x^- - 0.40° die tilt

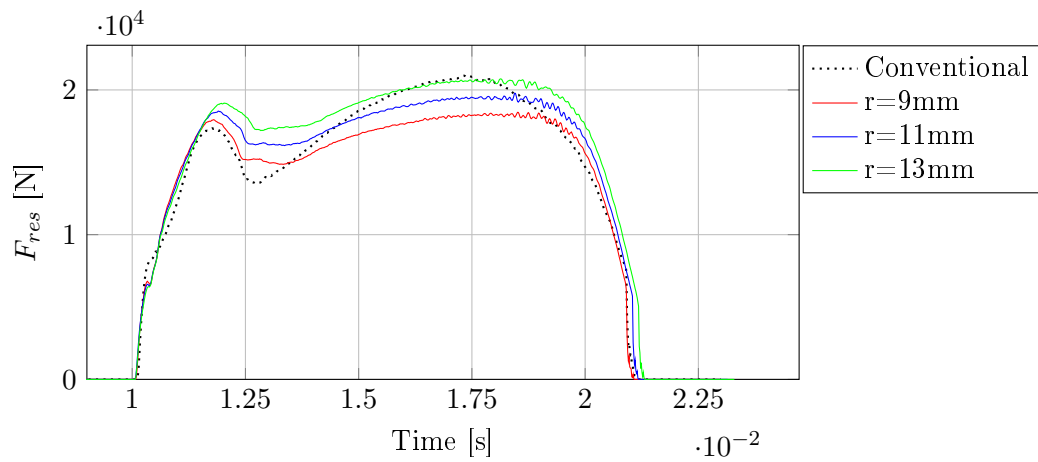


Figure D.143. F_{res} - Station 1 - Die 2 x^+ - 0.40° die tilt

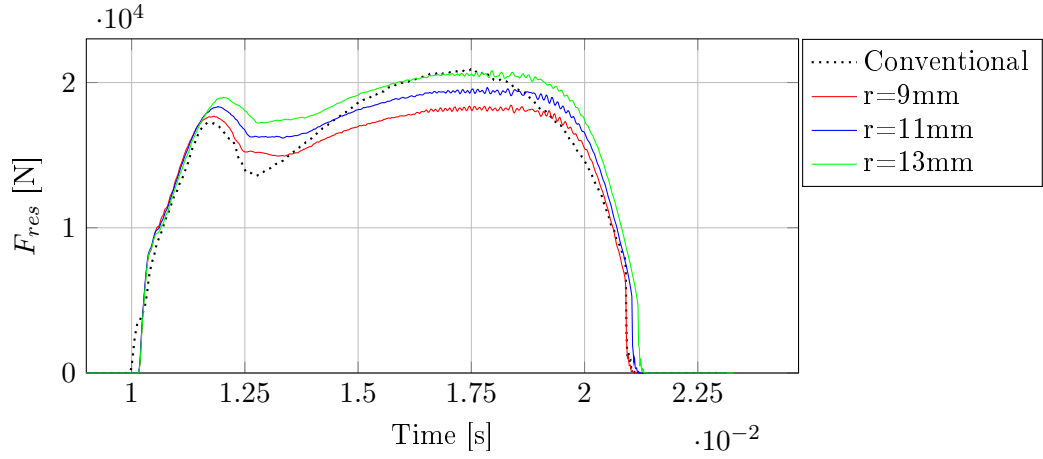


Figure D.144. F_{res} - Station 1 - Die 2 x^- - 0.40° die tilt

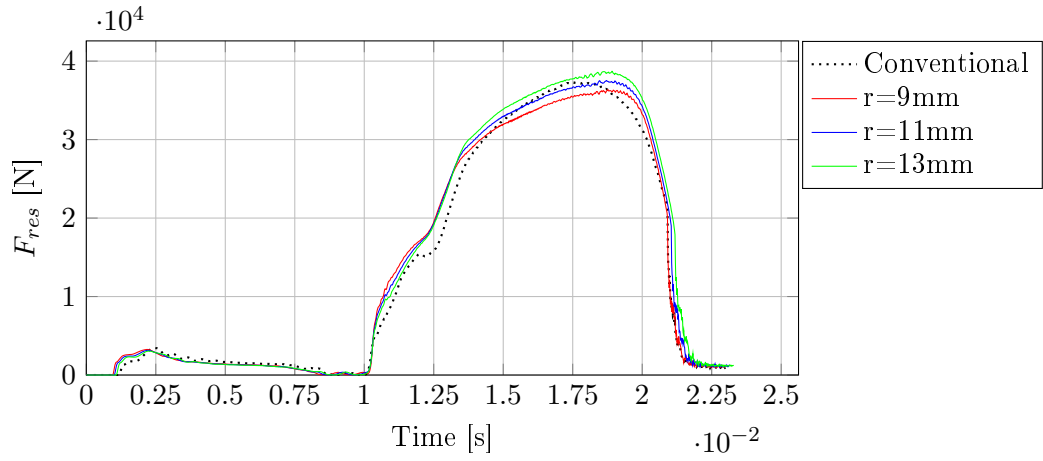


Figure D.145. F_{res} - Station 1 - Punch - 0.40° die tilt

D.3.1.3 x-forces

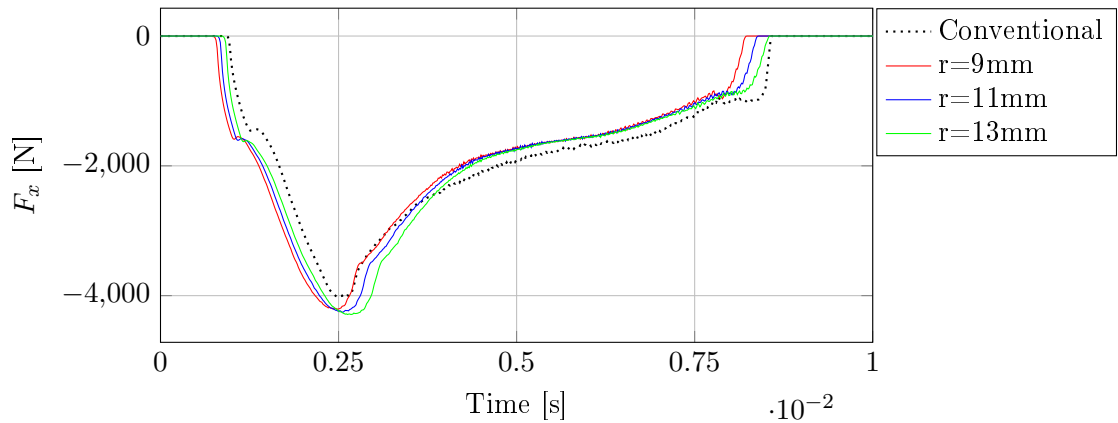


Figure D.146. F_x - Station 1 - Die 1 x^+ - 0.40° die tilt

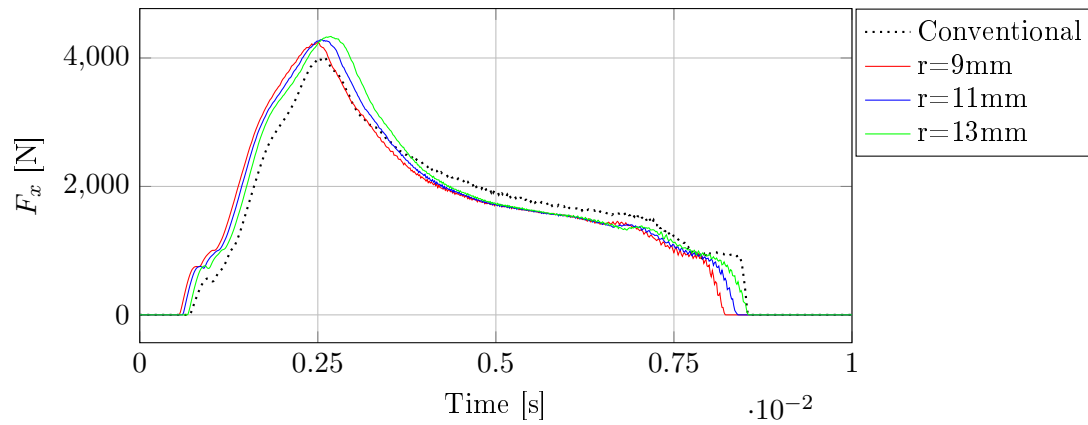


Figure D.147. F_x - Station 1 - Die 1 x^- - 0.40° die tilt

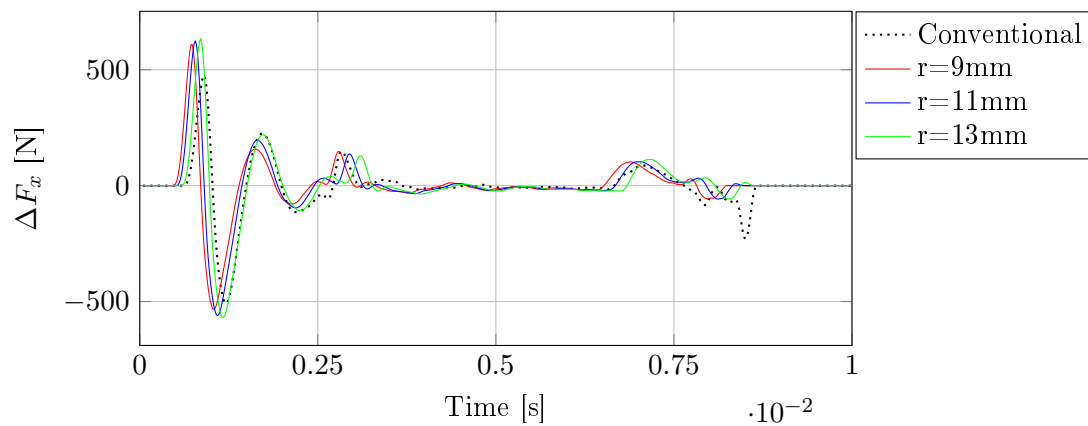


Figure D.148. ΔF_x - Station 1 - Die 1 - 0.40° die tilt

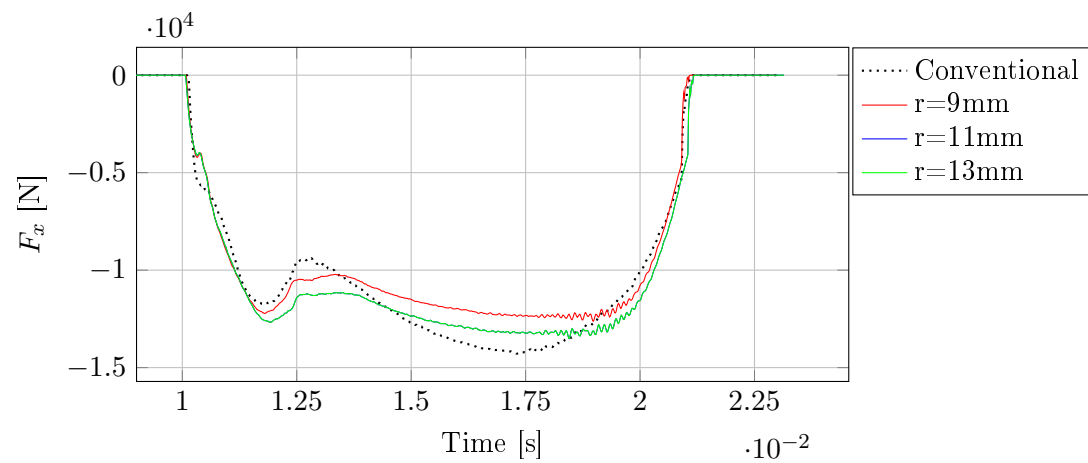


Figure D.149. F_x - Station 1 - Die 2 x^+ - 0.40° die tilt

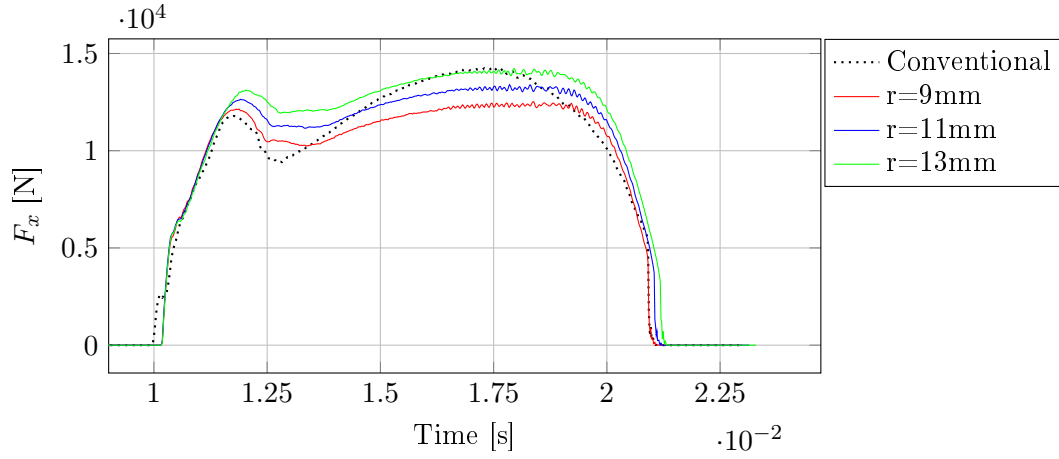


Figure D.150. F_x - Station 1 - Die 2 x^- - 0.40° die tilt

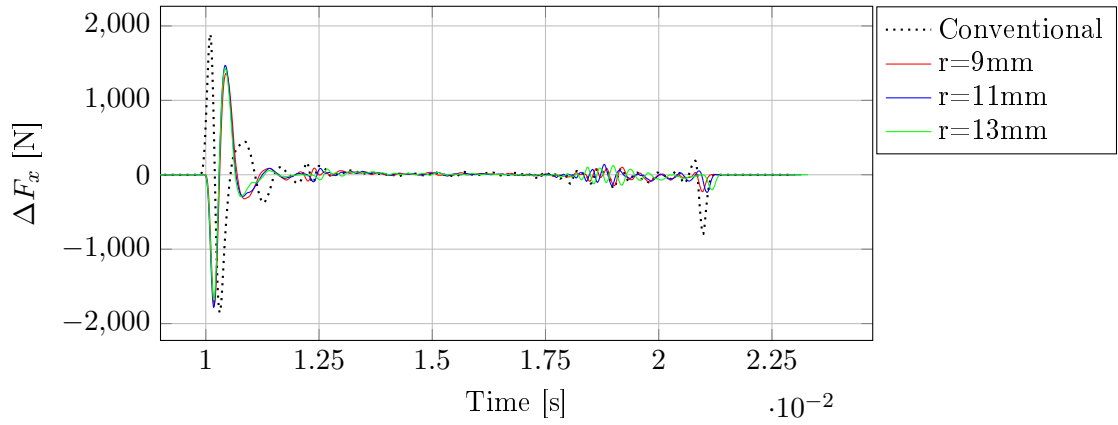


Figure D.151. ΔF_x - Station 1 - Die 2 - 0.40° die tilt

D.3.1.4 z-forces

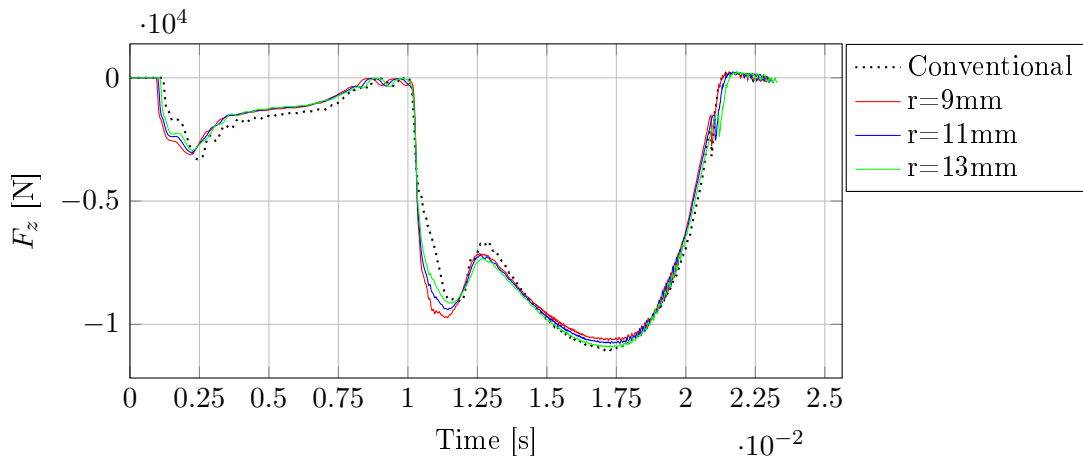


Figure D.152. F_z - Station 1 - Punch - 0.40° die tilt

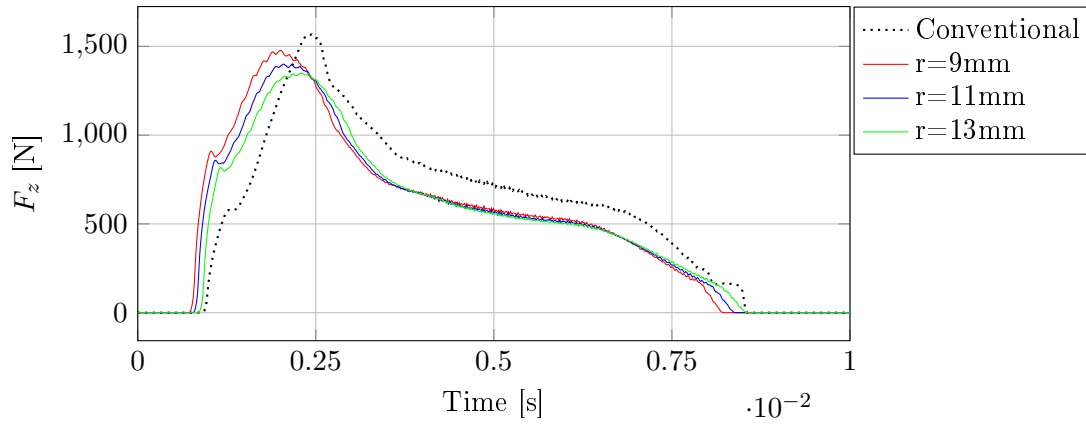


Figure D.153. F_z - Station 1 - Die 1 x^+ - 0.40° die tilt

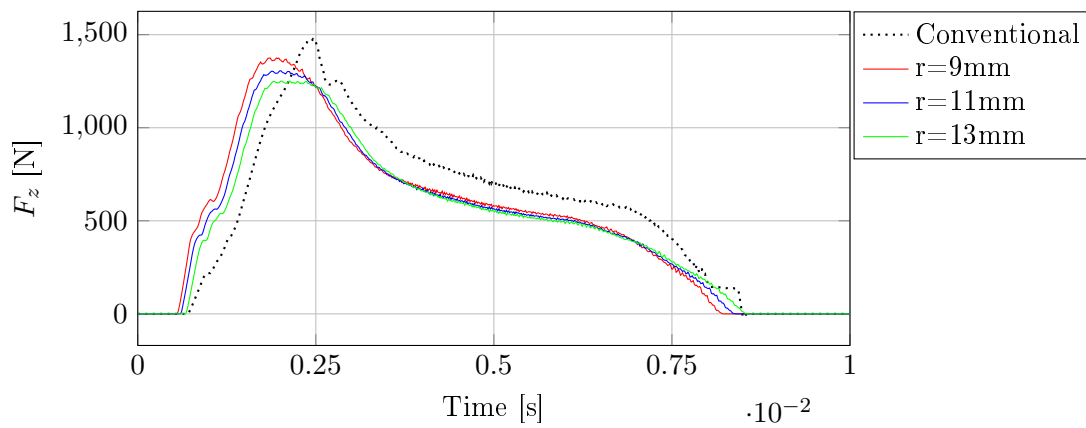


Figure D.154. F_z - Station 1 - Die 1 x^- - 0.40° die tilt

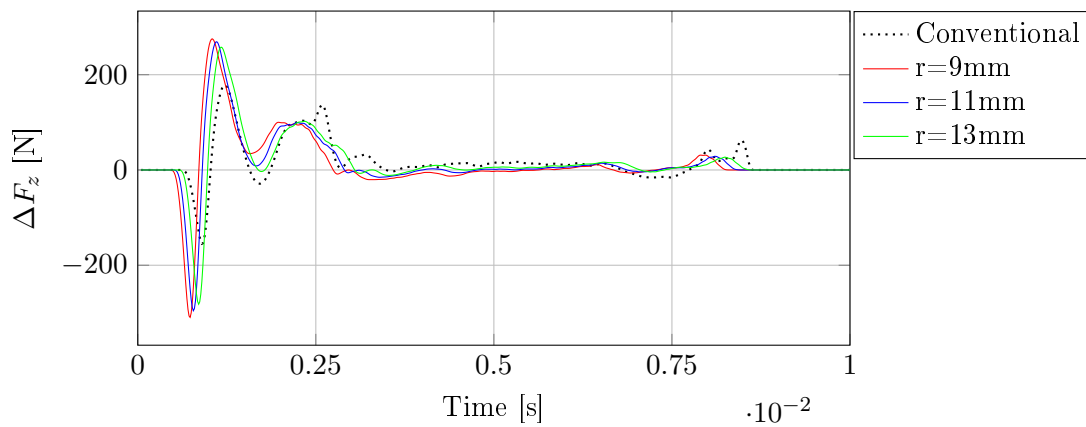


Figure D.155. ΔF_z - Station 1 - Die 1 - 0.40° die tilt

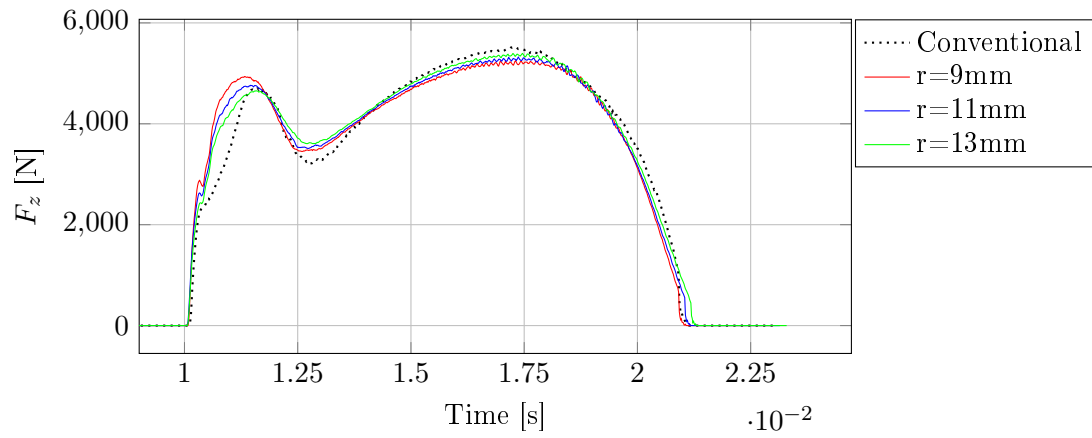


Figure D.156. F_z - Station 1 - Die 2 x^+ - 0.40° die tilt

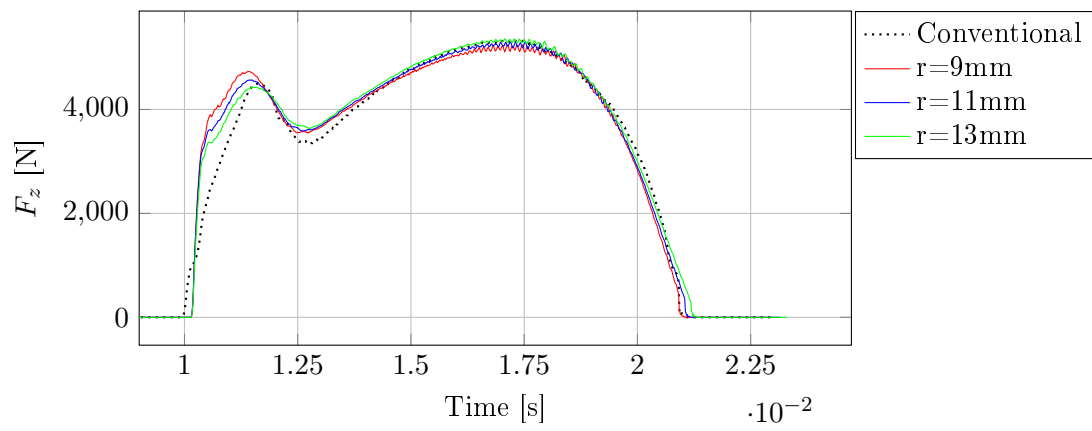


Figure D.157. F_z - Station 1 - Die 2 x^- - 0.40° die tilt

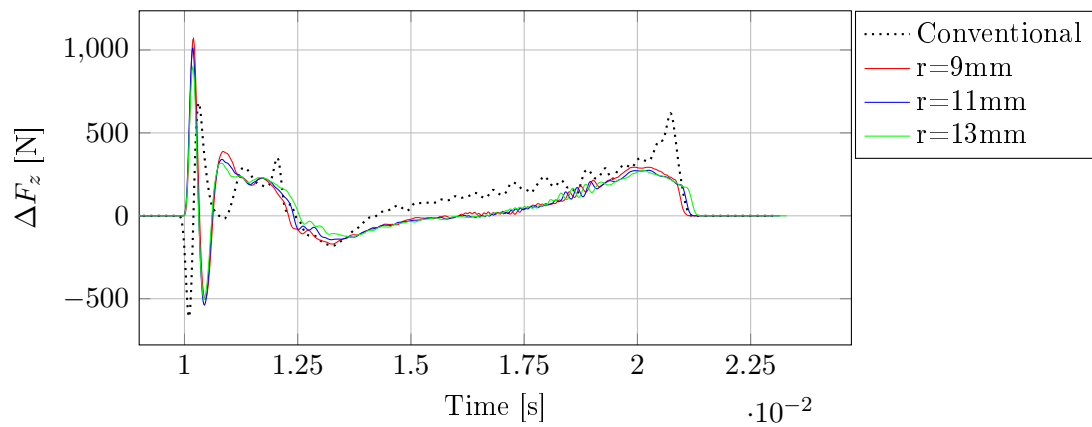


Figure D.158. ΔF_z - Station 1 - Die 2 - 0.40° die tilt

D.3.1.5 Interface pressure

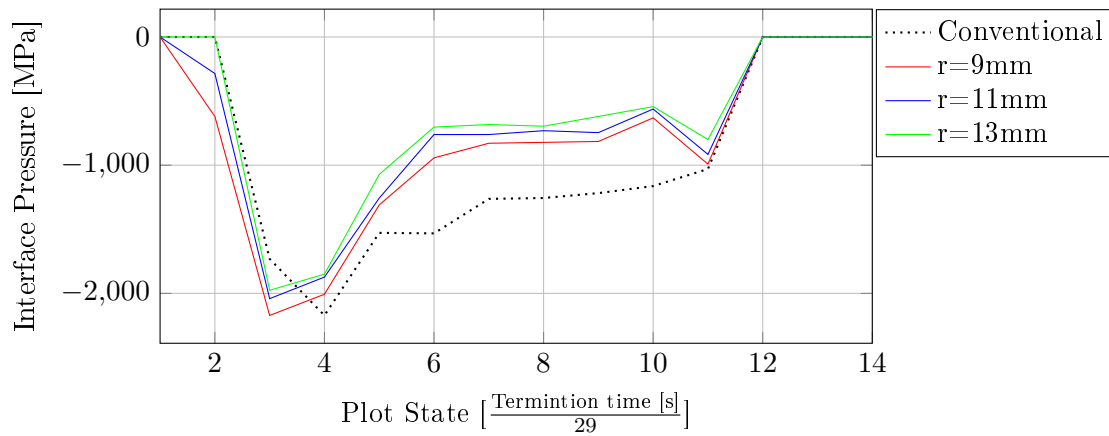


Figure D.159. Maximum interface pressure - Station 1 - Die 1 x^+ - 0.40° die tilt

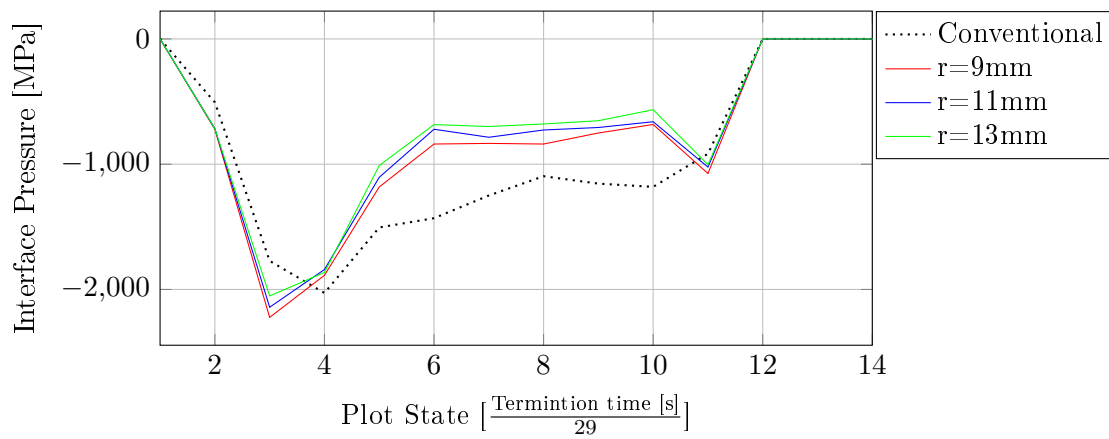


Figure D.160. Maximum interface pressure - Station 1 - Die 1 x^- - 0.40° die tilt

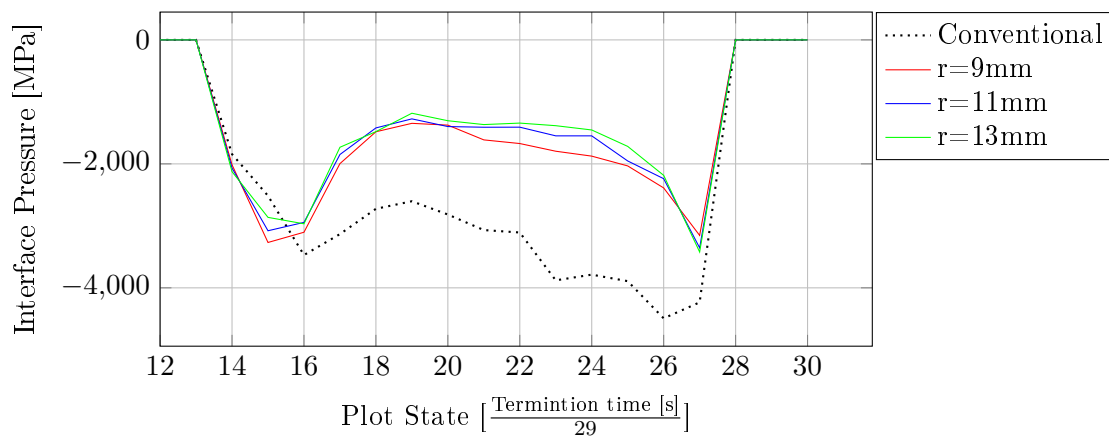


Figure D.161. Maximum interface pressure - Station 1 - Die 2 x^+ - 0.40° die tilt

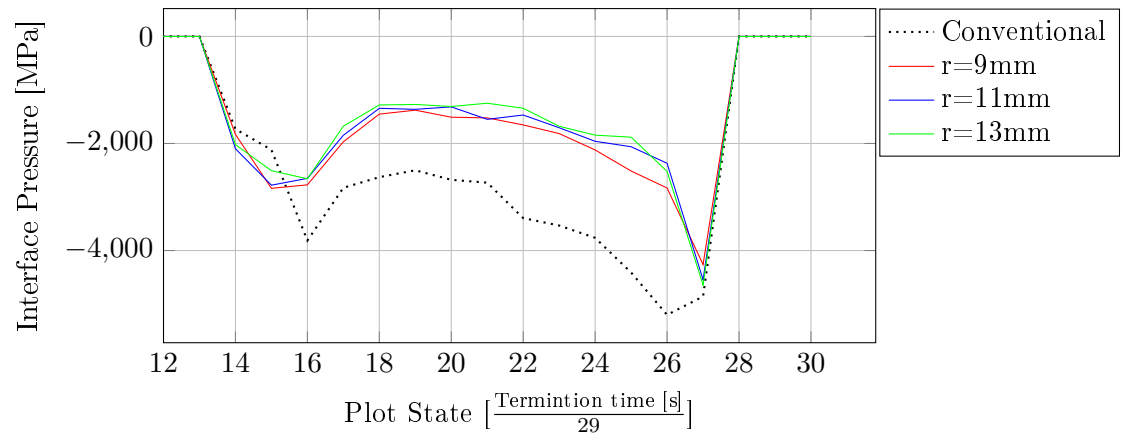


Figure D.162. Maximum interface pressure - Station 1 - Die 2 x^- - 0.40° die tilt

D.3.2 Station 2

D.3.2.1 Effective plastic strain

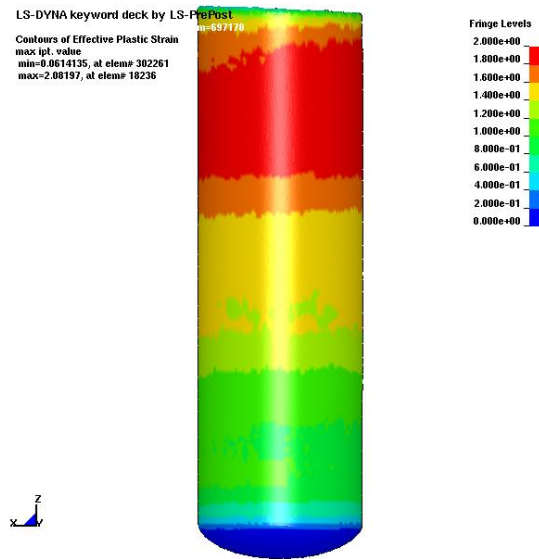


Figure D.163. Effective plastic strain - Station 2 - 0.40° die tilt - Conventional die design

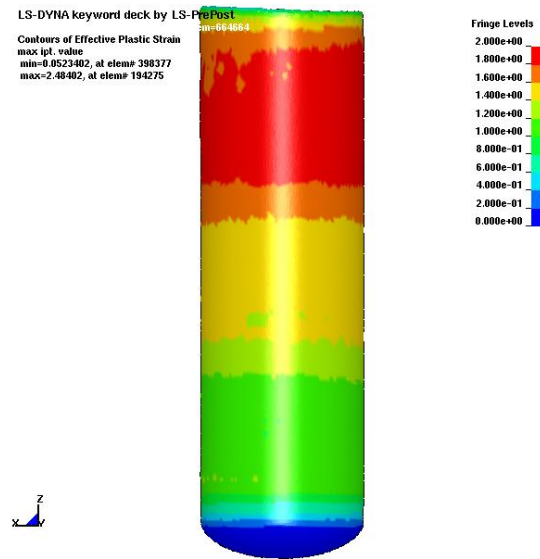


Figure D.164. Effective plastic strain - Station 2 - 0.40° die tilt - $r = 9mm$

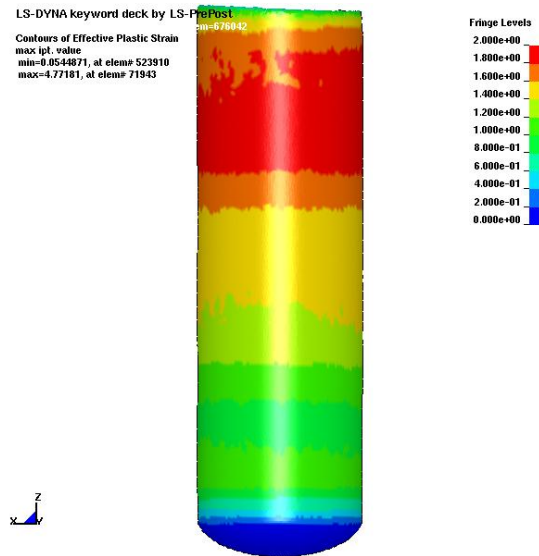


Figure D.165. Effective plastic strain - Station 2 - 0.40° die tilt - $r = 11mm$

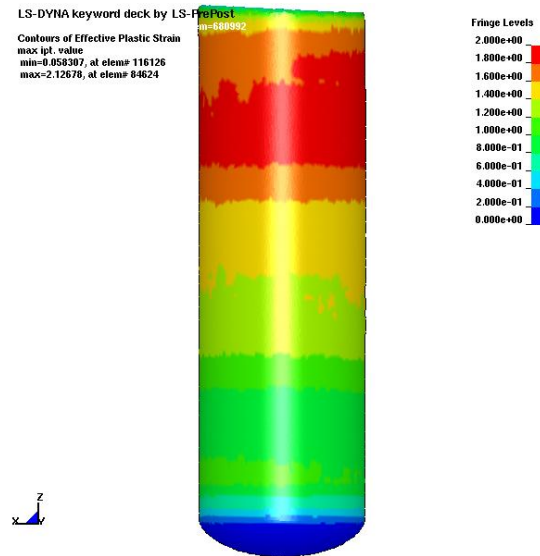


Figure D.166. Effective plastic strain - Station 2 - 0.40° die tilt - $r = 13mm$

D.3.2.2 Resultant forces

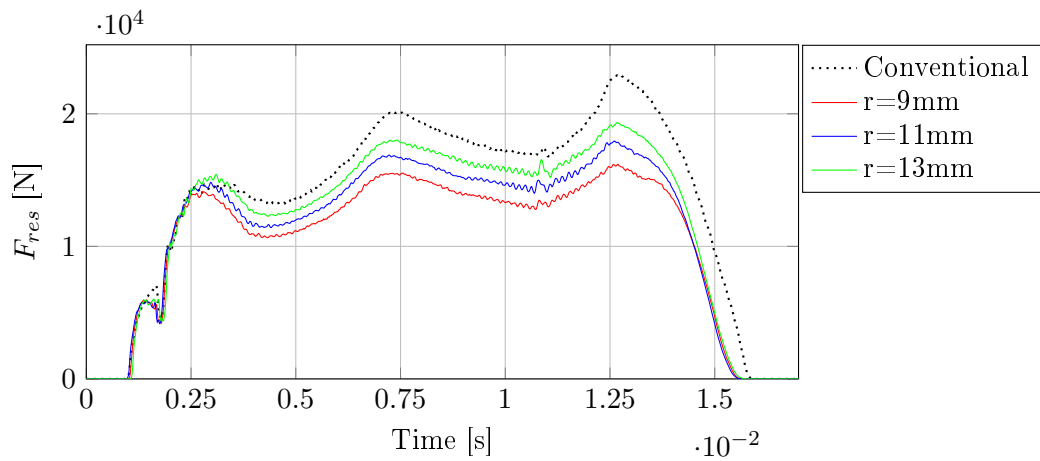


Figure D.167. F_{res} - Station 2 - Die 1 x^+ - 0.40° die tilt

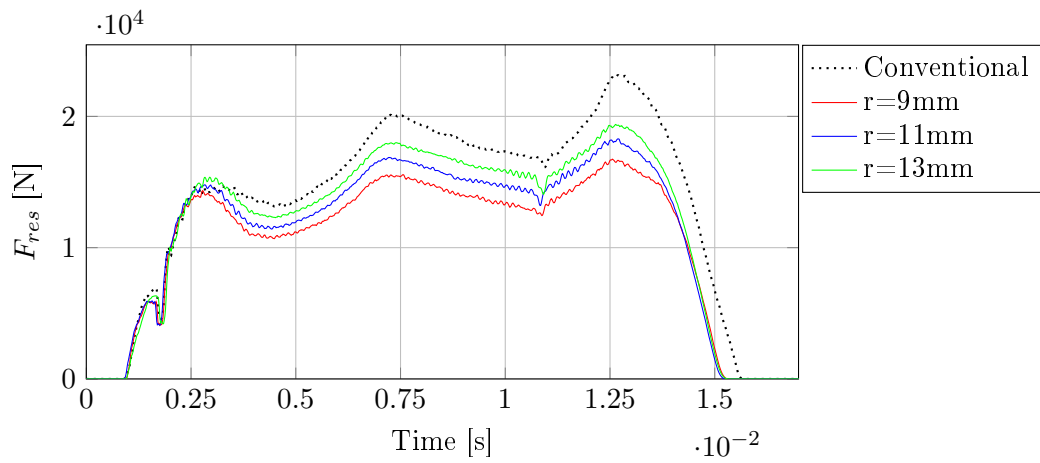


Figure D.168. F_{res} - Station 2 - Die 1 x^- - 0.40° die tilt

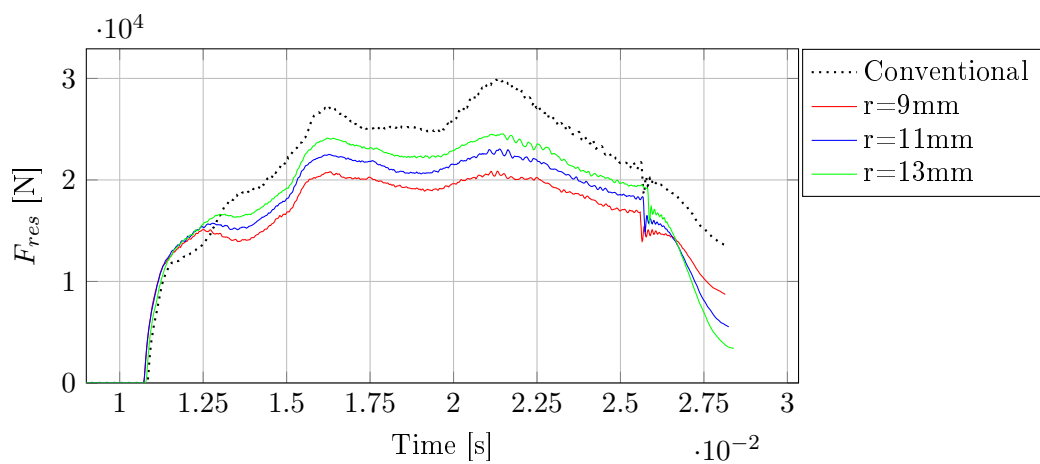


Figure D.169. F_{res} - Station 2 - Die 2 x^+ - 0.40° die tilt

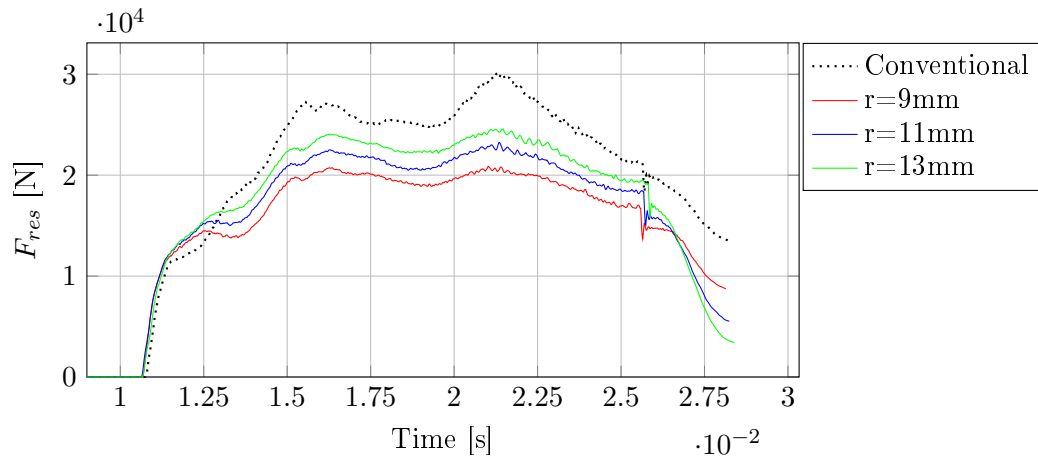


Figure D.170. F_{res} - Station 2 - Die 2 x^- - 0.40° die tilt

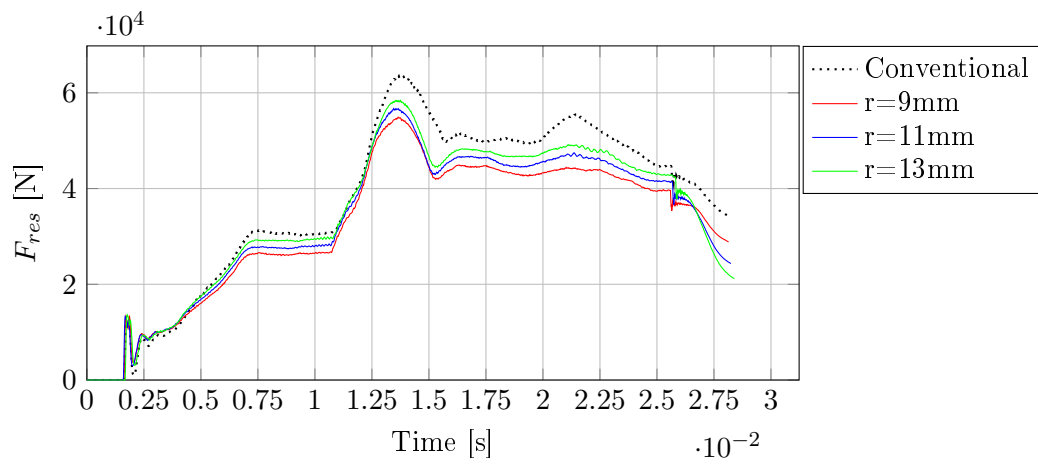


Figure D.171. F_{res} - Station 2 - Punch - 0.40° die tilt

D.3.2.3 x-forces

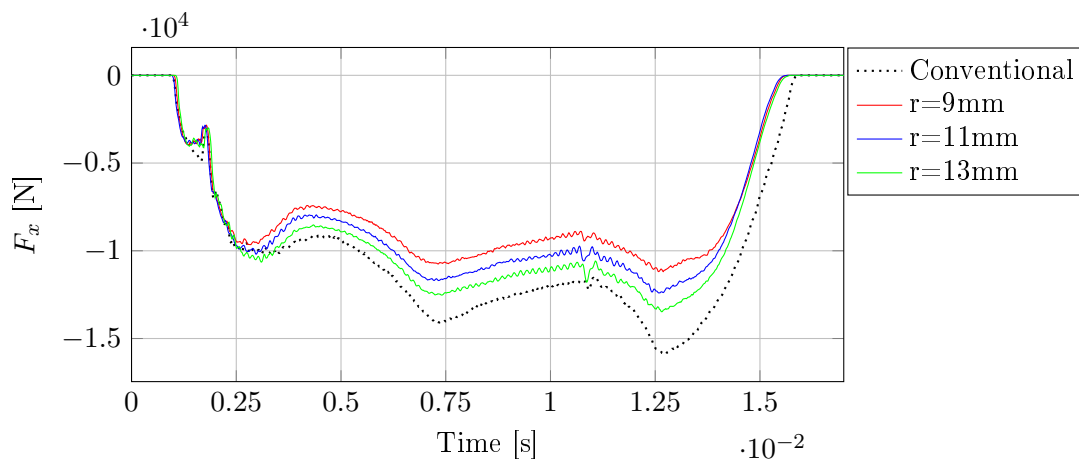


Figure D.172. F_x - Station 2 - Die 1 x^+ - 0.40° die tilt

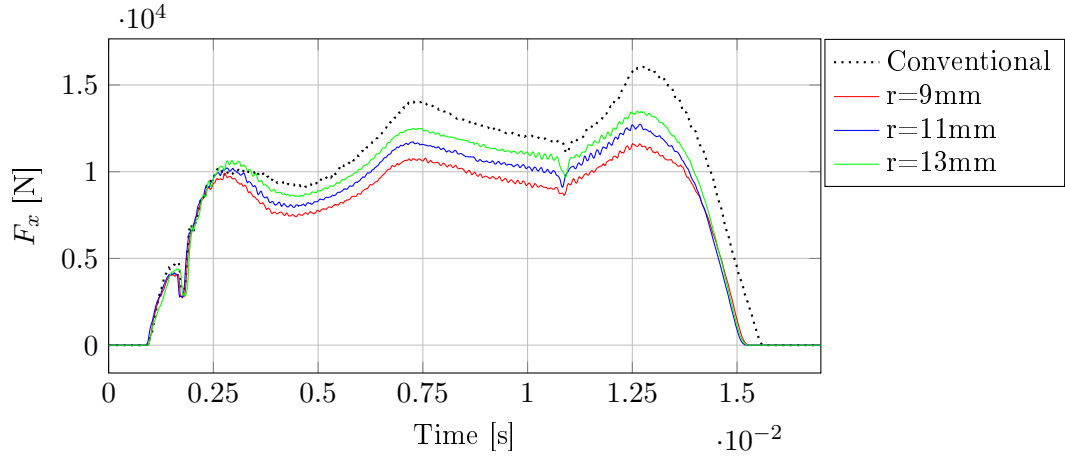


Figure D.173. F_x - Station 2 - Die 1 x^- - 0.40° die tilt

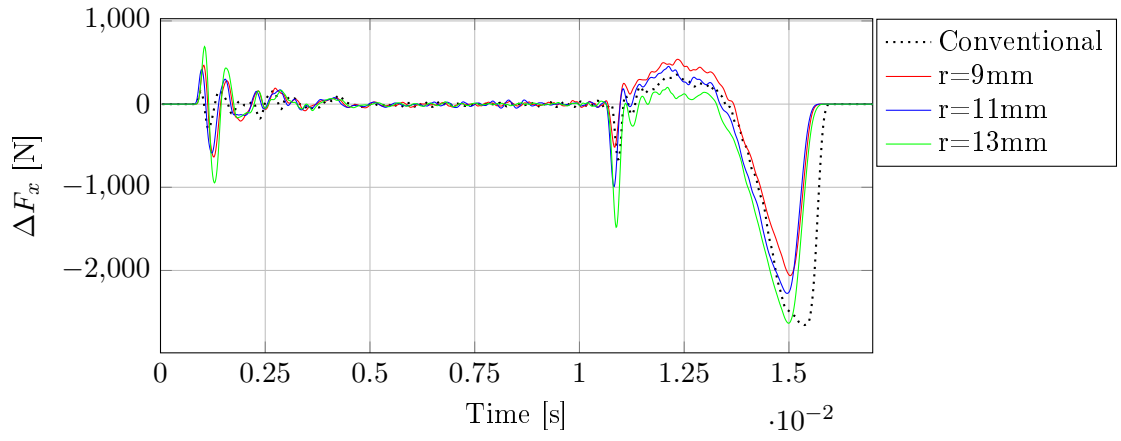


Figure D.174. ΔF_x - Station 2 - Die 1 - 0.40° die tilt

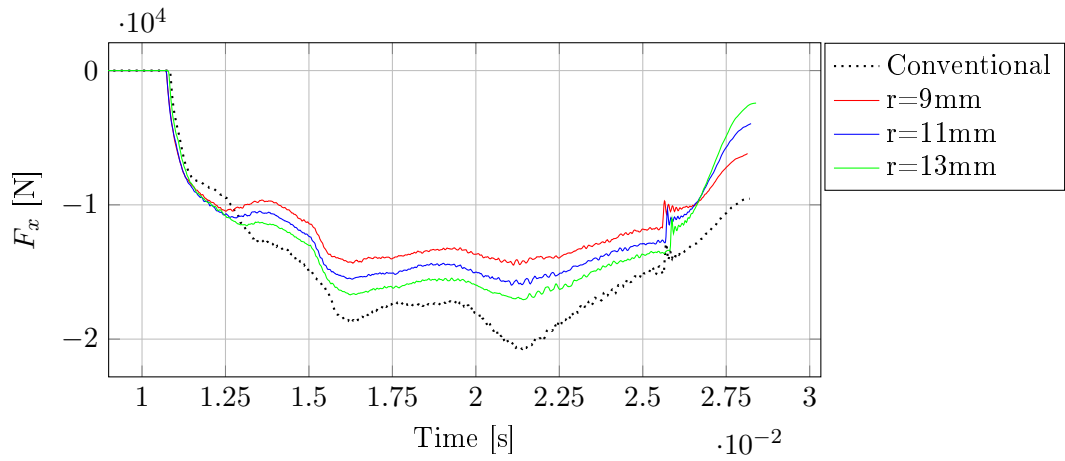


Figure D.175. F_x - Station 2 - Die 2 x^+ - 0.40° die tilt

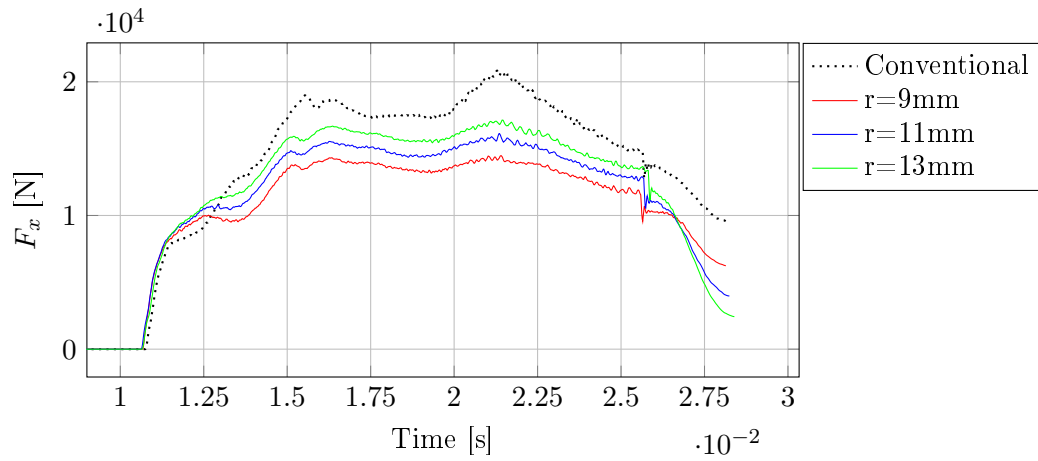


Figure D.176. F_x - Station 2 - Die 2 x^- - 0.40° die tilt

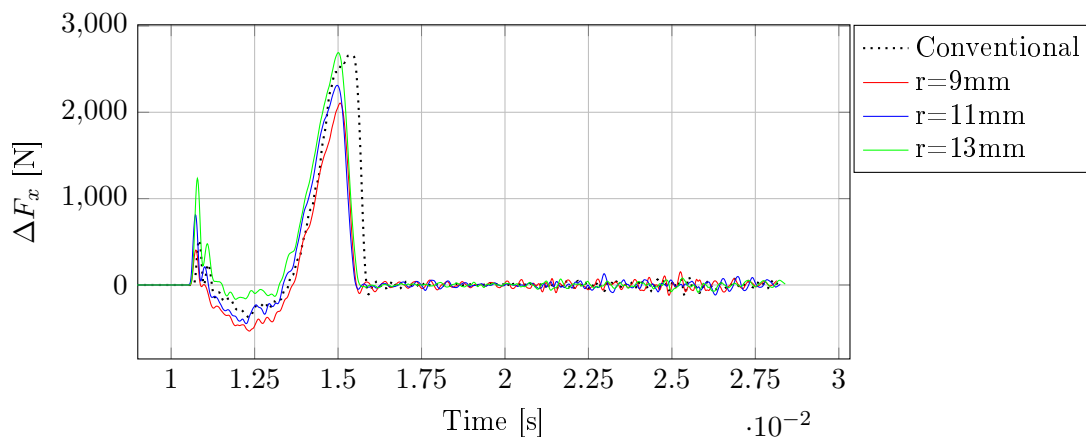


Figure D.177. ΔF_x - Station 2 - Die 2 - 0.40° die tilt

D.3.2.4 z-forces

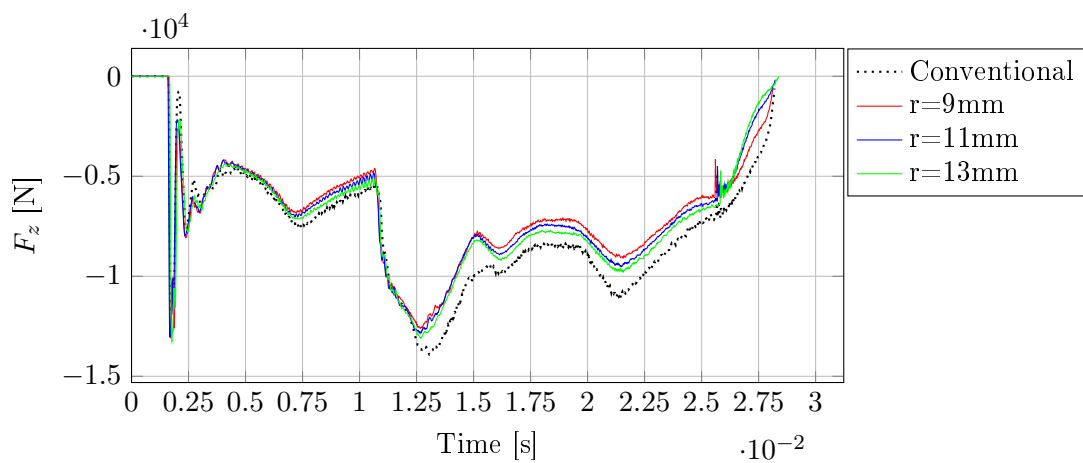


Figure D.178. F_z - Station 2 - Punch - 0.40° die tilt

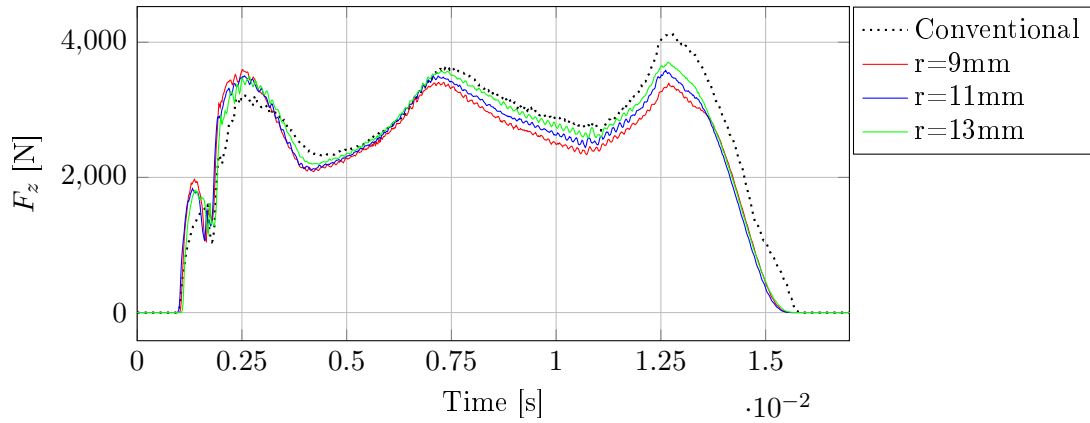


Figure D.179. F_z - Station 2 - Die 1 x^+ - 0.40° die tilt

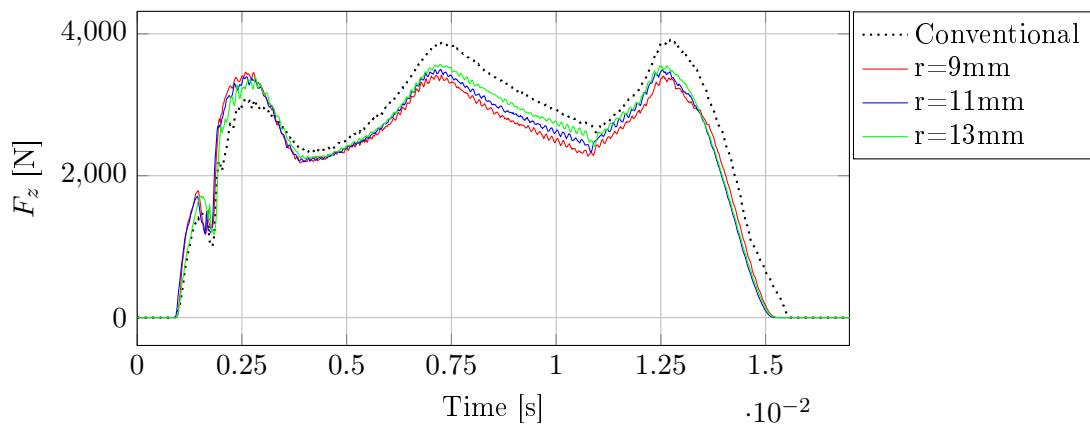


Figure D.180. F_z - Station 2 - Die 1 x^- - 0.40° die tilt

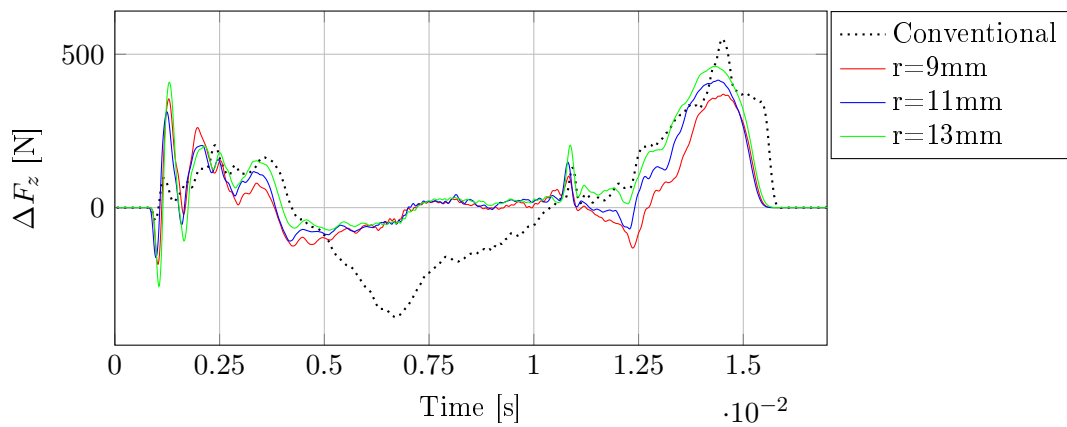


Figure D.181. ΔF_z - Station 2 - Die 1 - 0.40° die tilt

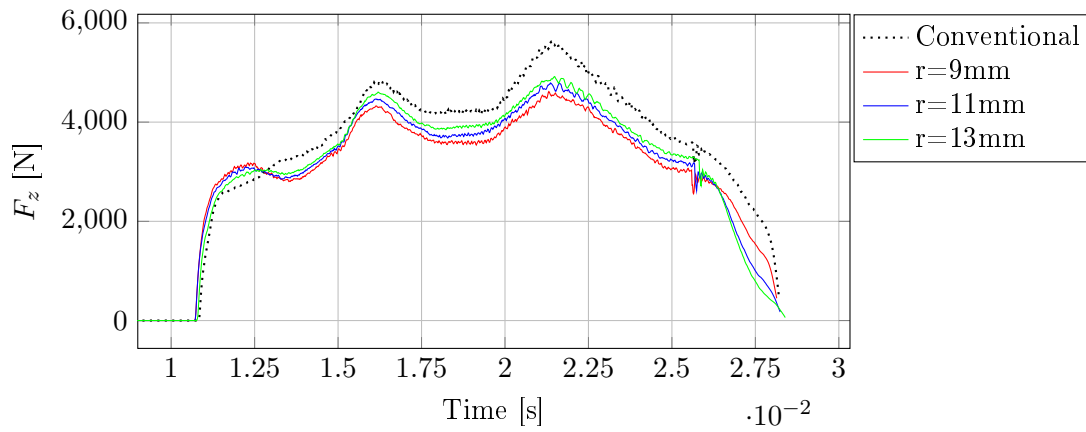


Figure D.182. F_z - Station 2 - Die 2 x^+ - 0.40° die tilt

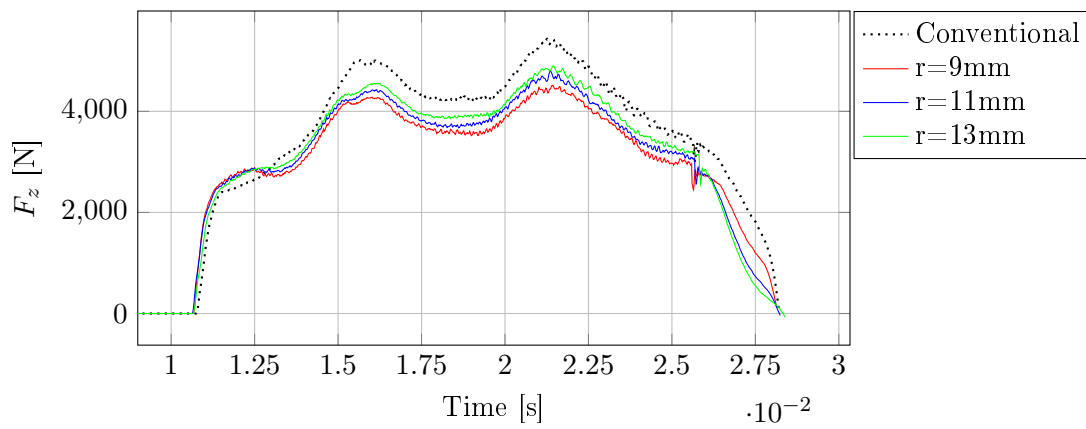


Figure D.183. F_z - Station 2 - Die 2 x^- - 0.40° die tilt

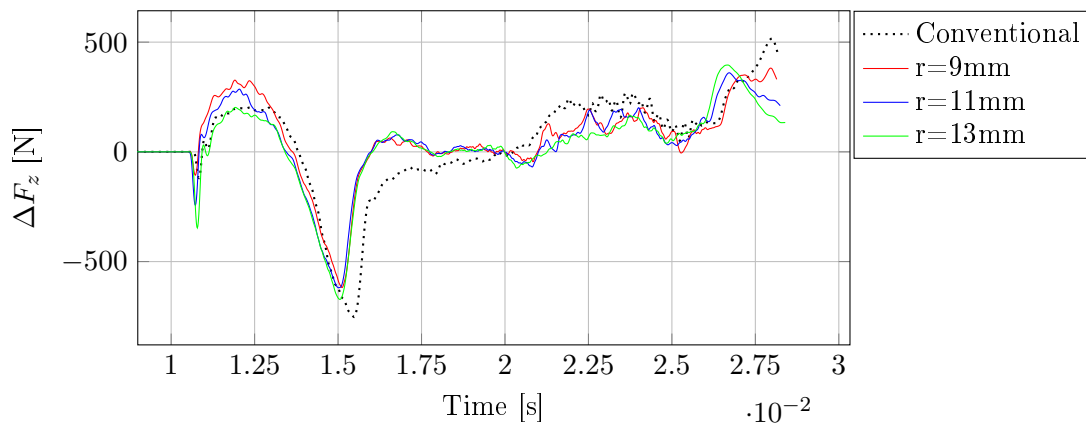


Figure D.184. ΔF_z - Station 2 - Die 2 - 0.40° die tilt

D.3.2.5 Interface pressure

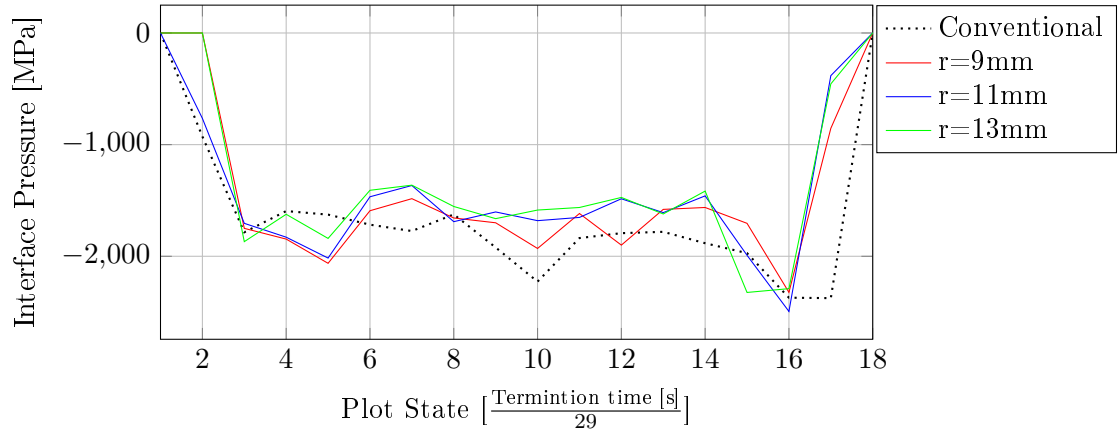


Figure D.185. Maximum interface pressure - Station 2 - Die 1 x^+ - 0.40° die tilt

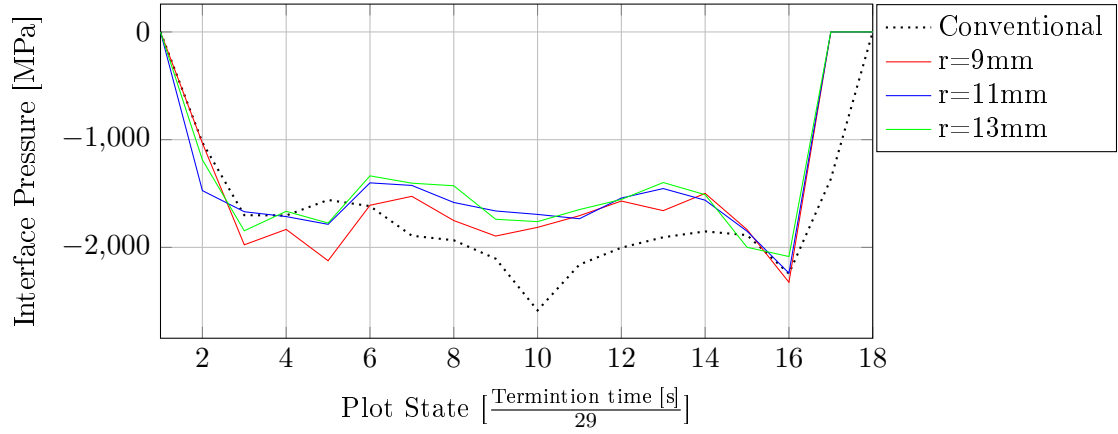


Figure D.186. Maximum interface pressure - Station 2 - Die 1 x^- - 0.40° die tilt

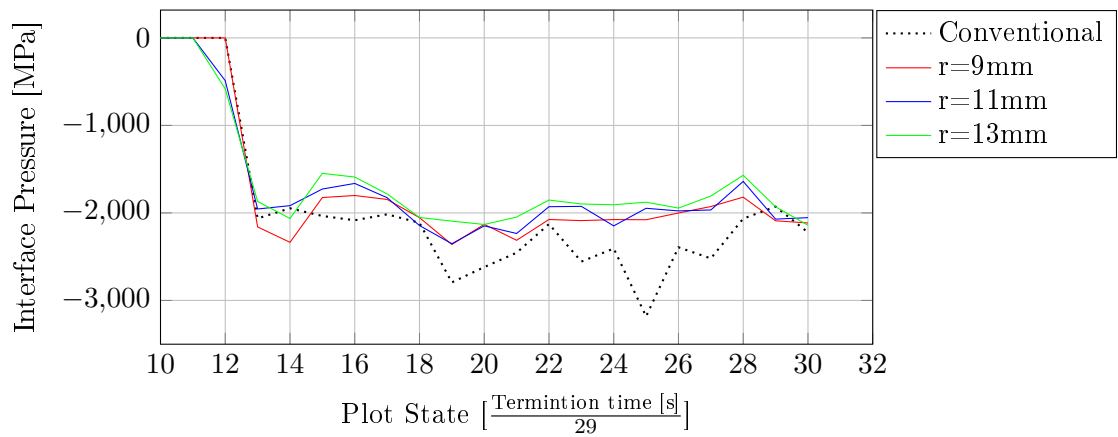


Figure D.187. Maximum interface pressure - Station 2 - Die 2 x^+ - 0.40° die tilt

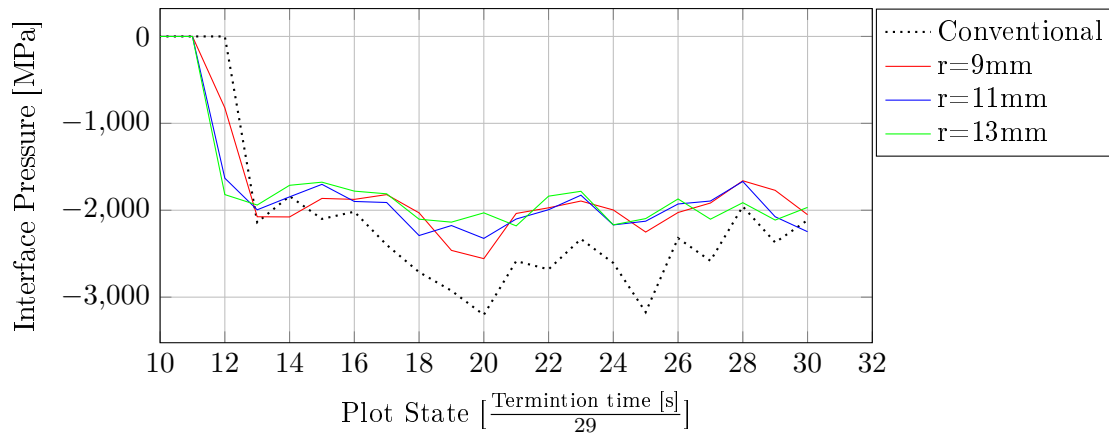


Figure D.188. Maximum interface pressure - Station 2 - Die 2 x^- - 0.40° die tilt

D.3.3 Station 3

D.3.3.1 Effective plastic strain

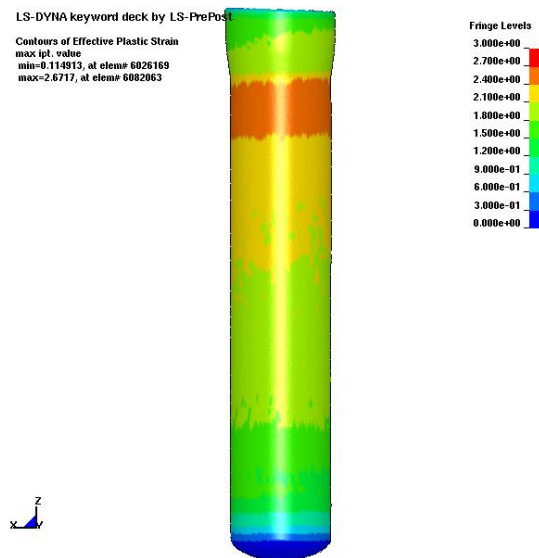


Figure D.189. Effective plastic strain - Station 3 - 0.40° die tilt - Conventional die design

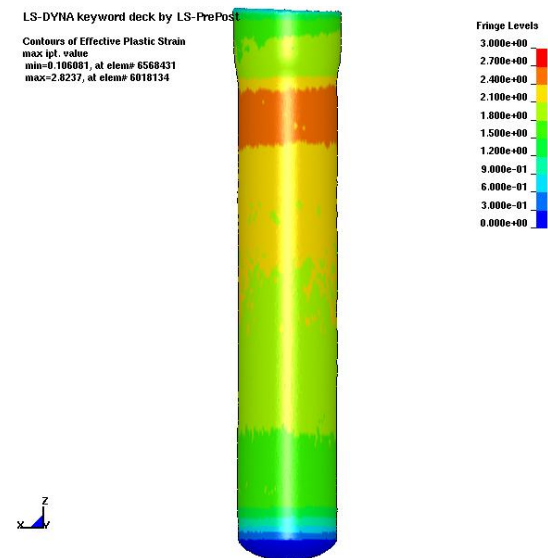


Figure D.190. Effective plastic strain - Station 3 - 0.40° die tilt - $r = 9mm$

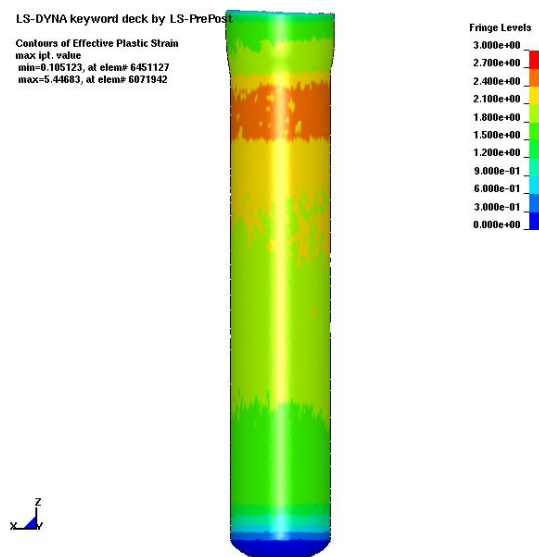


Figure D.191. Effective plastic strain - Station 3 - 0.40° die tilt - $r = 11mm$

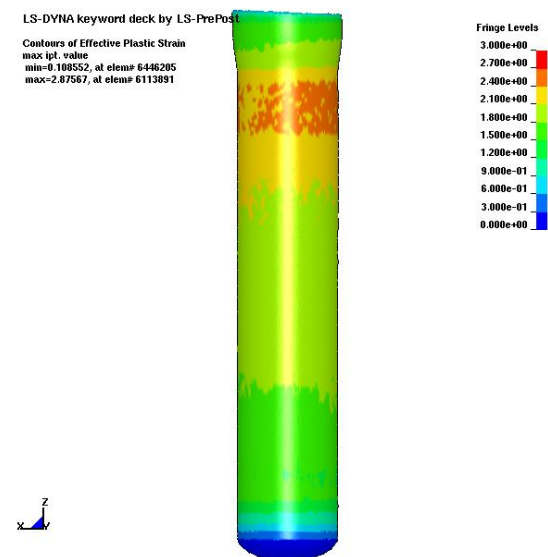


Figure D.192. Effective plastic strain - Station 3 - 0.40° die tilt - $r = 13mm$

D.3.3.2 Resultant forces

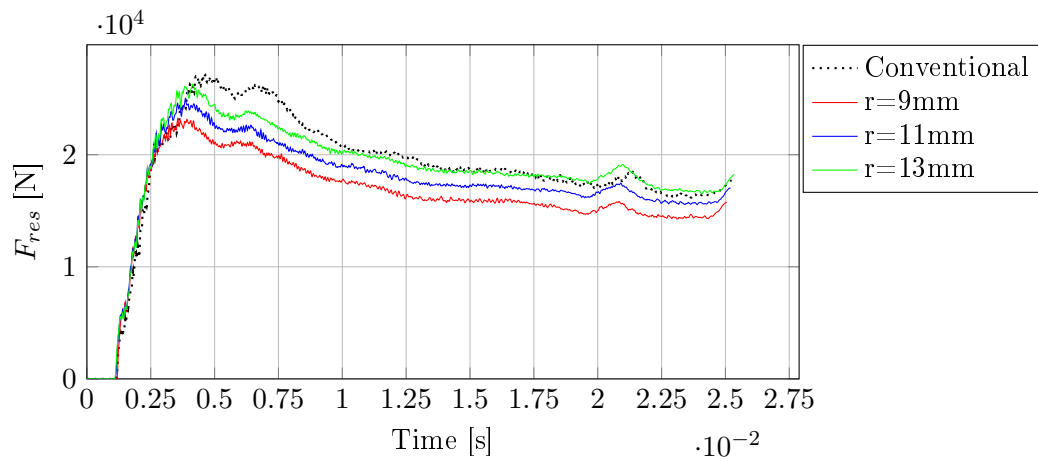


Figure D.193. F_{res} - Station 3 - Die 1 x^+ - 0.40° die tilt

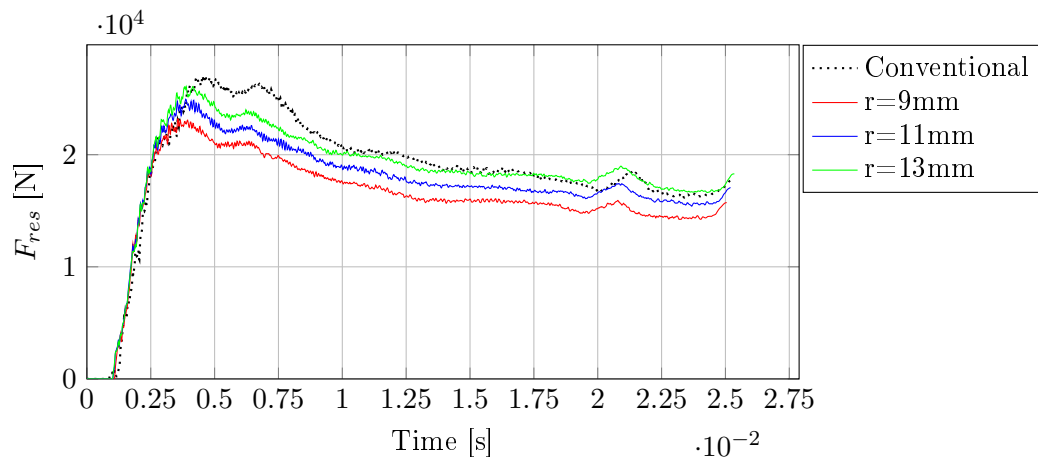


Figure D.194. F_{res} - Station 3 - Die 1 x^- - 0.40° die tilt

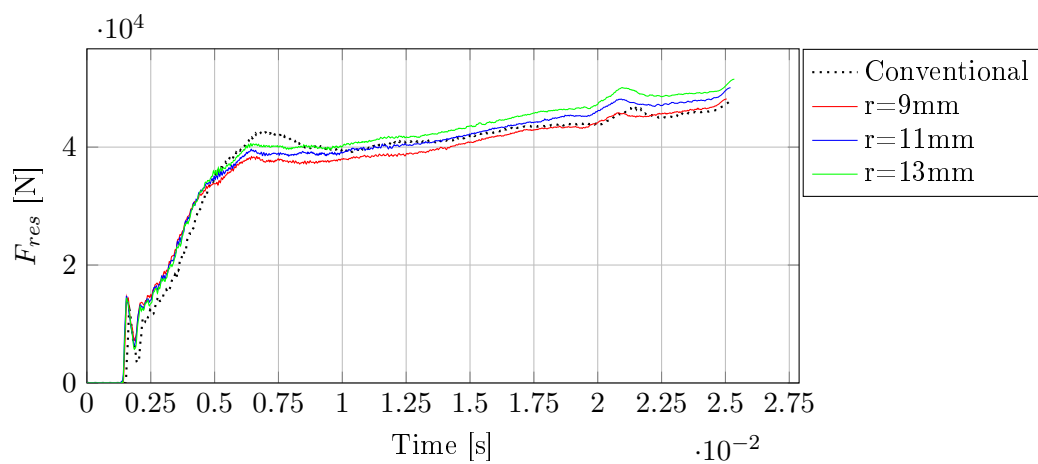
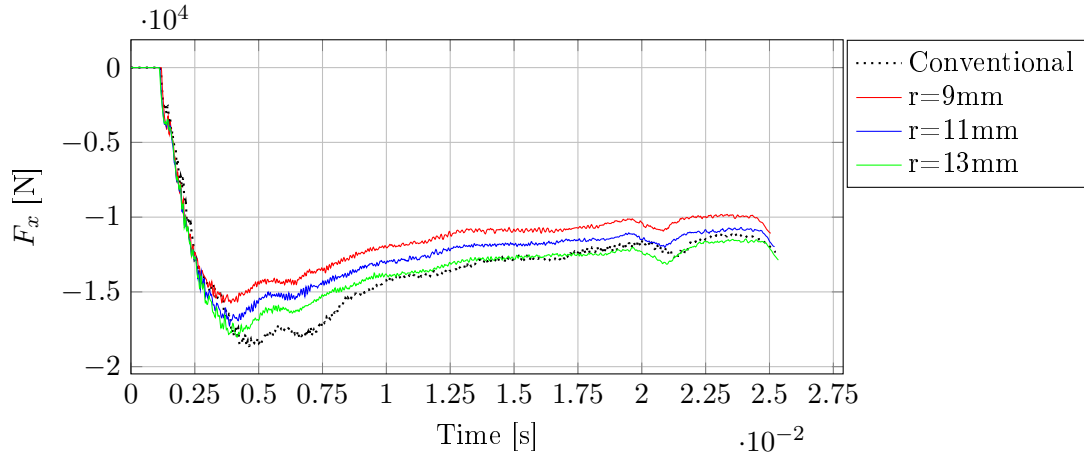
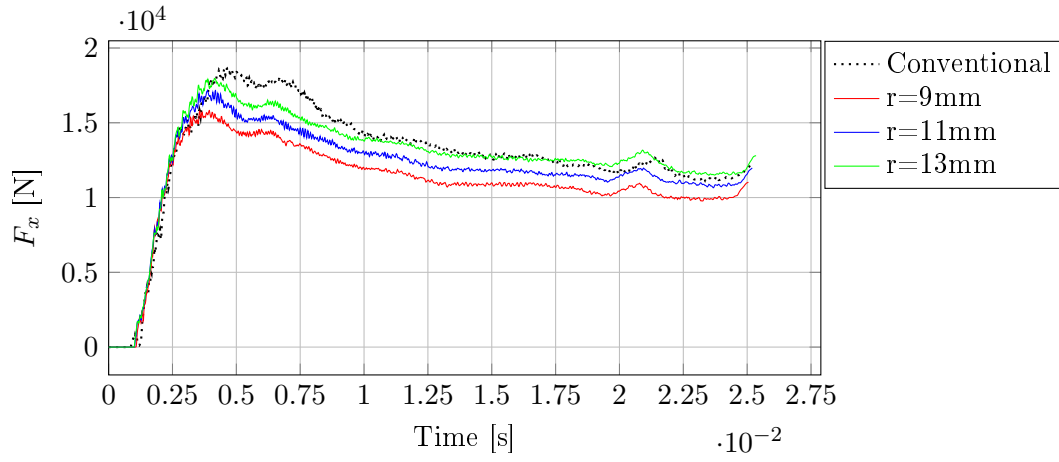
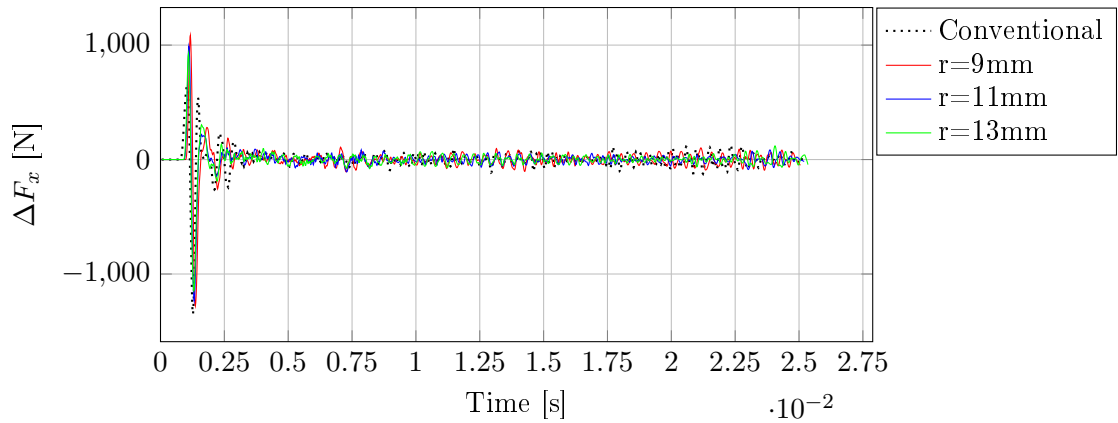


Figure D.195. F_{res} - Station 3 - Punch - 0.40° die tilt

D.3.3.3 x-forces

Figure D.196. F_x - Station 3 - Die 1 x^+ - 0.40° die tiltFigure D.197. F_x - Station 3 - Die 1 x^- - 0.40° die tiltFigure D.198. ΔF_x - Station 3 - Die 1 - 0.40° die tilt

D.3.3.4 z-forces

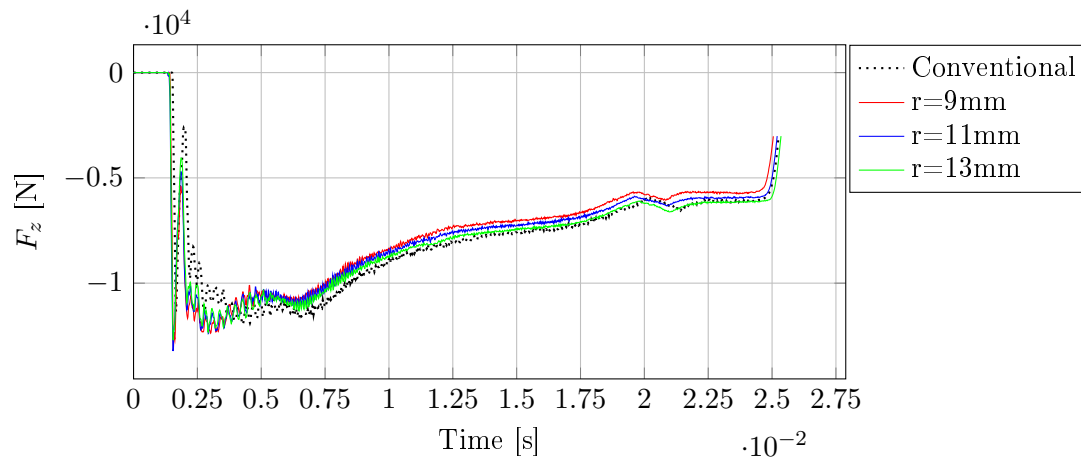


Figure D.199. F_z - Station 3 - Punch - 0.40° die tilt

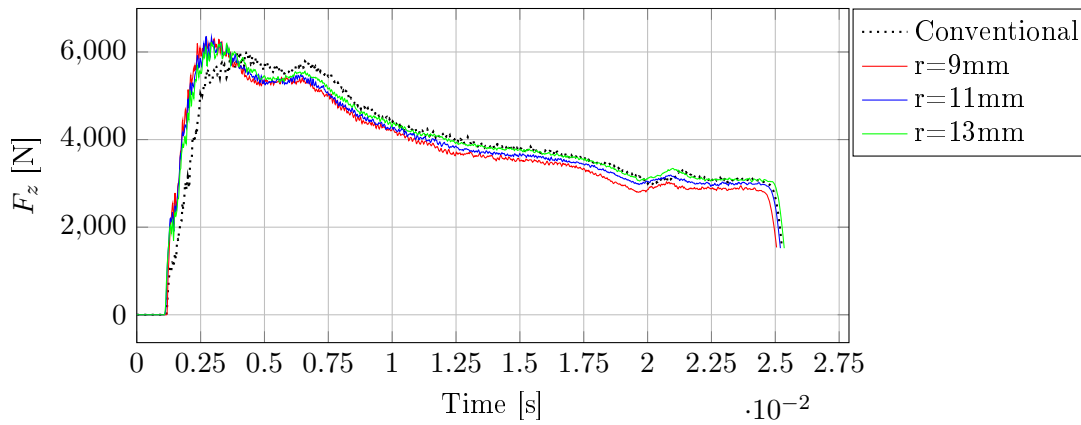


Figure D.200. F_z - Station 3 - Die 1 x^+ - 0.40° die tilt

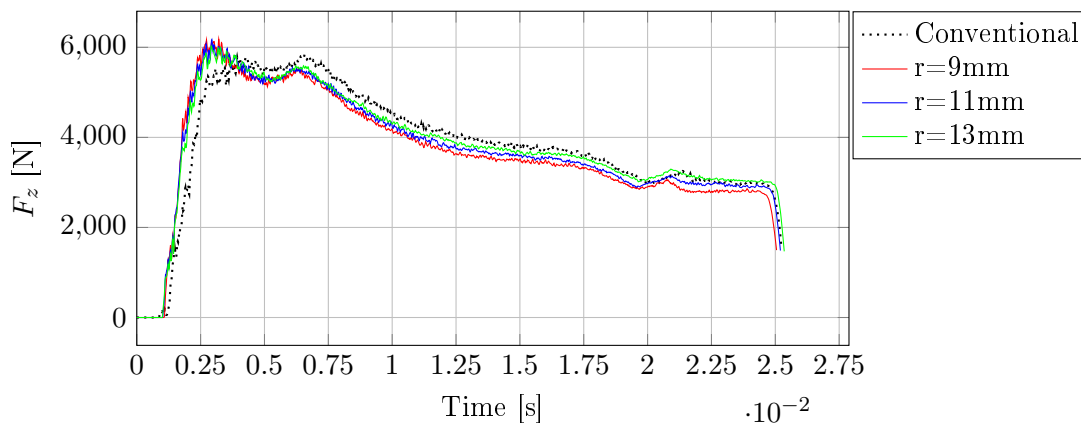


Figure D.201. F_z - Station 3 - Die 1 x^- - 0.40° die tilt

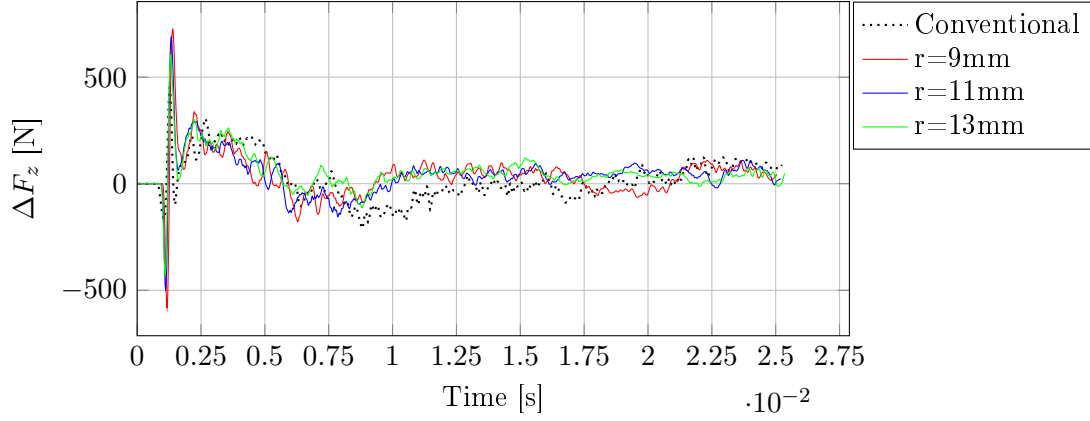


Figure D.202. ΔF_z - Station 3 - Die 1 - 0.40° die tilt

D.3.3.5 Interface pressure

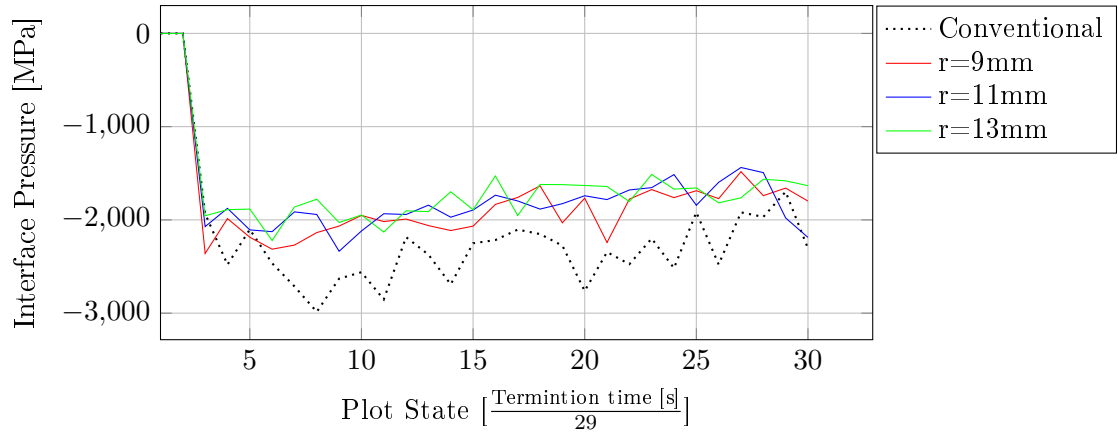


Figure D.203. Maximum interface pressure - Station 3 - Die 1 x^+ - 0.40° die tilt

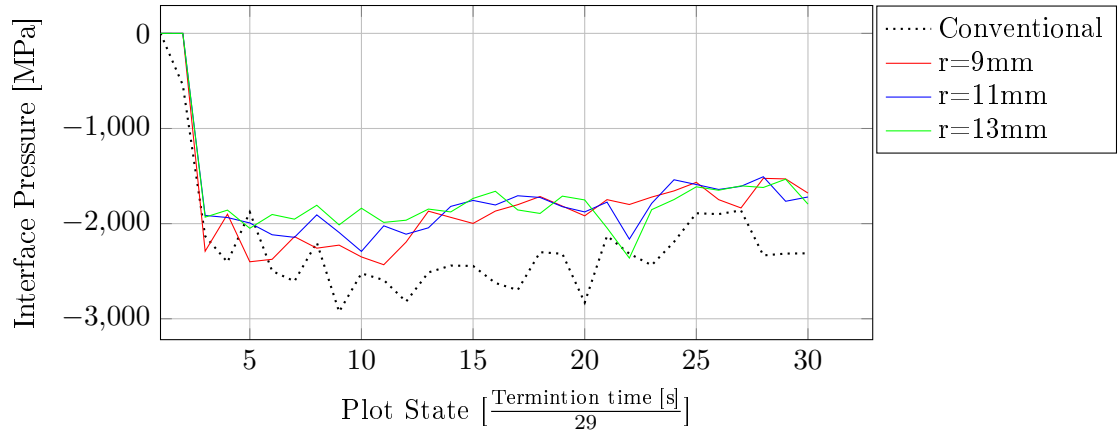


Figure D.204. Maximum interface pressure - Station 3 - Die 1 x^- - 0.40° die tilt

D.4 Geometric evaluation

D.4.1 Station 1

D.4.1.1 Punch displacement

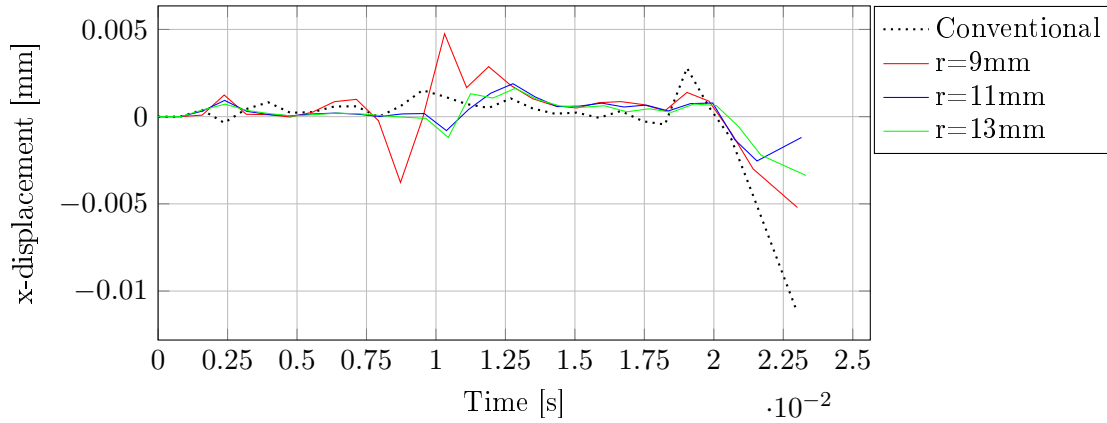


Figure D.205. x-displacement - Station 1 - Punch - 0.00° die tilt

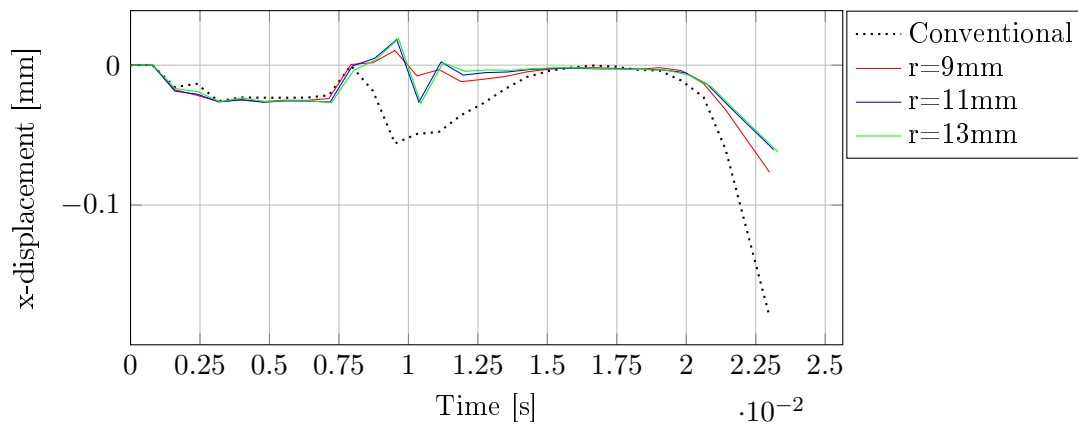


Figure D.206. x-displacement - Station 1 - Punch - 0.20° die tilt

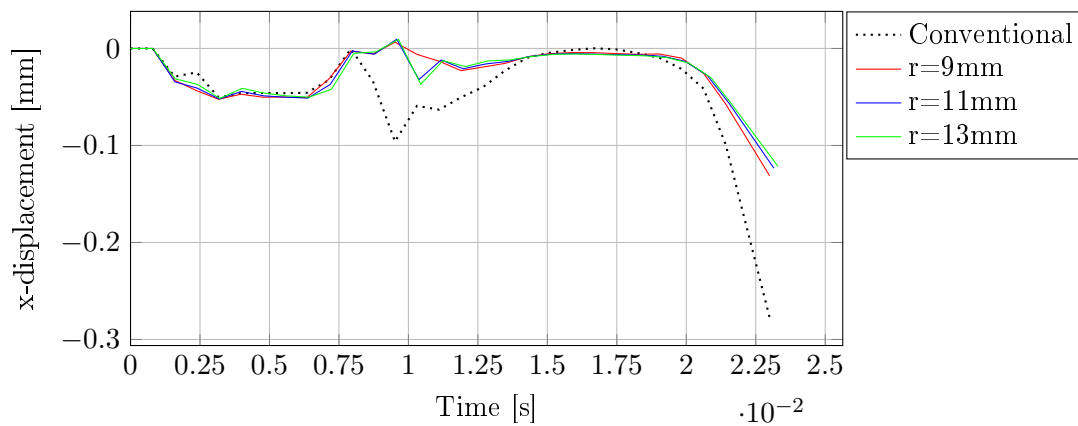


Figure D.207. x-displacement - Station 1 - Punch - 0.40° die tilt

D.4.1.2 Cartridge height

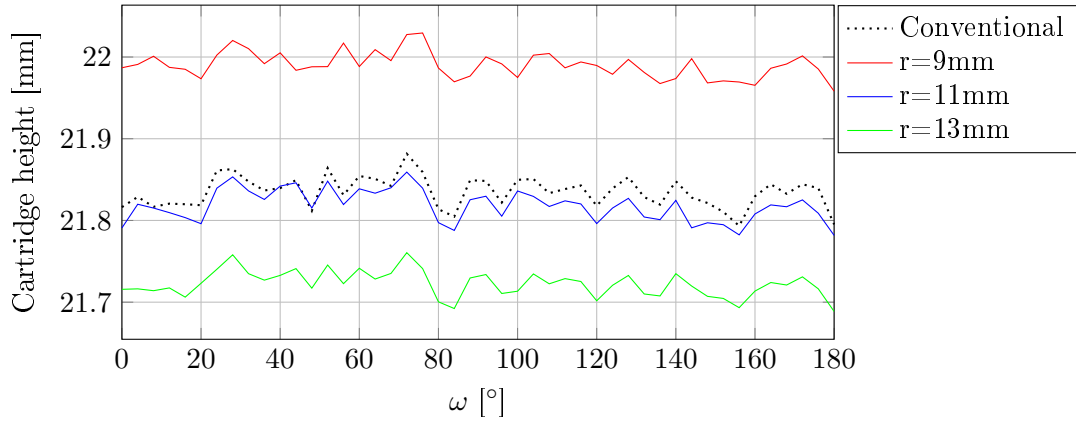


Figure D.208. Cartridge height - Station 1 - 0.00° die tilt

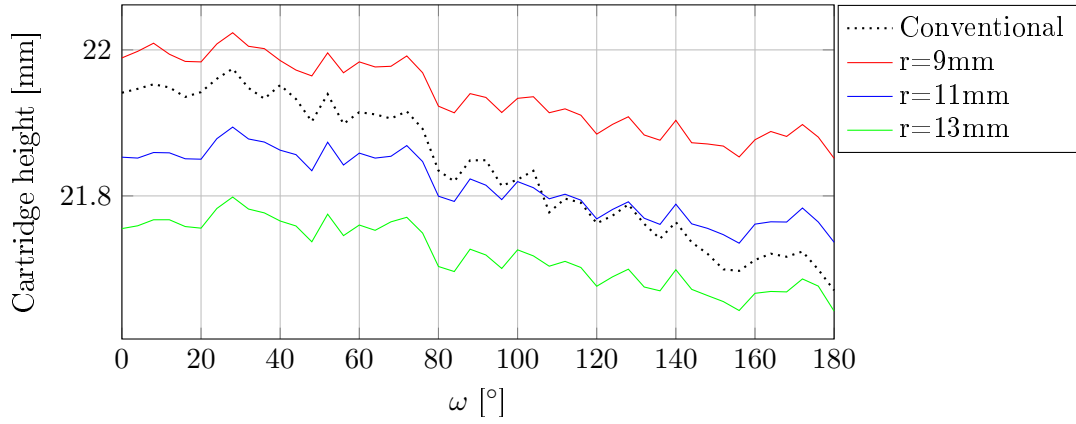


Figure D.209. Cartridge height - Station 1 - 0.20° die tilt

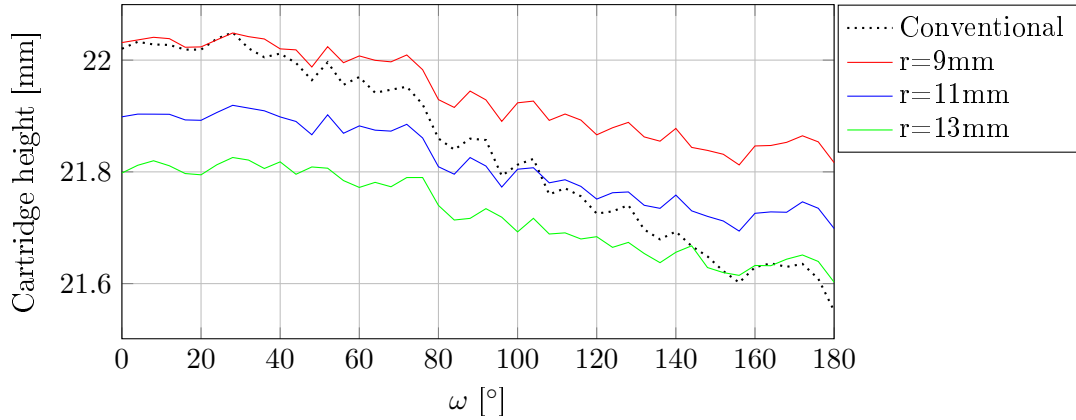


Figure D.210. Cartridge height - Station 1 - 0.40° die tilt

D.4.1.3 Projected cartridge height difference

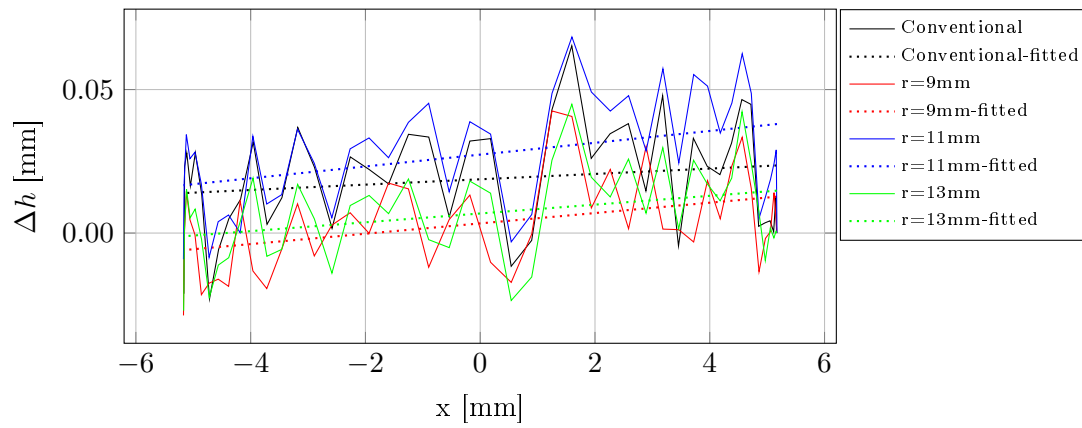


Figure D.211. Projected cartridge height difference - Station 1 - 0.00° die tilt

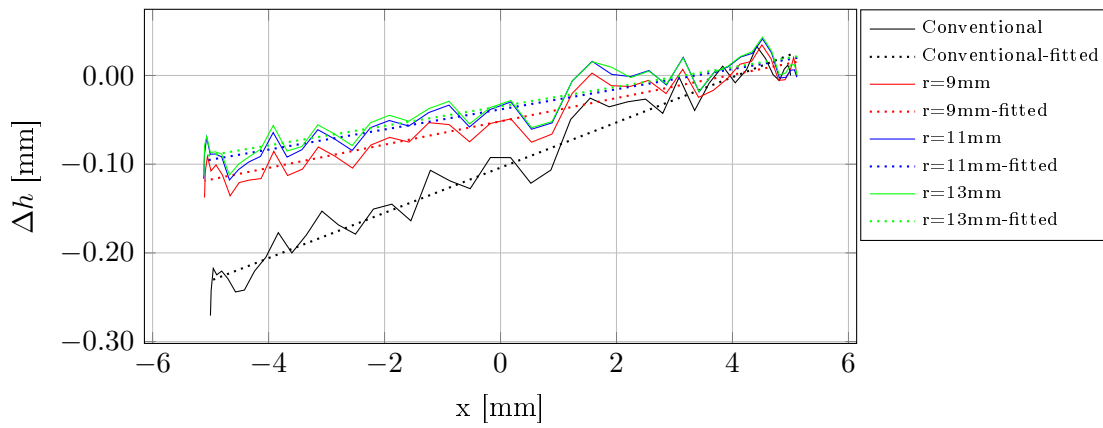


Figure D.212. Projected cartridge height difference - Station 1 - 0.20° die tilt

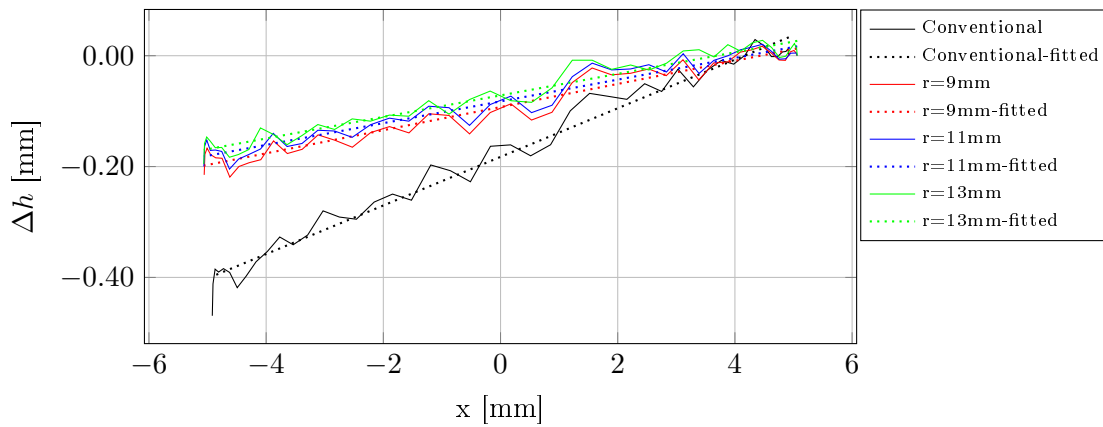


Figure D.213. Projected cartridge height difference - Station 1 - 0.40° die tilt

D.4.1.4 Cartridge bottom profile

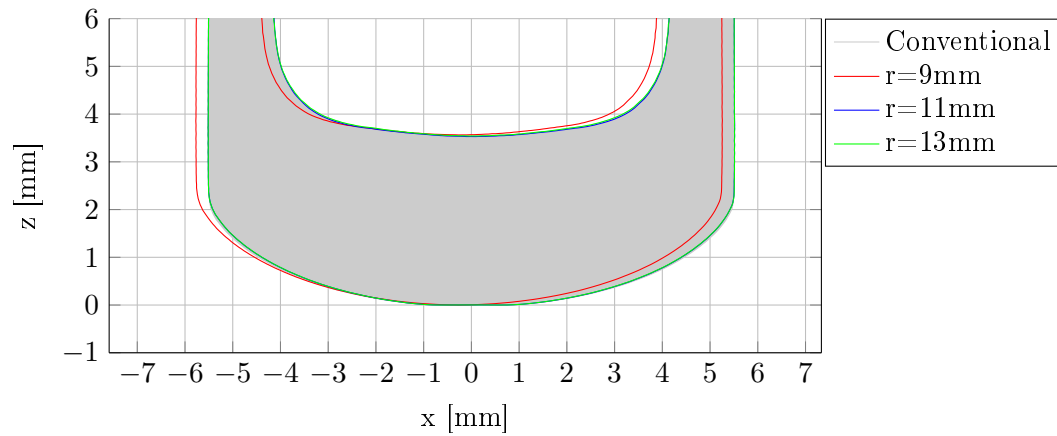


Figure D.214. Cartridge bottom profile - Station 1 - 0.00° die tilt

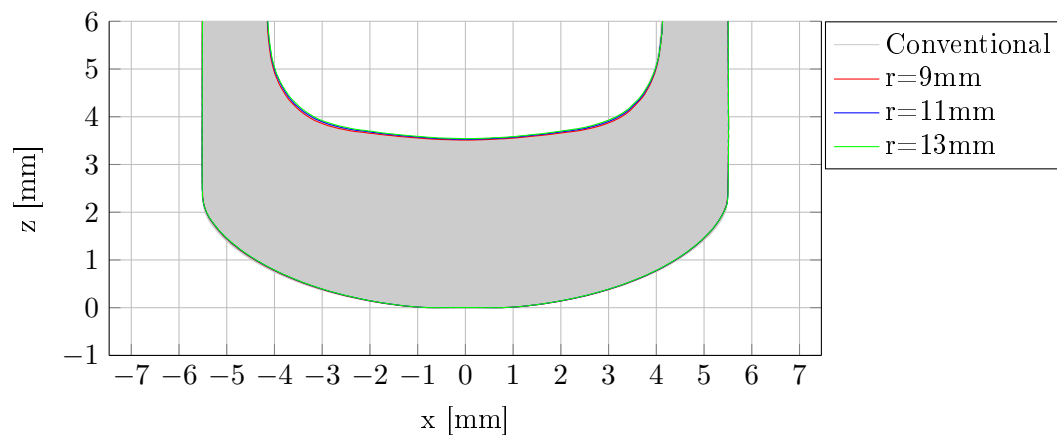


Figure D.215. Cartridge bottom profile - Station 1 - 0.20° die tilt

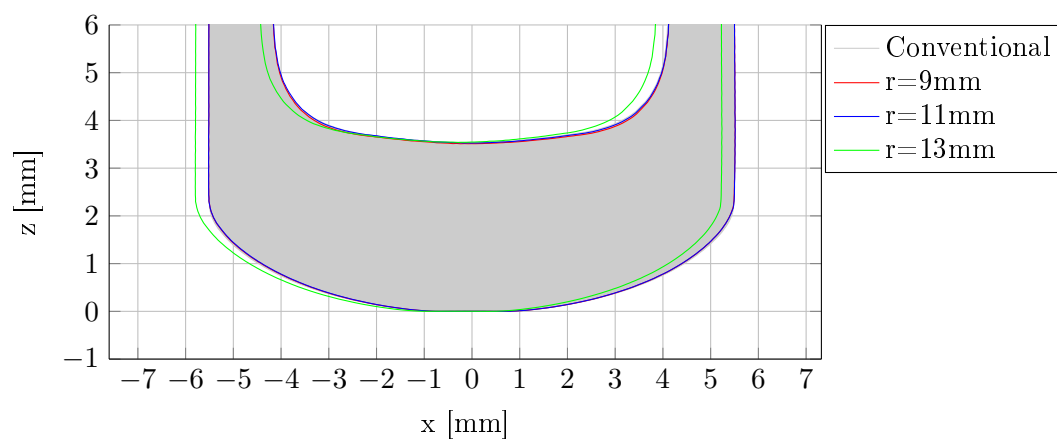


Figure D.216. Cartridge bottom profile - Station 1 - 0.40° die tilt

D.4.2 Station 2

D.4.2.1 Punch displacement

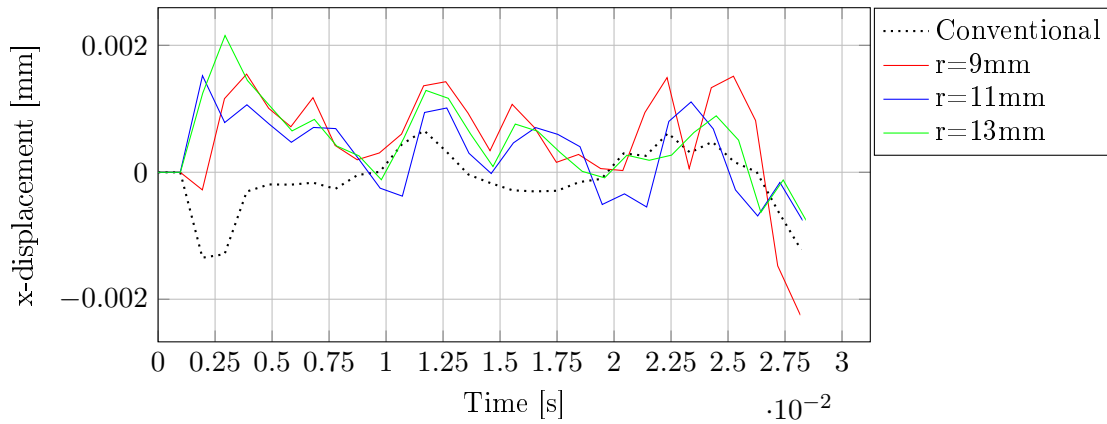


Figure D.217. x-displacement - Station 2 - Punch - 0.00° die tilt

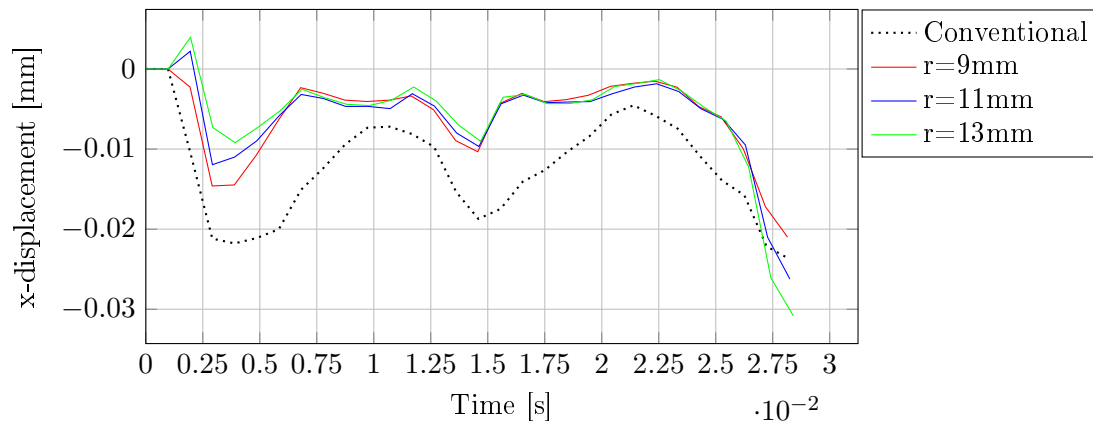


Figure D.218. x-displacement - Station 2 - Punch - 0.20° die tilt

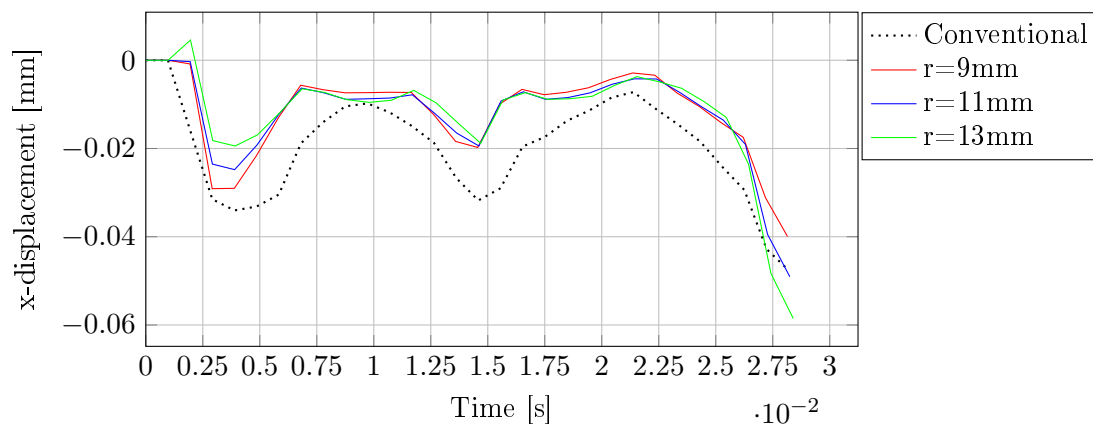


Figure D.219. x-displacement - Station 2 - Punch - 0.40° die tilt

D.4.2.2 Cartridge height

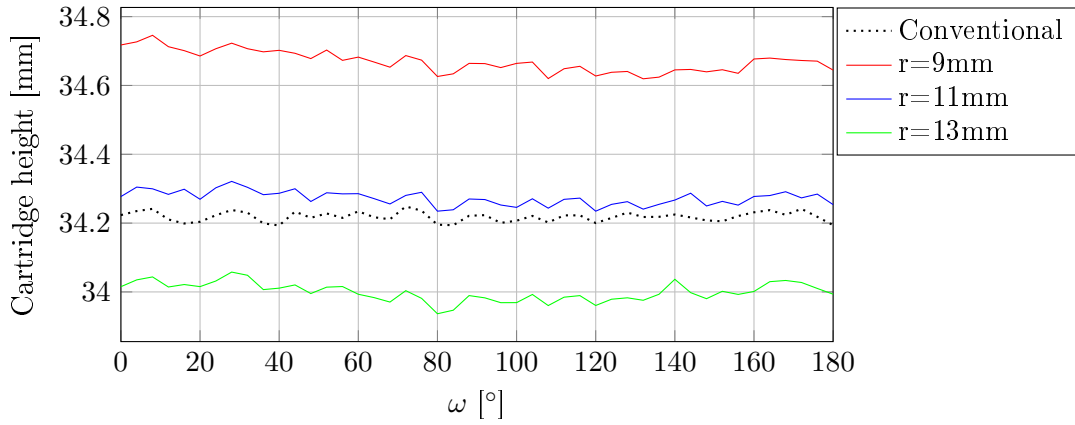


Figure D.220. Cartridge height - Station 2 - 0.00° die tilt

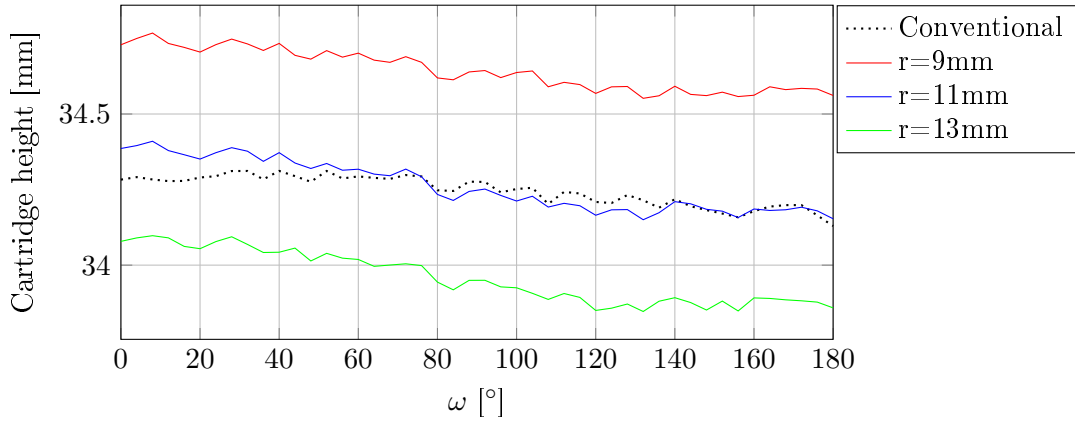


Figure D.221. Cartridge height - Station 2 - 0.20° die tilt

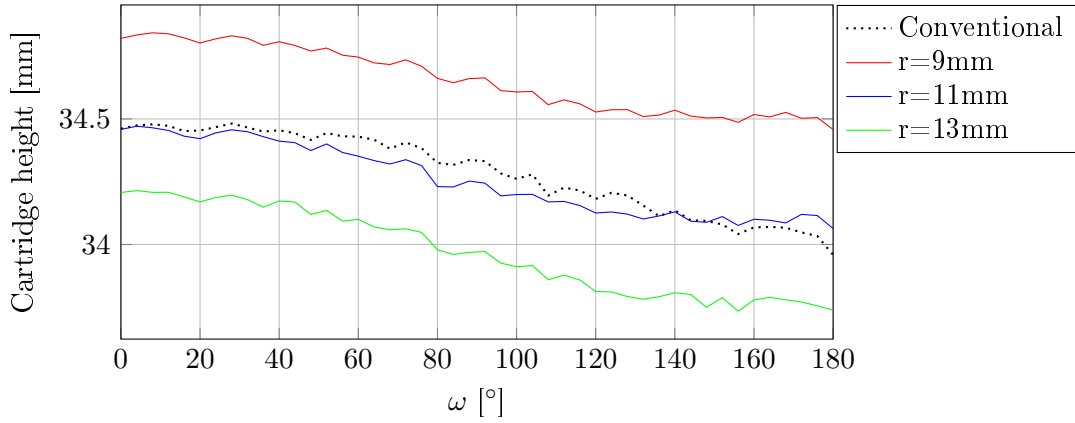


Figure D.222. Cartridge height - Station 2 - 0.40° die tilt

D.4.2.3 Projected cartridge height difference

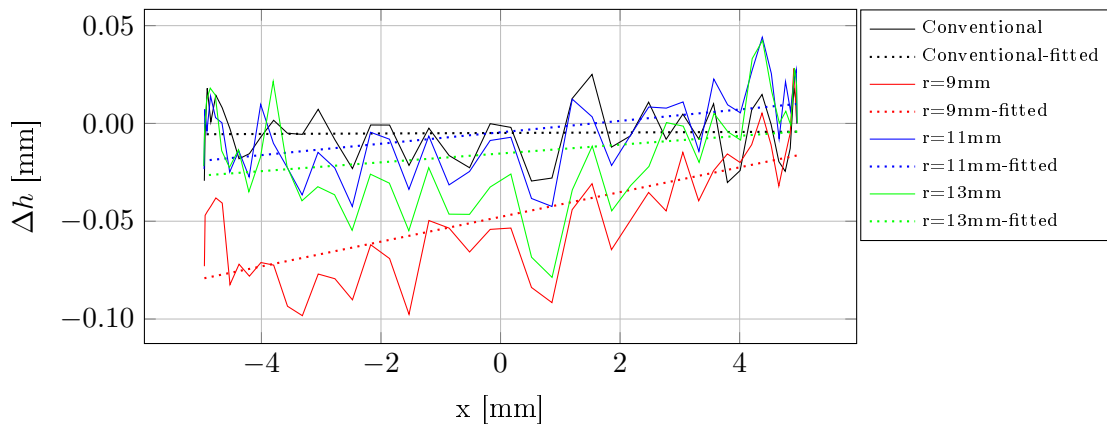


Figure D.223. Projected cartridge height difference - Station 2 - 0.00° die tilt

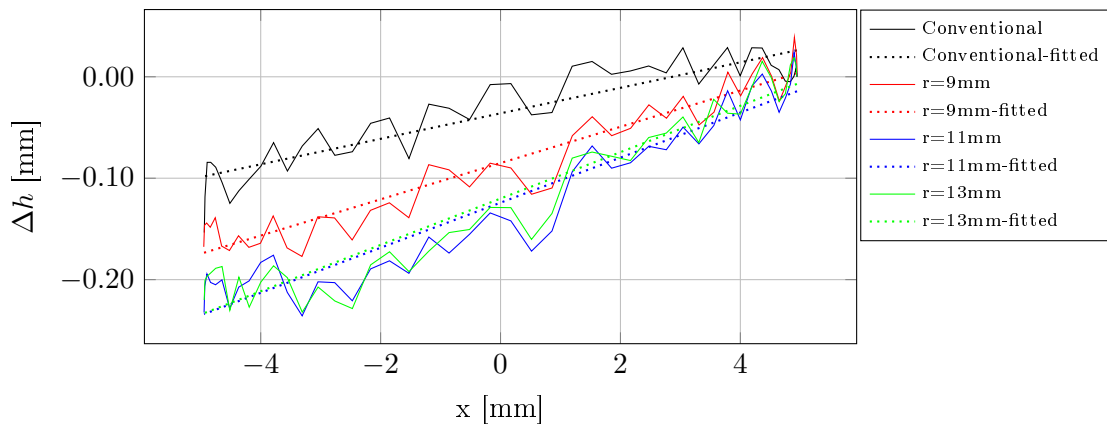


Figure D.224. Projected cartridge height difference - Station 2 - 0.20° die tilt

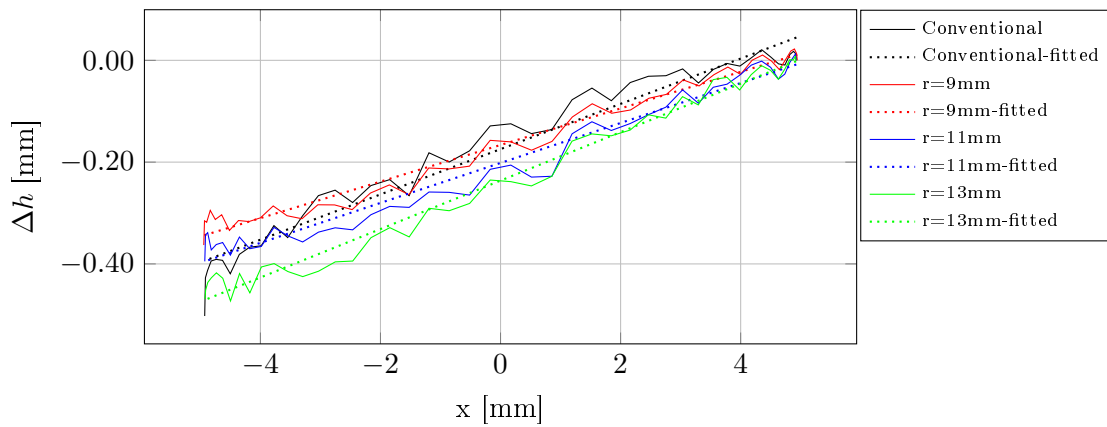


Figure D.225. Projected cartridge height difference - Station 2 - 0.40° die tilt

D.4.2.4 Cartridge bottom profile

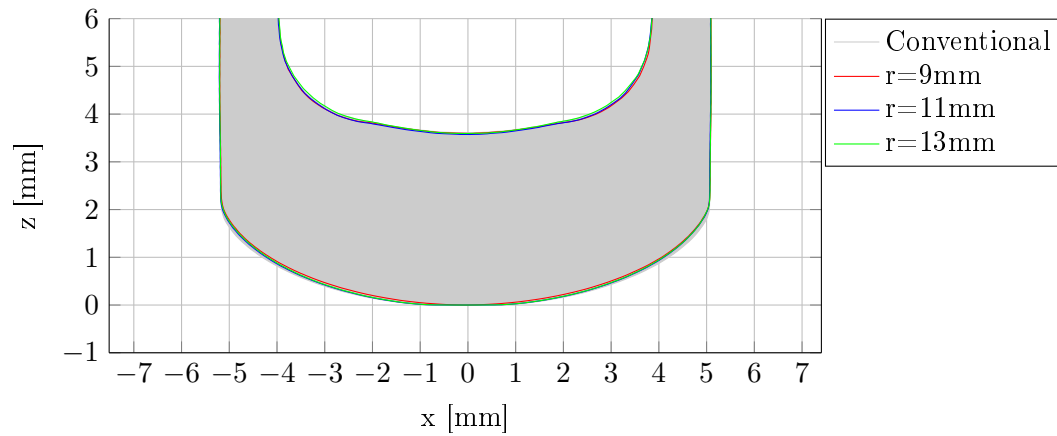


Figure D.226. Cartridge bottom profile - Station 2 - 0.00° die tilt

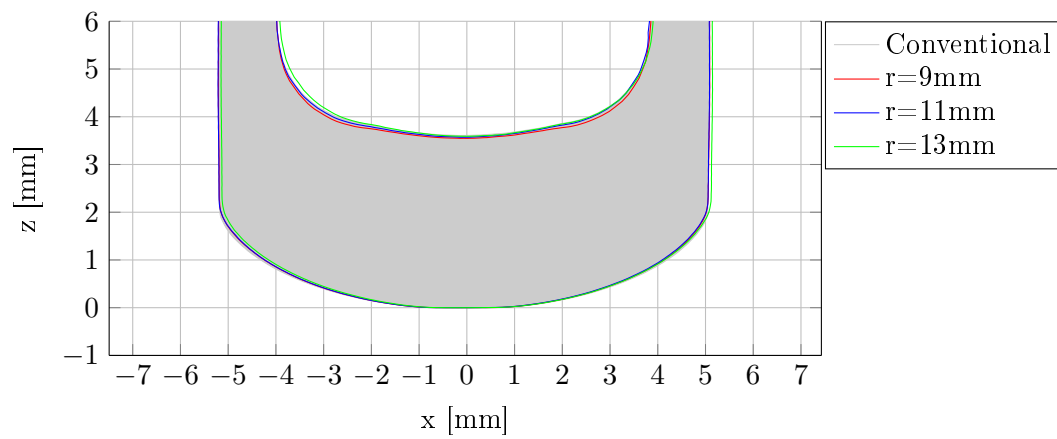


Figure D.227. Cartridge bottom profile - Station 2 - 0.20° die tilt

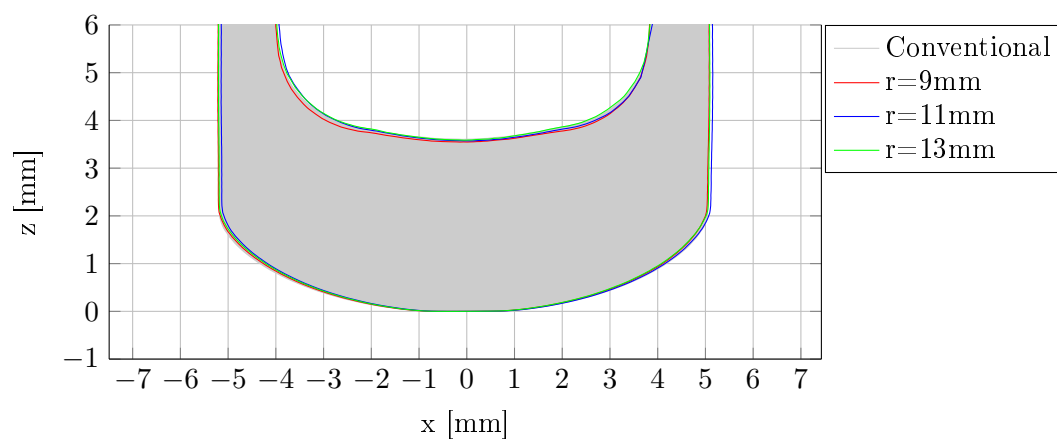


Figure D.228. Cartridge bottom profile - Station 2 - 0.40° die tilt

D.4.3 Station 3

D.4.3.1 Punch displacement

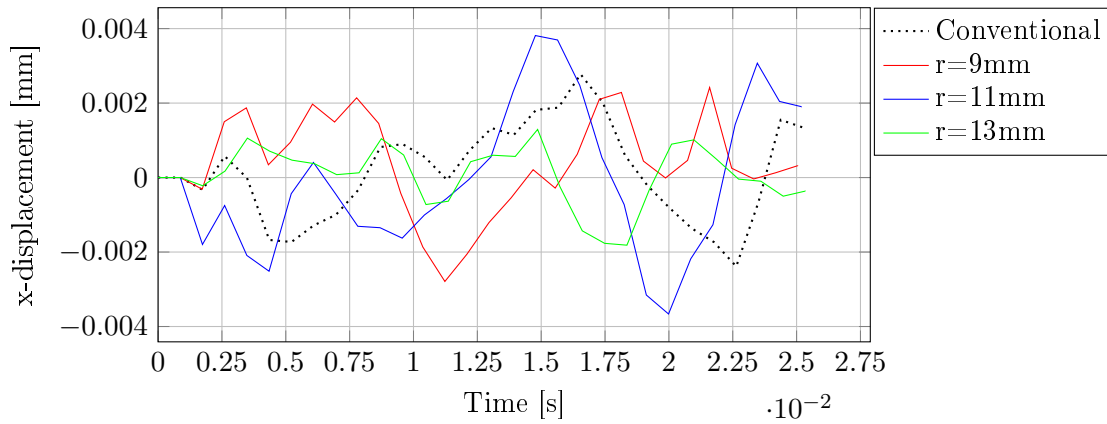


Figure D.229. x-displacement - Station 3 - Punch - 0.00° die tilt

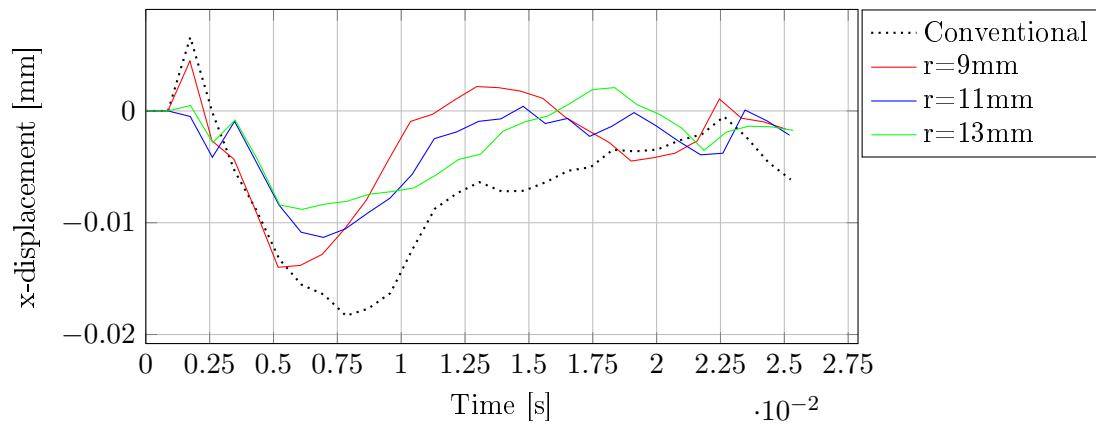


Figure D.230. x-displacement - Station 3 - Punch - 0.20° die tilt

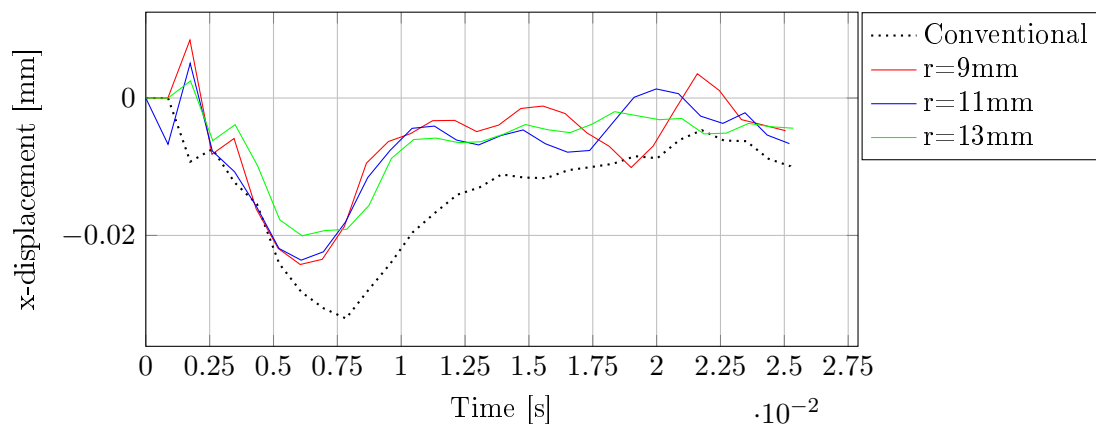


Figure D.231. x-displacement - Station 3 - Punch - 0.40° die tilt

D.4.3.2 Cartridge height

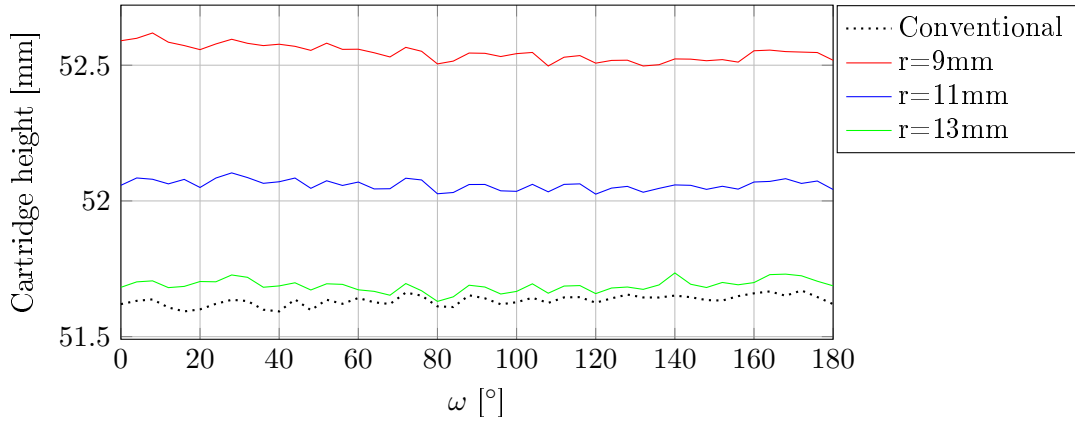


Figure D.232. Cartridge height - Station 3 - 0.00° die tilt

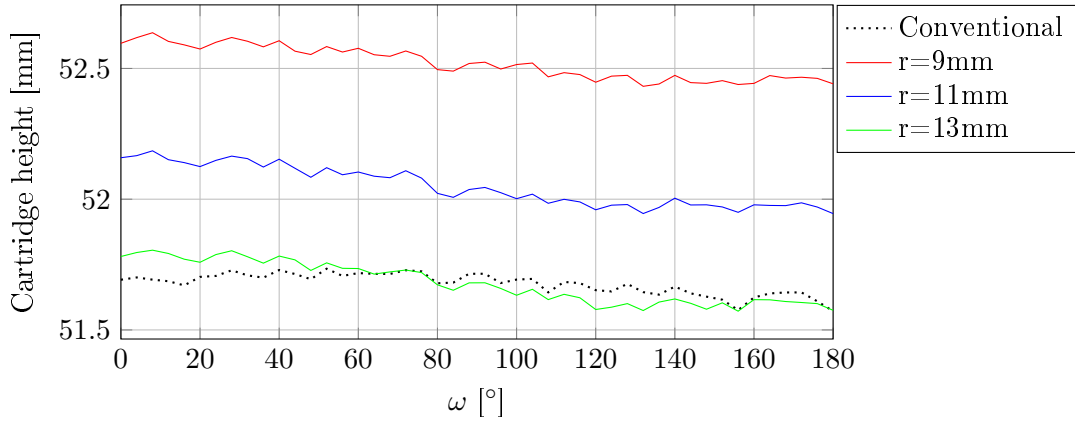


Figure D.233. Cartridge height - Station 3 - 0.20° die tilt

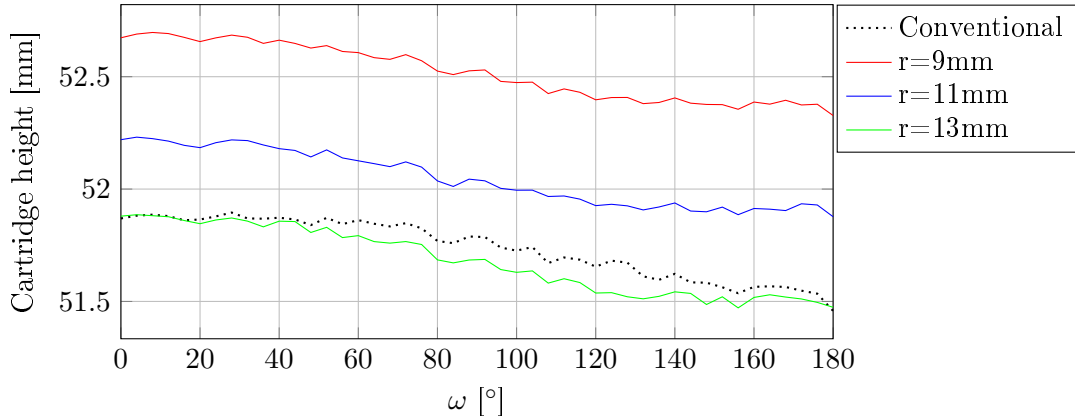


Figure D.234. Cartridge height - Station 3 - 0.40° die tilt

D.4.3.3 Projected cartridge height difference

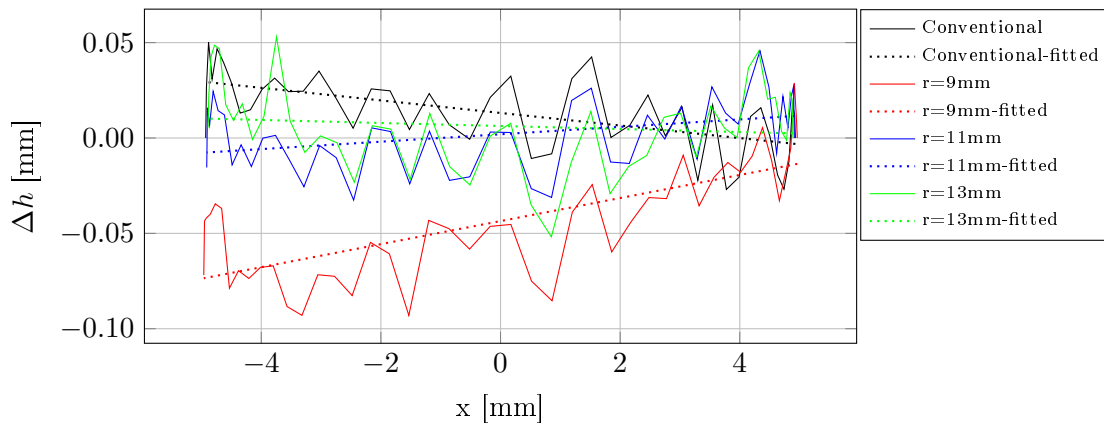


Figure D.235. Projected cartridge height difference - Station 3 - 0.00° die tilt

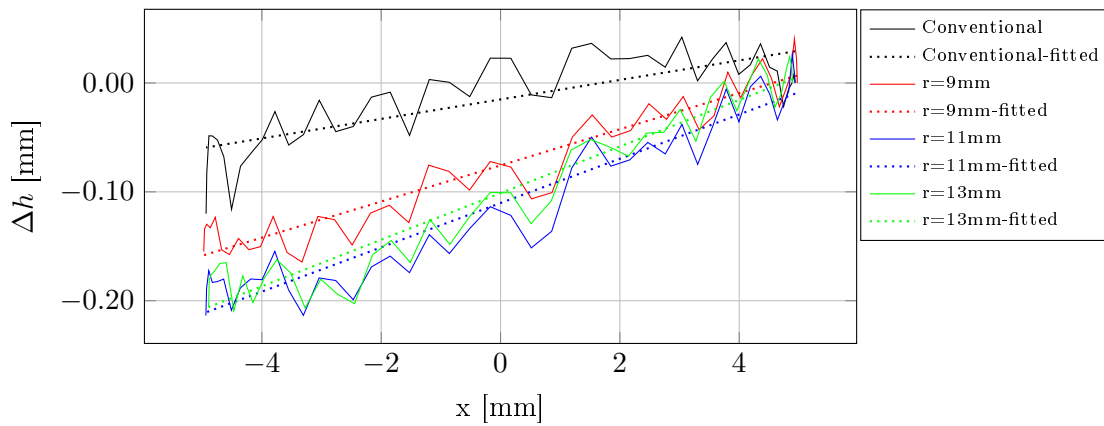


Figure D.236. Projected cartridge height difference - Station 3 - 0.20° die tilt

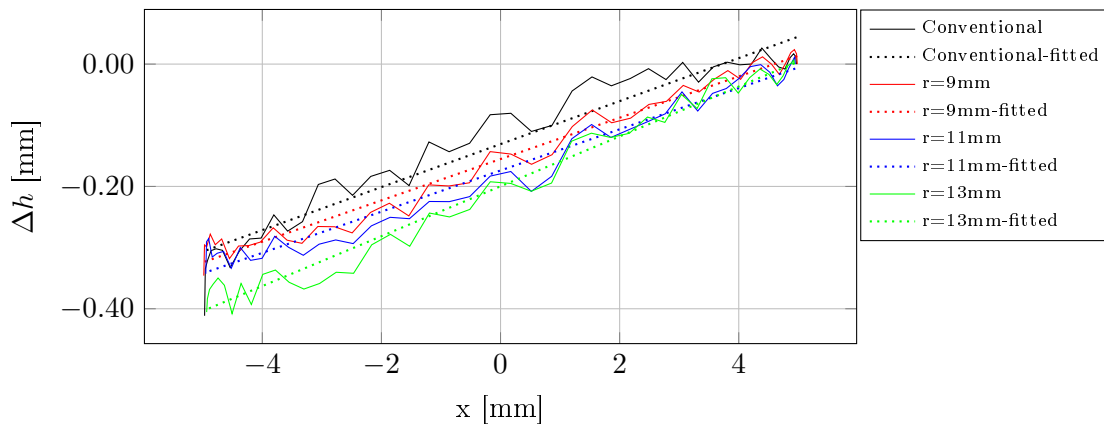


Figure D.237. Projected cartridge height difference - Station 3 - 0.40° die tilt

D.4.3.4 Cartridge bottom profile

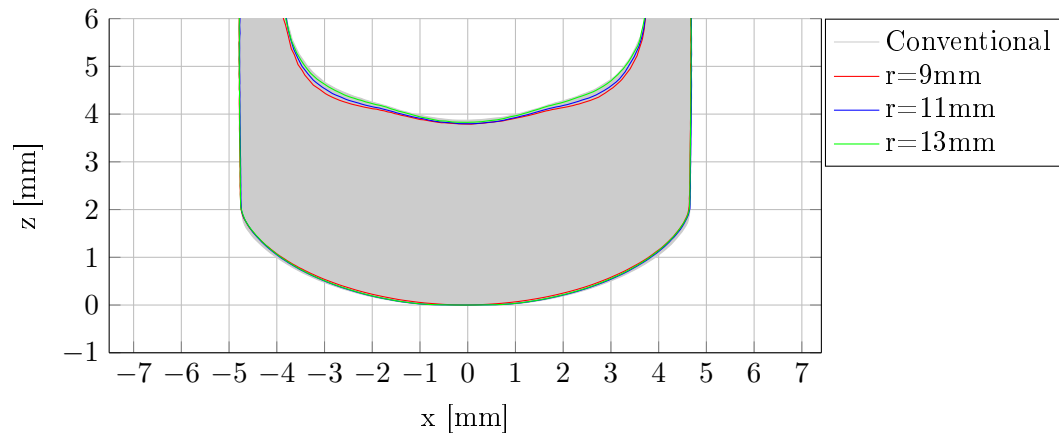


Figure D.238. Cartridge bottom profile - Station 3 - 0.00° die tilt

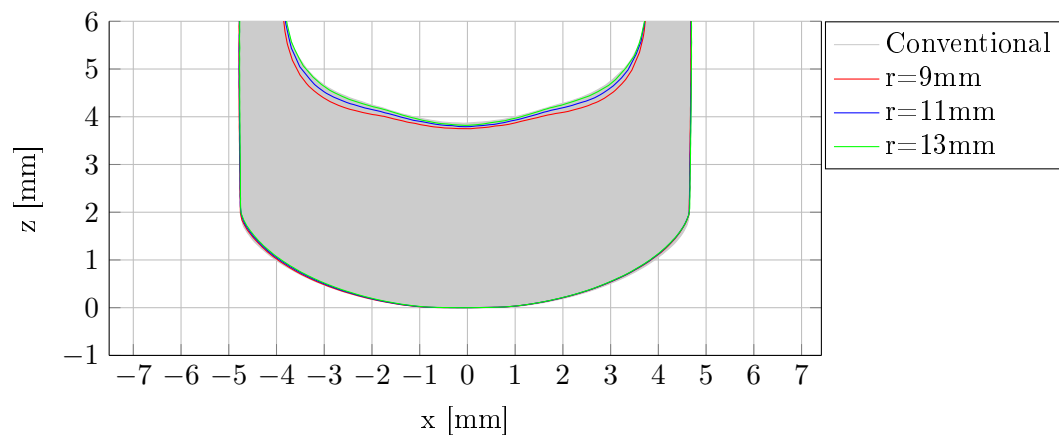


Figure D.239. Cartridge bottom profile - Station 3 - 0.20° die tilt

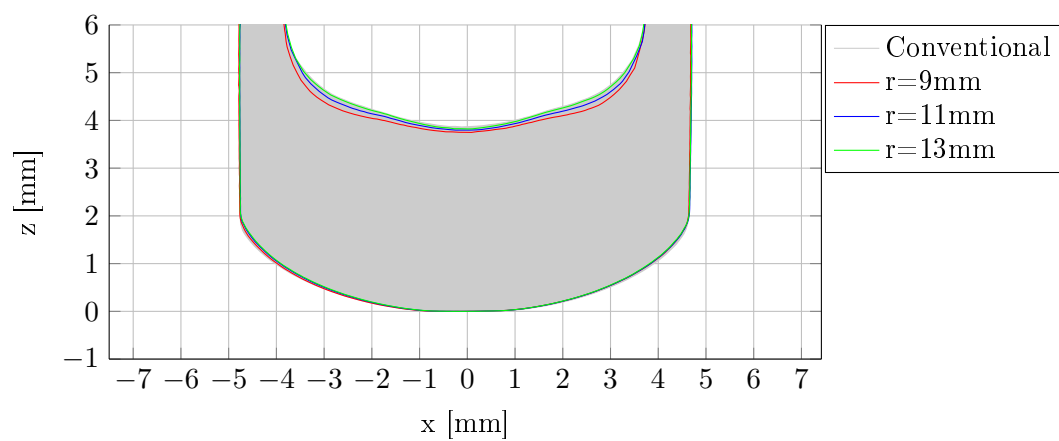


Figure D.240. Cartridge bottom profile - Station 3 - 0.40° die tilt

D.4.4 Height difference

0.00° die tilt

| Die design | Δh [mm] | | |
|--------------|-----------------|-----------|-----------|
| | Station 1 | Station 2 | Station 3 |
| Conventional | 0.0211 | 0.0293 | 0.0000 |
| r=9mm | 0.0287 | 0.0730 | 0.0719 |
| r=11mm | 0.0091 | 0.0234 | 0.0155 |
| r=13mm | 0.0270 | 0.0218 | 0.0055 |

Table D.1. Height difference - 0.00° die tilt

0.20° die tilt

| Die design | Δh [mm] | | |
|--------------|-----------------|-----------|-----------|
| | Station 1 | Station 2 | Station 3 |
| Conventional | 0.2707 | 0.1535 | 0.1200 |
| r=9mm | 0.1376 | 0.1676 | 0.1549 |
| r=11mm | 0.1165 | 0.2325 | 0.2137 |
| r=13mm | 0.1131 | 0.2201 | 0.2058 |

Table D.2. Height difference - 0.20° die tilt

0.40° die tilt

| Die design | Δh [mm] | | |
|--------------|-----------------|-----------|-----------|
| | Station 1 | Station 2 | Station 3 |
| Conventional | 0.4692 | 0.5024 | 0.4115 |
| r=9mm | 0.2149 | 0.3630 | 0.3459 |
| r=11mm | 0.1999 | 0.3950 | 0.3428 |
| r=13mm | 0.1954 | 0.4688 | 0.4054 |

Table D.3. Height difference - 0.40° die tilt

D.4.5 Line fitting parameters

$$h(x) = p_1 \cdot x + p_2$$

| 0.00° die tilt | | | | | | | | | |
|----------------|-----------|---------|--------|-----------|---------|--------|-----------|---------|--------|
| Die design | Station 1 | | | Station 2 | | | Station 3 | | |
| | p_1 | p_2 | r^2 | p_1 | p_2 | r^2 | p_1 | p_2 | r^2 |
| Conventional | 0.0009 | 21.8350 | 0.0339 | 0.0001 | 34.2184 | 0.0010 | -0.0033 | 51.6330 | 0.3650 |
| r=9mm | 0.0018 | 21.9902 | 0.1738 | 0.0063 | 34.6699 | 0.5269 | 0.0060 | 52.5466 | 0.5368 |
| r=11mm | 0.0021 | 21.8182 | 0.1569 | 0.0029 | 34.2726 | 0.2567 | 0.0019 | 52.0595 | 0.1408 |
| r=13mm | 0.0015 | 21.7225 | 0.1305 | 0.0023 | 33.9999 | 0.0912 | -0.0008 | 51.6880 | 0.0157 |

Table D.4. Height fit parameters - 0.00° die tilt

| 0.20° die tilt | | | | | | | | | |
|----------------|-----------|---------|--------|-----------|---------|--------|-----------|---------|--------|
| Die design | Station 1 | | | Station 2 | | | Station 3 | | |
| | p_1 | p_2 | r^2 | p_1 | p_2 | r^2 | p_1 | p_2 | r^2 |
| Conventional | 0.0255 | 21.8375 | 0.9613 | 0.0126 | 34.2469 | 0.8294 | 0.0090 | 51.6769 | 0.6247 |
| r=9mm | 0.0131 | 21.9373 | 0.9109 | 0.0179 | 34.6440 | 0.9212 | 0.0166 | 52.5205 | 0.9107 |
| r=11mm | 0.0113 | 21.8148 | 0.8700 | 0.0222 | 34.2618 | 0.9166 | 0.0203 | 52.0483 | 0.9146 |
| r=13mm | 0.0110 | 21.7205 | 0.8697 | 0.0229 | 33.9586 | 0.9215 | 0.0214 | 51.6797 | 0.9289 |

Table D.5. Height fit parameters - 0.20° die tilt

| 0.40° die tilt | | | | | | | | | |
|----------------|-----------|---------|--------|-----------|---------|--------|-----------|---------|--------|
| Die design | Station 1 | | | Station 2 | | | Station 3 | | |
| | p_1 | p_2 | r^2 | p_1 | p_2 | r^2 | p_1 | p_2 | r^2 |
| Conventional | 0.0438 | 21.8378 | 0.9789 | 0.0445 | 34.2865 | 0.9605 | 0.0351 | 51.7384 | 0.9397 |
| r=9mm | 0.0209 | 21.9388 | 0.9522 | 0.0359 | 34.6545 | 0.9787 | 0.0338 | 52.5179 | 0.9783 |
| r=11mm | 0.0196 | 21.8161 | 0.9490 | 0.0393 | 34.2568 | 0.9716 | 0.0337 | 52.0458 | 0.9671 |
| r=13mm | 0.0194 | 21.7264 | 0.9529 | 0.0476 | 33.9706 | 0.9835 | 0.0408 | 51.6796 | 0.9784 |

Table D.6. Height fit parameters - 0.40° die tilt

LS-Dyna model E

This appendix contains the LS-Dyna code used for the modelling the ironing process of 556mm cartridge cases, though the geometry files will not be presented.

The structure for the code used at the three ironing stations is illustrated at figure E.1.

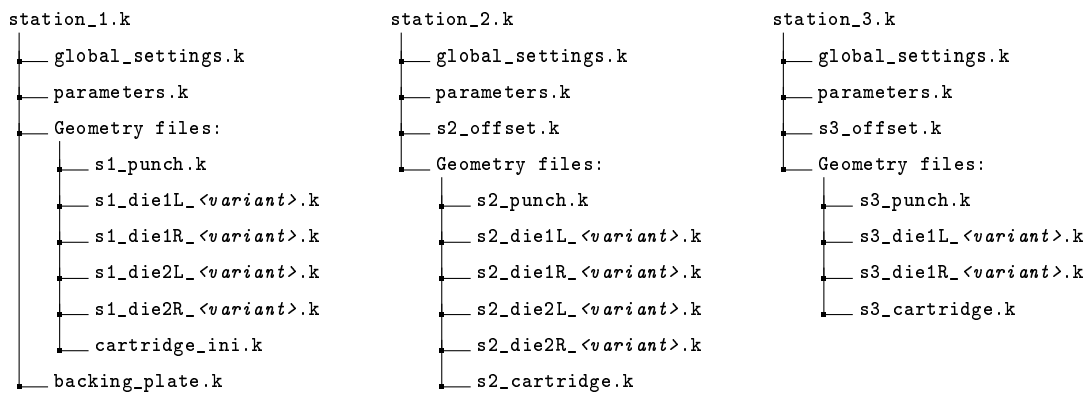


Figure E.1. Code structure for the LS-Dyna models

Note that the *global_settings.k* and *parameters.k* files are the same across all three ironing stations.

E.1 global_settings.k

```
1 #####
2 *KEYWORD
3 $ -----
4 $ Part          | PID | SEC | MAT |
5 $ Punch         | 1   | 10  | 10  |
6 $ Die 1 right   | 2   | 30  | 30  |
7 $ Die 1 left    | 3   | 30  | 30  |
8 $ Die 2 right   | 4   | 30  | 30  |
9 $ Die 2 left    | 5   | 30  | 30  |
10 $ Cartridge     | 6   | 50  | 50  |
11 $ Baking plate  | 9   | 90  | 90  |
12 $-----
13 $ Units:
14 $- Length: [mm]
15 $- Mass: [kg/mm^3]
16 $- Time: [s]
17 $- Weight: [kg]
18 $- pressure: [MPa]
```

```

19 $=====
20 $----- Controls -----
21 $=====
22 *CONTROL_BULK_VISCOSITY
23 $#      q1      q2      type      btype
24      0.0      0.0      1      0
25 $-----
26 *CONTROL_CONTACT
27 $#  slsfac  rwpnal  islchk  shlthk  penopt  thkchg  orien  enmass
28      0.0      0.0      2      0      0      0      2      0
29 $#  usrstr  usrfric  nsbcs  interm  xpene  ssthk  ecdt  tiedprj
30      0      0      0      0      0.0      0      0      0
31 $#  sfriac  dfriac  edc  vfc  th  th_sf  pen_sf
32      0.0      0.0      0.0      0.0      0.0      0.0      0.0
33 $#  ignore  frceng  skiprwg  outseg  spotstp  spotdel  spothin
34      0      0      0      0      0      0      0.0
35 $#  isym  nserod  rwgaps  rwgdt  rwsf  icov  swradf  ithoff
36      0      0      1      0.0      1.0      0      0.0      0
37 $#  shldg  pstiff  ithcnt  tdcnof  ftall  unused  shltrw
38      0      0      0      0      0      0.0
39 $-----
40 *CONTROL_OUTPUT
41 $#  npopt  neecho  nrefup  iaccop  opifs  ipnint  ikedit  iflush
42      0      0      0      0      0.0      0      0      5000
43 $#  iprtf  ierode  tet10s8  msgmax  ipcurv  gmdt  ip1dbl  eocs
44      0      0      2      50      0      0.0      0      0
45 $#  tolev  newleg  frfreq  minfo  solsig  msgflg  cdetol
46      2      0      1      0      0      0      10.0
47 $-----
48 *CONTROL_SHELL
49 $#  wrpang  esort  irnxx  istupd  theory  bwc  miter  proj
50      0.0      0      0      0      2      2      1      0
51 $#  rotasc  intgrd  lamsht  cstyp6  tshell
52      1.0      0      0      1      0
53 $#  psstup  sidt4tu  cntco  itsflg  irquad
54      0      0      0      0      2
55 $#  nfail1  nfail4  psnfail  keepcs  delfr  drcpsid  drcprm
56      0      0      0      0      0      0      1.0
57 $-----
58 *CONTROL_TERMINATION
59 $#  endtim  endcyc  dtmin  endeng  endmas
60      &term      0      0.0      0.0      1.0
61 $-----
62 *CONTROL_TIMESTEP
63 $#  dtinit  tssfacc  isdo  tslimt  dt2ms  lctm  erode  ms1st
64      0.0      0.0      0      0.0  &dt2ms      0      0      0
65 $#  dt2msf  dt2mslc  imsc1  unused  unused  rmscl
66      0.0      0      0      0.0
67 $=====
68 $----- Database Outputs -----
69 $=====
70 *CONTROL_DEBUG
71 *DATABASE_BINARY_D3PLOT
72 $#  dt  lcdt  beam  npltc  psetid
73      &d3dump      0      0      0      0
74 $#  ioopt
75      0

```



```

76 *DATABASE_BINARY_INTFOR
77 $#      dt      lcdt      beam      npltc      psetid
78      &d3dump      0      0      0      0
79 $#      ioopt
80      0
81 $-----
82 *DATABASE_EXTENT_BINARY
83 $#      neiph      neips      maxint      strflg      sigflg      epsflg      rltflg      engflg
84      0      0      7      1      1      1      1      1
85 $#      cmpflg      ieverp      beamip      dcomp      shge      stssz      n3thdt      ialemat
86      0      0      0      1      1      3      2      1
87 $#      nintsls      pkp_sen      sclp      hydro      msscl      therm      intout      nodout
88      0      0      1.0      0      0      0
89 $#      dtdt      resplt      neipb
90      0      0      0
91 $-----
92 *DATABASE_GLSTAT
93 $#      dt      binary      lcur      ioopt
94      1.50000E-5      0      0      1
95 $-----
96 *DATABASE_MATSUM
97 $#      dt      binary      lcur      ioopt
98      3.00000E-5      0      0      1
99 $-----
100 *DATABASE_NODOUT
101 $#      dt      binary      lcur      ioopt      option1      option2
102      2.00000E-5      0      0      1      0.0      0
103 $-----
104 *DATABASE_RBDOUT
105 $#      dt      binary      lcur      ioopt
106      3.00000E-5      0      0      1
107 $-----
108 *DATABASE_RCFORC
109 $#      dt      binary      lcur      ioopt
110      1.50000E-5      0      0      1
111 $=====
112 $----- Contacts -----
113 $=====
114 *CONTACT_CONSTRAINT_SURFACE_TO_SURFACE_ID
115 $#      cid      title
116      1Die 1 Right
117 $#      ssid      msid      sstyp      mstyp      sboxid      mboxid      spr      mpr
118      6      2      3      3      0      0      1      1
119 $#      fs      fd      dc      vc      vdc      penchk      bt      dt
120      &mys      &myd      0.0      &vc      &vcd      0      0.01.00000E20
121 $#      sfs      sfm      sst      mst      sfst      sfmt      fsf      vsf
122      0.0      1.0      0.0      0.0      1.0      1.0      1.0      1.0
123 $#      KPF
124      0.0
125 $-----
126 *CONTACT_CONSTRAINT_SURFACE_TO_SURFACE_ID
127 $#      cid      title
128      2Die 1 Left
129 $#      ssid      msid      sstyp      mstyp      sboxid      mboxid      spr      mpr
130      6      3      3      3      0      0      1      1
131 $#      fs      fd      dc      vc      vdc      penchk      bt      dt
132      &mys      &myd      0.0      &vc      &vcd      0      0.01.00000E20

```

```

133 $#      sfs      sfm      sst      mst      sfst      sfmt      fsf      vsf
134      0.0      1.0      0.0      0.0      1.0      1.0      1.0      1.0
135 $#      KPF
136      0.0
137 $-----
138 *CONTACT_CONSTRAINT_SURFACE_TO_SURFACE_ID
139 $#      cid                                     title
140      3Die 2 Right
141 $#      ssid      msid      sstyp      mstyp      sboxid      mboxid      spr      mpr
142      6          4          3          3          0          0          1          1
143 $#      fs      fd      dc      vc      vdc      penchk      bt      dt
144      &mys      &myd      0.0      &vc      &vcd      0          0.01.00000E20
145 $#      sfs      sfm      sst      mst      sfst      sfmt      fsf      vsf
146      0.0      1.0      0.0      0.0      1.0      1.0      1.0      1.0
147 $#      KPF
148      0.0
149 $-----
150 *CONTACT_CONSTRAINT_SURFACE_TO_SURFACE_ID
151 $#      cid                                     title
152      4Die 2 Left
153 $#      ssid      msid      sstyp      mstyp      sboxid      mboxid      spr      mpr
154      6          5          3          3          0          0          1          1
155 $#      fs      fd      dc      vc      vdc      penchk      bt      dt
156      &mys      &myd      0.0      &vc      &vcd      0          0.01.00000E20
157 $#      sfs      sfm      sst      mst      sfst      sfmt      fsf      vsf
158      0.0      1.0      0.0      0.0      1.0      1.0      1.0      1.0
159 $#      KPF
160      0.0
161 $-----
162 *CONTACT_SURFACE_TO_SURFACE_ID
163 $#      cid                                     title
164      5Punch
165 $#      ssid      msid      sstyp      mstyp      sboxid      mboxid      spr      mpr
166      6          1          3          3          0          0          1          1
167 $#      fs      fd      dc      vc      vdc      penchk      bt      dt
168      &mys      &myd      0.0      &vc      &vcd      0          0.01.00000E20
169 $#      sfs      sfm      sst      mst      sfst      sfmt      fsf      vsf
170      0.0      1.0      0.0      0.0      1.0      1.0      1.0      1.0
171 $#      soft      sofsc1      lcidab      maxpar      sbopt      depth      bsort      frcfrq
172      1          0.1          0          1.025      2.0          2          0          1
173 $=====
174 $----- Hourglass Control -----
175 $=====
176 *CONTROL_ENERGY
177 $#      hgen      rwen      slnten      rylen
178      2          1          2          2
179 $-----
180 *CONTROL_HOURLASS
181 $#      ihq      qh
182      0          0.0
183 $-----
184 *HOURLASS
185 $#      hgid      ihq      qm      ibq      q1      q2      qb/vdc      qw
186 $      1          5          0.1          1          1.5      0.06      0.1          0.1
187      1          4          0.1          0          1.5      0.06      0.1          0.1
188 $=====
189 $----- Parts -----

```

```

190 $=====
191 *PART
192 Punch - Shell
193 $#      pid      secid      mid      eosid      hgid      grav      adpopt      tmid
194         1         10         10         0         1         0         0         0
195 $-----
196 *PART
197 Die 1 Right
198 $#      pid      secid      mid      eosid      hgid      grav      adpopt      tmid
199         2         20         30         0         1         0         0         0
200 $-----
201 *PART
202 Die 1 Left
203 $#      pid      secid      mid      eosid      hgid      grav      adpopt      tmid
204         3         20         30         0         1         0         0         0
205 $-----
206 *PART
207 Die 2 Right
208 $#      pid      secid      mid      eosid      hgid      grav      adpopt      tmid
209         4         20         30         0         1         0         0         0
210 $-----
211 *PART
212 Die 2 Left
213 $#      pid      secid      mid      eosid      hgid      grav      adpopt      tmid
214         5         20         30         0         1         0         0         0
215 $-----
216 *PART
217 Cartridge case
218 $#      pid      secid      mid      eosid      hgid      grav      adpopt      tmid
219         6         50         50         0         1         0         2         0
220 $=====
221 $----- Sections -----
222 $=====
223 *SECTION_SHELL_TITLE
224 Rigid shell - Punch
225 $#      secid      elform      shrf      nip      propt      qr/irid      icomp      setyp
226         10         2         1.0         2         1.0         0         0         1
227 $#      t1         t2         t3         t4         nloc      marea      idof      edgset
228         1.0         1.0         1.0         1.0         0.0         0.0         0.0         0
229 $-----
230 *SECTION_SHELL_TITLE
231 Rigid shell - Dies
232 $#      secid      elform      shrf      nip      propt      qr/irid      icomp      setyp
233         20         2         1.0         2         1.0         0         0         1
234 $#      t1         t2         t3         t4         nloc      marea      idof      edgset
235         1.0         1.0         1.0         1.0         0.0         0.0         0.0         0
236 $-----
237 *SECTION_SOLID_TITLE
238 Solid tetrahegon - Cartridge case
239 $#      secid      elform      aet
240         50         13         0
241 $=====
242 $----- Material -----
243 $=====
244 *MAT_RIGID_TITLE
245 Punch
246 $ Rigid material, constrained y-z translation and x-y-z rotation

```

```

247 $#      mid      ro      e      pr      n      couple      m      alias
248      10      &pden      &pyoung &ppoisson      0.0      0.0      0.0
249 $#      cmo      con1      con2
250      1.0      5      7
251 $#lco or a1      a2      a3      v1      v2      v3
252      0.0      0.0      0.0      0.0      0.0      0.0
253 $-----
254 *MAT_RIGID_TITLE
255 Dies
256 $ Rigid materiall, constrained x-y translation and x-y-z rotation
257 $#      mid      ro      e      pr      n      couple      m      alias
258      30      &tdden      &tyoung &tpoisson      0.0      0.0      0.0
259 $#      cmo      con1      con2
260      1.0      4      7
261 $#lco or a1      a2      a3      v1      v2      v3
262      0.0      0.0      0.0      0.0      0.0      0.0
263 $-----
264 *MAT_POWER_LAW_PLASTICITY_TITLE
265 Cartridge Case
266 $#      mid      ro      e      pr      k      n      src      srp
267      50      &cdden      &cyoung &cpoisson      &ck      &cn      0.0      0.0
268 $#      sigy      vp      epsf
269      0.0      0.0      0.0
270 $=====
271 $----- Control Remeshing -----
272 $=====
273 *CONTROL_ADAPTIVE
274 $# adpfreq      adptol      adpopt      maxlvl      tbirth      tdeath      lcadp      ioflag
275      &mfreq 1.000E20      7      3      0.01.00000E20      0      0
276 $# adpsize      adpass      ireflg      adpene      adpth      memory      orient      maxel
277      0.0      0      0      0.0      0.0      0      0      0
278 $-----
279 *CONTROL_REMESHING
280 $#      rmin      rmax      vf_loss      mfrac      dt_min      icurv      iadp10      sefang
281      &rmin      &rmax      1.0      0.0      0.0      4      0      0.0
282 $-----
283 *CONTROL_SOLID
284 $#      esort      fmatrix      niptets      swlocl      psfail      t10jtol      icohed      tet13k
285      1      0      4      2      0      0.0      0      0
286 $#      pm1      pm2      pm3      pm4      pm5      pm6      pm7      pm8      pm9      pm10
287      0      0      0      0      0      0      0      0      0      0
288 $=====
289 $----- Movements and forces -----
290 $=====
291 *BOUNDARY_PRESCRIBED_MOTION_RIGID_ID
292 $#      id                                     heading
293      1 Die 1 Right
294 $#      pid      dof      vad      lcld      sf      vid      death      birth
295      2      3      0      20      1      01.00000E28      0.0
296 $-----
297 *BOUNDARY_PRESCRIBED_MOTION_RIGID_ID
298 $#      id                                     heading
299      2 Die 1 Left
300 $#      pid      dof      vad      lcld      sf      vid      death      birth
301      3      3      0      20      1      01.00000E28      0.0
302 $-----
303 *BOUNDARY_PRESCRIBED_MOTION_RIGID_ID

```

```

304  $#      id                                     heading
305      3 Die 2 Right
306  $#      pid      dof      vad      lcid      sf      vid      death      birth
307      4          3          0          20          1          01.00000E28          0.0
308  $-----
309  *BOUNDARY_PRESCRIBED_MOTION_RIGID_ID
310  $#      id                                     heading
311      4 Die 2 Left
312  $#      pid      dof      vad      lcid      sf      vid      death      birth
313      5          3          0          20          1          01.00000E28          0.0
314  $-----
315  *DEFINE_CURVE
316  $#      lcid      sidr      sfa      sfo      offa      offo      dattyp      lcint
317      20          0          1.0          1.0          0.0          0.0          0          0
318  $#              a1              o1
319              0.0              0.0
320              0.002              2000.0
321              &tfall              2000.0
322              &term              0.0
323  $=====
324  $----- Constraints -----
325  $=====
326  *CONSTRAINED_GLOBAL
327  $#      tc      rc      dir      x      y      z
328  $      1          5          1          0.0          0.0          0.0
329      2          6          2          0.0          0.0          0.0
330  *end
331  #####

```

E.2 parameters.k

```

1  #####
2  *PARAMETER
3  $=====
4  $----- Cartridge case material parameters -----
5  $=====
6  Rcden      8.53E-9      $ Density
7  Rcyoung    110000.0     $ Modulus of elasticity
8  Rcpoisson  0.35        $ Poissons ratio
9  Rck        896         $ Strength coefficient
10 Rcn         0.49        $ Hardening exponent
11 Rcy        50          $ Estimated initial yield stress
12 $=====
13 $----- Die material parameters -----
14 $=====
15 Rtden      15.5E-9      $ Density
16 Rtyoung    650000.0     $ Modulus of elasticity
17 Rtpoisson  0.2         $ Poissons ratio
18 $=====
19 $----- Punch material parameters -----
20 $=====
21 Rpden      7.85000E-9   $ Density
22 Rpyoung    210000       $ Modulus of elasticity
23 Rppoison   0.3         $ Poissons ratio
24 $=====
25 $----- Punch stroke depth -----
26 $=====
27 $$ Measured from top surface of top die to punch nose
28 Rstroke1   44           $ station 1 stroke depth
29 Rstroke2   53.3         $ station 2 stroke depth
30 Rstroke3   46.3         $ station 2 stroke depth
31 $=====
32 $----- Simulation settings -----
33 $=====
34 Rncpm      1500         $ Number of cycles pr. mm punch travel
35 $=====
36 $----- Global contact settings -----
37 $=====
38 RmyS       0.1          $ Static coefficient of friction
39 RmyD       0.08         $ Dynamic coefficient of friction
40 *PARAMETER_EXPRESSION
41 $Rvc       cy/sqrt(3)    $ Coefficient of viscous friction
42 Rvc        0            $ Coefficient of viscous friction
43 Rvcd       70           $ Viscous damping coefficient
44 #####

```

E.3 station_1.k

```

1 #####
2 *KEYWORD 1000000000 ncpu=8
3 $=====
4 $----- Include Global Parameters -----
5 $=====
6 *INCLUDE
7 ../parameters.k
8 $=====
9 $----- Local Parameters -----
10 $=====
11 *PARAMETER
12 Rccorrect -3.5          $ Cartridge placement correction in the z-direction
13 Rdcorrect 2             $ Die placement correction in the z-direction
14 Rrmin      0.17         $ Minimum element leg length when remeshing
15 Rrmax      0.23         $ Maximum element leg length when remeshing
16 $-----
17 *PARAMETER_EXPRESSION
18 Rzd1      dcorrect      $ Die 1 placement correction in the z-direction
19 Rzd2      dcorrect-18n   $ Die 2 placement correction in the z-direction
20 Rdistp    stroke1-dcorrect $ Stoke length
21 Rnegdistp (distp)*(-1)   $ Sign conversion for stroke length
22 Rterm     (2+(distp/2))/1000 $ Calulation of needed termination time
23 Rdt2ms    1/(2*ncpm)*0.001 $ Calcualtion of time step size
24 Rtfall    term-0.002     $ Calculation of start time for punch velocity slope down
25 Rd3dump   term/29        $ Dump frequency of d3plot files
26 Rmfreq    term/1.1       $ remeshing frequency
27 $=====
28 $----- Input settings and parts -----
29 $=====
30 *include
31 ../global_settings.k
32 s1_punch.k
33 s1_die1R_<variant>.k
34 s1_die1L_<variant>.k
35 s1_die2R_<variant>.k
36 s1_die2L_<variant>.k
37 cartridge_ini.k
38 backing_plate.k
39 $=====
40 $----- Move parts -----
41 $=====
42 $ Punch - Shell
43 *PART_MOVE
44 $#   pid          xmov          ymov          zmov          cid          iset
45     1             0.0            0.0            0             0             0
46 $-----
47 $ Die 1 Right
48 *PART_MOVE
49 $#   pid          xmov          ymov          zmov          cid          iset
50     2             0.0            0.0            &zdz1          0             0
51 $-----
52 $ Die 1 Left
53 *PART_MOVE
54 $#   pid          xmov          ymov          zmov          cid          iset

```

```

55      3      0.0      0.0      &zdz1      0      0
56 $-----
57 $ Die 2 Right
58 *PART_MOVE
59 $#  pid      xmov      ymov      zmov      cid      iset
60      4      0.0      0.0      &zdz2      0      0
61 $-----
62 $ Die 2 Left
63 *PART_MOVE
64 $#  pid      xmov      ymov      zmov      cid      iset
65      5      0.0      0.0      &zdz2      0      0
66 $-----
67 $ Cartridge case
68 *PART_MOVE
69 $#  pid      xmov      ymov      zmov      cid      iset
70      6      0.0      0.0      &ccorrect      0      0
71 *END
72 $#####

```


E.4 backing_plate.k

```

1 #####
2 *SECTION_SHELL_TITLE
3 Rigid shell - Backing plate
4 $#      secid      elform      shrf      nip      propt      qr/irid      icomp      setyp
5          90          2          1.0          2          1.0          0          0          1
6 $#      t1          t2          t3          t4          nloc      marea      idof      edgset
7          1.0          1.0          1.0          1.0          0.0          0.0          0.0          0
8 $-----
9 *CONTACT_SURFACE_TO_SURFACE_ID
10 $#      cid                                     title
11          9Backing
12 $#      ssid      msid      sstyp      mstyp      sboxid      mboxid      spr      mpr
13          6          9          3          3          0          0          1          1
14 $#      fs          fd          dc          vc          vdc      penchk      bt      dt
15          &mys      &myd      0.0          &vc      &vcd      0          0.01.00000E20
16 $#      sfs      sfm      sst      mst      sfst      sfmt      fsf      vsf
17          0.0          1.0          0.0          0.0          1.0          1.0          1.0          1.0
18 $#      soft      sofscl      lcidab      maxpar      sbopt      depth      bsort      frcfrq
19          1          0.1          0          1.025          2.0          2          0          1
20 $-----
21 *MAT_RIGID_TITLE
22 Backing plate
23 $ Rigid material, fixed x-y translation and x-y-z rotation
24 $#      mid      ro      e      pr      n      couple      m      alias
25          90      &pden      &pyoung      &ppoisson      0.0          0.0          0.0
26 $#      cmo      con1      con2
27          1.0          4          7
28 $#lc or a1      a2      a3      v1      v2      v3
29          0.0          0.0          0.0          0.0          0.0          0.0
30 $-----
31 *DEFINE_CURVE
32 $#      lcid      sidr      sfa      sfo      offa      offo      dattyp      lcint
33          90          0          1.0          1.0          0.0          0.0          0          0
34 $#          a1          o1
35          0.0          0.0
36          0.006          1.0
37          &term          1.0
38 *LOAD_RIGID_BODY
39 $#      pid      dof      lcid      sf      cid      m1      m2      m3
40          9          3          90          150          0          0          0          0
41 *PART
42 Backing plate
43 $#      pid      secid      mid      eosid      hgid      grav      adpopt      tmid
44          9          90          90          0          1          0          0          0
45 *PART_MOVE
46 $#      pid      xmov      ymov      zmov      cid      iset
47          9          0.0          0.0          -3.6          0          0
48 #####

```

E.5 station_2.k

```

1  #####
2  *KEYWORD 1000000000 ncpu=8
3  $=====
4  $----- Global Parameters -----
5  $=====
6  *INCLUDE
7  ../parameters.k
8  $=====
9  $----- Local Parameters -----
10 $=====
11 *PARAMETER
12 Rccorrect 0.1          $ Cartridge placement correction in the z-direction
13 Rdcorrect 0.9          $ Die placement correction in the z-direction
14 Rrmin      0.17        $ Minimum element leg length when remeshing
15 Rrmax      0.23        $ Maximum element leg length when remeshing
16 $-----
17 *PARAMETER_EXPRESSION
18 Rzd1      dcorrect      $ Die 1 placement correction in the z-direction
19 Rzd2      dcorrect-18    $ Die 2 placement correction in the z-direction
20 Rdistp     stroke2-dcorrect $ Stoke length
21 Rnegdistp (distp)*(-1)   $ Sign conversion for stroke length
22 Rterm      (2+(distp/2))/1000 $ Calculation of needed termination time
23 Rdt2ms     1/(2*ncpm)*0.001 $ Calculation of time step size
24 Rtfall     term-0.002    $ Calculation of start time for punch velocity slope down
25 Rd3dump    term/29       $ Dump frequency of d3plot files
26 Rmfreq     term/1.1      $ remeshing frequency
27 $=====
28 $----- Input settings and parts -----
29 $=====
30 *include
31 ../global_settings.k
32 s2_punch.k
33 s2_die1R_<variant>.k
34 s2_die1L_<variant>.k
35 s2_die2R_<variant>.k
36 s2_die2L_<variant>.k
37 s2_cartridge.k
38 s2_offset.k
39 $=====
40 $----- Move parts -----
41 $=====
42 $ Punch - Shell
43 *PART_MOVE
44 $#      pid      xmov      ymov      zmov      cid      iset
45      1          0.0        0.0        0          0          0
46 $-----
47 $ Die 1 Right
48 *PART_MOVE
49 $#      pid      xmov      ymov      zmov      cid      iset
50      2          0.0        0.0      &zsd1      0          0
51 $-----
52 $ Die 1 Left
53 *PART_MOVE
54 $#      pid      xmov      ymov      zmov      cid      iset

```

```

55      3          0.0          0.0          &z d1          0          0
56  $-----
57  $ Die 2 Right
58  *PART_MOVE
59  $#   pid          xmov          ymov          zmov          cid          iset
60      4          0.0          0.0          &z d2          0          0
61  $-----
62  $ Die 2 Left
63  *PART_MOVE
64  $#   pid          xmov          ymov          zmov          cid          iset
65      5          0.0          0.0          &z d2          0          0
66  $-----
67  $ Cartridge case
68  *PART_MOVE
69  $#   pid          xmov          ymov          zmov          cid          iset
70      6          &movec          0.0          &ccorrect          0          0
71  *END
72  #####

```

E.6 s2_offset.k

The *s2_offset.k* file is produced by the automated post processing for cartridge transfer between station 1 and 2. The value of *movect* is the x-displacement of the punch at ended simulation of station 1, and is used for re-centering the cartridge fro the simulation of station 2.

```

1  #####
2  *PARAMETER_EXPRESSION
3  Rmovect      -1.121200e-02
4  Rmovec       -1*movect
5  #####

```

E.7 station_3.k

```

1 #####
2 *KEYWORD 1000000000 ncpu=8
3 $=====
4 $----- Global Parameters -----
5 $=====
6 *INCLUDE
7 ../parameters.k
8 $=====
9 $----- Local Parameters -----
10 $=====
11 *PARAMETER
12 Rccorrect 0          $ Cartridge placement correction in the z-dirction
13 Rdcorrect -0.2       $ Die placement correction in the z-dirction
14 Rrmin      0.15      $ Minimum element leg length when remeshing
15 Rrmax      0.225     $ Maximum element leg length when remeshing
16 $-----
17 *PARAMETER_EXPRESSION
18 Rzd1      dcorrect   $ Die 1 placement correction in the z-dirction
19 Rdistp     stroke3-dcorrect $ Stoke length
20 Rnegdistp  (distp)*(-1) $ Sign conversion for stroke length
21 Rterm      (2+(distp/2))/1000 $ Calculation of needed termination time
22 Rdt2ms     1/(2*ncpm)*0.001 $ Calculaution of time step size
23 Rtfall     term-0.002 $ Calculation of start time for punch velocity slope down
24 Rd3dump    term/29    $ Dump frequency of d3plot files
25 Rmfreq     term/0.9    $ remeshing frequency
26 $=====
27 $----- Input settings and parts -----
28 $=====
29 *include
30 ../global_settings.k
31 s3_punch.k
32 s3_die1R_<variant>.k
33 s3_die1L_<variant>.k
34 s3_cartridge.k
35 s3_offset.k
36 $=====
37 $----- Move parts -----
38 $=====
39 $ Punch - Shell
40 *PART_MOVE
41 $#      pid      xmov      ymov      zmov      cid      iset
42      1          0.0        0.0        0          0          0
43 $-----
44 $ Die 1 Right
45 *PART_MOVE
46 $#      pid      xmov      ymov      zmov      cid      iset
47      2          0.0        0.0        &zd1        0          0
48 $-----
49 $ Die 1 Left
50 *PART_MOVE
51 $#      pid      xmov      ymov      zmov      cid      iset
52      3          0.0        0.0        &zd1        0          0
53 $-----
54 $ Cartridge case

```

```

55 *PART_MOVE
56 $#   pid          xmov          ymov          zmov          cid    iset
57     6             &movec        0.0          &ccorrect      0      0
58 *END
59 #####

```

E.8 s3_offset.k

The *s3_offset.k* file is produced by the automated post processing for cartridge transfer between station 2 and 3. The value of *movect* is the x-displacement of the punch at ended simulation of station 2, and is used for re-centering the cartridge for the simulation of station 3.

```

1  *PARAMETER_EXPRESSION
2  Rmovect    -1.217264e-03
3  Rmovec     -1*movect

```